MPC REPORT NO. 93-18-A

Tests and Analysis of Mixed Wood-Concrete Beams (Preliminary Report)

Tser-Ming Chen
Richard M. Gutkowski

March 1993

TESTS AND ANALYSIS OF MIXED CONCRETE-WOOD BEAMS

Tser-Ming Chen, Research Assistant
Richard M. Gutkowski, Professor

Department of Civil Engineering
Colorado State University
Ft. Collins, Colorado

March 1993

ACKNOWLEDGEMENTS

Support for this project described herein was provided through the Mountain Plains Consortium as part of the University Transportation Centers Program (UTCP). The MPC member universities include North Dakota State University, Colorado State University, University of Wyoming and Utah State University. The UTCP is funded by the U.S. Department of Transportation.

The authors would like to thank Drs. M. E. Criswell, and P. J. Pellicane, for their assistance during the course of his study. Experimental tests were conducted in the Structural Engineering Laboratory at the Engineering Research Center on the campus of Colorado State University. Computer facilities in the Department of Civil Engineering were also employed in the research. The donated use of these facilities is gratefully acknowledged.

Preface

As concrete and wood are low cost materials and require low skill levels in construction, their combined use as bridge materials is attractive to rural settings. Concrete is strong in compression and weak in tension. Wood is strong in tension parallel to grain but subject to buckling in compression. Thus, composite T-beams constructed to stress concrete in compression and wood in tension may have performance advantages for bridges. Basic research on the composite behavier of mixed concrete-wood beam construction is a first step toward understanding their potential use in bridge constructions.

This project included two laboratory studies and analytical work dealing with T-beams comprised of a concrete flange connected to wood beam plus plywood sheathing. Based on the experimental results of tests of 72 slip specimens and 4 full-scale layered T-beams, the mechanical behavior of different materials in layered structure was studied. In the slip tests, concrete-wood members were tested for two different ages of concrete, 4 types of nails and two different embedment lengths. The slip modulus and ultimate load of each specimen were determined after testing. In T-beam bending tests, the deflection and the interlayer slip were measured at varying load level. The experimental results of the T-beam tests are compared favorably to theoretical values that were obtained by use of an existing computer program, FEABEA, originally configured for composite wood to wood construction.

The report material which follow was submitted by Mr. Tser-Ming Chen as his thesis in partial fulfillment of the degree of Master of Science in Civil Engineering at Colorado State University. Except for modification of the format to comply with MPC requirement, it is the verbatim duplicate of that thesis body and is titled the same. Dr. Richard M. Gutkowski directed the work and was his Faculty Advisor.

Tser-Ming Chen, Research Assistant
Richard M. Gutkowski, Professor
Department of Civil Engineering
Colorado State University
Ft. Collins, Colorado 80523

TABLE OF CONTENTS

LIST OF TABLES

LIST OF FIGURES

CHAPTER 1

INTRODUCTION

"T-beam construction" has been well known and widely used in modern engineering structures. This construction is an example of layered structural systems. In layered structural systems, different components are interconnected to form one assembly. In such assemblages, designers can effectively utilize the different characteristics of materials and use every piece of material in the most economical way.

Layered structures generally have a quite simple outside appearance, but like any composite structure, they exhibit several complex mechanical behaviors. These behaviors include incomplete composite action, two-way action, discontinuous action, and slippage of connections. Material properties, connector characteristics, connection type, and configuration of structure are all important factors which influence these behaviors. In the early design of layered systems, many assumptions were made to simplify the analysis, but some of them could not match actual conditions.

In the past thirty years, researchers have developed more accurate methods to model the action of layered wood systems. In 1971, a research team was organized at Colorado State University (CSU) to develop rational analysis and design procedures for wood joist floor systems. A computer program, FEAFLO (Finite Element Analysis of FLOors), was written after the appropriate mathematical model was developed and several related laboratory test programs were completed. In FEAFLO, the complete modeling procedure accounts for variable material properties, incomplete composite action of the layered beams, two-way action of the floor, and sheathing interlayer gaps. In past studies, wood was the only material used in the FEAFLO mathematical model and supporting experiments.

Light-frame construction is the most common application of layered wood structural systems. This system constitutes a major part of residential buildings under four stories in the United States. However, wood is not the only component utilized in layered structures. During the general theoretical development of mathematical models for layered structures, other components such as steel and concrete have been included the research and experimental verifications. In the study reported herein, wood and concrete, two of the most common materials in building constructions, are chosen to make 3-layer T-beam specimen. Such members might have potential application in floor and bridge construction.

The objective of this study is to explore the laboratory behavior of such members to determine critical variables that affect performance. Aspects of the applicability of the FEAFLO model to such construction is examined. The goal of the work is to examine the degree of composite action evident in the test members.

After load tests on simply supported beams, the measured behavior of T-beams is compared with the results of theoretical analyses. The slipping action of the interlayer connectors between concrete and wood is likely an important variable in these tests. Therefore, tests for different nail connectors and spacing between concrete and wood were designed and investigated in this study.

CHAPTER 2

LITERATURE REVIEW

Wood-joist floor systems are generally designed by assuming that the joists act alone as simple beams. The design procedure is conservative but the overdesign results in an ineffective use of materials. This is because many factors which contribute to the strength and stiffness of the systems are neglected. A complete mathematical model that could more precisely describe the behavior of laminated floor systems consists of extremely complex steps.

Under a given load, a beam that is composed of laminations placed freely upon one another deflects more than a solid beam of the same cross section under the same loading condition. This is because the freely laminated beam cannot resist horizontal shear between the layers. In order to make a laminated beam act more like a solid beam, various devices such as nails, bolts, and glue are used to connect the laminations. The resulting behavior is partially composite, so neither the model of ideal solid beams (fully composite) nor of freely laminated beams (non-composite) can properly predict the action of connected layered beam.

In 1951, Clark [12] developed a theory for predicting the deflection of laminated beams. In his theory, the connectors between two layers were assumed to be rigid, and the deflection and separation of laminations were considered to be very small. By these assumptions the layered beams were rigidly connected at discrete intervals along the beams. It was assumed that there is no slip occurring between layers, so the total elongation at the contact plane of each of the two laminations is equal. Based on this concept, a layered beam theory was developed.

A comparison between mathematical analysis and results of laboratory tests of sandwich construction has been made by Norris, et al [14]. This work included two series of test beams comprised of 3-ply strips having cores of low density wood and theoretical analysis based on a

low shear rigidity existing between layers. The theoretical analysis not only involved the modulus of elasticity of materials but also introduced shearing modulus into the model. An extension by Kuenzi and Wilkinson [18] introduced additional parameters into theoretical expressions for deflection and stresses of composite beams with finite adhesive or fastener rigidity.

Newmark, Siess and Viest [13] reported results of tests and analyses of composite beams with incomplete composite action. Composite steel and concrete T-beam specimens and push-out specimens were utilized in these tests. The T-beam specimens were designed to allow measurement of the important actions of composite beams. The purpose of the push-out test specimens was to study the behavior of individual shear connectors.

Kuenzi [19] reported a mathematical method to determine the allowable lateral load of a single nail or bolt joint. His method combines various parameters involving the member and connector properties. The basic concept of his work is to consider the connectors as being supported on an elastic foundation with a foundation modulus equal to the modulus of elasticity. The advantage of this method is that it could be applied to any construction without need of test data on joints. Wilkinson [20, 21, 22, 23] continued Kuenzi's research to make a series of analyses and experiments consisting of several different kinds of connectors. McCutcheon [24] further developed Kuenzi and Wilkinson's research [18] to derive a procedure for computing the deflection of wood-joist two layer floors and combined the effects of fastener stiffness and gaps.

In Clark's research [14] the joints were assumed to be rigid, but for some composite structures like layered wood constructions connected by nails, the relative motion (slip) between layers affects the action of the structures significantly. Goodman [1, 2] investigated a mathematical model governing the behavior of a 3-layer beam with each layer having the same thickness and symmetrical mechanical properties. The primary difference in Goodman's mathematical model as compared to Clark's is that Goodman took the slip between two layers as being equal to the difference between the total elongation of the two layers. Thus, the connector modulus (slip modulus) played an important role in Goodman's model and significantly influenced later research.

Ko [31] expanded Goodman's theory by using the numerical solution and the closed form solution to express an approximate solution with beam and connector properties. Good agreement between the experimental results and both theoretical values were shown in Ko's reported results.

Ko's report was a part of the extended research program conducted at CSU beginning in 1971. The computer program FEAFLO for wood joist floor system was developed by Thompson, et al [5, 11], Vanderbilt, et al [7], and Liu [28]. A subprogram FEABEA was previously used by Kuo [32], Tremblay [6], and Pault [17] to analyze multilayered T-beams. The details of the FEABEA mathematical model are discussed in chapter 3. Complete series of laboratory verification tests for FEABEA and FEAFLO were included in that research program.

Interlayer slip, slip modulus, load sharing and two-way action are the main influences discussed in research on partially composite wood joist floor systems. Several reports [8, 10, 16] involved the issue of interlayer slip and derived various testing methods to measure slip modulus. Basically, the slip modulus is a function of both the connector properties and the material properties of the joists and flooring. Slip modulus is defined as the slope of the load-slip curve for a full-scale shear test of the connected materials. The relationship of load and slip in interlayer action is nonlinear, but it is often simplified by assuming linearity. The simplification was incorporated in FEAFLO. In the researches of Ko [31], Kuo [32], and Pault [17], the linear elastic theory was used to investigate T-beam systems and analyze composite action in glulam bridges. Tremblay [6] derived a nonlinear slip modulus and modulus of elasticity of materials from tests and introduced these nonlinear moduli into T-beam system analysis.

Wheat [25, 26] developed and verified a nonlinear analysis method to predict deflection of layered floor by an iteration procedure. This method is implemented in program NONFLO. McLain [16] developed an empirical equation to characterize the load-slip relation. The equation is $P = A\log_{10}(1 + B\delta)$, in which P = the nail lateral load, δ = the nail slip, and A and B = parameters based on the specific gravity of the connected materials. Pellicane, et al [10] and Jizba [27] developed a technique to predict the A and B parameters.

The interlayer slip modulus is a critical variable in modeling composite action. The effect of this parameter has previously been demonstrated in Goodman [3, 4] and Pault's [17] reports. The two-way action was also discussed in related reports [3, 4, 7]. Another significant factor in wood floor system construction is interlayer gaps. Gaps have a significant effect on connector stiffness. Antonides [15, 33] presented a complete discussion.

The FEAFLO program has been widely applied in analysis for wood floor systems. Similar research has been conducted by U.S. Forest Products Laboratory (FPL). In McCutcheon's report [35], there is a detailed presentation and discussion of the research effort at CSU and the FPL. In the most recent development at CSU, Stonebraker [29] and Glasco [30] applied the concept of an expert system to develop a program CADFLO (Computer Aided Design of FLOor systems). CADFLO was developed by combining the FEAFLO program and graphic capabilities of C language to build an interactive graphical input based design system.

Foschi [34] developed a more rigorous floor analysis based on the finite strip method. The lateral bending deflection of the joists and their torsional deformation were included. This rigorous model included all degrees of freedom to avoid the need to introduce the parameters that are difficult to determine such as the flexible gaps.

McCutcheon [36] presented a simplified method for predicting the performance of a wood floor under uniform loads. The method was based on his earlier analog which represented a floor as a beam supported by elastic springs. Load sharing and two-way action were both considered in this study. The bending stiffness of wood member with sheathing attached nonrigidly is included by use of the transformed area concept [37].

The study reported herein focuses on a preliminary study of the basic mixed material T-beam behavior. The FEABEA model was applied to the mixed material layered system. It is the preparation for later advanced research on mixed material structures.

CHAPTER 3

THE MATHEMATICAL MODEL FOR A T-BEAM

INTRODUCTION

The major purpose of this study is to investigate the FEABEA mathematical model, that has previously been applied in wood joist system research, to assess the behavior of the mixed material T-beams. The test results of the T-beam specimens are compared to the predictions obtained from FEABEA. The development of mathematical model is presented in section 3.2. Two values, the deflection of T-beam and the slip between layers, were measured in the tests. These results are discussed in section 6.3. In section 7.3, the comparison of the theoretical results and the test results are presented.

DEVELOPMENT OF MATHEMATICAL MODEL

As stated earlier, a mathematical model for the investigation of a layered beam was presented by Goodman [1, 2] and later extended by Ko [31]. The theoretical solution for this model was based on beam theory with consideration of interlayer slip. In Ko's studies, the closed form solution and a finite difference solution were presented for two and three layer beams. The typical two-layer beam system and its internal moments, shears, and axial forces required to maintain equilibrium are shown in Figure 3.1.

A finite element solution based on the mathematical model was developed by Thompson [5, 11]. The principle of minimum potential energy is the basic consideration in the finite element solution. In Thompson's report, the following assumptions were made in this mathematical model:

1. Material properties are elastic.

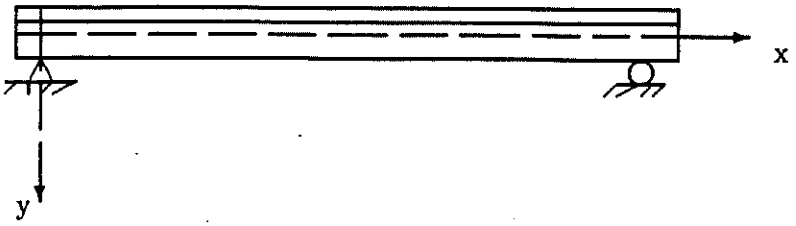

(a) Beam with sign convention

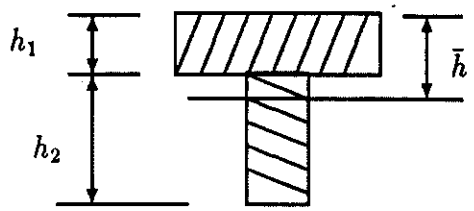

(b) Cross-section

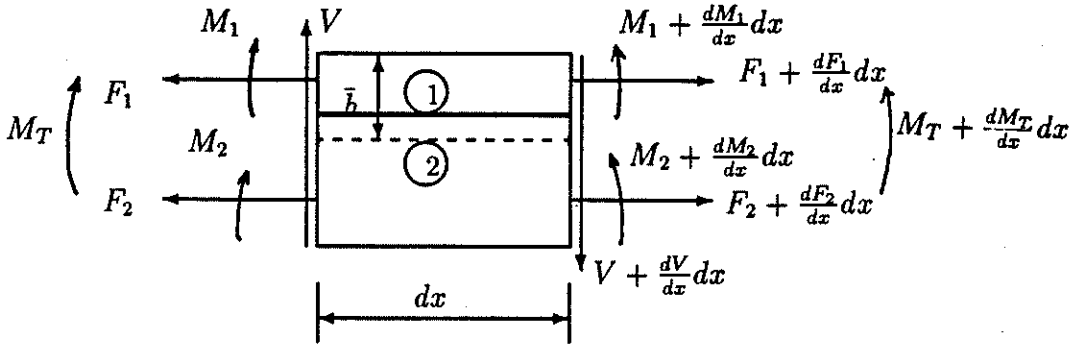

(c) Beam element

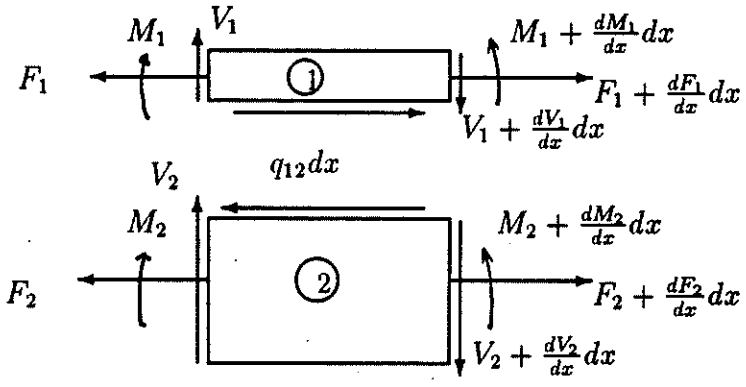

(d) Layer element

Figure 3.1: The Internal Forces of a Layered T-Beam

2. Deflection is small.

3. Shear deformation and friction are neglected.

4. The slip modulus of the interlayer connection is elastic.

5. The radius of curvature is the same for all layers.

6. Gaps create discontinuous axial displacement and force.

In accordance with these assumptions, the potential energy of a layered beam is considered as composed of four components:

1. pure bending of each layer, J^b,

2. axial deformation of each layer, J^u,

3. slip deformation of the connections between each layer, J^c, and

4. external loads on the beam, J^w.

The third energy component, that due to the slip deformation of connectors, can be written as

$$J^c = \sum_{i=1}^{n_L-1} \frac{1}{2} \int_0^l (\frac{k_i n_i}{s_i})(\Delta_{si})^2 dx \tag{3.1}$$

Δ_{si} is the interlayer slip, $(\frac{k_i n_i}{s_i})\Delta_{si}dx$ represents the average force along a length of beam dx. From Figure 3.2, the interlayer slip, Δ_{si} can be expressed as the combined effects of the beam deflection and the axial displacements.

$$\Delta_{si} = (u_{i+1} - \frac{h_{i+1}}{2}\frac{dy}{dx}) - (u_i + \frac{h_i}{2}\frac{dy}{dx}) \tag{3.2}$$

The total potential energy of the layered beam is given as

$$\begin{aligned} J &= J^b + J^u + J^c + J^w \\ &= \sum_{i=1}^{n_L} \int_0^l [\frac{1}{2} E_i I_i (\frac{d^2y}{dx^2})^2 + \frac{1}{2} E_i A_i (\frac{du_i}{dx})^2] dx + \\ &\quad \sum_{i=1}^{n_L-1} \int_0^l \frac{1}{2} (\frac{k_i n_i}{s_i}) [(u_{i+1} - u_i) - \frac{1}{2}(h_{i+1} + h_i)\frac{dx}{dy}]^2 dx - \int_0^l w(y) dx \end{aligned} \tag{3.3}$$

in which

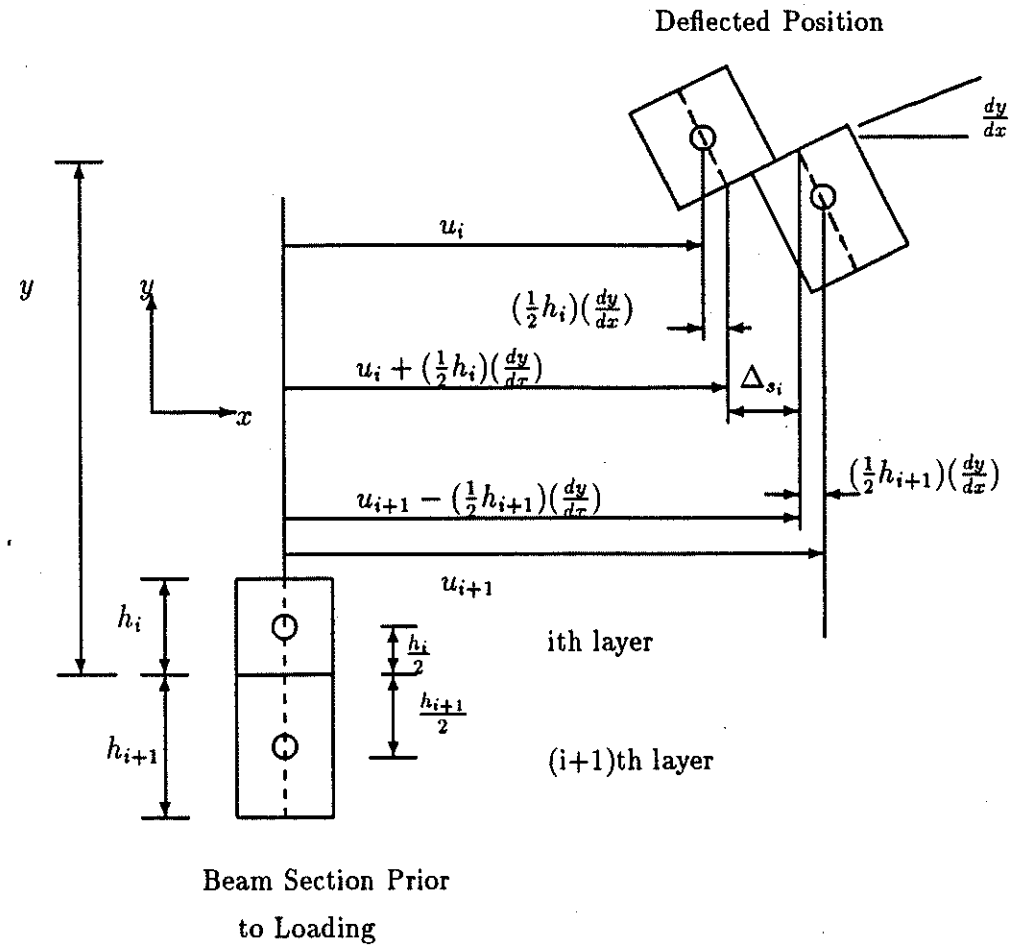

Figure 3.2: The Deflection of A T-Beam

A_i = cross section area of the ith layer,

E_i = modulus of elasticity of the ith layer,

I_i = moment of inertia of the ith layer,

k_i = slip modulus of connector between the ith and $(i+1)$th layers,

l = length of beam,

n_i = number of rows of connectors between the ith and $(i+1)$th layers,

n_l = number of layers

s_i = spacing of connectors between the ith and $(i+1)$th layers,

u_i = axial deformation of the ith layer,

w = loading on the beam,

x = coordinate along the length of beam,

y = vertical displacement of the beam, and

h_i = depth of the ith layer.

The principle of virtual work requires that the potential energy have a stationary value for the equilibrium position of the layered beam. Using calculus of variations, the requirement of the equilibrium is expressed as:

$\delta J = 0$

in which

$$\begin{aligned}\delta J \;=\; & \sum_{i=1}^{n_L}[\int_0^l E_i I_i(\frac{d^2y}{dx^2})\delta(\frac{d^2y}{dx^2})dx + \int_0^l E_i A_i(\frac{du_i}{dx})\delta(\frac{du_i}{dx})dx] + \\ & \sum_{i=1}^{n_L-1}\{\int_0^l(\frac{k_i n_i}{s_i})[(u_{i+1}-u_i) - \frac{1}{2}(h_{i+1}+h_i)\frac{dy}{dx}]\delta(u_{i+1}-u_i)dx - \\ & \int_0^l(\frac{k_i n_i}{s_i})[(u_{i+1}-u_i) - \frac{1}{2}(h_{i+1}+h_i)\frac{dx}{dy}]\frac{1}{2}(h_{i+1}+h_i)\delta(\frac{dy}{dx})dx\} - \\ & \int_0^l w\delta y dx \end{aligned} \tag{3.4}$$

In equation 3.4, the deflection and axial displacement can be approximated using the finite element form of the Rayleigh-Ritz procedure. The variables, y and u_i, in the potential energy equation are functions only of the distance along the beam. In order to satisfy the finite element formulation, the beam has to be divided into linear elements as shown in Figure 3.3. The variables, y and u_i, are approximated by polynomials in x in each element of the beam. The approximations of y and u_i in element j are expressed as

$$y = [N_y]\{Y\}_j \tag{3.5}$$

$$u_i = [N_u]\{U_i\} \tag{3.6}$$

in which

$[N_y]$ = shape functions for a cubic approximation to y,

$[N_u]$ = shape functions for a linear approximation to u,

$\{Y\}_j$ = nodal point values for deflection and slope for element j, and

$\{U_i\}_j$ = nodal point values for the axial displacements of layer i of element j.

The first derivatives of u_i and the first and second derivatives of y appear in the potential energy equation. They are

$$\frac{dy}{dx} = [N_y']\{Y\}_j \tag{3.7}$$

$$\frac{d^2y}{dx^2} = [N_y'']\{Y\}_j \tag{3.8}$$

$$\frac{du_i}{dx} = [N_u']\{U_i\}_j \tag{3.9}$$

The variation of potential energy for any element can be approximated in term of the nodal point values for $y, dy/dx$, and u_i, such that

$$\sum_{i=1}^{n_L}[\int_0^{l_j} E_i I_i(\frac{d^2y}{dx^2})\delta(\frac{d^2y}{dx^2})]dx = \{\delta Y\}_j^T \int_0^{l_j} [N_y'']^T EI[N_y'']dx\{Y\}_j \tag{3.10}$$

and

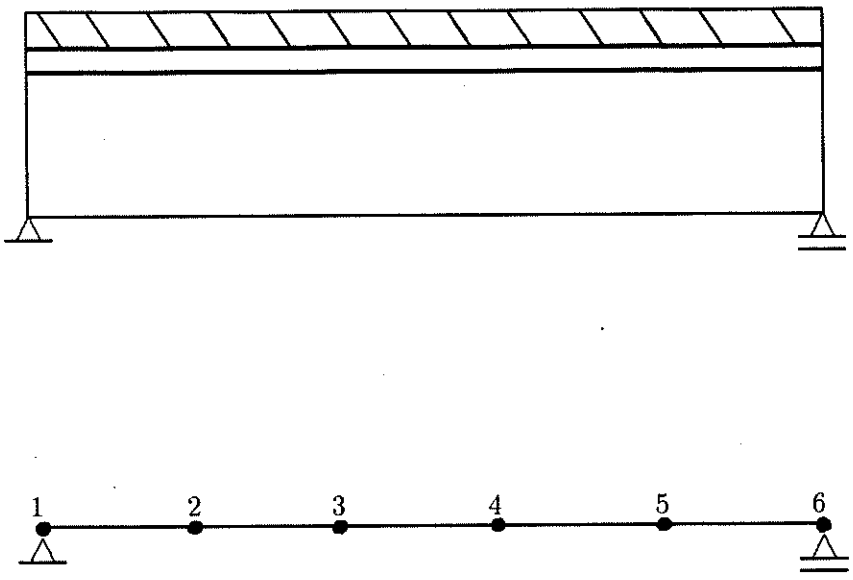

Figure 3.3: The Finite Element Representation of T-Beam

$$\sum_{i=1}^{n_L-1}\{\int_0^{l_j}(\frac{k_i n_i}{s_i})[-\frac{1}{2}(h_{i+1}+h_i)\frac{dy}{dx}]\delta u_{i+1}dx\}$$
$$= \sum_{i=1}^{n_L-1}\{\delta U_i\}_j^T \int_0^l [N_u]^T C_i [N_y']dx\{\delta Y\}_j \tag{3.11}$$

in which

$$EI = \sum_{i=1}^{n_L} E_i I_i \tag{3.12}$$

$$C_i = -\frac{1}{2}(h_{i+1}+h_i)\frac{k_i n_i}{s_i} \tag{3.13}$$

and l_j is the length of element j of the n_L element. By combining all terms into one matrix expression, the variation of the potential energy for a single element can be expressed as

$$\delta J_j = \{\delta s\}_j^T [k]_j \{s\}_j - \{\delta s\}_j^T \{f\}_j \tag{3.14}$$

in which

$\{s\}$ =a matrix combining all the generalized displacements for y, dy/dx, and u_i,

$[k]_j$ =the stiffness matrix for element j, and

$\{f\}_j$ =a matrix combining all generalized external forces corresponding to $\{s\}$.

By direct assembly of element matrices, the general equilibrium equation for the entire beam can be expressed as

$$[K]\{S\} = \{F\} \tag{3.15}$$

in which $[K]$, $\{S\}$, and $\{F\}$ are the system equivalents of $[k]_i$, $\{s\}_i$, and $\{f\}_i$.

Thompson developed the finite element formulation for beams and utilized it to build the computer program FEABEA. From the observed results of T-beam bending tests, it is known that the effect of the gaps on the stiffness of layered beam can be significant. In FEABEA,

there are two methods to incorporate gaps. For the finite element formulation, when an open gap exists in a layer, the axial displacement of this layer is no longer continuous and the transmission of axial force is interrupted. The first method is to use a special element with the length equaling zero, and the axial force for the both sides of the element is set at zero for the layer for which the open gap exists. This method produces an element of zero length at every gap point. The second method is to model a small element at the gap point and give a low modulus of MOE to this element. This method can be used to handle the gap problem, when the gaps are filled with another material.

CHAPTER 4

TESTING EQUIPMENT AND PROCEDURE

INTRODUCTION

Two fundamental types of tests were conducted in this study. One is the slip test of connectors used between the concrete and the wood. Similar tests had been done by other researchers for determining connector slip moduli between plywood sheathing and wood joist. These works were published in reports cited earlier. Most of the steps in the experimental work in the present study are the same as in the past research. One noteworthy difference is that the properties of concrete are variable with age. In the next chapter, a discussion of basic material properties is presented. In addition, the vital material property, connector slip modulus, was determined from the slip tests and utilized in the theoretical model analysis of composite T-beams. The behavior of the joints and results of the slip tests are discussed in section 6.2.

The second type of test in this study is a full-size bending test of three-layer T-beams. The purpose of the T-beam tests is to examine the applicability of the existing FEABEA model by the comparison of the predicted and measured relationships of load level to deflection and slip. The T-beam testing procedure and testing equipment are described in section 4.3.

SLIP TEST

The American Society for Testing and Materials (ASTM) specifies standard methods for testing mechanical properties of mechanical fasteners used with wood, including the slip modulus for metal connectors. The slip test setup is illustrated in Figure 4.1a. The test method has been questioned by various investigators, so several testing procedures have been developed to

improve the ASTM standard test. Pellicane and Bodig [39] made a complete comparison of six different nail joint test methods that had been used in different research studies.

In the study reported herein, the single-connector tension test method was selected (Figure 4.1b). The particular test devices used was originally developed by DeBonis [38] and later used and modified by McLain [16], Antonides [15, 33], Pellicane et al [10], and Pault [17]. The testing apparatus of this method includes four aluminum plates that serve to hold the specimen and two LVDT's (Linear Variable Differential Transformer) set on plates to measure the deformation of the specimen. The specimens used in this test method are comprised of a main member and a side member jointed by a single connector. These four aluminum plates were designed to be a special anti-symmetric device (Figure 4.2) so that an applied tensile load can be located directly along the interface between two members to produce pure shear at specimens. The hydraulic loading system that is connected to a controller is designed to apply tension on the test apparatus. The loading can be controlled so as to be applied at a constant rate (ramp load). An LVDT is mounted in each side plate of the aluminum apparatus. The load and average value of the interface displacement measured by each of these two LVDT's are recorded simultaneously and continuously. These data of load and slip are input to an X-Y recorder to plot a continuous curve. The load-slip curves are the source of slip modulus values.

A total of 72 specimens were built in wood, concrete, and nail connector. Each slip test specimen used in this study was composed of a main wood member and a side concrete member connected by a single nail. Four different sizes of nails were selected to be the connectors of specimens. The connections can be divided into 8 types according to the different penetration depths into the wood members. For each connection type, 9 replications of the test specimen were used. The detailed dimension of specimen and connection types are illustrated in Figure 4.3 and Table 4.1. In order to confirm the influence of the time dependent strength of concrete, the specimens in each chosen connection type were divided into two sets. In each type of connection, six specimens were tested after the concrete had cured for 14 days, and the other

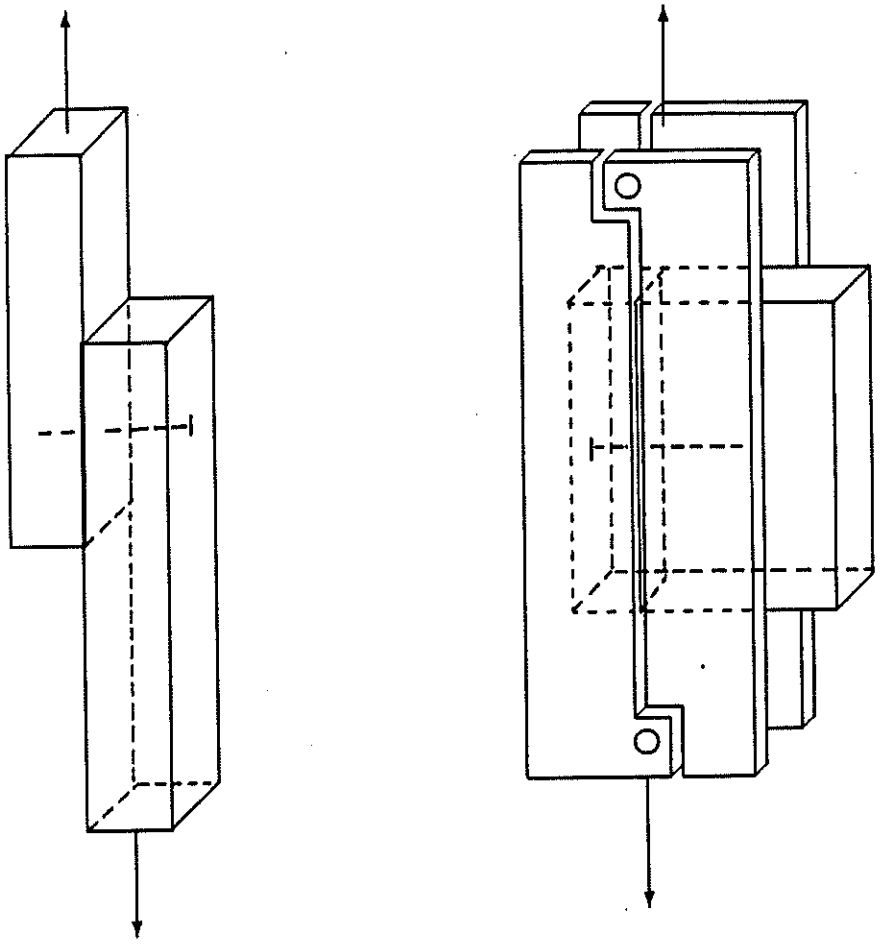

a b

Figure 4.1: The Slip Test Set-Up, a) The Slip Test Set-Up in ASTM and b) The Set-Up of Slip Test in The Study.

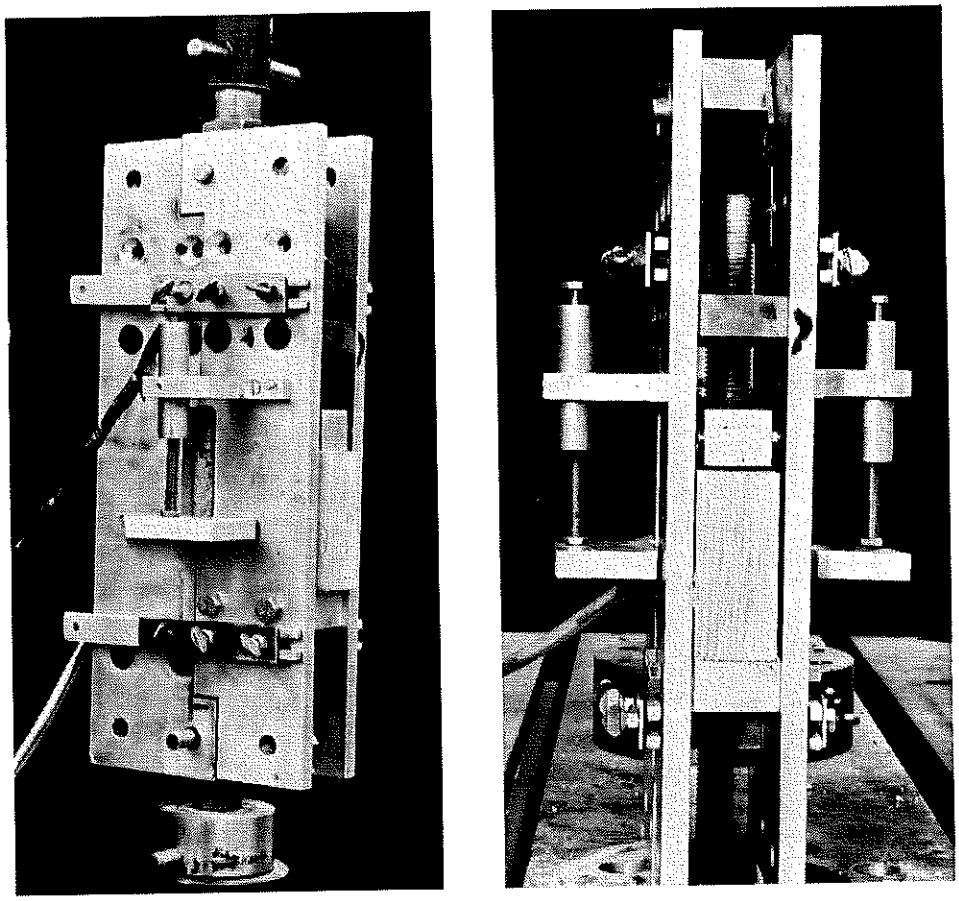

Figure 4.2: The detailed configuration of slip test device

three specimens were tested at 28-day age. Concrete of 14-day and 28-day age have different strengths. The strength of concrete is discussed in section 5.2.

The slip modulus is commonly defined either as the initial tangent to the load-slip curve at the origin or as an appropriate secant value. A representation of a typical load-slip curve and the two slip modulus definitions are shown in Figure 4.4. In Appendix A, the load-slip curves of all test specimens are presented, and an average curve of every type of connection is shown. For illustration, an actual load-slip curve is shown in Figure 4.5.

THREE-LAYER T-BEAM TEST

Test Specimen

Four T-beam specimens built in concrete, plywood, and hem-fir lumber were tested in bending. The detailed configuration of these T-beams is shown in Figure 4.6. The stem was a nominal 2x10 in. x in. The plywood was 3/4 inch thick Douglas-fir. Due to the length of the plywood, there are one or two gaps existing in the plywood layer. All four T-beams were built in the same connection type, 10d nail with one inch embedment length in concrete, and in two different spacings, namely 2 and 6 inches. The specimen span was 16 feet.

The specimen casting procedure was to nail plywood and lumber together first and leave one inch of the nail protruding from the plywood. After these two layers are connected, this two layer T-beam was placed on a form that supported the T-beam under the plywood layer and kept the plywood layer flat. Then, the concrete was cast on the top of the two layer beam. The concrete used in this study was ready-mixed concrete which was the same kind of concrete used in the slip tests. Results of standard tests conducted to determine the strength of the mix are reported subsequently. The concrete thickness could not be controlled exactly, so the actual thickness of the concrete layer was measured after the form was taken off. The values of thickness used in computing theoretical values are the average of measurements taken at several

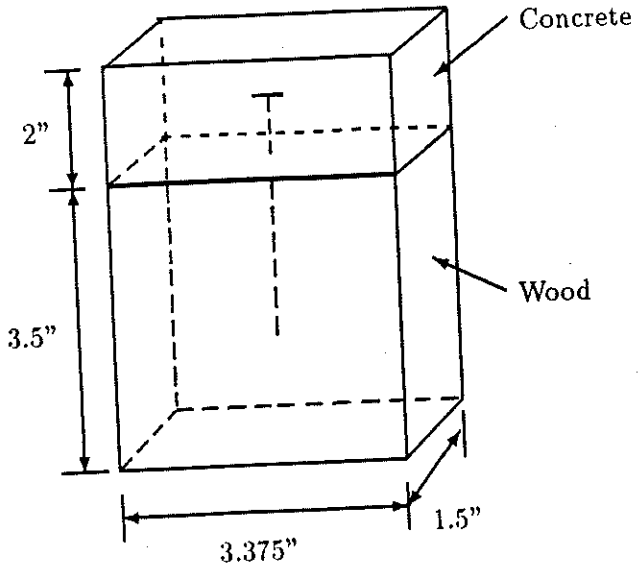

Figure 4.3: The Dimensions of The Slip Test Specimens

Table 4.1: The Connection Types for The Slip Tests

type	connector style (l=length, d=diameter)	length in wood member (in)	length in concrete member(in)
1	doublehead nail	1.75	1.75
2	l=3.5 in. d=0.139 in.	2.50	1.00
3	common nail (6d)	1.00	1.00
4	l=2 in. d=0.115 in.	1.50	0.50
5	common nail (20d)	2.25	1.75
6	l=4 in. d=0.148 in.	3.00	1.00
7	common nail (10d)	1.50	1.50
8	l=3 in. d=0.130 in.	2.00	1.00

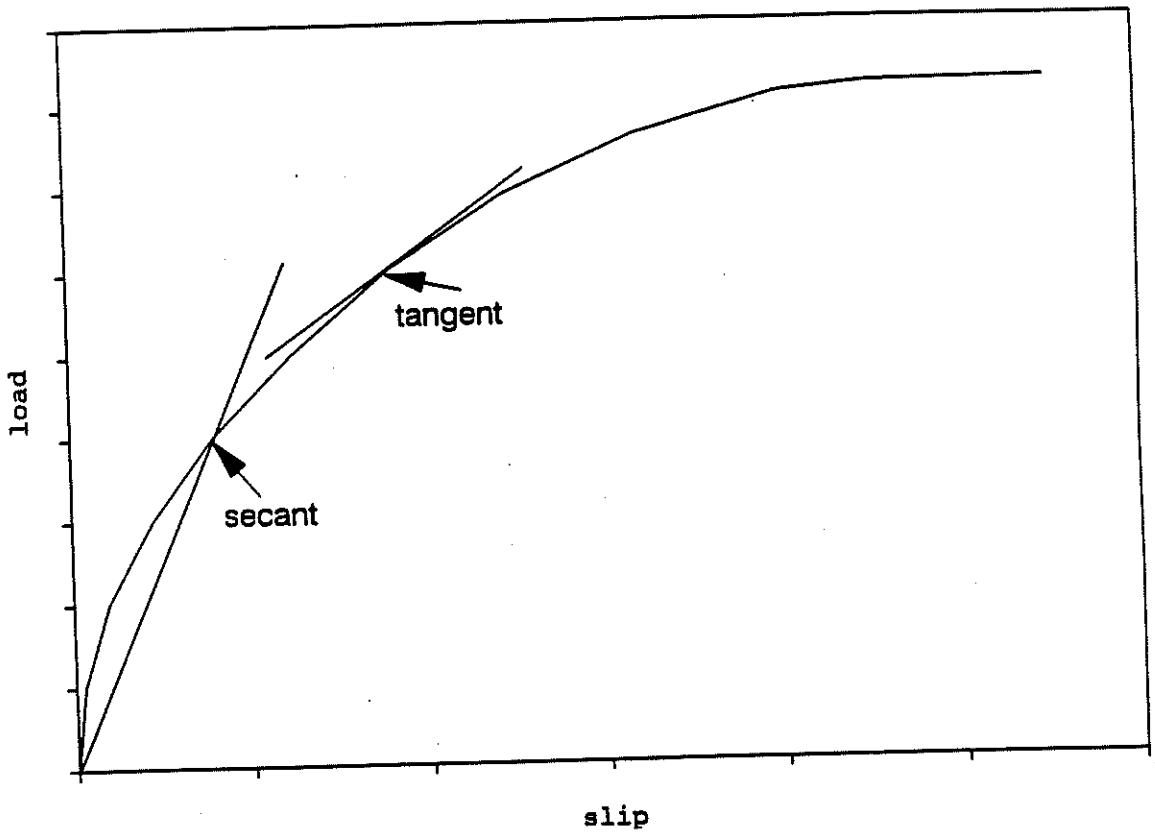

Figure 4.4: The Typical Theoretical Load-Slip Curve

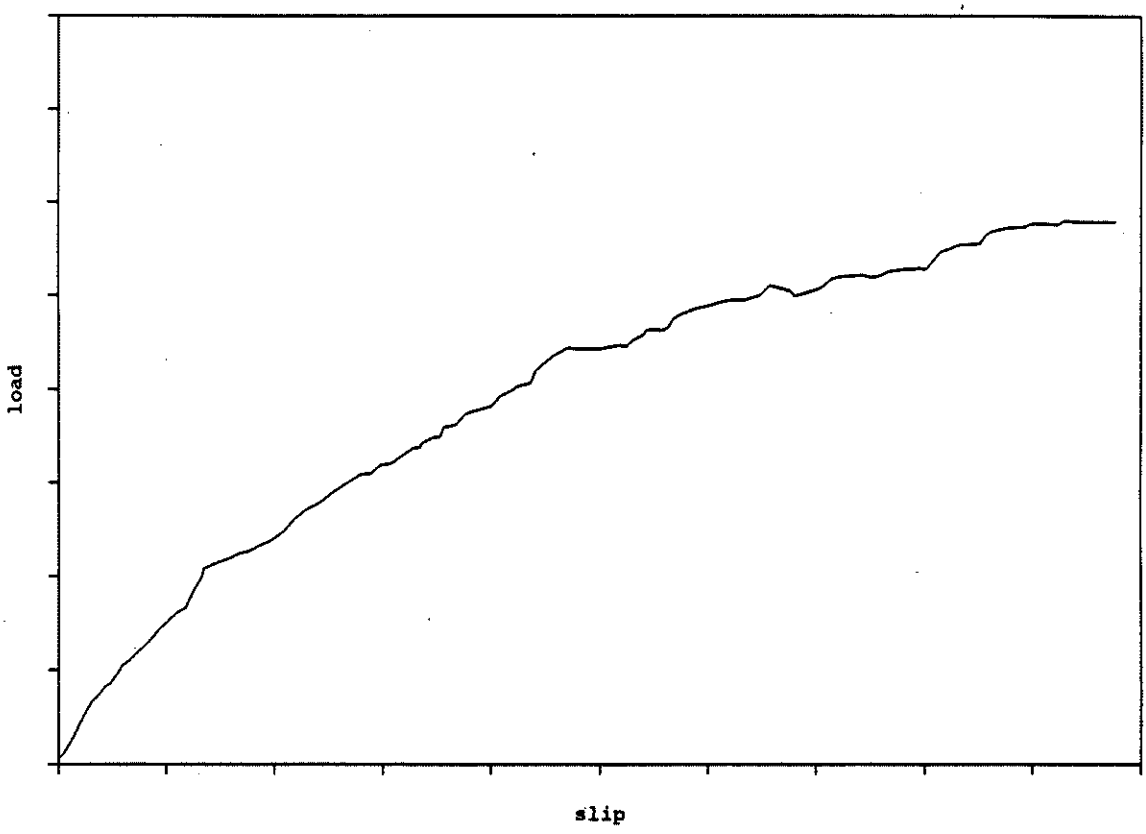

Figure 4.5: An Example of An Actual Load-Slip Curve

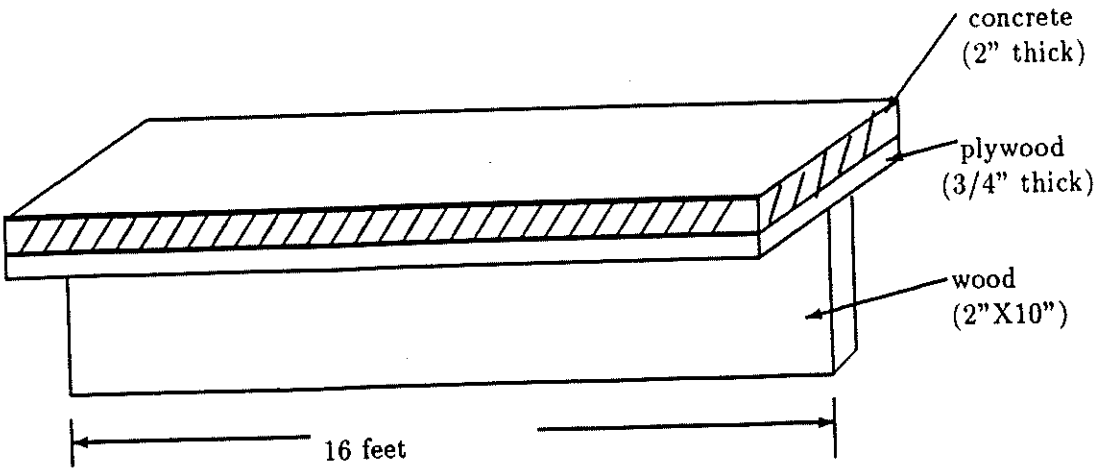

a

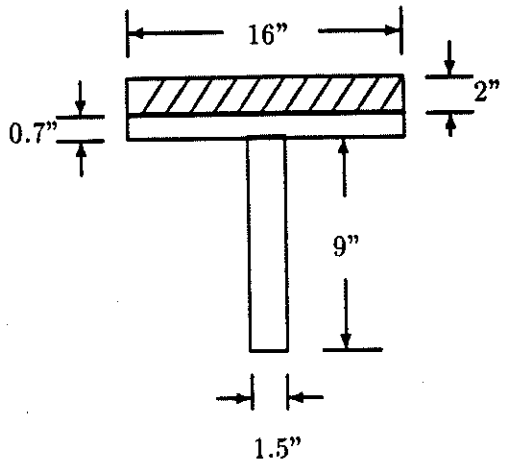

b

Figure 4.6: The Configuration of T-Beam Specimens, a) Span and Nominal Sizes, and b) Example Measured Dimensions.

locations along the concrete layers. The measured thickness ranged from 1.89 to 2.02 inches. The average thickness values of concrete layer for all specimens are listed in Table 4.2.

Table 4.2: The Average Thickness of The Concrete Flange of The T-Beam Specimens

	specimen 1	specimen 2	specimen 3	specimen 4
thickness (in.)	1.96	1.94	1.98	1.94

Loading System

Facilities used for the structural testing of the T-beam specimens are located in the Structural Engineering Laboratory at the Engineering Research Center at CSU. The major components of the loading system were a 100 kip-capacity MTS hydraulic actuator and associated control equipment.

The MTS closed-looped system is comprised of 3 main components: The central power supply unit, two actuators, and a control console. The two actuators were placed on a steel frame with two separate skeletons. The distance between the center of the two actuators was fixed as 5 feet. The whole system is shown in Figure 4.7. In order to produce two concentrated loads on the 16 inch wide T-beam specimen, the force from each actuator was transmitted to a T-section steel pad that was built in two 16 inches long 0.5x1.5 in. x in. steel plates. The hydraulic power supply unit is the source of the pressure that actuates the load cells to place the load on specimens. The control console is the main control system that can control the hydraulic power unit and adjust the load on the actuators. The load from load cell can be set at a constant amount by the set point switch on the control console. Each load cell had a capacity of 100 kips, but for experimental requirements, the range of load was 0 to 10000 lbs.

The ends of the T-beam specimens were supported by rollers fixed on concrete blocks. Each roller was located at a distance of 5 feet from the load points. The clear span of the beam was 15 feet and the loads were applied at the third points.

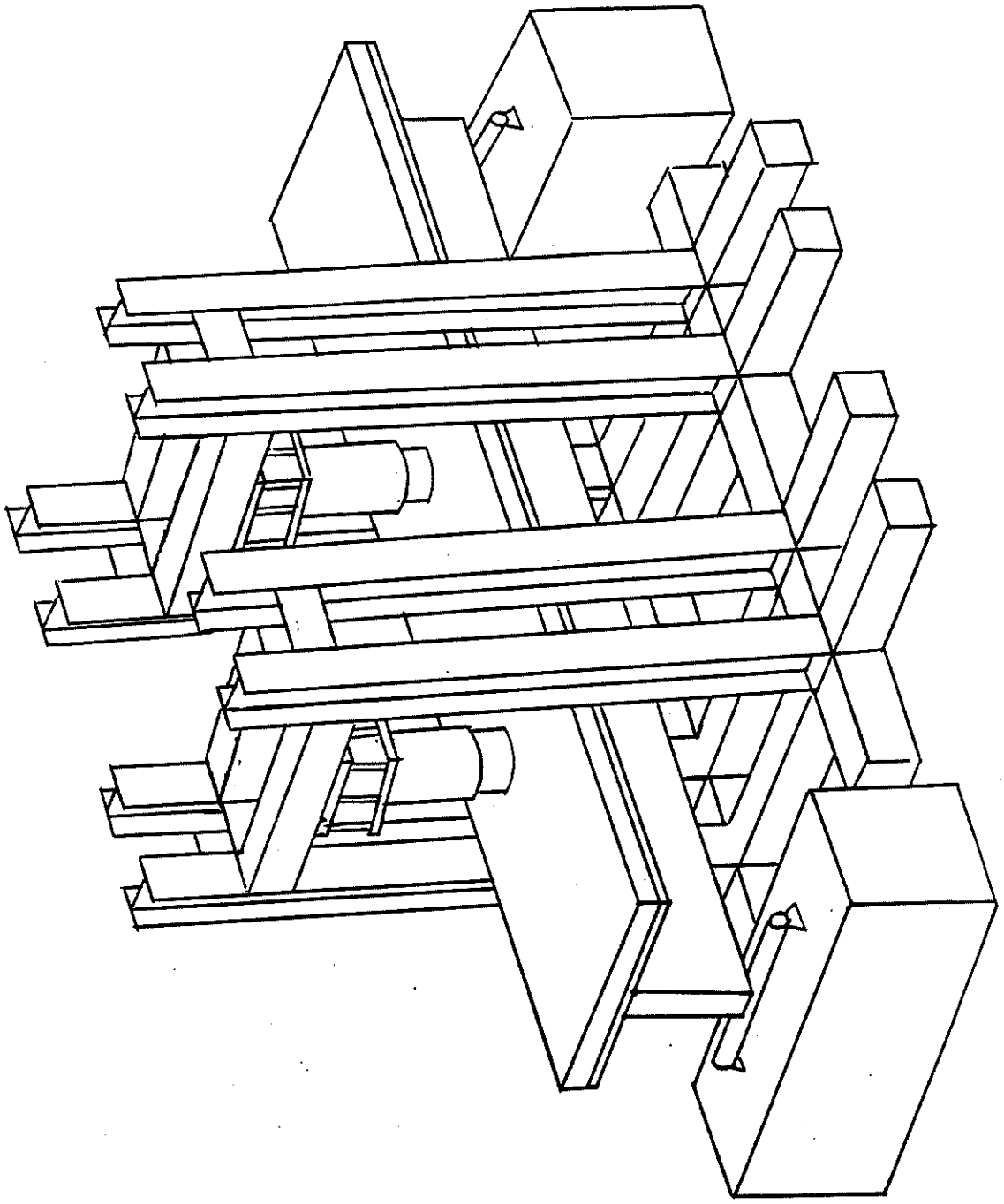

Figure 4.7: The Loading System for T-Beam Bending Test

DATA COLLECTION

Two values, deflection and slip, were measured during the T-beams testing. The deflections of T-beam specimens were detected by three LVIT's (Linear Variable Inductive Transducers) that were placed at three different positions underneath the joist of each T-beam specimen. The three LVIT's and the control console were connected to an HP computer for data logging and processing. The computer can record readings from assigned channels at the same time. In this experiment, 5 channels were used to transmit the values of voltage from load cells and LVIT's to the computer. Because the readings on the computer represented the voltage signal, the LVIT's and load cells needed to be calibrated before the testing. Thus the increasing or decreasing of the values of voltage on the channels expressed the relationship between the loads and deflections.

The slip between layers was measured by dial gages that were fastened to wood blocks attached on the sides of concrete and lumber layers. The positions of LVIT's and dial gages for every specimen are shown in Figures 4.8 and 4.9. In order to establish the relation between load, deflection, and slip, the dial gages were read at the same time when the computer recorded the loads and deflections.

Test Procedure

The procedure for testing each T-beam is summarized below:

1. Put the T-beam in place.
2. Install the LVIT's at the designated positions.
3. Mount the dial gages on the T-beam.
4. Record the initial readings of the channels on computer and the dial gages.
5. Increase the loads. The readings were recorded for every 100 lbs (approximately) load increment.

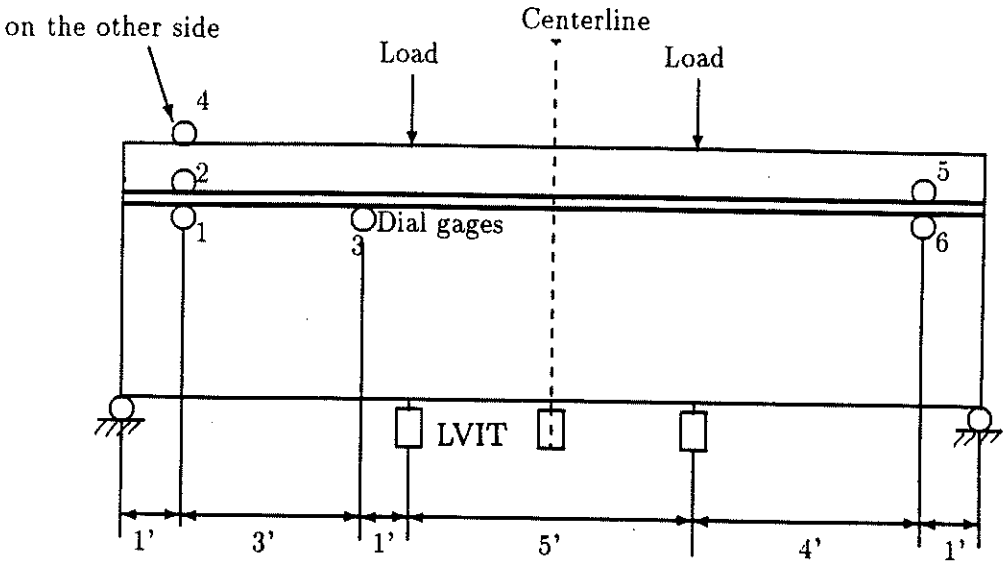

Specimen 1

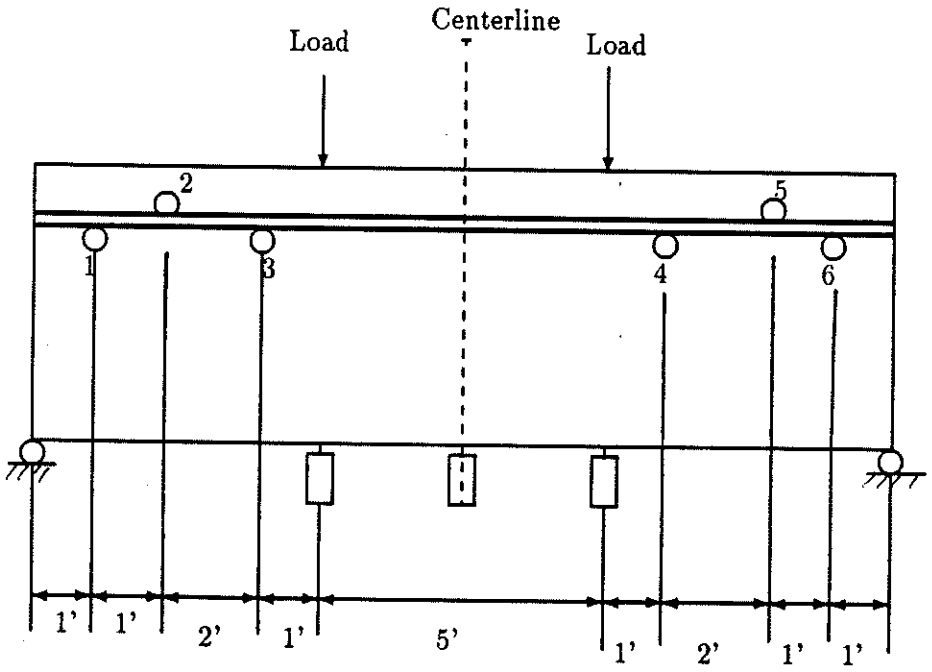

Specimens 2,3,4

Figure 4.8: The Position of LVIT's and Dial Gages

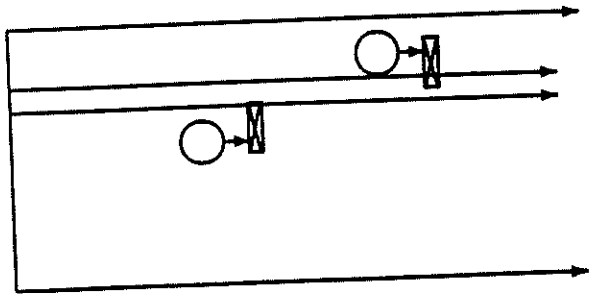

a) side view

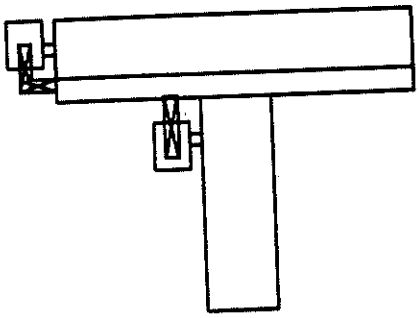

b) cross section

Figure 4.9: The Location of Dial Gages on T-Beam Specimens, a) Side View, and b)Cross-Section.

Table 4.3: The Measured Deflection Results of T-Beams

specimen	load (lbs)		deflection (in.)		
	actuator position		at LVIT position		
	left	right	left	center	right
1	81.80	106.90	0.09288	0.11381	0.10825
	181.60	208.50	0.17231	0.21469	0.19425
	280.20	348.20	0.27325	0.33969	0.30625
	401.60	399.60	0.35231	0.43700	0.39381
	497.20	493.30	0.44163	0.54844	0.50194
	591.00	598.30	0.54825	0.67800	0.62400
2	100.50	103.00	0.07131	0.07675	0.06650
	203.30	201.30	0.16331	0.17962	0.15506
	296.60	301.90	0.27038	0.29881	0.25656
	400.30	397.30	0.40137	0.43669	0.37519
	494.10	502.60	0.51831	0.56062	0.48306
	595.40	600.10	0.67081	0.73219	0.63212
3	97.30	96.50	0.09944	0.10988	0.09419
	196.50	198.10	0.16750	0.18406	0.15006
	300.20	299.50	0.26144	0.28388	0.23825
	394.00	398.40	0.34806	0.38231	0.32306
	494.30	499.40	0.44225	0.48650	0.41725
	595.00	597.70	0.53006	0.58081	0.50625
4	102.10	98.70	0.05019	0.04944	0.04044
	198.90	200.40	0.09687	0.10644	0.08200
	300.70	302.80	0.15094	0.16831	0.13531
	400.70	400.70	0.20512	0.22981	0.18819
	499.40	497.20	0.26075	0.29131	0.23675
	596.00	596.50	0.32012	0.49394	0.28712

6. After the loads were increased to 400 or 500 lbs, decrease the loads to zero in 100 lbs increments.

7. Repeat the fifth step until the T-beam fails.

In order to avoid damage to the LVIT's, they were removed when the first crack was heard. Basically, the deflection and slip measurements were recorded for every 100 lb load increment, but the loads could not be controlled in an exact 100 lbs variation. Figure 4.10 is the example of experimental behavior of specimen 1. The results of all the T-beam tests are presented in Table 4.3-4 and Appendix B.

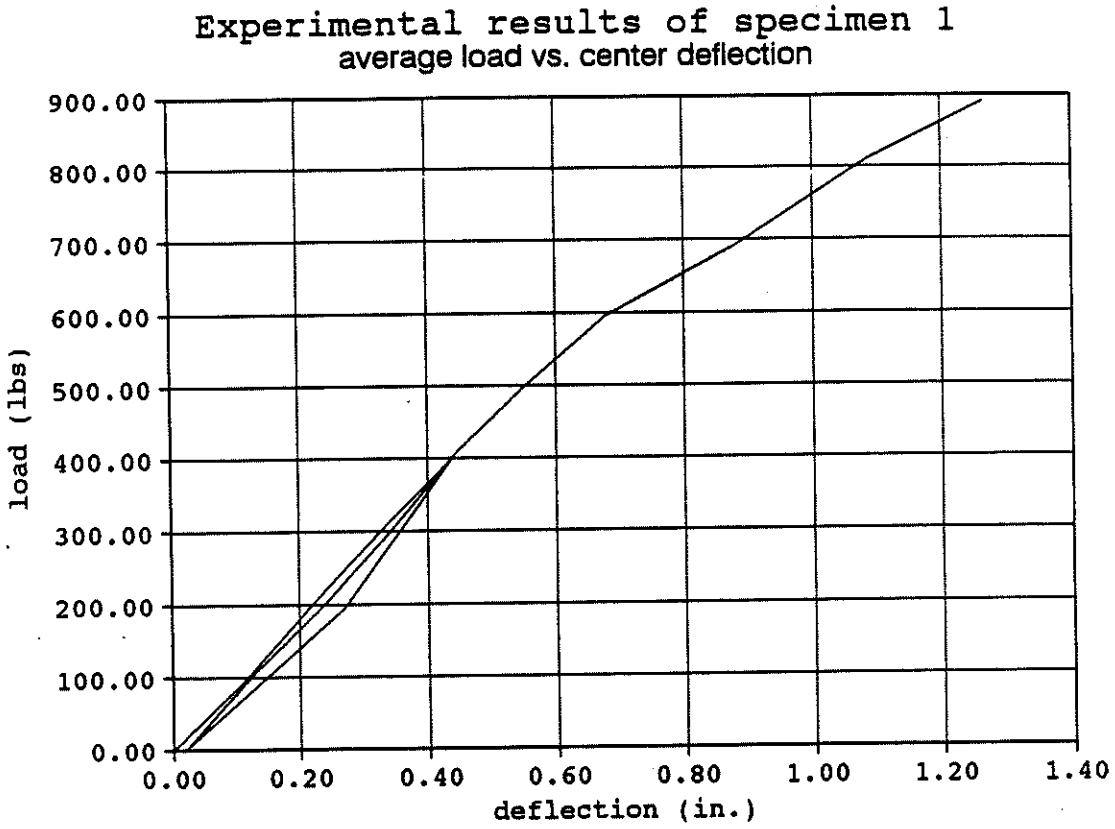

Figure 4.10: The Load-Deflection Curve of Specimen 1

Table 4.4: The Measured Slip Results of T-Beams

specimen	load (lbs)		slip at position (in.)					
	actuator position		at dial gage position					
	left	right	1	2	3	4	5	6
1	81.80	106.90	0.007	0	0.005	0	0.005	0.012
	181.60	208.50	0.014	0	0.010	0	0.008	0.020
	280.20	348.20	0.021	0	0.016	0	0.013	0.029
	401.60	399.60	0.028	0	0.020	0	0.015	0.033
	497.20	493.30	0.035	0	0.025	0	0.020	0.042
	591.00	598.30	0.045	0	0.031	0	0.025	0.052
2	100.50	103.00	0.006	0.002	0.005	0.003	0.002	0.004
	203.30	201.30	0.014	0.005	0.010	0.008	0.005	0.013
	296.60	301.90	0.024	0.010	0.019	0.017	0.010	0.023
	400.30	397.30	0.036	0.015	0.029	0.024	0.013	0.034
	494.10	502.60	0.048	0.020	0.037	0.032	0.017	0.045
	595.40	600.10	0.065	0.027	0.050	0.042	0.022	0.058
3	97.30	96.50	0.004	0.003	0.003	0	0	0.004
	196.50	198.10	0.010	0.003	0.008	0.002	0	0.011
	300.20	299.50	0.019	0.006	0.015	0.006	0	0.019
	394.00	398.40	0.028	0.010	0.023	0.009	0	0.027
	494.30	499.40	0.038	0.014	0.032	0.013	0	0.035
	595.00	597.70	0.048	0.016	0.040	0.017	0	0.043
4	102.10	98.70	0.003	0.002	0.002	0.002	0.001	0.003
	198.90	200.40	0.005	0.003	0.004	0.004	0.002	0.005
	300.70	302.80	0.008	0.005	0.006	0.006	0.004	0.008
	400.70	400.70	0.011	0.007	0.009	0.009	0.005	0.015
	499.40	497.20	0.014	0.008	0.011	0.011	0.005	0.015
	596.00	596.50	0.018	0.010	0.014	0.014	0.006	0.019

CHAPTER 5

PROPERTIES OF MATERIALS

INTRODUCTION

When two or more kinds of materials are used in a structure, the different characteristics of these materials influence the actions of the structure. Generally, the moduli of elasticity of the materials are the most important basic material properties influencing the behavior of the structure and must be utilized in the mathematical models. For a laminated structure, the slip moduli of connectors between layers also directly influence the composite behavior of the structure.

Wood and concrete are the two materials used in this study. The evaluation of the material properties is in accordance with the related tests. The recommended methods for determining the properties of concrete and wood are listed in the ASTM standards, and several substitute methods have been used in previous reports. The standard method specified in ASTM C39-86 is widely accepted as the means to evaluate the mechanical properties of concrete. The properties of wood usually exhibit a high degree of variability. Many unavoidable physical factors such as grain angle and knot size and location affect the properties of wood.

Because wood is a nonhomogeneous and anisotropic material, it is not possible to establish a constant value for the MOE. Different values of the MOE of wood exist for each species and for different orthotropic directions. A standard method for testing the mechanical properties of lumber and plywood is difficult to specify. ASTM D198-84 presents a test method that was originally designed for solid sawn materials (such as bridge girders and floor joists) to evaluate the flexure properties of timber. For the flexure properties of plywood, ASTM D3042-76 also specifies three methods for determination. However, for the dimensions of lumber and plywood

used in this study, these methods are not suitable. The specified test specimen dimensions by ASTM cannot represent the characteristics of lumber and plywood that were used in the T-beam bending test. In addition, the lumber and plywood that were used in T-beam beading tests are difficult to be cut as the dimensions that are specified by ASTM. A simple method used in this study is presented in section 5.3.

Slip modulus of connectors between layers is the other main point discussed in this chapter. It is one of the major factors influencing the composite behavior of layered structures.

PROPERTIES OF CONCRETE

Because concrete has very good compressive strength, the common applications of concrete in construction are designed for compressive resistance. For design requirements, the general strength of the concrete is taken from uniaxial compressive strength of a standard test cylinder. The standard test method and specimen are presented in ASTM C39-86. The specified compressive strength f'_c is the basic concrete design strength in structural design procedure. It is generally measured by a compression test on a standard cylinder after 28 days of moist curing.

The factors affecting concrete strength include water-cement ratio, type of cement, aggregate, moisture condition during curing, temperature, and age of concrete. In this study, the same ready-mixed concrete was used to cast all specimens. Water content and curing condition were almost the same for all specimens. The only controlled variable, age of concrete, is discussed in this study.

ACI (American Concrete Institute) Committee 209 has recommended the following equation to represent the rate of strength gain for normal weight concrete in wet-cured condition.

$$(f'_c)_t = \frac{t}{4.00 + 0.85t}(f'_c)_{28} \tag{5.1}$$

In Equation 5.1, $(f'_c)_{28}$ is the compressive strength at 28 days and $(f'_c)_t$ is the strength at time t in days.

In the tests described in chapter 4, three concrete cylinders were cast at the same time with mixed T-beam and wet-cured 28 days in the same condition with T-beam specimens. After the compressive strength test, the specified compressive strength f'_c was measured from three specimens. The average of f'_c is equal to 2506 psi. From equation (5.1), $(f'_c)_{28} = 2506psi$, $(f'_c)_{14} = 2206psi$.

ASTM also recommends two types of tests for determining the tensile strength of concrete. One is the modulus of rupture or flexural test. The other is the split cylinder test. These two methods give different strength values. Generally they vary between 8 and 15% of the compressive strength.

ACI section 9.5.2.3 defines the modulus of rupture for bending:

$$f_r = 7.5\sqrt{f'_c} \tag{5.2}$$

In common applications, concrete is considered as an linear-elastic material. The value of modulus of elasticity of concrete basically is determined from the stress-strain curve of concrete in compression. The slope of the line from the origin to the point on the curve corresponding to stress of $0.45f'_c$ is defined as modulus of elasticity E_c. ACI section 8.5.1 defines the following equation for modulus of elasticity of concrete

$$E_c = 33W_c^{1.5}\sqrt{f'_c} \tag{5.3}$$

for the value of unit weight W_c between 90 and 155 lb/ft^3. For normal weight concrete $W_c = 145$ lb/ft^3 and, thus

$$E_c = 57000\sqrt{f'_c} \tag{5.4}$$

For the three cylinder specimens cast for the T-beams tested in this research, the average unit weight was 139.4 lb/ft^3. From equation 5.3, the corresponding value of E_c is $2.72 \times 10^6 psi$.

PROPERTIES OF LUMBER AND PLYWOOD

In the mathematical model used in this study, all properties are assumed to be linear. In order to get the value of the MOE directly from the lumber and plywood material used in T-beam tests, specimens that were used in the material property tests were extracted from undamaged part of the T-beams.

After the T-beam testing, the lumber was the major broken material, so small specimens were extracted from the undamaged portions. Considering the influence of the direction of load on the properties of wood, these small specimens were placed in the same direction of load as in the T-beam test to evaluate the MOE, and the ratio of length and depth for small lumber specimens was similar to the original lumber. Each joist was then assigned a constant value of the MOE that was equal to the average of the MOE values obtained for small specimens extracted from it.

In the T-beam specimens, there were two different types of configurations of plywood (Figure 5.2a,b). The difference is the number and locations of butt joints (gaps) in the plywood. After the T-beam testing, every complete plywood panel was subsequently load tested and assigned a constant value of the MOE.

The loading test for determining the MOE of lumber and plywood was based on the basic relation of loading and deflection on a simply supported beam. After positioning the small specimens or plywood plates on two roller supports, a concentrated load was placed at the midspan of the specimen (Figure 5.1). The clear span of small specimens was about 40 inches, and the depth of the small lumber specimens was about 2 inches. This ratio of depth and length is close to the ratio of lumber in T-beam test. The midspan deflection of each specimen was measured by a LVIT. From the measured load and deflection, the MOE value of each specimen can be obtained from the equation

$$E = \frac{PL^3}{48I\Delta} \tag{5.5}$$

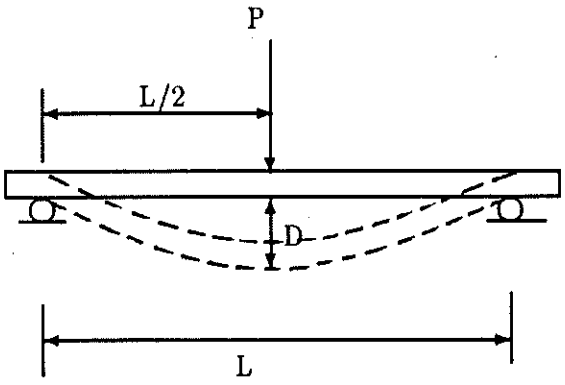

Figure 5.1: The Test Set-Up for The Plywood and Lumber

in which E = the MOE of specimen, P = the concentrated load, I = the moment of inertia of the section of specimens, $\frac{bh^3}{12}$, (b, h are the width and depth of the specimen's cross section), Δ = the deflection at the midspan, L = the span.

The load-deflection properties of plywood and lumber generally are nonlinear. Only constant values of the MOE for the joist and plywood plate can be used in the FEABEA mathematical model. The load-deflection tests were conducted in the elastic range with load specified at 50 lb increments. An example load-deflection curve for a lumber specimen that was extracted from T-beam specimen 1 is shown in Figure 5.3. For all extracted lumber and plywood specimens, each load-deflection curve is approximatedly linear when load was below 150 lbs and deflection was less than 0.8 inch. Therefore, an constant value of the MOE for lumber joist and plywood plate is reasonable. The value of the MOE for all T-beam specimens are listed in Table 5.1a,b.

SLIP MODULUS

There are several factors influencing the slip modulus. They are the properties of connected materials, the properties of connectors, and the gaps existing between materials. The slip modulus of the connection between layers in a laminated structure is the important factor affecting

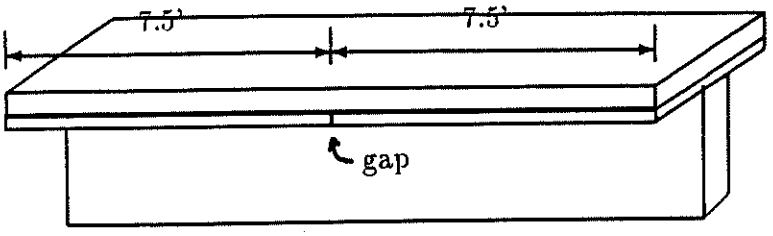

Figure 5.1a: The Configurations of T-Beam Specimens 1 and 3

Table 5.1a The Material Properties of Specimens 1 and 3

Specimen	MOE of concrete(psi)	MOE of plywood (psi) 0-7.5 ft	7.5-15 ft	MOE of lumber (psi)
specimen 1	3.30×10^6	1.32×10^6	1.43×10^6	1.22×10^6
specimen 3	2.74×10^6	1.19×10^6	1.25×10^6	1.80×10^6

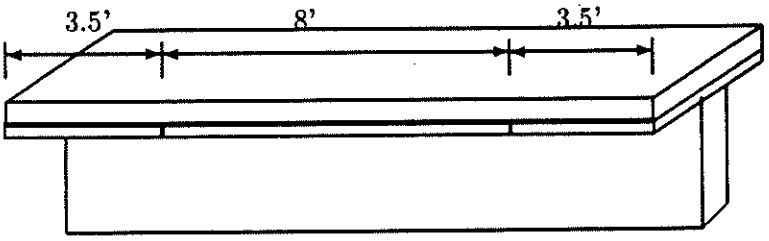

Figure 5.1b: The Configurations of T-Beam Specimens 2 and 4

Table 5.1b The Material Properties of Specimens 2 and 4

Specimen	MOE of concrete(psi)	MOE of plywood (psi) 0-3.5 ft	3.5-11.5 ft	11.5-15 ft	MOE of lumber (psi)
specimen 2	2.78×10^6	1.56×10^6	0.97×10^6	1.57×10^6	1.16×10^6
specimen 4	2.69×10^6	0.91×10^6	1.32×10^6	0.93×10^6	1.56×10^6

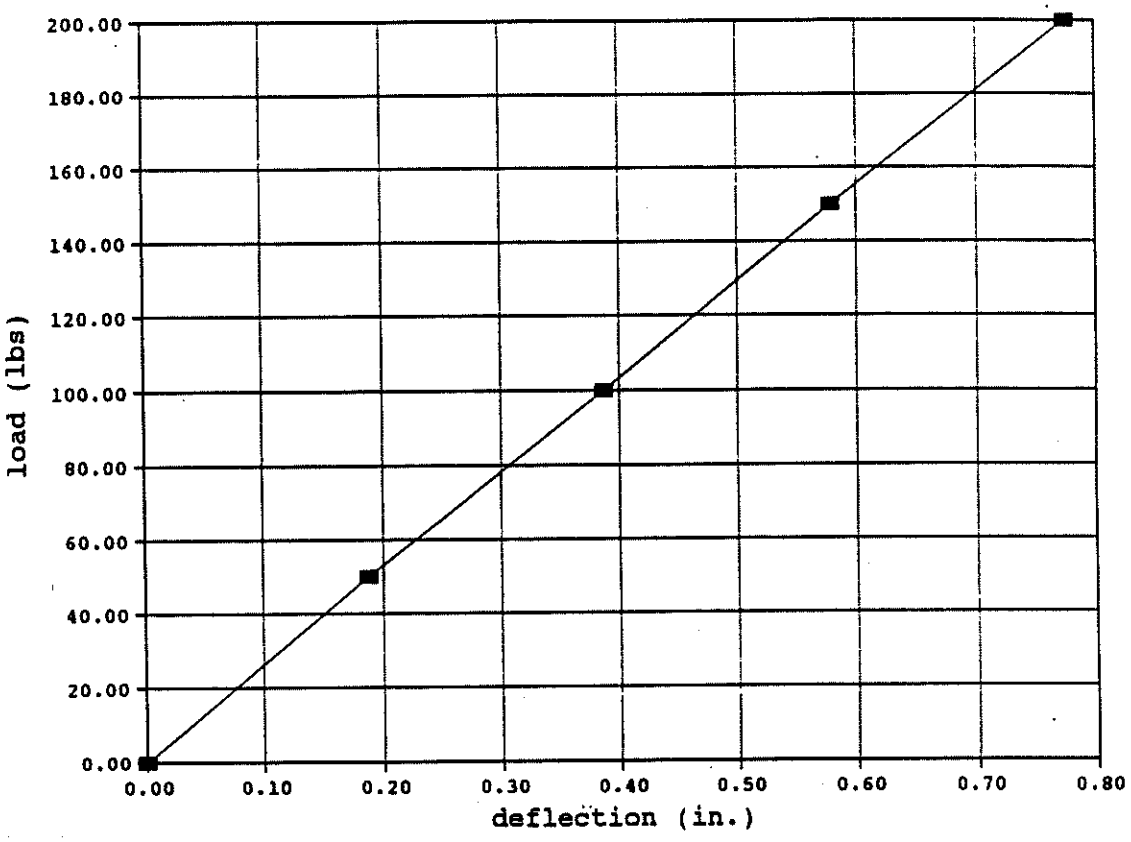

Figure 5.2: A Typical Load-Deflection Curve for Lumber

the composite action of the structures. Goodman [9] developed an equation for describing the relationship between interlayer slip and lateral load. It is based on fitting the equation to the load-slip curve from slip tests. Patterson [8] extended the equation to reflect the results of slip tests from 128 specimens. These specimens were made in lumber and plywood connected by nails. Several different kinds of lumber and plywood were used in that tests. The results of that experimentation were utilized by Kuo [32] and Tremblay [6] in their studies of slip moduli. In Patterson's report, the slip modulus values were determined using both the secant and tangent modulus concepts. The secant and tangent modulus values (KS and KT, respectively) were determined at loads equaling to 25, 50, 100, and 150 lbs (KS25 to KS150, KT25 to KT150).

In chapter 4, the secant slip modulus of connectors between concrete and wood was determined at a slip equal to 0.015 in.. In Patterson's report, the load-slip curves from experiments were matched by the equation

$$\Delta = C_1(e^{C_2F}) + C_3(e^{C_4F} - 1) + C_5(e^{C_6F} - 1) \tag{5.6}$$

where

Δ = deformation,

F = load, and

$C_1, C_2 ... C_6$ = constants.

Goodman assumed $C_2 = 0.01$, $C_4 = 0.002$, $C_6 = 0.0002$. The other three unknown constants (C_1, C_3, and C_5) are obtained by taking the deformations corresponding to three load levels along the experimental load-slip curve. The slip moduli that were used in Patterson's report were selected by obtaining equation 5.6 for the tangent of the load-slip curve or the secant to the curve at a chosen load level. In order to get the secant modulus at slip equaling to 0.015 in. from Patterson's laboratory results, the experimental results from Patterson's report were reanalyzed.

In Patterson's report [8], the slip modulus was determined from specimens with two nail-holding interfaces. The number of nails for each interface was varied. From the results of test, the unknown constants in equation 5.5 can be determined by taking the deformations corresponding to load levels along the load-slip curve. Two lateral load direction, parallel to grain and perpendicular to grain were discussed in that report. The parallel load direction is similar to the condition that used for T-beam bending test in this study. In Patterson's research, the unknown constants (in Equation 5.6) had been determined for each specimen. Therefore, the relation of load and slip can be represented by the equations. From these equations of the load-slip relationship, the load level corresponding 0.015 inch slip can be determined. In order to match the characteristics of the T-beam specimens in this study, the results of the specimens subjected the load that was parallel to grain were selected from Patterson's report.

The average slip modulus at 0.015 inch slip from 58 specimens that were subjected to parallel load was calculated to be 12397lbs/in.. The average slip modulu at 0.04 inch slip was 6286 lbs/in..

CHAPTER 6

EXPERIMENTAL RESULTS

INTRODUCTION

In order to analyze the behavior of mixed material T-beams, two primary works have been done in this study. One is the observation of the actions of 3-layer T-beams in the bending tests that was described in chapter 3. The other work is to compute the theoretical results for the behaviors of layered T-beams from the mathematical model based on computer program FEABEA. The mathematical model was presented in chapter 3.

Before the discussion of the behaviors of 3-layer T-beams, one important property of the T-beam system has to be clarified. It is the slip modulus of connection between the two interlayers of the T-beam specimens.

Slip modulus is one of the critical factors that affect the interlayer actions of composite structures. In past studies, the slip modulus of interlayer between two wood layers has been discussed and determined in experiments. In this study, the interlayer actions occur in three layer systems with two dependent interlayers actions. From the slip tests described in chapter 4, the basic characteristics of the slipping action of different type connectors between concrete and wood were observed. The discussion of the slip modulus of nail connectors between concrete and wood is presented in section 6.2.

For the 3-layer mixed material T-beams in this study, 10d common nails were used to connect the three layers together. The degree of composite action of one interlayer affects the action of the other interlayer. Therefore, the slip modulus of the two interlayer connections are interrelated, so the slip modulus of the connection in the 3-layer T-beams in this study cannot be determined from a test that only involved the interaction between two layers. Because

the nails are continuous material through the three layers, a precise analysis of the type of connection has to consider the transmission of internal forces in nails. This concept makes the behavior of whole systems much more complicated. In this preliminary study, the slip moduli at each of the two interlayer connections are assumed to be independent of each other, then these two interfaces can be assumed to be connected by individual nails.

In this chapter, the experimental behavior of slipping action of a single-interface nail connection between concrete and wood members is presented. The former discussion of the slip modulus used in the 3-layer T-beam is presented in chapter 7.

The bending test set-up used in the T-beam specimens is a simply supported beam subjected to two concentrated loads at the third points. The deflections and slipping actions represent the external behaviors of layered structures. The theoretical values of deflection and slip also can be predicted from the mathematical model derived for FEABEA. The comparison of experimental results and the theoretical values is discussed in chapter 7. The results of the mixed material T-beam tests are discussed in section 6.3.

THE RESULTS OF SLIP TESTS

An accurate determination of the mechanical properties of structures is the first step needed to build a mathematical model. Some special properties such as slip modulus involve very complex interaction of several materials. As the discussion in chapter 5, the slip modulus is defined as the tangent to the load-slip curve at specified load level or the appropriate secant modulus. The MOE of connected materials, the properties of connectors, and the geometry of the connection all are important factors that affect the slip modulus of connection. In slip tests that were presented in chapter 4, the selected variables were the penetrations of the nail in the main members of specimens, the types of nails, and the age of concrete.

In addition to the slip modulus of connectors, the ultimate loads of the interlayer connection also are important in the design requirements. From the load-slip curves (Figure 6.1), when the lateral load reaches the ultimate load the interlayer slip increases without the lateral load

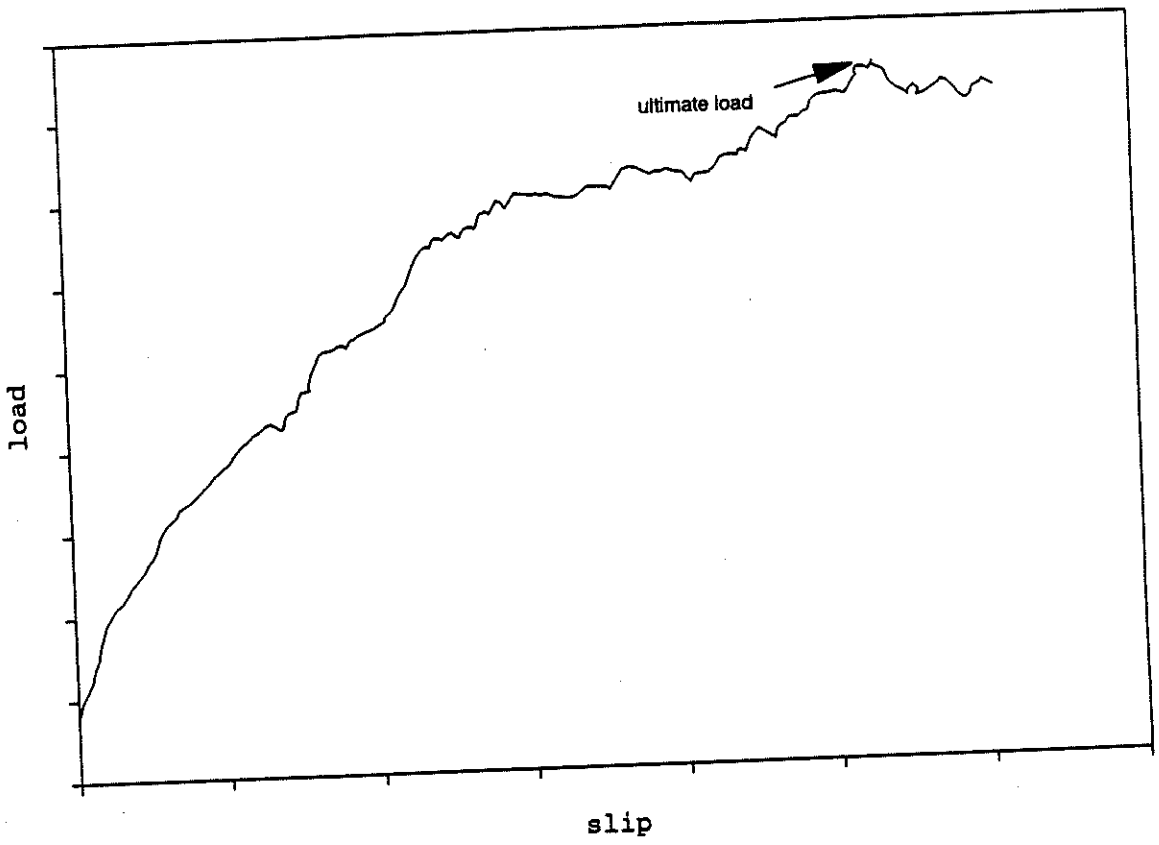

Figure 6.1: An Example of The Ultimate Load of Slip Test

increasing further. The average of ultimate loads and the appropriate secant modulus at slip equaling 0.015 (K15) and 0.04 (K40) inch for all specimens in eight types of connectors and in two selected ages of concrete are listed in Tables 6.1-6.4.

Nails are the most commonly used connectors in light-frame wood structures. For the different applications, nails are made in the different dimensions and appearances. In this study, only four types of nails were used to analyze the connector behaviors. As stated earlier, they are 3.5 inches long, doubleheaded, 8d, 10d, and 20d common nails. These four kinds of nails were used to configure 8 types of connection conditions as presented earlier in Table 4.1.

In the slip test specimens, the nails are penetrated into wood members so as to be perpendicular to the interface with concrete members. The penetrations of nails are different for each type of connection. When the wood main member and concrete side member were pulled to move in opposite directions, the nail is loaded by shear. If the frictional resistances of the interlayer between two members are neglected, the nails are the only materials to undertake the lateral load. Thus, the nail stiffness affects the amount of slip of the specimens. The nails are not the only deforming material in the specimens. The concrete members and wood members also deform due to the bearing of the nails against them.

From Table 6.1, the average ultimate lateral loads of the specimens that were connected by the same kind of nail distribute in a small range, even when the penetrations of nails are different.

Two different ages of concrete, 14 days and 28 days, were studied in slip tests. The compressive strength of concrete does not change greatly, when the concrete is cured for 28 days. From equation 5.1, the compressive strength of concrete of 14 day age is about 12% less than the concrete of 28 day age.

In Table 6.1, the average slip moduli of the specimens of 28 day age are greater than those of the specimens of 14 day age in the same type of connection. The difference in the slip modulus values for specimens of 28 day age and 14 day age are not in regular ratio. Therefore, the concrete strength would not be the only factor that affects the slip modulus of the connection,

Table 6.1: The K15 and K40 Values of Slip Test Specimens of 28 Day Age

Type	K15 (lbs/in)				K40 (lbs/in)			
	A	B	C	ave.	A	B	C	ave.
1	11502	8130	20545	13390	12812	10005	21348	14722
2	13972	17663	15994	15860	12900	16170	12380	13816
3	22034	23096	—-	22565	13600	12839	—-	13220
4	6811	10249	16744	11268	6173	6606	9950	7576
5	9513	16114	—-	12814	10540	11354	—-	10947
6	15053	19850	10908	15270	12950	12496	8005	11150
7	14158	12957	—-	13557	9665	9320	—-	9492
8	15774	15733	28461	19989	12805	9559	13431	11932

Table 6.2: The K15 values of slip test specimens of 14 day age

Type	K15 (lbs/in)						
	A	B	C	D	E	F	ave.
1	14487	5420	14293	11965	12306	—-	11694
2	10198	3557	24584	17179	4324	—-	11969
3	6429	12045	9731	10651	13629	12216	10784
4	10002	10027	8652	3192	14851	5677	8733
5	12370	15357	9419	12870	14641	9988	12441
6	14782	10471	10367	8983	11136	6397	10351
7	6415	8673	8764	14100	15530	7988	10245
8	12973	10280	10224	3288	8803	—-	9114

Table 6.3: The K40 values of slip test specimens of 14 day age

Type	K40 (lbs/in)						
	A	B	C	D	E	F	ave.
1	13712	5038	13445	12313	10698	—-	11026
2	9156	10515	19540	13744	6378	—-	10552
3	6146	7396	7216	9628	8862	8058	7884
4	8587	7537	6840	3203	9693	5243	6851
5	11248	13770	8868	12017	10548	9651	10934
6	12543	7388	9804	8619	9268	6051	8962
7	6248	7132	5272	11570	11171	6739	8022
8	14700	8329	6620	4281	7874	—-	8361

Table 6.4: The Ultimate Load and Slip Modulus Obtained from Slip Tests

connection type	age (days)	No. of specimens	ave. ultimate load (lbs)	ave. modulus K15 (lbs/in.)
1	14	6	1192	11694
	28	3	1130	13390
2	14	6	1290	11969
	28	3	987	15860
3	14	6	730	10784
	28	3	797	22565
4	14	6	843	8733
	28	3	653	11268
5	14	6	1077	12441
	28	3	1010	12814
6	14	6	1087	10351
	28	3	810	15270
7	14	6	883	10245
	28	3	767	13557
8	14	6	934	9114
	28	3	780	19989

but it should be an important factor. Comparing the influence of the nail types and the strength of concrete to the slip moduli, the strength of concrete affects the values of the slip modulus and the types of nails is reflected in the ultimate loads of connections. These phenomenon may reflect that when the slip initiates, the major deformation occurs in the interaction of concrete, wood and nails. But when the amount of slip increases, the subsequent failing material is the nail.

In a slip test specimen, the nail head is embedded in the concrete side member and the shank of the nail penetrates into wood main member. After testing, in order to observe the deformation of connector, the nails were pulled out of wood members. The typical deformation of a nail is shown in Figure 6.2. It appears that the only part of the nails that deformed is that which is close to the interface between wood and concrete members. The other portion of the nail that was embedded in the wood member was still straight. Because the nails were vertically penetrated in test specimens, when the slip occurs, the lateral load subjects the nails to shearing deformation. If the penetration of nails in wood members and the enclosed length in concrete member are long enough, the nails are not pulled out when the slip occurs. The necessary penetration length depends on the diameter and the surface condition of nails and the properties of the materials that enclose nails.

The slip modulus K15 of each type of nail in different penetration conditions has very similar values, except for the 6d nails. The 6d nails were used to make connection types 3 and type 4. The connection type 3 had 1.0 inch penetration in the wood member and 1.0 inch embedment length in the concrete. The type 4 connection was 1.5 inch penetration in the wood member and 0.5 inch embedment in concrete member. The slip modulus of 28 day old specimens in connection type 3 is almost triple that the K15 value of specimens in type 4. A possible reason is that the 0.5 inch embedment length of 6d nails in concrete is insufficient to prevent the nails from being pulled out of the concrete members.

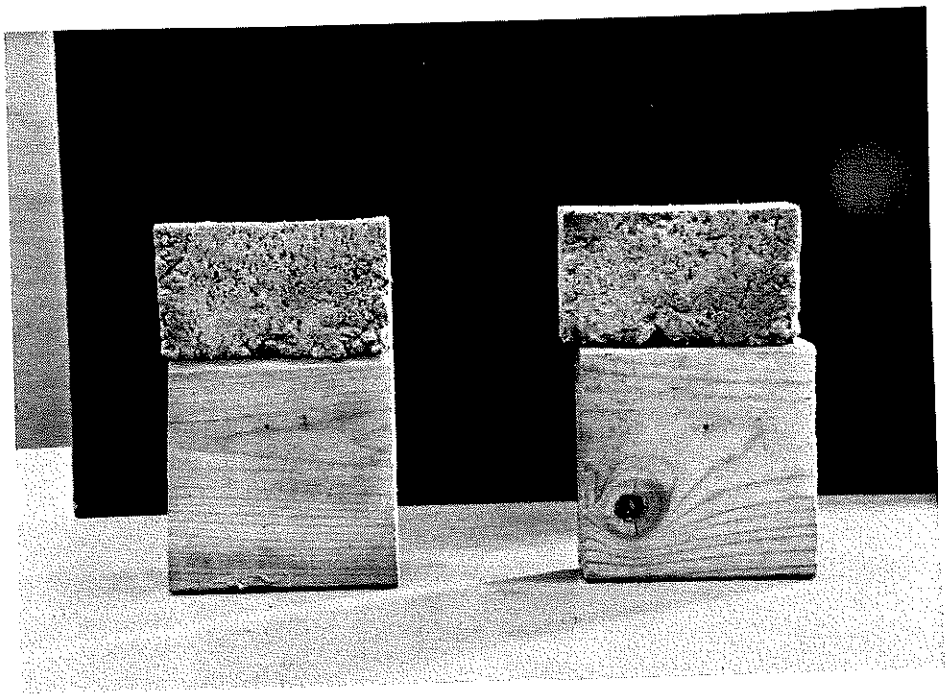

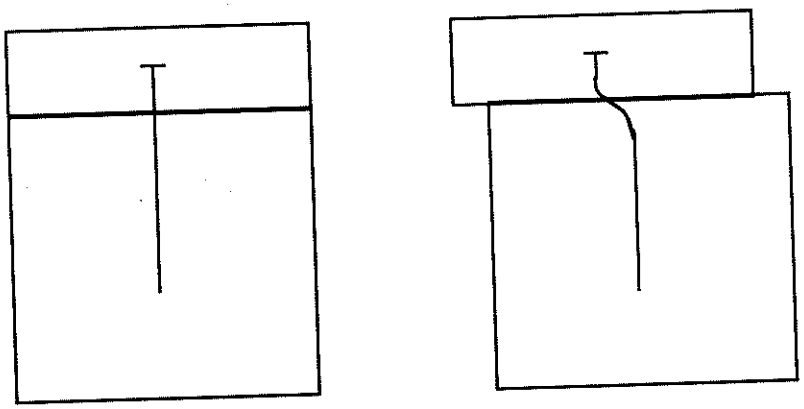

a) before test

b) after test

Figure 6.2: The deformation of a nail on slip tests

In the specimen casting procedure, the concrete cannot be uniformly arranged in concrete member, so vacant space may exist especially in the part touching the wood member. The actual holding length in concrete may be less than the expected amount.

The exact relation of penetration and slip modulus may not be determined from the slip test. The analysis of the exact relationship of slip modulus and embedded length need more precise tests and statistical analysis.

T-BEAM TEST RESULTS

The experimental behaviors exhibited by the T-beam specimens are the sources that are used to examine the accuracy of the existing FEABEA model. By comparing the data that were recorded from the conduct of the T-beam tests to the predicted results from mathematical model, the accuracy of the mathematical model can be studied. A carefully designed experiment and instrumentation can express the real action of specimens. Developing procedures to mathematically predict this real action is the information needed for structural design.

The basic response of a simply supported T-beam during loading is its deflection. The properties of the beam and the load level directly influence the deflection. For a layered beam, the interactions between layers create the composite action. The specimen deflection and the slip between layers were the two detectable variables that were measured in the tests.

The T-beam specimens used in this study were comprised of three layers. Of the three layers, the unit weight of concrete layer was much greater than the other two layers. The total weight of a 16-feet-long T-beam specimen was more than 500 lbs. When the specimens were placed on the testing frame, the specimens were immediately subjected to the distributed dead load. Thus, dead load deflection and slip also already existed before the concentrated loads were applied to the specimens. The subsequent loading of the specimen just took very short time (about 30 minutes), so the effect of creep and shrinkage was not considered. One other assumption has to be satisfied, namely, that the specimens were still in elastic condition before appling load.

Deflection of Specimens

As described in chapter 3, the four T-beam specimens were comprised of the same materials and dimensions. The differences in the four specimens configurations are the spacing of nails and the location of open gaps. Specimen 1 was used to adjust the loading systems and slip measuring locations, so the data of the test results of specimen 1 were used for reference. The comparison of the behavior of specimens was focused on specimens 2-4.

The specimen 2 differed from specimen 3 in the locations of gaps. In specimen 3, one open gap was at the midspan of the plywood layer. Specimen 2 had two open gaps in the plywood located 4 feet from each end. The spacing of nails for these two specimens was 6 inches. Theoretically, the average force along a unit length of the interlayer is the same value for these both specimens when they are subjected to the same amount of load.

From the Table 4.1, the MOE of the lumber joist of specimen 3 is greater than that of specimen 2, and the MOE of plywood layer of these two specimens are similar. Thus the specimen 3 should be stiffer than specimen 2, if the existence of gaps is neglected.

Observing the deflections of these two specimens (Figure 6.3), when the two concentrated loads were less than 300 lbs, the deflection of specimen 2 was smaller than for specimen 3. For loads above about 250 lbs, the situations reversed. When the loads increased, the deflections of specimen 2 increased faster than specimen 3. The configuration of specimen 1 is similar to specimen 3. Referring to the deflection data, the relative behavior of specimen 1 and specimen 2 is very similar to the relative behavior of specimen 3 and specimen 2.

The open gaps that existed in the plywood layer of specimens were only about 1/16 inch long. When they are at the midspan of beams, they make the beams deform noticeably at low load levels. But after the deflection of the T-beams increases, the slip between layers also increases. The average force along the interlayer becomes greater. On comparison, the stiffness of the beam increases. Therefore, the effect of the locations of gaps to the deflection of the T-beams is particularly significant in the low load levels.

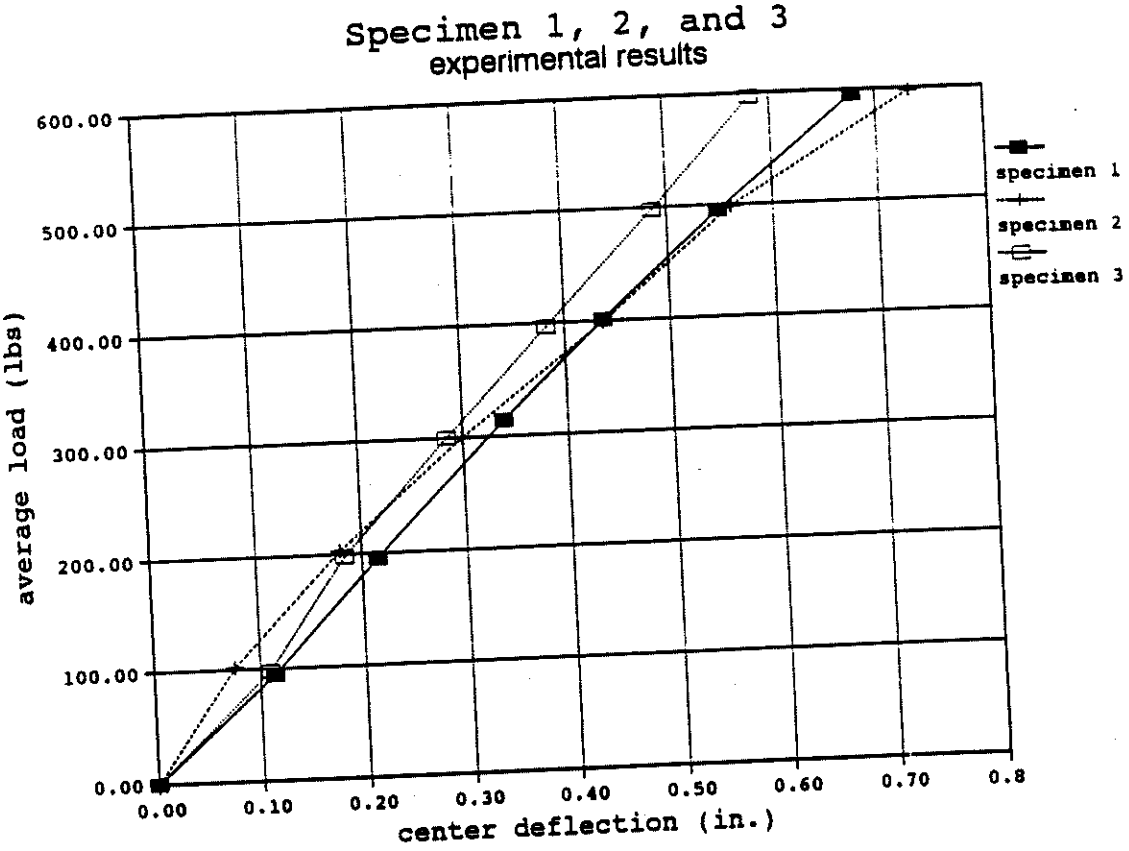

Figure 6.3: Comparison of The Experimental Results of Specimens 1, 2 and 3 on Deflection

In order to increase connection rigidity, specimen 4 was built with a nail spacing equal to two inches as compared to six inches for the previous specimens. The locations of gaps for specimen 4 are the same as in specimen 2. Therefore, the connection rigidity of specimen 4 is triple that of specimen 2, and the other properties of these two specimens are similar. Comparing the deflection of the specimen 2 and 4 at the same load level (Figure 6.4), the ratio of the deflection of specimen 2 to that of specimen 4 range from 1.42 to 1.92. The average ratio is 1.74, so the increasing connection rigidity makes the stiffness of specimen increase about 74%. The detailed effect of the slip modulus to the flexural stiffness of T-beams are discussed in next chapter.

Although the properties of the lumber joists were considered as isotropic, the actual condition of lumber is not uniform, especially close to knots. Except for specimen 3, the T-beam specimens all failed at a lumber layer knot. Failure modes were typical tension failures at the position close to midspan. No significant damage to plywood and concrete layers was realized. When the first crack occurs in a specimen, the deflection of the specimen increases rapidly without increasing loads.

Specimens' Slip

Except for specimen 1, the specimen slip was detected by dial gages placed in six locations that were symmetric to the center line of the beam (Figure 4.8). For specimens 1 and 3, the recorded slip values at some locations stayed at essentially zero until the loads increased to their higher limits. These zero slip values occurred only between the interlayer of concrete and plywood. The area of the interface of concrete layer and plywood layer in a specimen is much larger than the interface of plywood layer and lumber layer. The locations for measuring the slip were on the side of T-beams but not exactly at the connector locations (Figure 4.9), so the measured slip values of the interlayer between concrete and plywood layers do not represent the slipping action of the connection. On the other hand, the measured slips between plywood

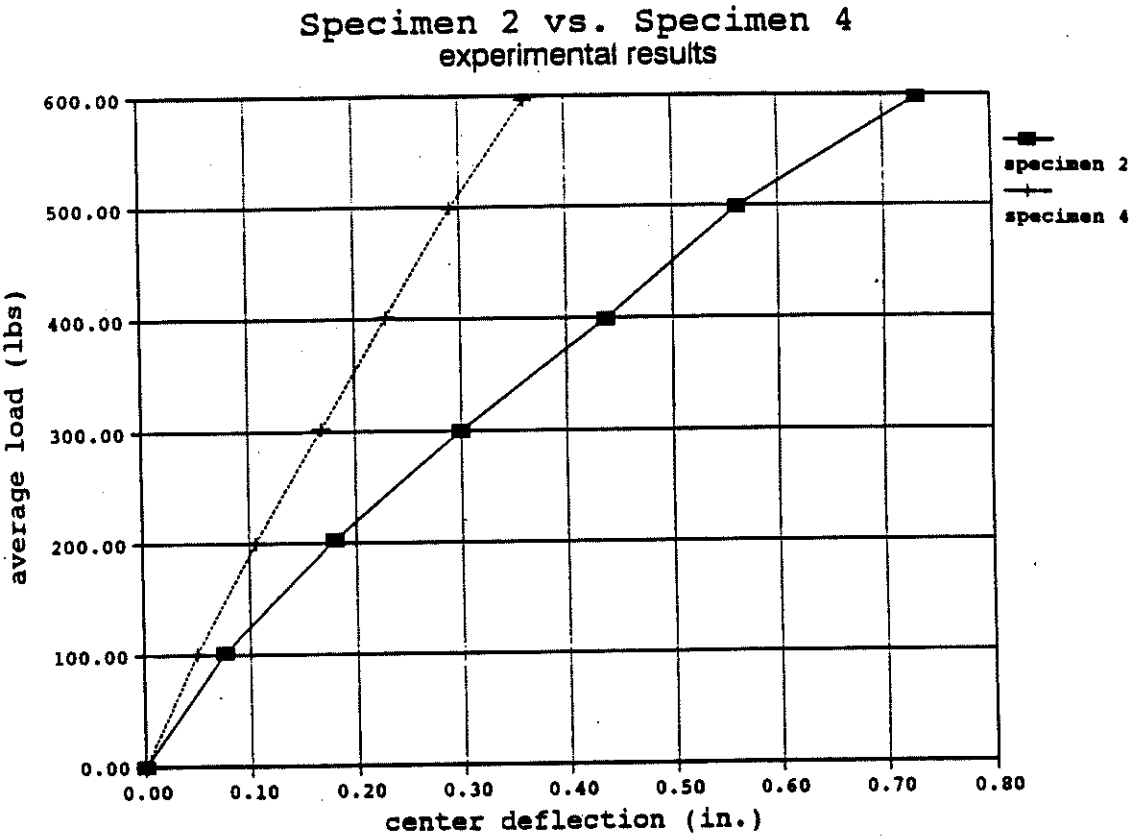

Figure 6.4: Comparison of The Experimental Results of Specimens 2 and 4 on Deflection

and lumber layers are more reliable for expressing the behavior of interlayer connections. The relation of slip and load from the result of test were presented by graphs in Appendix B.

Similar to the discussion in preceding subsection, the interlayer slip of specimens 1, 2, and 3 were compared. The slip of specimen 2 was much greater than specimens 1 and 3 (Figure 6.5). The existence of two open gaps in specimen 2 allowed the plywood layer to move more in that specimen. In addition, the two gaps of specimen 2 were on the locations 4 feet from each end. The interlayer slip at these two locations theoretically is greater than that at midspan. When the nail spacing decreases, the rigidity of the interlayer connection increases. Specimen 4 has the one third nail spacing of specimen 2. The ratio of these two specimens' slip is also about 1:3 after the loads were beyond the 200 lbs level (Figure 6.6). Theoretically, the force that nails are subjected to is to the interlayer slip. The interlayer slip of specimen 2 is triple of specimen 4 and the interlayer rigidity of specimen 2 is one third of specimen 4, so the nails of these two specimens were subjected to very approximate shearing force at the same load level.

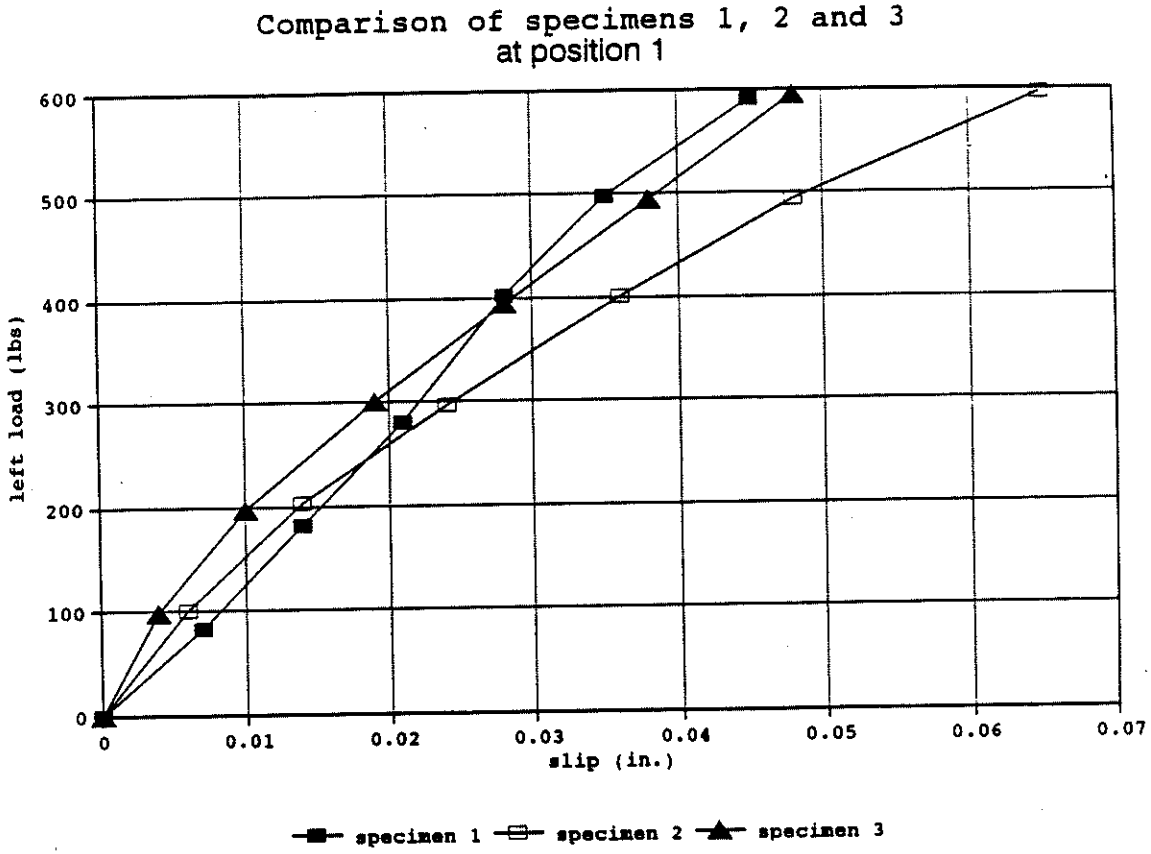

Figure 6.5: Comparison of The Experimental Resluts of Specimens 1, 2 and 3 on slip

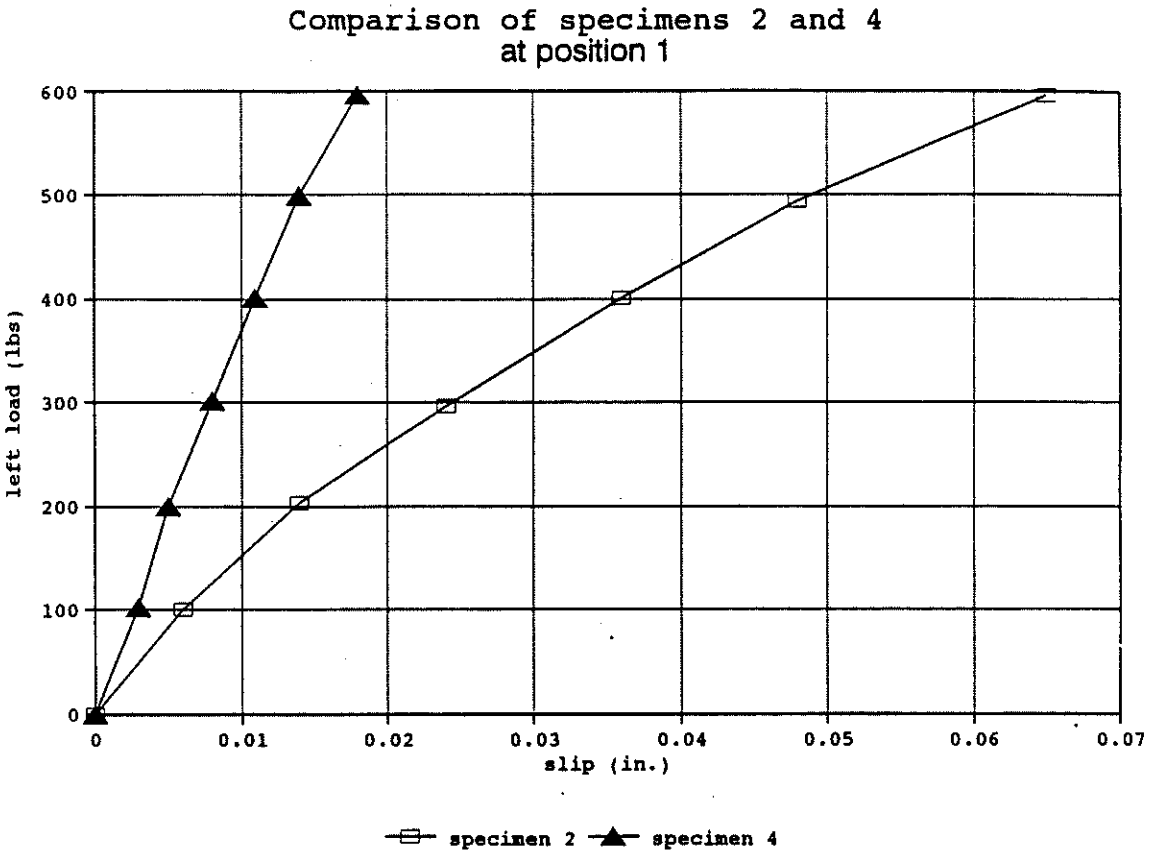

Figure 6.6: Comparison of The experimental Results of Specimens 2 and 4 on Slip

CHAPTER 7

VERIFICATION OF THE MATHEMATICAL MODEL

INTRODUCTION

The material properties used in mathematical model were discussed in chapter 5. The MOE of concrete, plywood, and lumber can be determined from the simple tests discussed earlier. One deficiency is that the slip moduli of two interlayer connections cannot be determined from the usual slip tests. The information about slip modulus from the slip tests in this study and from past researches only represented the approximate range of the slip modulus.

The MOE of concrete of all specimens are based on equations 5.1 and 5.3. The difference of the MOE of concrete reflects the different age of the specimens. The age of the four specimens were 40, 36, 33, and 26 days. The specified compressive strength of concrete at those ages for the four specimens are close (2637, 2607, 2580, and 2496 psi), so the influence of the age of concrete is negligible.

The MOE of the lumber joist for each specimen was assumed to be constant along the beam. In the bending test for determining the MOE of plywood and lumber, each small specimen extracted from undamaged portion of T-beam had a different value of MOE. In computer program FEABEA, a T-beam specimen is divided into 31 (one gap in the plywood layer) or 32 (two gaps in the plywood layer) elements (Figure 7.1), and each element was given the same value of MOE for each specimen. The value of MOE is the average of all small specimens for the particular beam. Similarly, the properties of plywood were assigned the same value for every complete plate. The MOE values used in mathematical model were listed earlier in Tables 5.1a,b.

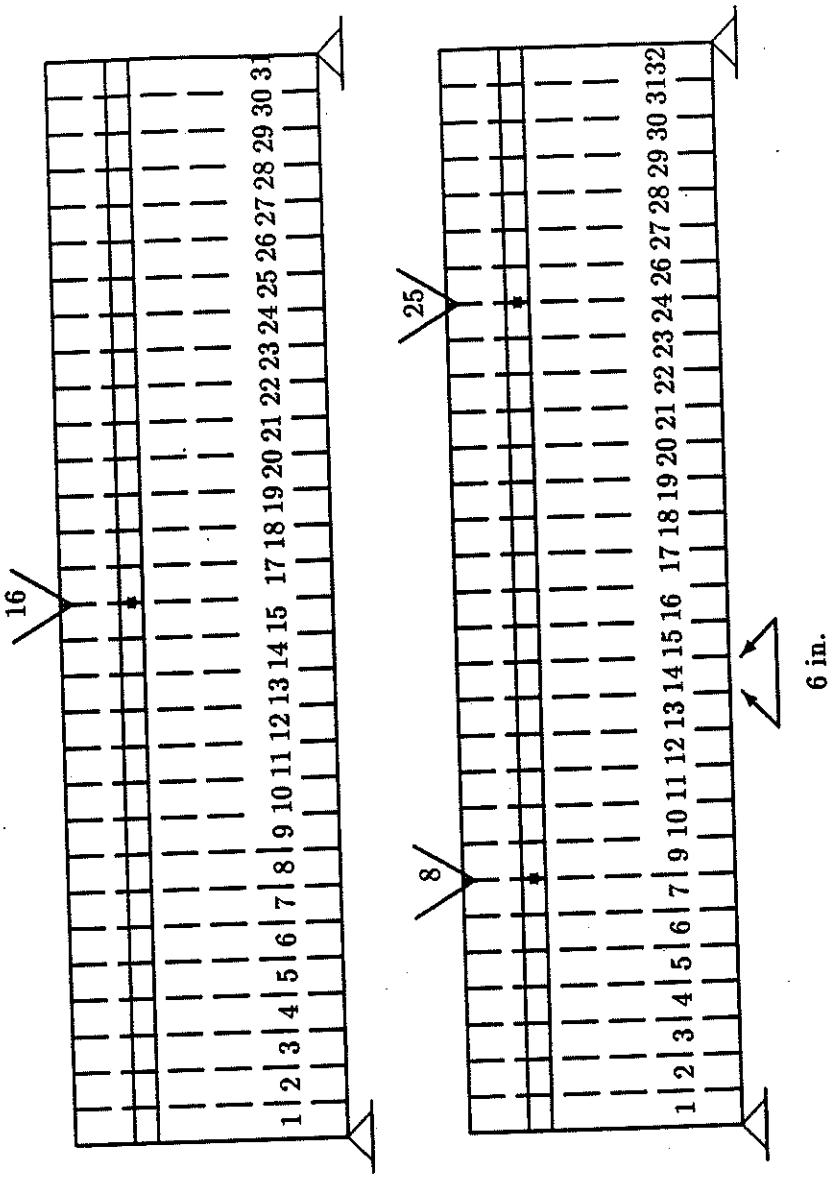

Figure 7.1: Discretization of The T-Beam Specimens

In the T-beam bending tests, 10d nails were used as the connectors. In accordance with the slip test data, the slip modulus, K15, of this type of nails for 28 day age are from 15730 to 28400 lb/in. The average value is about 20000 lb/in. From Patterson's report [8], the average value of approximate secant slip modulus, Kpl, of nail connection between plywood and dimension lumber at a slip equaling 0.015 inch is about 12000 lb/in (the range is from 9400 to 16300 lb/in.). If the assumption that the slip modulus of the same connector on each of two interfaces are independent can be recognized, the slip modulus of the two interlayer connection can be specified as two constant values. By the earlier discussion, the slip modulus of connection between concrete and plywood is selected as Kcp=20000 lb/in. A value of Kpl=12000 lb/in is used as the other interlayer slip modulus between plywood and lumber joist, based on the experimental results of Patterson's report.

For the gap problem, three different methods were used to compare the effect of gaps to the mathematical model. The first method is to neglect the existence of gaps. The other two methods, as discussed in chapter 3, are to use a special element with zero length or a small element with low a value of MOE.

THE EFFECT OF GAPS AND SLIP MODULUS IN MATHEMATICAL MODEL

Before computing the theoretical values of deflection and slip for the mixed material T-beam, three effects require discussion. The influence of slip modulus on the stiffness of layered beam, the effect of dead load on the deflection and slip, and the effect of gaps are three pertinent subjects in layered structures. The properties of T-beam specimen 1 are used to discuss these three subjects.

For a three layer T-beam with the three layers placed freely together, the moment of inertia for the plywood layer is only 0.1 % of the moment of inertia for the whole section. Thus, when the interlayer connection does not exist, the stiffness of a two layer T-beam comprised of concrete and lumber layers would be very similar to a three layer T-beam (Figure 7.2a). By comparing

the load-deflection curve for two layer model and three layer model by program FEABEA in Figure 7.2, the effect of the existence of plywood layer varies when the slip modulou values of the interlayer of two layer T-beam and the both interlayers of three layer T-beam change. When there is no connection between layers, the stiffness of beams does not increase much due to the plywood. When the slip modulus is not very large (less than 10000 lb/in) for each interlayer connection, the incomplete composite action makes the three layer T-beam deflect more than two layer T-beam. When the rigidity of the connection for interlayers increases to a very large value (K = 10^8 lb/in), the moment of interia of three layer beam becomes significantly greaterthan that of two layer beam. Therefore, the stiffness of three layer beam will greater than that of two layer beam. Thus, the stiffness of three layer beams is not always greater then that of two layer beams. The rigidity of the interlayer connection is the determinant. Therefore, when the slip modulus of the two interlayer is less than 10000 lb/in, the existence of a plywood layer makes the T-beam specimen less stiff than the T-beam only composed of concrete and a lumber joist. This effect in laminated structures is very important for selecting interlayer connectors.

By the discussion in chapter 4, the existence of gaps is unavoided. Therefore, the problem of gaps needs to be examined in FEABEA model. In Figure 7.3, when the slip moduli of two interlayers change, the effect of gaps on the deflection changes. If the slip moduli have very high magnitude, the deflection of the T-beam with and without gaps are essentially identical. When one interlayer slip modulus is very small and the other slip modulus is between 10000 and 1000000 lb/in., the deflection of T-beam with or without gaps is obviously different. By the discussion in section 7.1, if the slip moduli were both selected as secant modulus at 0.015 inch slip, two slip modulus are both at the range between 10000 and 30000 lb./in. (Figure 7.4). Therefore, the greater is the slip modulus of interlayers, the more significant is the difference in deflection of the T-beams with and without gaps. In Figure 7.3, when a slip modulus is very small and the other slip modulus is about 100000 lb/in, the different of the two deflection is the greatest.

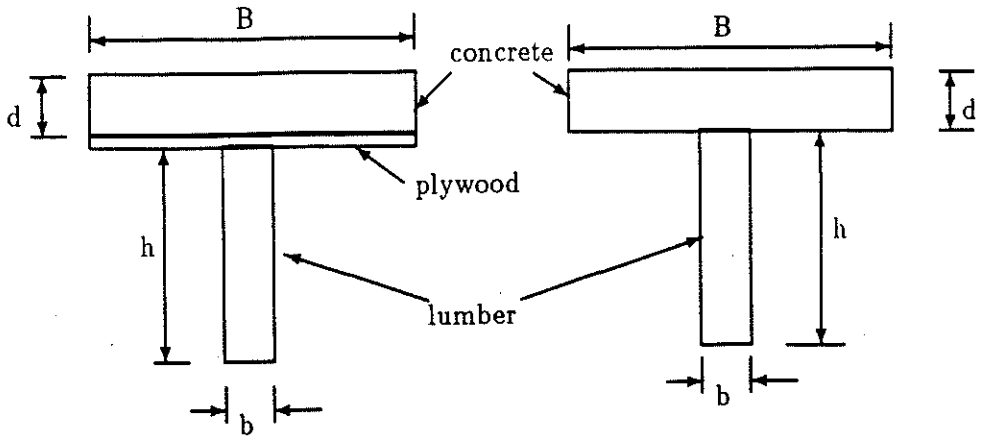

The cross section of concrete and lumber are the same for two layer and three layer T-beams.

Figure 7.2a: The Cross Section of Three Layer T-Beam and Two Layer(without plywwod) T-Beam

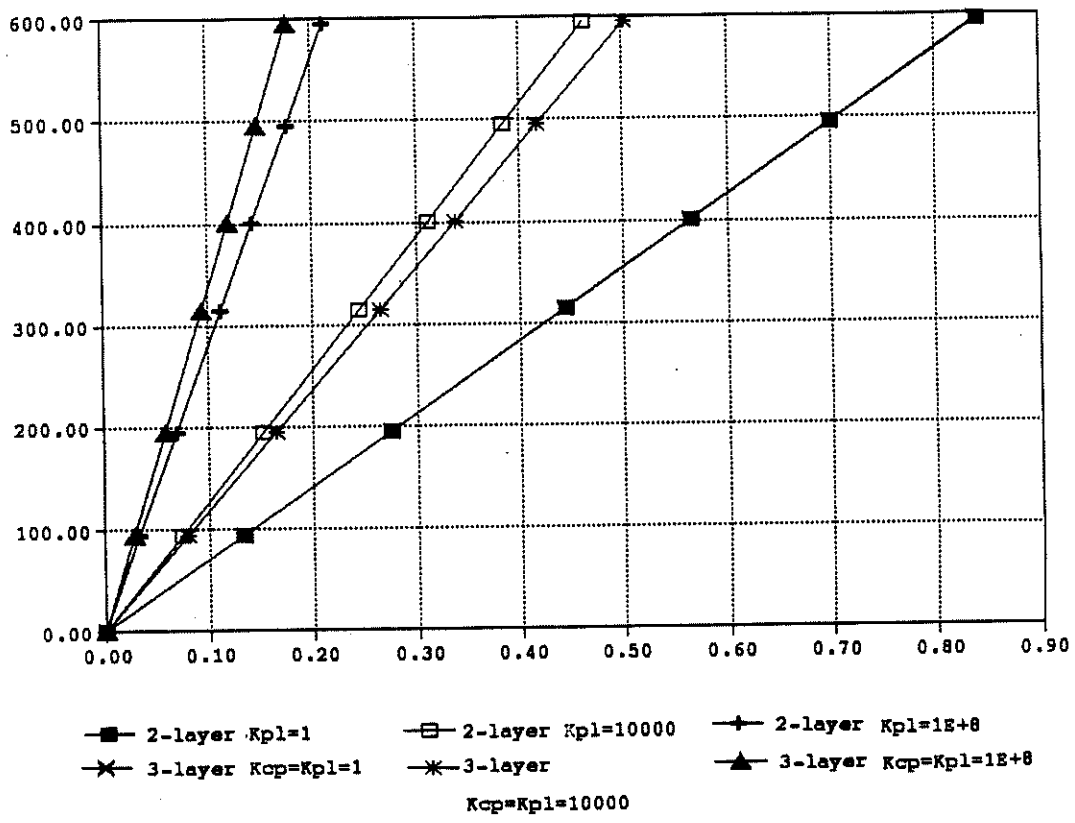

Figure 7.2: Comparison of The Deflection of Two Layer T-Beam and Three Layer T-beam

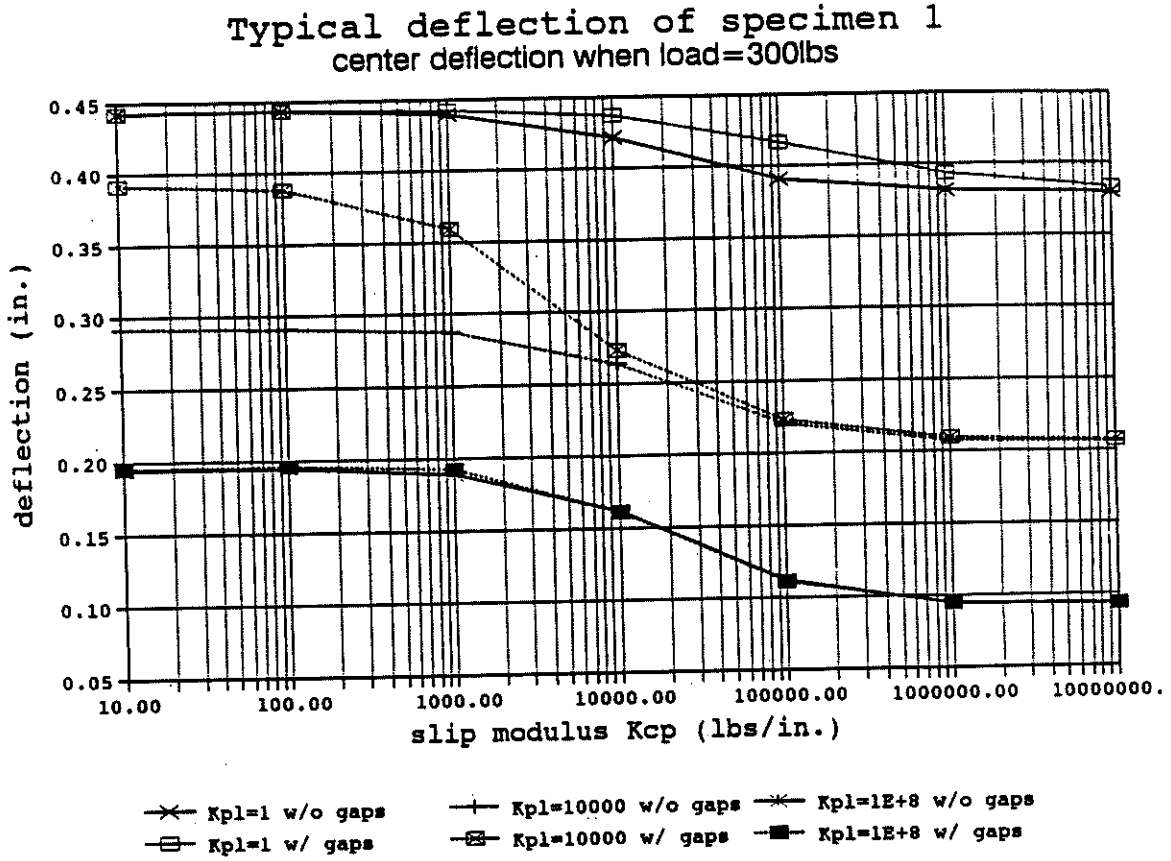

Figure 7.3: Comparison of The Effect of Gaps at Different Slip Moduli

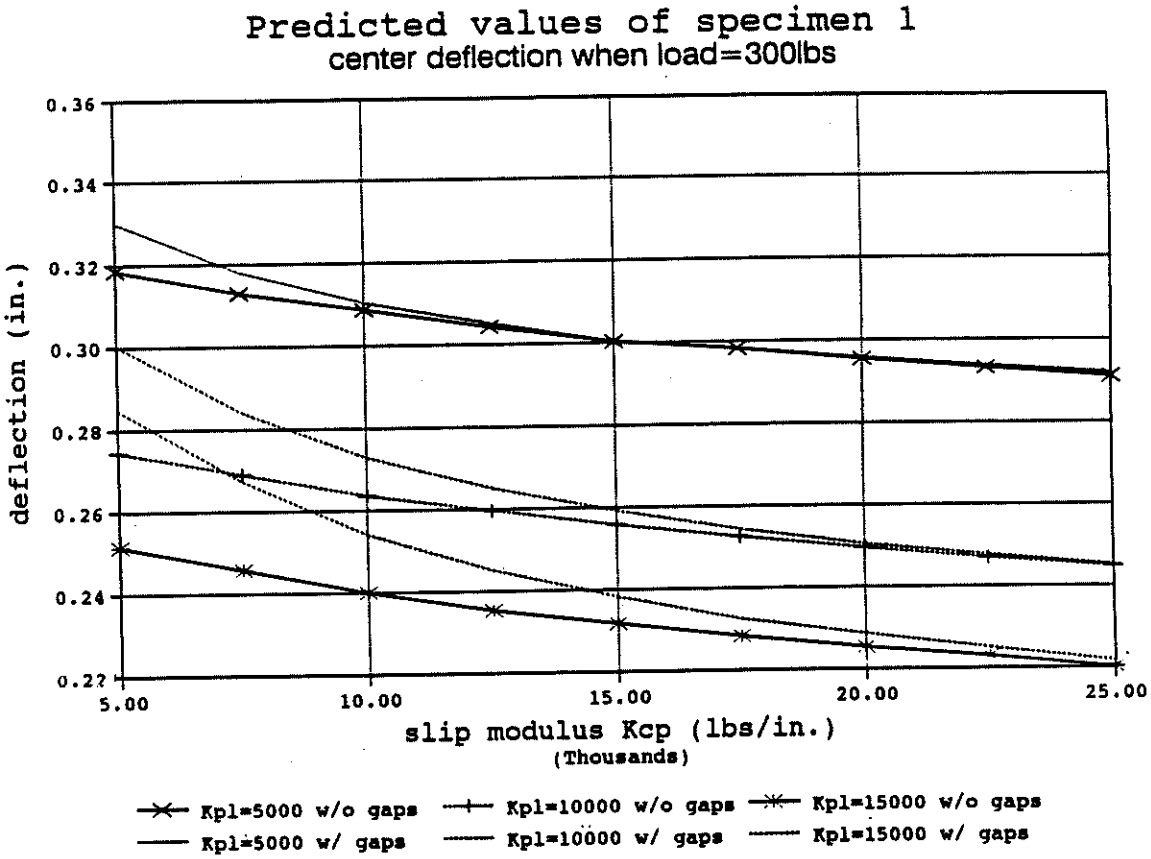

Figure 7.4: Comparison of The Effect of Gaps at Different Slip Moduli

Table 7.1: The Deflection and Slip of Specimens at Dead Load

	deflection (in.) at LVIT position			slip (in.) at dial gage position					
	left	center	right	1	2	3	4	5	6
1	0.15343	0.17621	0.15338	0.012	0.005	0.007	0.005	0.005	0.012
2	0.16019	0.18415	0.16019	0.012	0.005	0.010	0.010	0.005	0.012
3	0.13037	0.14973	0.13036	0.010	0.004	0.006	0.006	0.004	0.010
4	0.09599	0.11022	0.09599	0.006	0.003	0.006	0.006	0.003	0.006

The dead load of the mixed material T-beam in this study is about 500 lbs for each specimen. Most of the dead load is from the weight of concrete and it become a distributed load on the T-beam. Using the properties of specimens, the theoretical deflections are listed in Table 7.1. In section 5.3, in the tests for geting the MOE of plywood and lumber, the relation of deflection and load is almost linear for each specimen when the maximum deflection is not beyond 0.8 inch (Figure 5.3). so the amount of deflection may not significantly influence the elastic behaviors of T-beams in the bending tests. But, the slip amount at different positions on specimens 1, 2 and 3 have noteworthy difference that may affect the correction of selected slip modulus.

In Figure 7.5, the computed load-deflection results for specimen 1 for three different gap condition are shown. When gaps are neglected, the stiffness of beam is greater then the beams with gaps, but the difference between them is not significant. As noted in the earlier discussion, using slip modulus values of two interlayer connections equaling to 20000 and 12000 lb/in, respectively, cannot make the stiffness of three layer T-beam much greater than two layer (concrete and lumber) T-beam. In addition, the gaps occur in the plywood layer. The effect of these gaps on deflection in mathematical model is negligible. Comparing the two different techniques for handling the gap problem in FEABEA, the predicted values of these two methods are very similar.

On the other hand, the existence of gaps in FEABEA model affects the interlayer slip at the locations close to gaps. From Figure 5.1, the dial gage position 3 of specimen 2 is close to the location of gap at plywood layer, and the position 1 is near the left end of specimen 2.

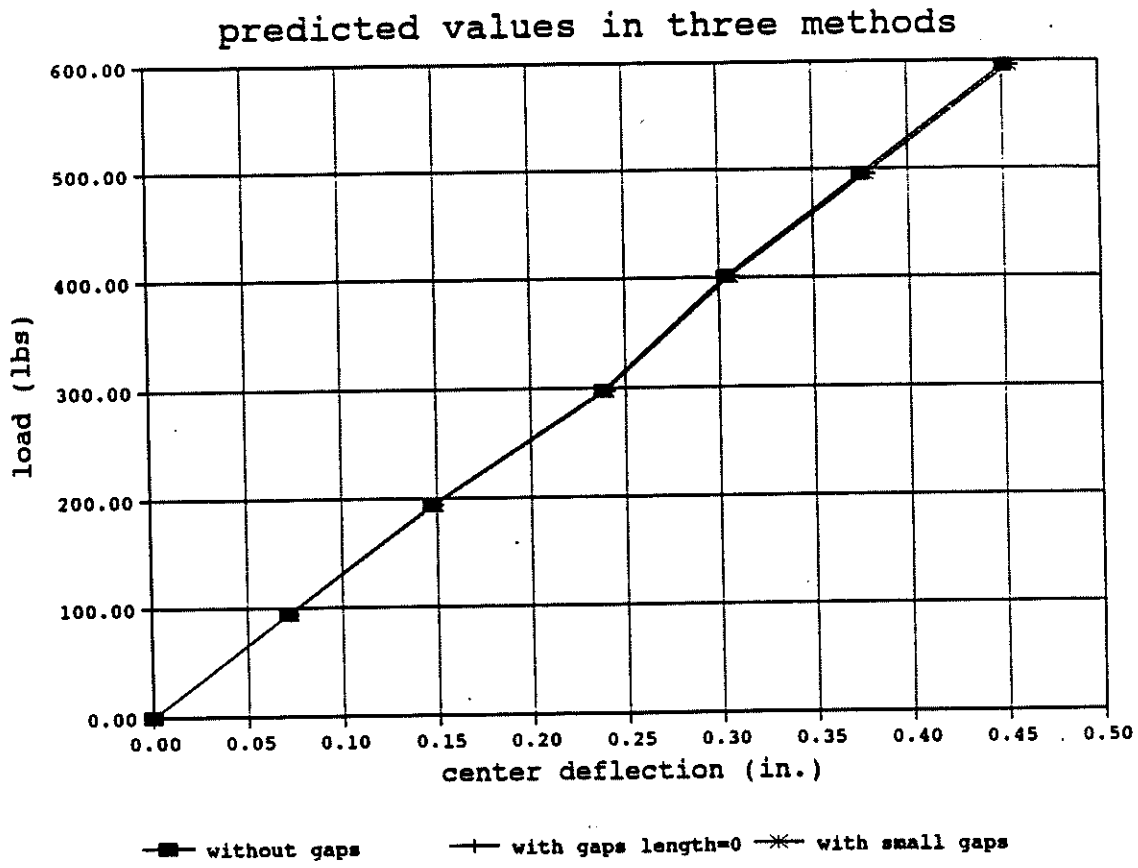

Figure 7.5: Comparison of Theoretical Values in Three Analysis Methods for Gaps

Computing by program FEABEA, when the gaps at plywood layer are included, the interlayer slip at position 3 is greater than when the gaps do not exist (Figure 7.6). At the position 1 of specimen 2, the effect of gaps to interlayer slip in FEABEA model is not significant (Figure 7.7). For T-beam specimen 3, the gap is located at the midspan of plywood layer, so the dial gage position 1 and 3 are not close to the gap. Therefore, the existence of this gap does not strongly affect the interlayer slip at position 1 and 3 in FEABEA model (Figures 7.8 and 7.9).

COMPARISON OF EXPERIMENTAL AND THEORETICAL RESULTS

Selected Slip Modulus K15

The predicted values from program FEABEA are compared to the experimental results in this section. The material properties of each T-beam specimen are only slightly different from one another. These differences in material properties will not apparently influence the comparison of the behavior of the specimens.

The values of material properties of specimens 1, 2, and 3 used in FEABEA are similar. The location of gaps is the only distinct difference. From the theoretical results of deflection of specimens 1, 2, and 3 (Figure 7.10), the deflection values of the three specimens are very close. Thus, the location of gaps are not very important in the theoretical results. Recall from section 7.1, that slip modulus values of the interlayer between concrete and plywood layer (Kcp) is 20000 lbs/in. and the slip modulus value of the other interlayer (Kpl) is 12000 lbs/in..

Nail spacing of specimen 4 is one third of the spacing in the other three specimens. Comparing the computed results for specimen 2 and specimen 4, the rigidity of the interlayer connection for the specimen 4 is triple that of specimen 2. The ratio of the deflections of these two specimens is about 1.75 (Figure 7.11), which matches the ratio observed in the laboratory test.

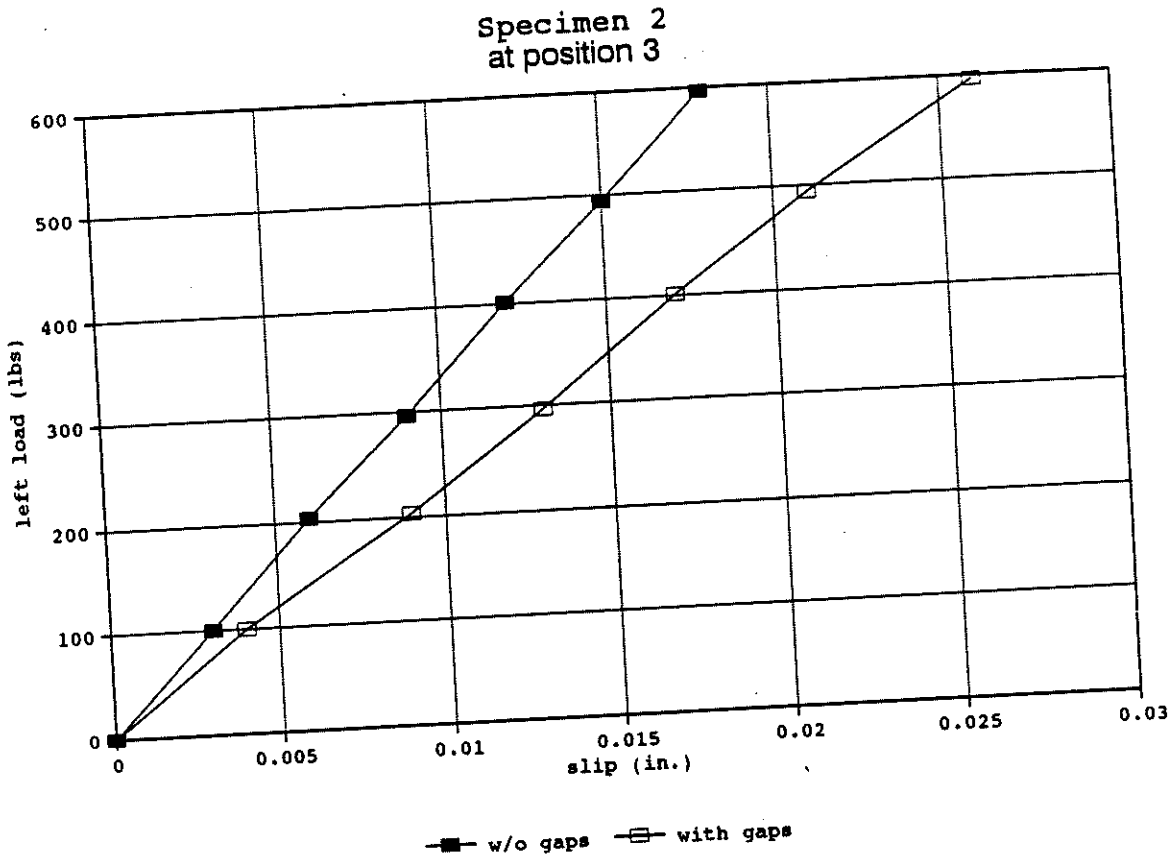

Figure 7.6: The Effect of Gaps on Slip

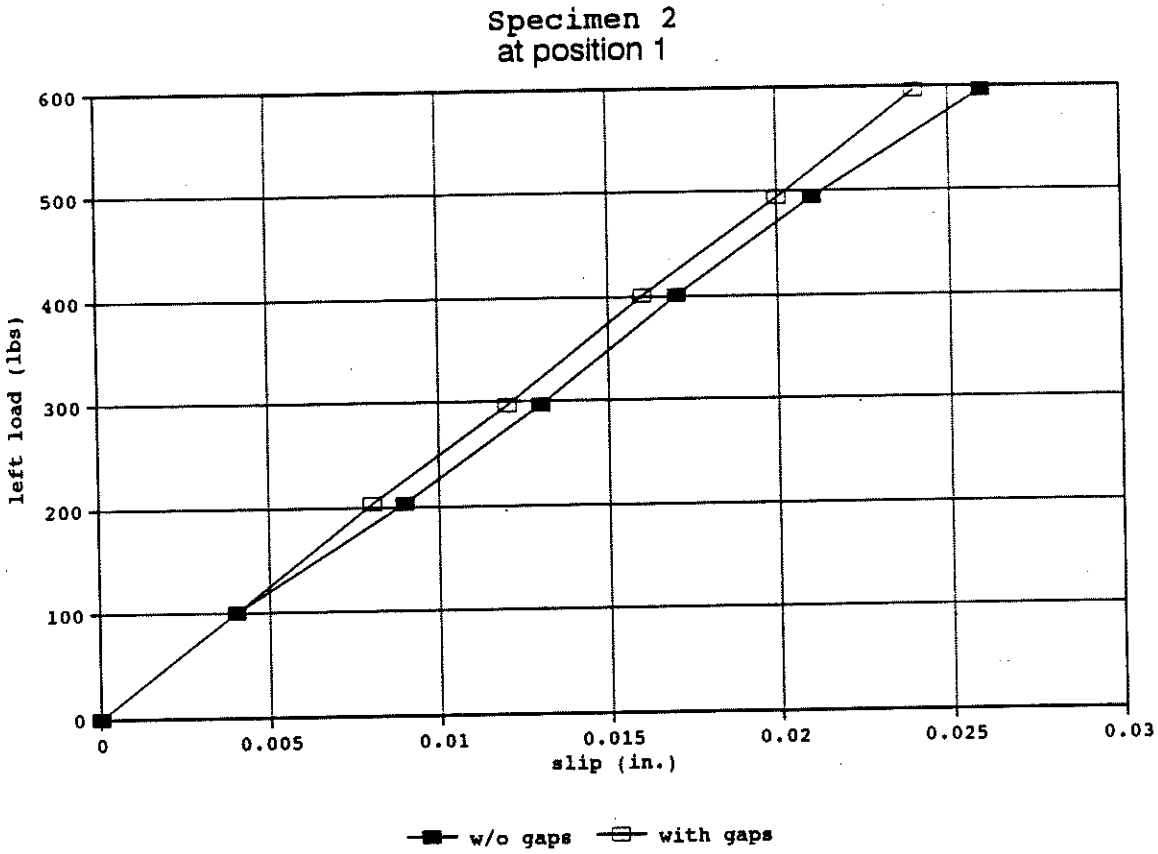

Figure 7.7: The Effect of Gaps on Slip

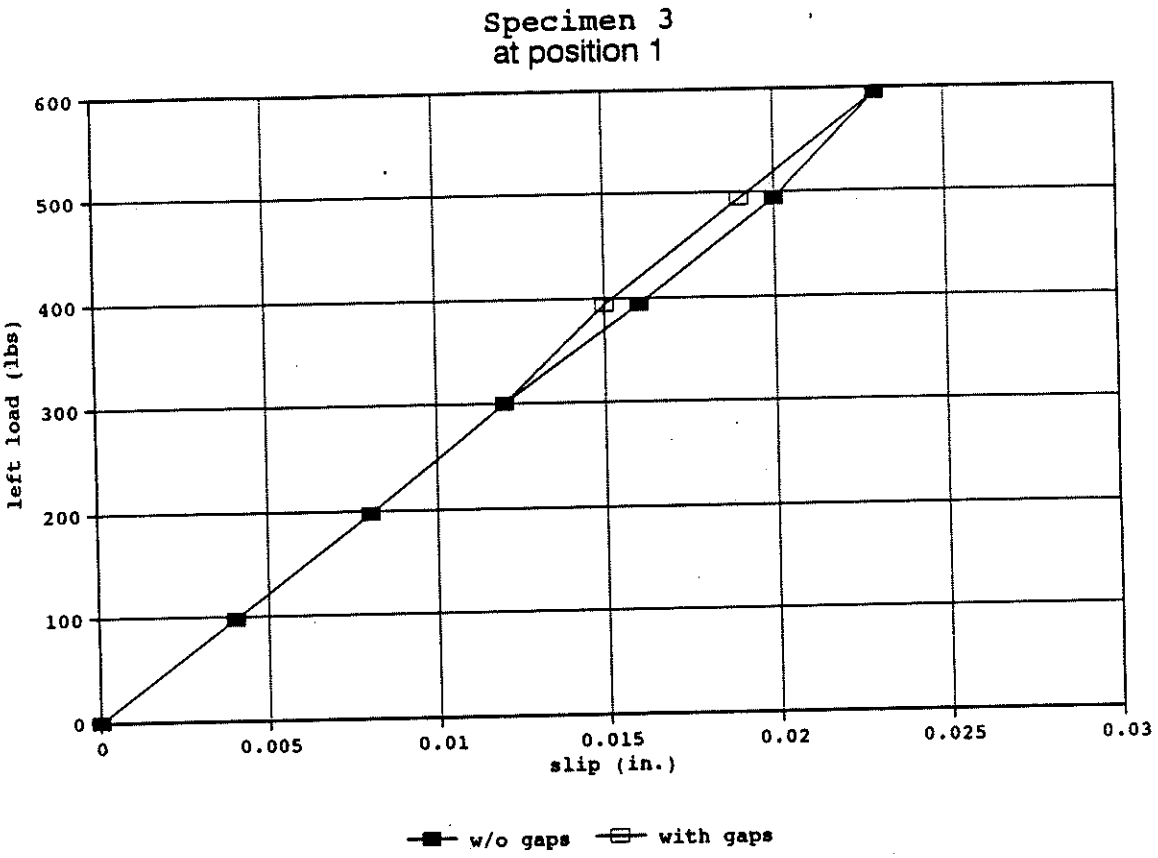

Figure 7.8: The Effect of Gaps on Slip

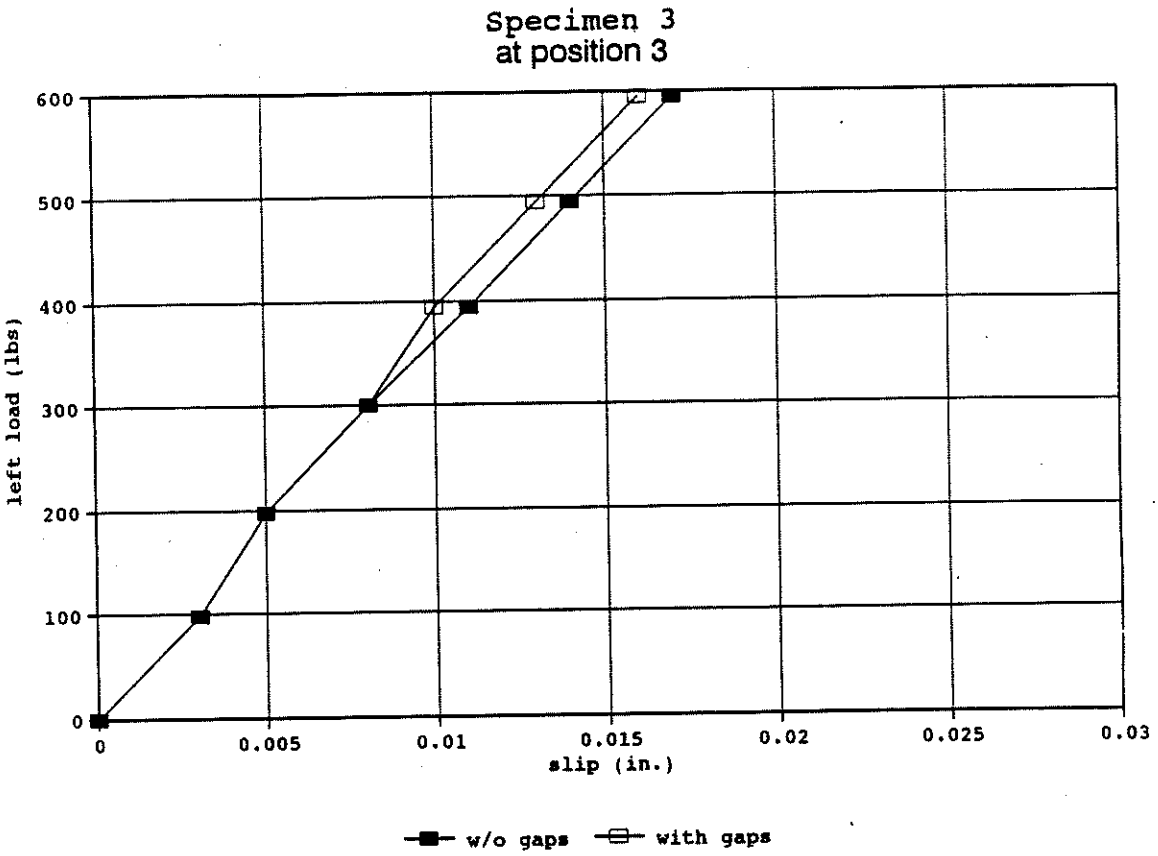

Figure 7.9: The Effect of Gaps on Slip

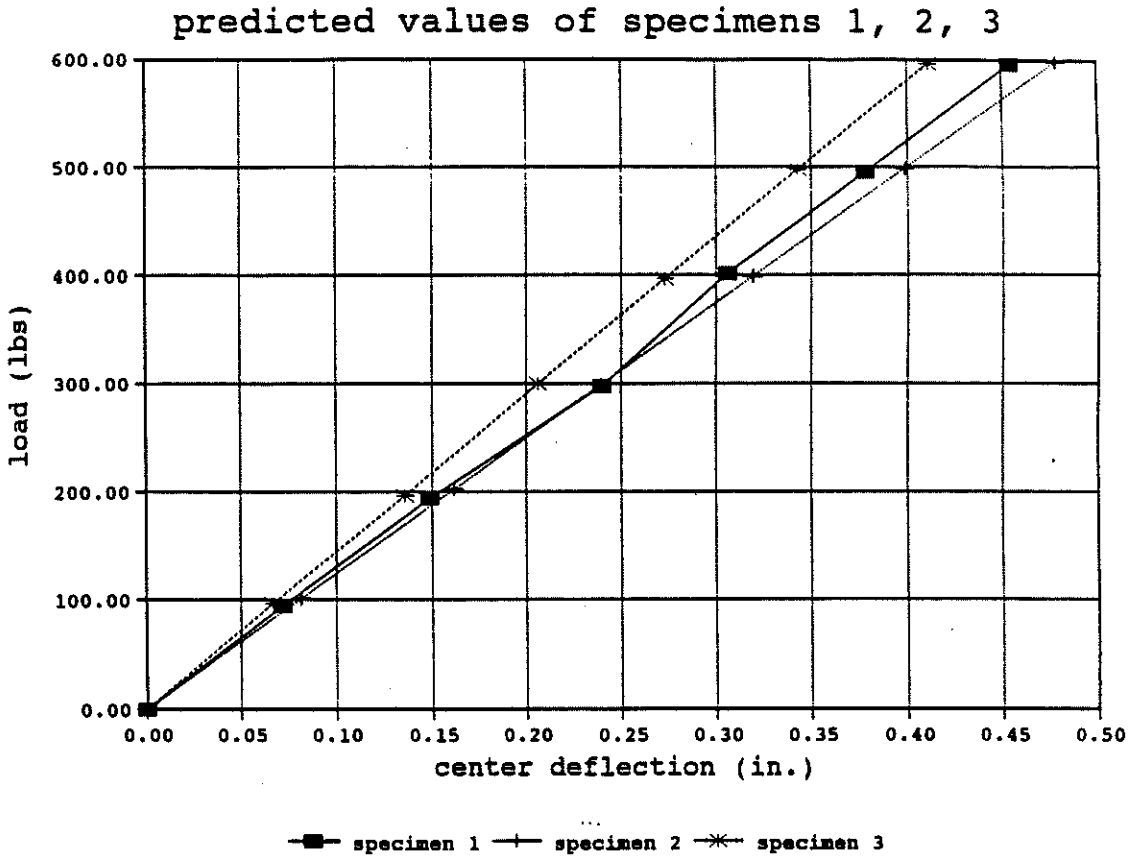

Figure 7.10: The Predicted Midspan Deflection Values of Specimen 1, 2 and 3

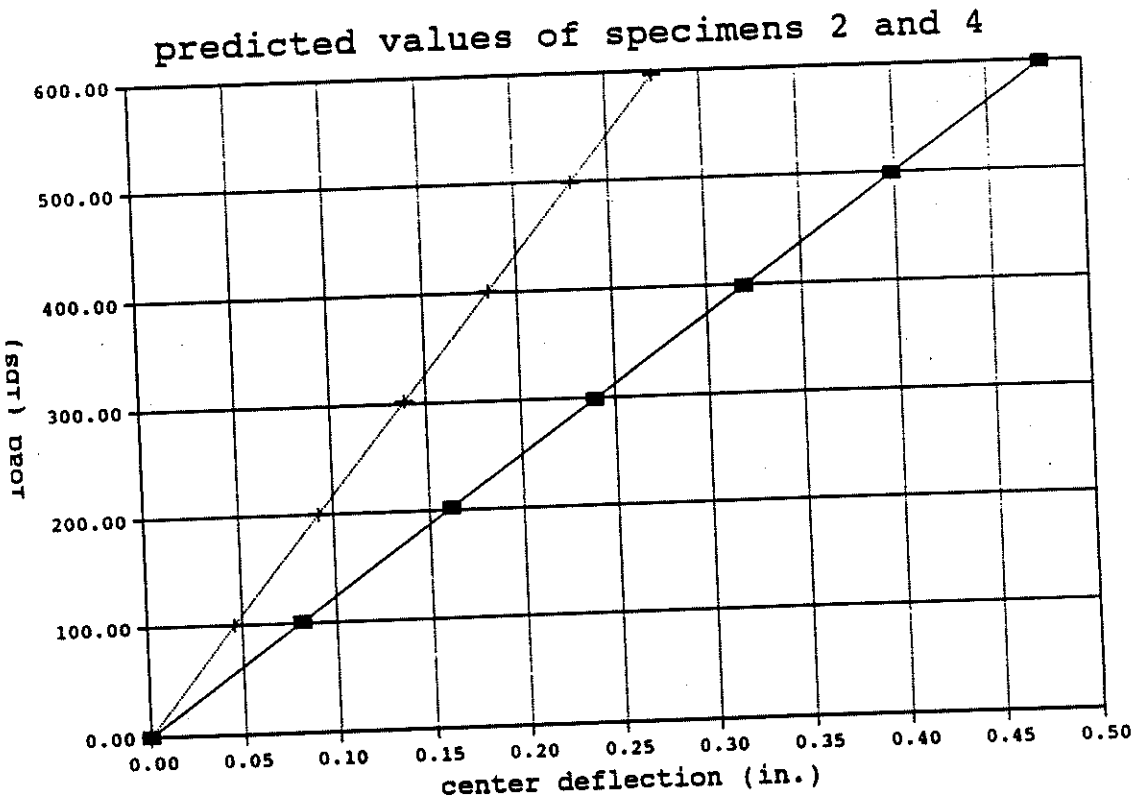

Figure 7.11: The Predicted Values of Specimens 2 and 4

The comparison of the T-beam specimen deflection of the theoretical (Kcp = 20000 lb./in. and Kpl = 12000 lb./in.) and experimental results for all 3-layer T-beam specimens are shown in Figures 7.12-7.15. The measured deflection of specimen 2 and specimen 4 are quite close to the computed results for load levels under 100 lbs. For specimen 1 and specimen 3, the predicted results and the measured values are obviously different at the low load levels. Referring to Figures 6.4 and 6.5 that were discussed in preceding chapter, when the gaps occur at the midspan of a beam, the effect on the deflection of the beam increases. If the gaps are far away the midspan of a beam, the effect of gaps to the stiffness of beam is limited. In Table 7.2, the comparison of the theoretical and experimental deflection values for each specimen are listed.

Observing the values of slip from mathematical model and laboratory work in Appendix C, for specimens 1, 2, and 3, when the load level exceed 300 lbs for both concentrated loads, the experimental values of slip is much greater than the predicted values (Figures C2.1-C2.30). This phenomenon is similar to the comparison of predicted and measured deflection values of specimen 2. At low load level, FEABEA model can predicted the deflection and slip values of specimen 2 (Figure 7.13). When the two concentrated loads increase, the theoretical values becomes too conservative. For specimen 4, except for the position 1 and 6 that had larger measured slip, the predicted slip values are reasonable close to measured values (Figures C2.31-C2.42).

Selected Slip Modulus K40

By using the measured slip modulus at slip equaling 0.015 inch, the theoretical value of slip in the T-beams at 300 lb load level are determined to be smaller than 0.015 inch. Therefore, the actual nail force is greater than the predicted value.

If the effect of dead load on slip is considered, the interlayer slip of T-beam specimens 1, 2 and 3 at some positions may exceed 0.015 inch when the two concentrated loads are still very small. Therefore, the selected slip modulus at 0.015 inch slip may not represent the

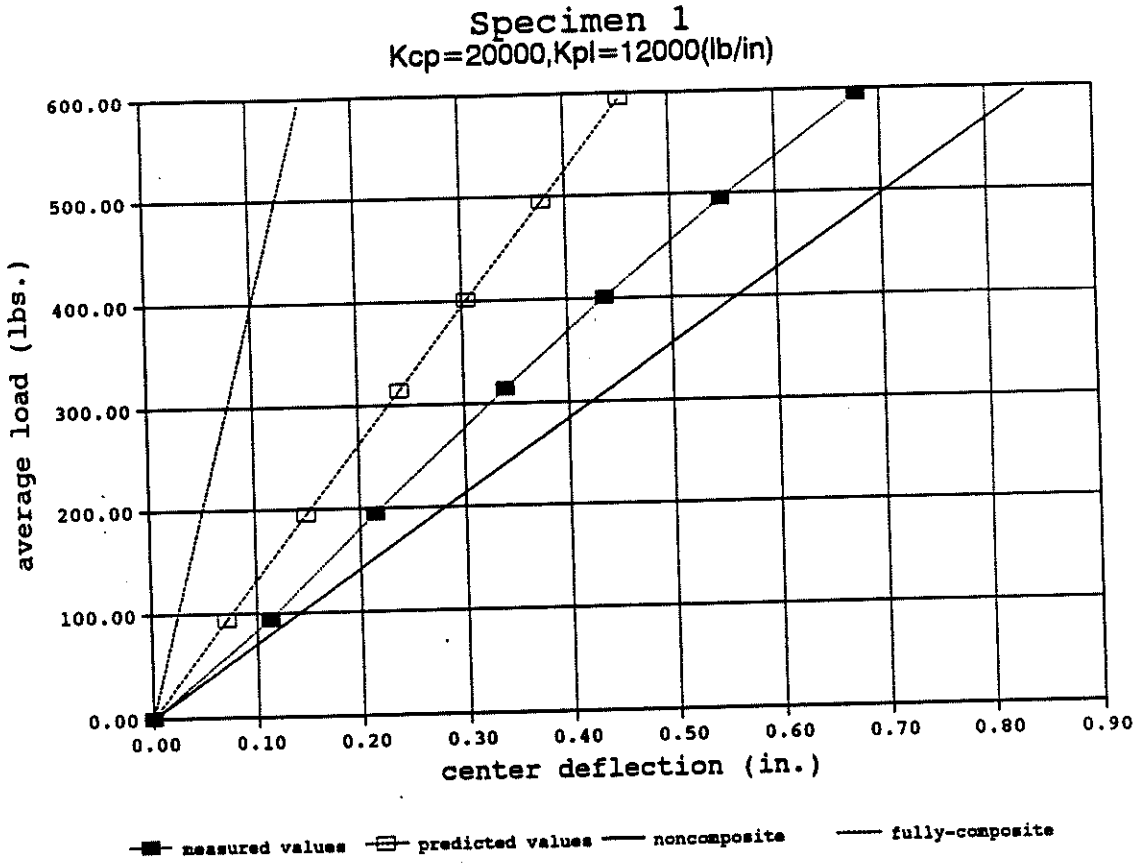

Figure 7.12: The Predicted Values and Experimental Results of Specimen 1

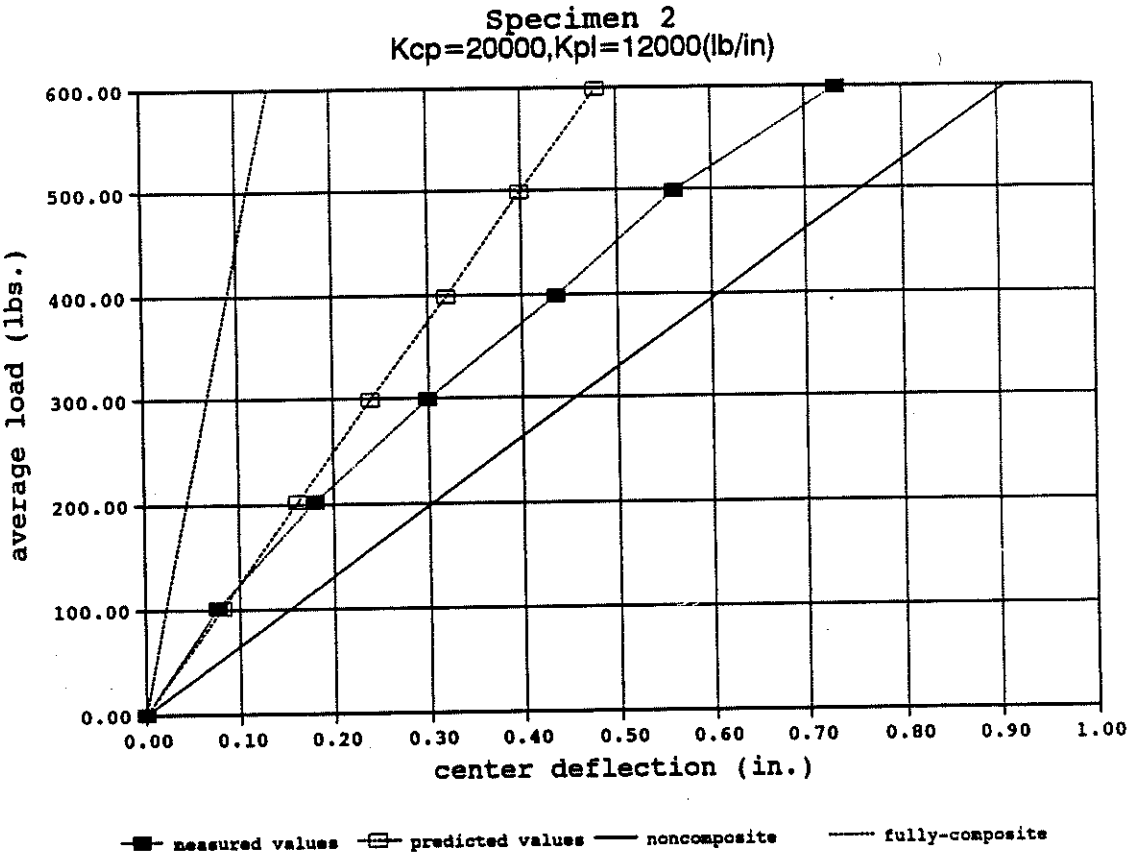

Figure 7.13: The Predicted Values and Experimental Results of Specimen 2

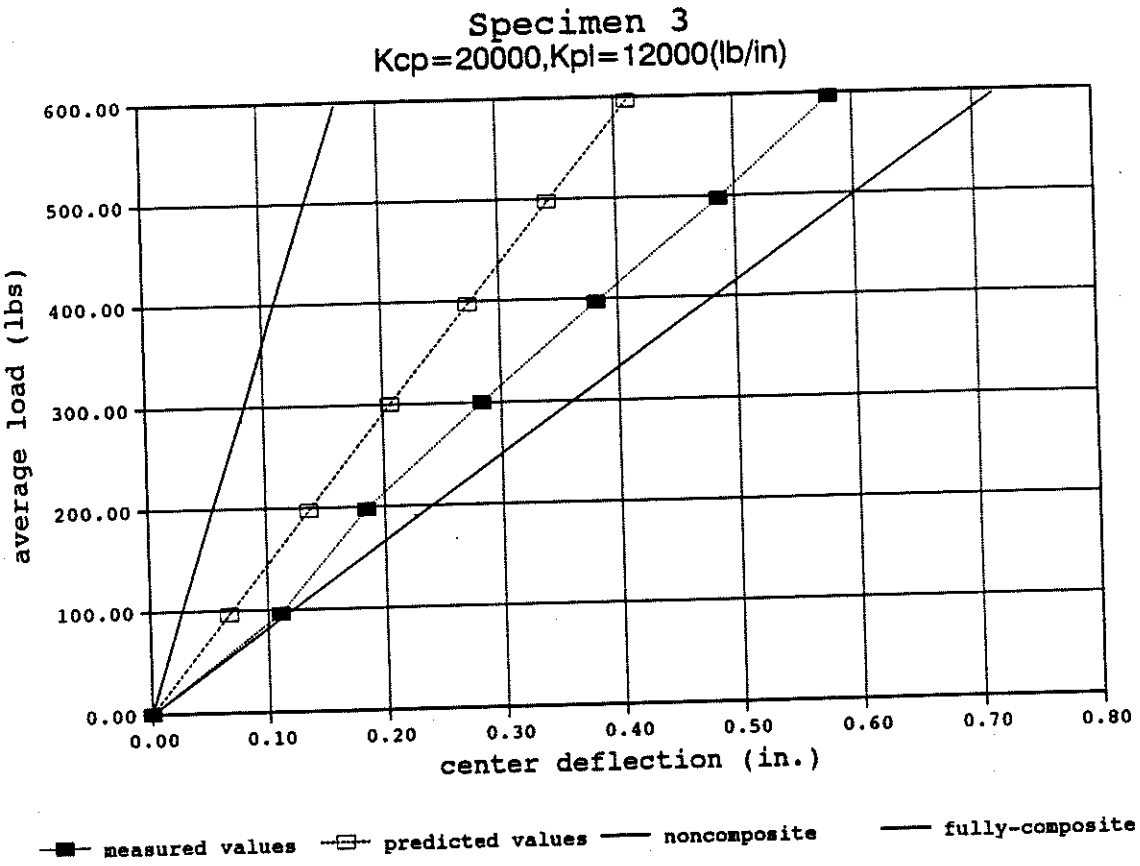

Figure 7.14: The Predicted Values and Experimental Results of Specimen 3

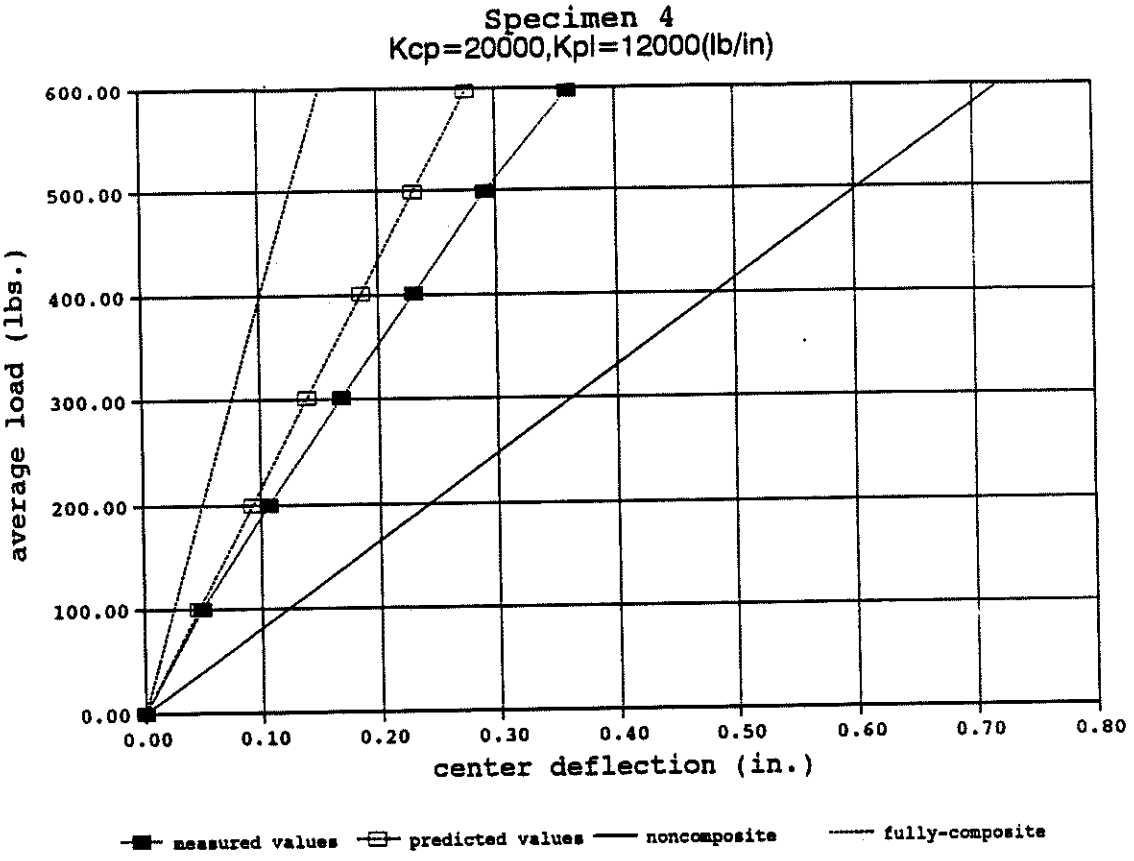

Figure 7.15: The Predicted Values and Experimental Results of Specimen 4

actual behavior of T-beams at the applied load level used in the FEABEA model. From the experimental results, the effect of dead load in theoretical model (using Kcp=20000 lb./in. and Kpl=12000lb./in.), the maximum interlayer slip of specimens 1, 2 and 3 would be about 0.04 inch when the concentrated loads are at 300 lbs. level.

Reviewing section 5.4, the selected slip modulus was based on 0.015 inch slip. Actually, in the slip test results and Patterson's report, the load-slip curves are not linear and the secant slip modulus varies at different selected slip. If the selected secant slip modulus is based on the slip equalling 0.04 inch, the slip modulus for the type 8 connection of 28 day age in slip test will be the range from 9560 to 13400 lb./in. and the average slip modulus is about 12000 lb/in.. Similarly, from Patterson's report, the interlayer slip modulus between plywood and lumber at 0.04 inch is in the range from 4850 to 8020 lb./in., and the average value is about 6000 lb./in. Using the two values (Kcp=12000 lb./in. and Kpl=6000 lb./in.) into FEABEA model, the load-deflection curves of FEABEA model were compared to experimental results in Figures 7.16-7.19 and Table 7.2.

Using these adjusted slip modulus, the theoretical deflection values of specimens 1, 2 and 3 become close to the measured values. Similarly, the slip values from theoretical model and test results are closer than when the slip modulus was selected at 0.015 inch slip (Appendix C). Focusing on specimen 2 (see Figure 7.17), the theoretical and measured load-deflection curves cross each other at about 300 lb loads, and the predicted and measured slip values at most positions are very close at that load level. Combining the effect of concentrated loads and dead load, the slip amount at the positions close to the two ends and the gaps of specimen 2 are approximately 0.04 inch, and for specimens 1 and 3, this slip amount only occurs at the positions close to the two ends. For this reason, the predicted values of specimen 2 at slip modulus K40 are closer to measured values than specimens 1 and 3 at 300 load level.

Table 7.2: Comparison of Measured and Predicted Midspan Deflection Values

			Specimen 1		
load level (lbs)	measured (in.)	predicted #1 (in.)	ratio	predicted #2 (in.)	ratio
100	0.1138	0.0720	1.58	0.0886	1.28
200	0.2147	0.1489	1.44	0.1831	1.17
300	0.3397	0.2380	1.41	0.2949	1.15
400	0.4370	0.3035	1.42	0.3760	1.16
500	0.5484	0.3752	1.45	0.4649	1.18
600	0.6780	0.4505	1.49	0.5582	1.21
			Specimen 2		
load level (lbs)	measured (in.)	predicted #1 (in.)	ratio	predicted #2 (in.)	ratio
100	0.0768	0.0815	0.94	0.1009	0.76
200	0.1796	0.1620	1.10	0.2006	0.90
300	0.2988	0.2396	1.25	0.2968	1.01
400	0.4366	0.3193	1.37	0.3955	1.10
500	0.5606	0.3990	1.41	0.4942	1.13
600	0.7322	0.4786	1.56	0.5927	1.23
			Specimen 3		
load level (lbs)	measured (in.)	predicted #1 (in.)	ratio	predicted #2 (in.)	ratio
100	0.1099	0.0668	1.64	0.0814	1.35
200	0.1841	0.1360	1.35	0.1658	1.11
300	0.2839	0.2067	1.37	0.2519	1.12
400	0.3823	0.2731	1.40	0.3329	1.15
500	0.4865	0.3425	1.42	0.4174	1.17
600	0.5808	0.4110	1.41	0.5010	1.16
			Specimen 4		
load level (lbs)	measured (in.)	predicted #1 (in.)	ratio	predicted #2 (in.)	ratio
100	0.0494	0.0464	1.06	0.0585	0.84
200	0.1064	0.0922	1.15	0.1163	0.91
300	0.1683	0.1393	1.20	0.1757	0.96
400	0.2298	0.1850	1.24	0.2334	0.98
500	0.2913	0.2301	1.27	0.2902	1.00
600	0.3606	0.2753	1.31	0.3472	1.04

Predicted #1 : Kcp=20000 lbs/in. Kpl=12000 lbs/in.
Predicted #2 : Kcp=12000 lbs/in. Kpl=6000 lbs/in.

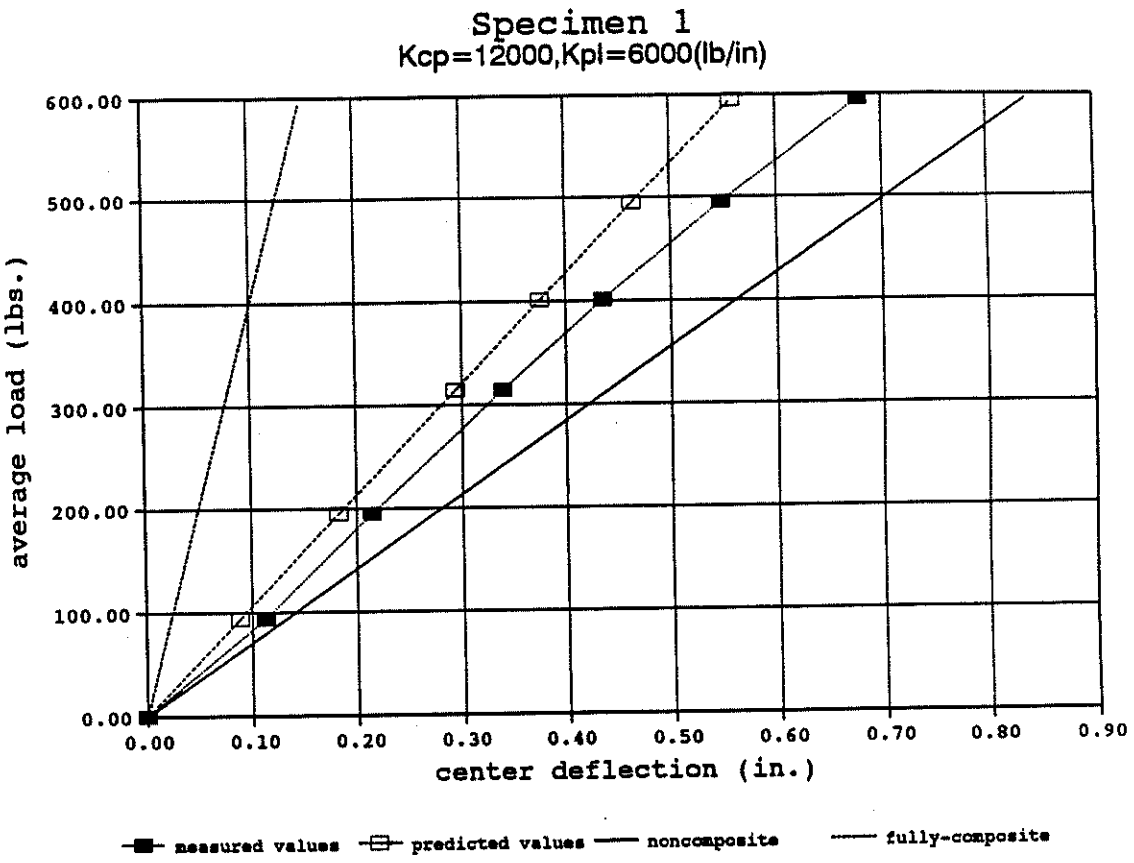

Figure 7.16: The Predicted Values and Experimental Results of Specimen 1

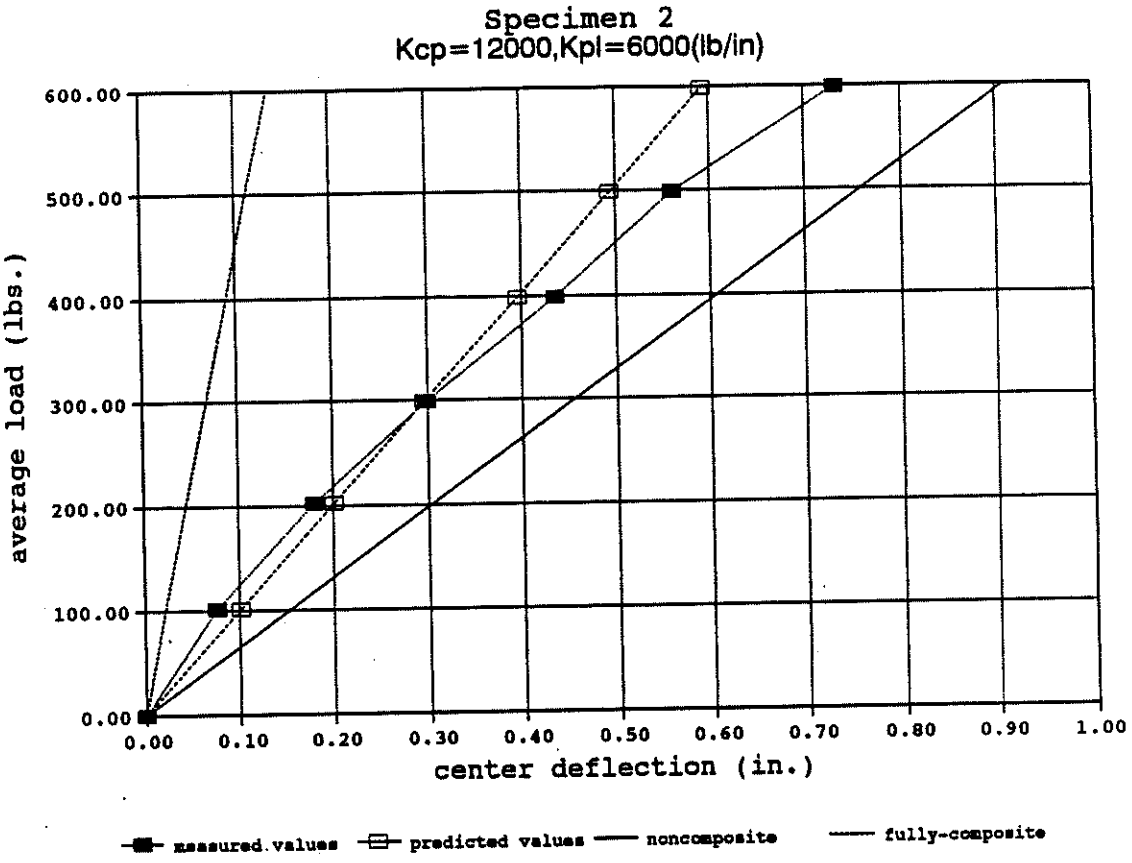

Figure 7.17: The Predicted Values and Experimental Results of Specimen 2

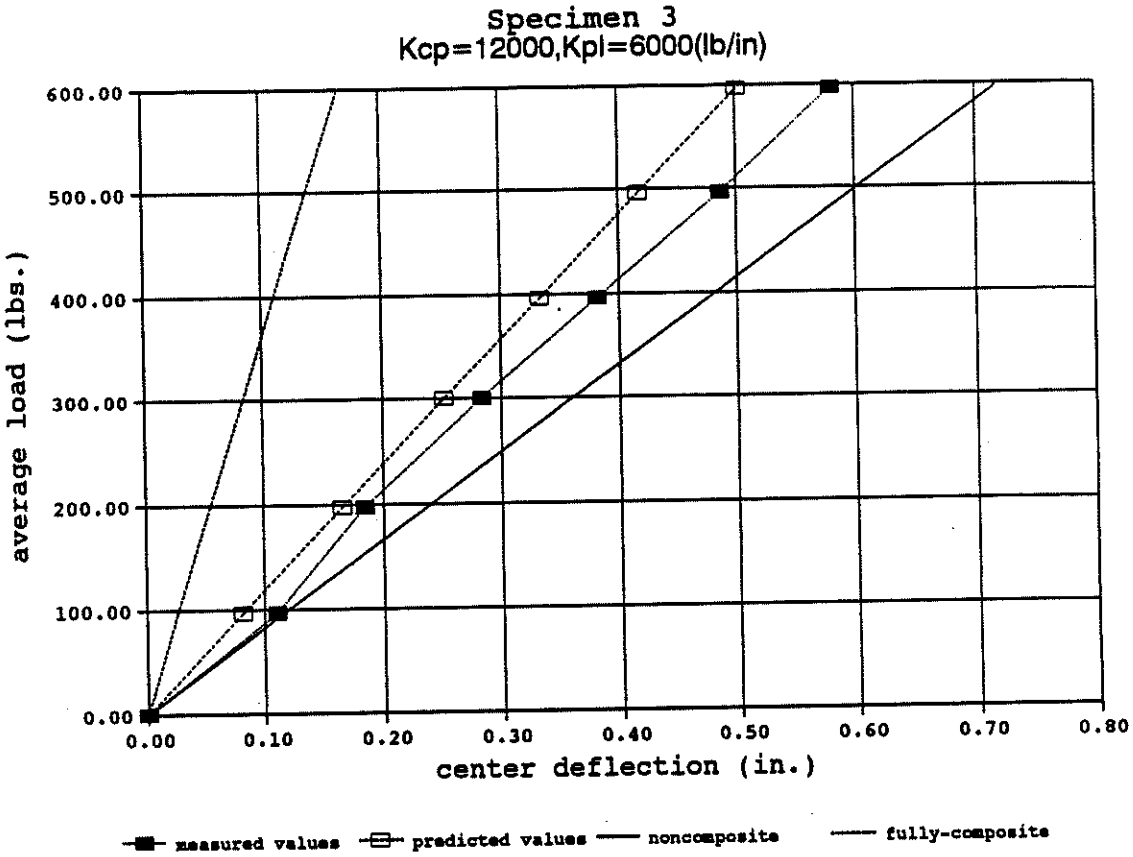

Figure 7.18: The Predicted Values and Experimental Results of Specimen 3

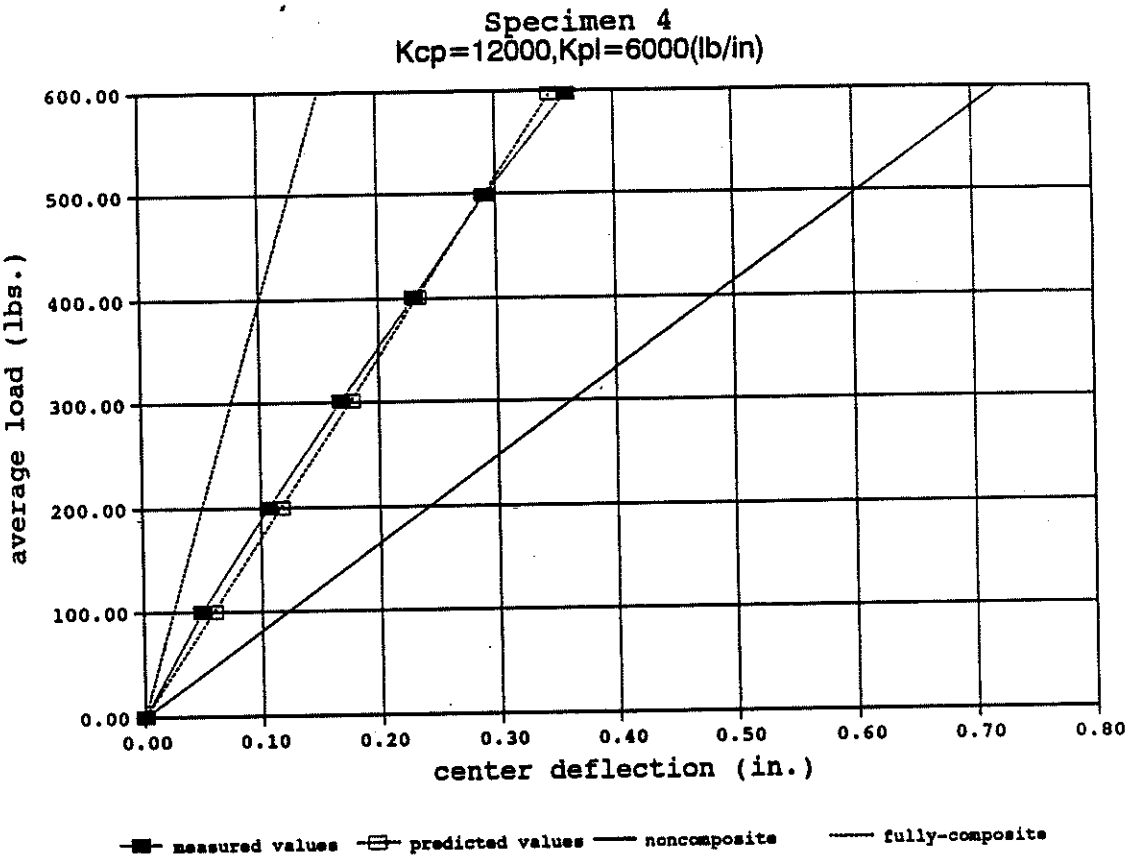

Figure 7.19: The Predicted Values and Experimental Results of Specimen 4

CHAPTER 8

SUMMARY AND CONCLUSIONS

SUMMARY

The outcomes of this work are from three primary studies. The first study was the slip test for determining the slip modulus of an interlayer connection between concrete and wood. Four types of nails, two ages of concrete, and two different configurations for each type of nail were using in the slip test. From the results of slip tests, the age of concrete and the embedment length of the connectors in the connected materials affect the slip modulus. The increase of the strength of concrete enhances the interlayer slip modulus. Like reinforcing steel enclosed in concrete, the embedment lengths of the nail connector in concrete members affect the rigidity of connection. The properties of connector also are an important factor for slip modulus, but the initial slip of connection is combination of the deformation of connected materials and connectors. The effect of properties of connector on slip modulus is difficult to determine in the study.

The second study was the mixed material T-beam bending test. Four specimens were used in the tests. The deflection and interlayer slip were measured to analyze the behavior of structure system. In testing the 3-layer T-beam specimens connected by nails, the effect of interlayer connection and the influence of the location of gaps reflect in the experimental results. Reducing the nail spacing effectively increases the stiffness of T-beam. Conversely, decreasing the amount of connectors inefficiently uses the materials. In the three layer specimens, the plywood layer is the least mass layer. When the interlayer connections are sufficiently rigid, the existence of plywood layer enhances the stiffness of the whole beam.

The locations of gaps in sheathings may change the stiffness of a multilayer beam. In specimens 1 and 3, an open gap occurs at the midspan of plywood layer. The stiffness of these two specimens does not decrease much due to the gap, but that gaps occur in the midspan affect the test results of layered beam in the earliest motion. When the gaps are not located at midspan (as in specimen 2), the earliest deflection (of specimen 2) is smaller (than that of specimen 1 and 3) for the same load level.

In the third study, computer program FEABEA was used to analyze the behavior of mixed material T-beams and compare the predicted values to the experimental results. Due to the fact that the properties of materials and modulus are assumed to be linear, the experimental results do not closely match the theoretical values when the tangent slip modulus at 0.015 inch slip (K15) was selected. Because the actual slip of specimens 1, 2 and 3 are greater than 0.015 inch for the full load level used, the secant slip modulus at 0.04 inch slip (K40) is more suitable to specimens 1, 2 and 3. From the comparison in chapter 7 and Appendix C, the effect of slip modulus on predicted values of deflection and slip can be verified. For more precise prediction, the slip modulus may need to be selected different values for different positions of interlayers and nonlinear analysis should be employed.

CONCLUSIONS

Based on the FEABEA model and experimental results, the quantities of the T-beams can be represented by the effective of composite action that was defined by Pault [17] from load-deflection curves. Three items were defined in Pault's report. The maximum percentage composite action available (C.A.A.) of completely composite system, the percentage of composite action observe (C.A.O.) in the actual system and the efficiency (EFF) were obtained by

$$C.A.A. = \frac{\Delta_N - \Delta_C}{\Delta_N} \tag{8.1}$$

$$EFF = \frac{\Delta_N - \Delta_I}{\Delta_N - \Delta_C} \tag{8.2}$$

$$C.A.O. = EFF \times C.A.A. \tag{8.3}$$

where

Δ_N = the theoretical deflection of the system if the behavior is not composite,

Δ_C = the theoretical deflection of the system if the behavior is completely composite, and

Δ_I = the measured deflection.

From the load-deflection curve figures in Appendix C, the experimental and theoretical midspan deflection values of each T-beam specimen at 300 lb load level are listed in Table 8.1. Theoretically the potential degree of composite action for the specimens is about 80%. However, modest effeciency reduces this to a range of 23.1% to 53.8% in the actual specimens.

Table 8.1: The Theoretical and Experimental Composite Action of T-Beam Specimens

specimen	Δ_N (in)	Δ_I (in)	Δ_C (in)	C.A.A. (%)	EFF (%)	C.A.O. (%)
1	0.07954	0.33969	0.44202	82.0	28.2	23.1
2	0.06748	0.29881	0.45459	81.2	40.2	32.7
3	0.08272	0.28388	0.36099	77.1	27.7	21.4
4	0.07588	0.16831	0.36429	79.2	68.0	53.8

The mass of connectors in the whole T-beam system is the less than any other material, but it can significantly enhance the stiffness of layered systems. When the number of connectors is tripled as specimen 4, the EFF and C.A.O. significantly increase, as evident in specimen 4. The effect of the locations of gaps is also evident in the values of EFF and C.A.O. as evdient in comparing specimens 1 and 3 with specimen 2.

From the comparison of the theoretical and measured results in Chapter 7, the applicability of the FEABEA model in predicting the behavior of mixed concrete-wood layered beams can be verified, but the consideration of the effect of dead load to the slip modulus of interlayer connection beforehand is necessary.

FUTURE RESEARCH NEEDS

From this study, the effect of properties of connected material and connector to slip modulus can be recognized, but the determination of a mathematical relationship between them needs a more comprehensive investigation. For multi-layer in a structure, the slip test may need to be based on multi-layer specimens. For a connector used to connect more than two layers, the relationship of slip behaviors of the different interlayers need to be Similar, a nonlinear model for program FEABEA is worth investigating in analysis of mixed material layered beam systems.

REFERENCES

1. J. R. Goodman and E. P. Popov "Layered beam systems with interlayer slip," *Journal of Structural Division,* ASCE, Vol. 94, St. 11, Paper No. 6214, Nov. 1968, pp. 2535-2547.

2. J. R. Goodman "Layered wood systems with interlayer slip," *Wood Science,* Vol. 1, No. 3, 1969, pp. 148-158.

3. J. R. Goodman, M. D. Vanderbilt, M. E. Criswell, and J. Bodig "Composite and two-way action in wood-joist floor systems," *Wood Science,* Vol. 7, No. 1, 1974, pp. 25-33.

4. J. R. Goodman "Composite and two-way action in wood-joist floor systems," *Wood science,* Vol. 7, No. 1, 1974, pp. 25-33.

5. E. G. Thompson, J. R. Goodman, and M. D. Vanderbilt "Finite element analysis of layered wood systems," *Journal of Structural Division,* ASCE, Vol. 101, St 12, Dec. 1975, pp. 2659-2672.

6. G. A. Tremblay "Nonlinear analysis of layered T-beams with interlayer slip," M.S. Thesis, Colorado State University, Fort Collins, CO, 1974.

7. M. D. Vanderblit, J. R. Goodman, M. E. Criswell, and J. Bodig "Service and overload behavior of wood joist floor systems," *Journal of Structural Division,* ASCE, Vol. 100, St. 1, Paper No. 10274, Jan. 1974, pp. 11-29.

8. D. W. Patterson "Nailed wood joints under lateral load," M.S. Thesis, Colorado State University, Fort Collins, CO, 1973.

9. J. R. Goodman "Layered wood systems with interlayer slip," Ph.D. dissertation, The University of California, at Berkeley, CA, 1967.

10. P. J. Pellicane, J. L. Stone, and M. D. Vanderbilt, "Generalized model for latered load slip of nail joints," *Journal of Material in Civil Engineering,* Vol. 3, No. 1, 1991, pp. 60-77.

11. E. G. Thompson, J. R. Goodman, and M. D. Vanderblit "FEAFLO: A program for analysis of layered wood systems," *Computers and Structures,* Vol. 7, 1977, pp. 237-248.

12. L. G. Clark "Deflection of laminated beams," *Transactions,* ASCE, Vol. 119, Paper No. 2694, 1954, pp. 721-736.

13. N. M. Newmark, C. P. Seiss, and I. M. Viest "Tests and analysis of composite beams with incomposite interaction," *Proceedings,* Society for Experimental Stress Analysis, Vol. 19, No. 1, 1951.

14. C. B. Norris, W. S. Erickson, and W. J. Kommars "Flexural rigidity of a rectangular strip of sandwich construction - Comparison between mathematical analysis and results of tests," USDA Forest Service, *Forest Product laboratory,* Report 1505A, May 1952.

15. C. E. Antonides, M. D. Vanderbilt, and J. R. Goodman "Interlayer gap effect on nailed joint stiffness," *Wood Science,* Vol. 13, No. 1, 1980.

16. T. E. McLain "Curvilinear load-slip relations in laterally-load nailed joints," M.S. Thesis, Colorado State University, Fort Collins, CO, 1975.

17. J. D. Pault "Composite action in glulam timber bridge systems," M.S. Thesis, Colorado State University, Fort Collins, CO, 1977.

18. E. W. Kuenzi and T. L. Wilkinson "Composite beams-effect of adhesive or fastener rigidity," USDA, Forest Service, *Forest Products Laboratory FLP152,* 1971.

19. E. W. Kuenzi "Theoretical design of a nailed or bolted joint under lateral load," USDA, Forest Service, *Forest Products Laboratory Report D1951*, 1955.

20. T. L. Wilkinson "Elastic bearing constants for sheathing materials," USDA, Forest Service, *Forest Products Laboratory,* 1973.

21. T. L. Wilkinson "Effect of deformed shanks, prebored lead holes, and grain orientation on the elastic bearing constant for laterally loaded nail joints," USDA, Forest Service, *Forest Products Laboratory, FPL 192*, 1972.

22. T. L. Wilkinson "Theoretical lateral resistance of nailed joints," *Journal of Structural Division*, ASCE Vol. 97, No. ST5, 1971.

23. T. L. Wilkinson "Analysis of nailed joints with dissimilar members," *Journal of Structural Division*, ASCE Vol. 98, No. ST9, 1972.

24. W. J. McCutcheon "Method for predicting the stiffness of wood-joist floor systems with partial composite action," USDA, Forest Service, *Forest Products Laboratory, ,FPL 289*, 1977.

25. D. L. Wheat, M. D. Vanderbilt, J. R. Goodman "Wood floor with nonlinear nail stiffness,"*Journal of Structural Division*, ASCE Vol. 109, No. ST5, May 1983.

26. D. L. Wheat "Nonlinear analysis of wood joist floors," Ph.D. dissertation , Colorado State University, Fort Collins, CO, 1980.

27. T. D. Jizba "Sheathing joint stiffness for wood joist floors," M.S. Thesis, Colorado State University, Fort Collins, CO, 1979.

28. J. S. Liu " Verification of a mathematical model for wood joist floor systems," Ph.D. dissertation, Colorado State University, Fort Collins, CO, 1974.

29. C. P. Stonebraker "Computer aided design of light frame structure," M.S. Thesis, Colorado State University, Fort Collins, CO, 1988.

30. G. E. Glasco "Computer aided design of wood-joist floor system for static and dynamic load," M.S. Thesis, Colorado State University, FOrt Collins, CO, 1990.

31. M. F. Ko "Layered beam systems with interlayer slip," M.S. Thesis, Colorado State University, Fort Collins, CO, Dec. 1972.

32. M. L. Kuo "Verification of a mathematical model for layered T-beams," M.S. Thesis, Colorado State University, Fort Collins, CO, March 1974.

33. C. E. Antonides "Interlayer gap effect on nail slip model," M.S. Thesis, Colorado State University, Fort Collins, CO, 1979.

34. R. O. Foschi 'Structural Analysis of Wood Floor Systems,"*Journal of Structural Division*, ASCE Vol. 108, No. ST7, 1982.

35. W. J. McCutheon, M. D. Vanderbilt, J. R. Goodman, and M. E. Criswell "Wood Joist Floors: Effects of Joist Variability on Floor Stiffness," USDA, Forest Service, *Forest Products Laboratory,* em FPL 405, Sep. 1981.

36. W. J. McCutcheon "Deflections of Uniformly Loaded Floors: A Beam- Spring Analog," USDA, Forest Service, *Forest Products Laboratory, FPL 449*, 1984.

37. W. J. McCutcheon "Stiffness of Framing Members with Partial Composite Action," *Journal of Structural Division*, ASCE Vol. 112, No. 7, 1985.

38. A. L. DeBonis and J. Bodig,"Nailed Wood Joints Under Combined Loading," *Wood Science and Technology*, Vol 9, No. 2, 1975.

39. P. J. Pellicane and J. Bodig,"Comparison of Nailed Joint Test Methods," *Journal of Testing and Evaluation*, Vol. 12, No. 5, Sept. 1984.

APPENDIX A

THE LOAD-SLIP CURVES OF SLIP TESTS

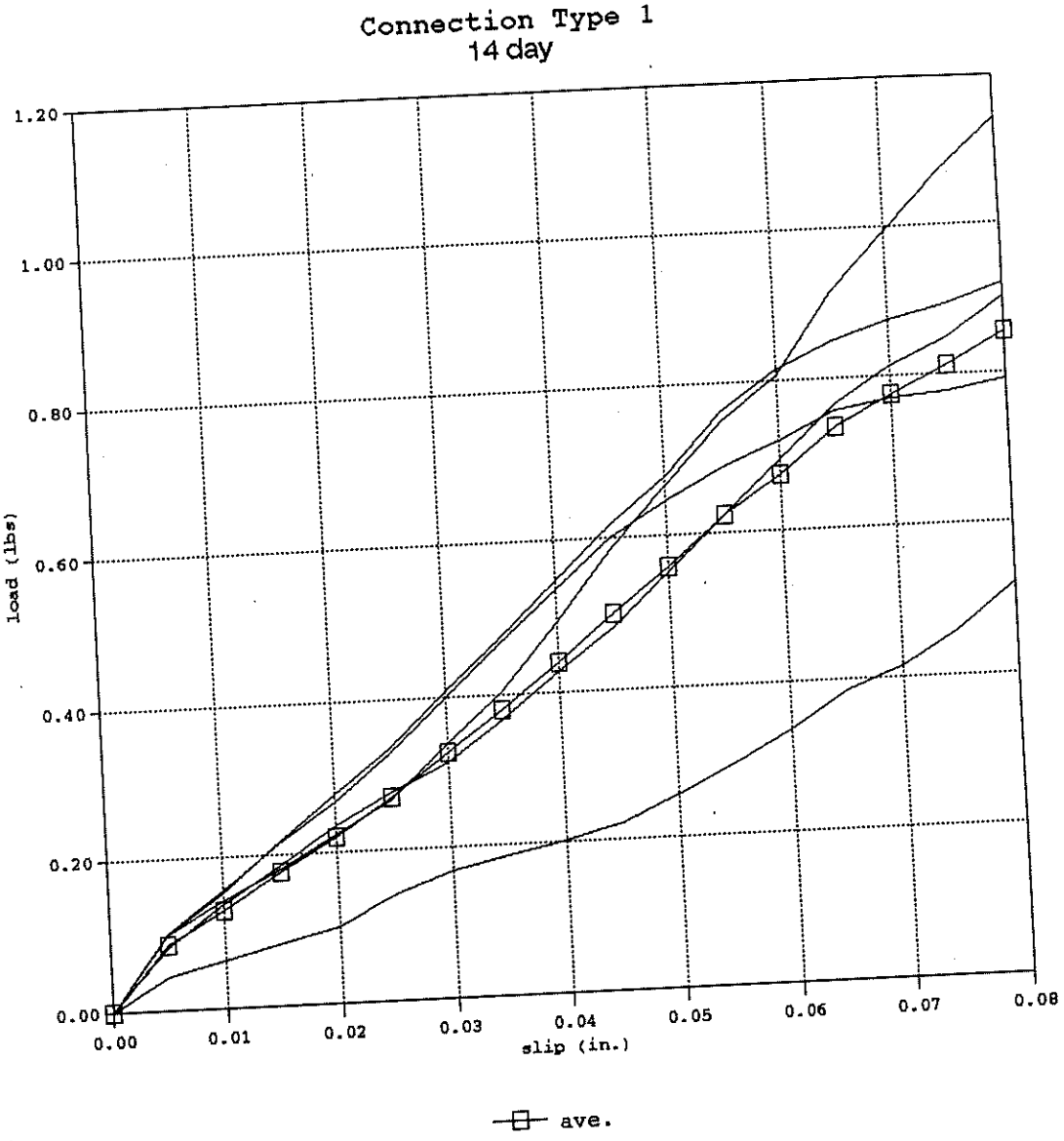

Figure A.1: The load-slip curves of specimens in connection type 1 (14days)

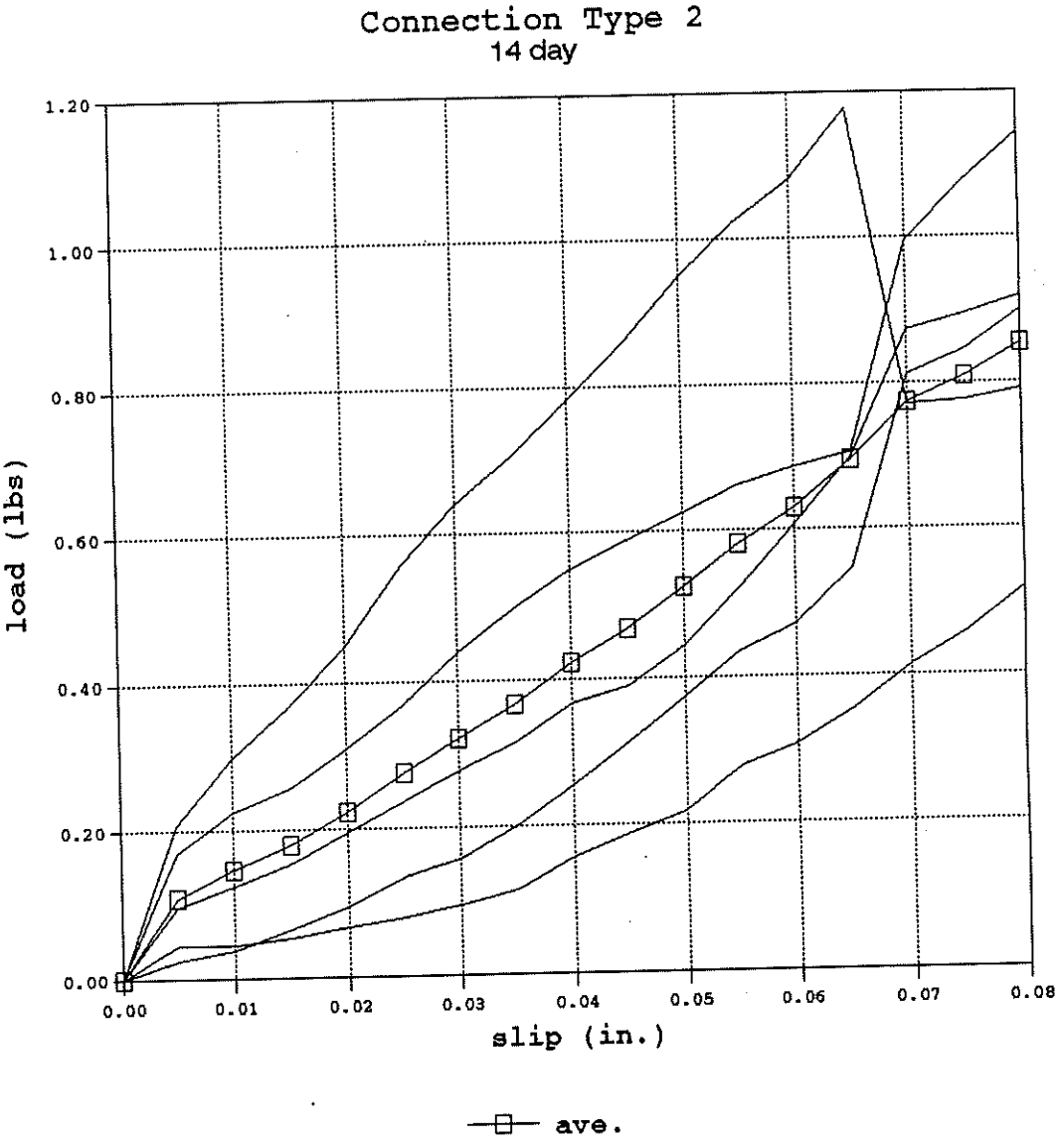

Figure A.2: The load-slip curves of specimens in connection type 2 (14 days)

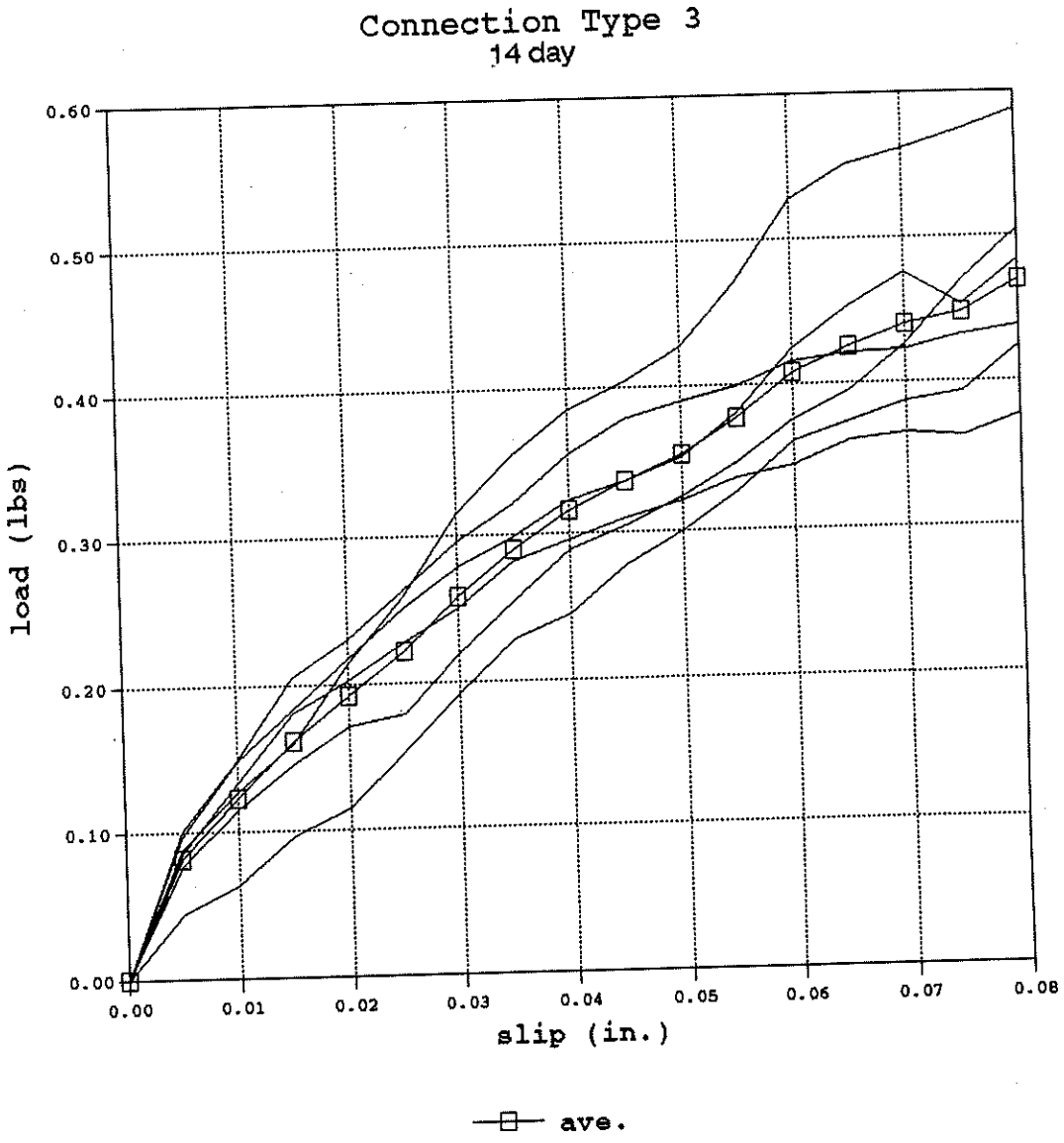

Figure A.3: The load-slip curves of specimens in connection type 3 (14 days)

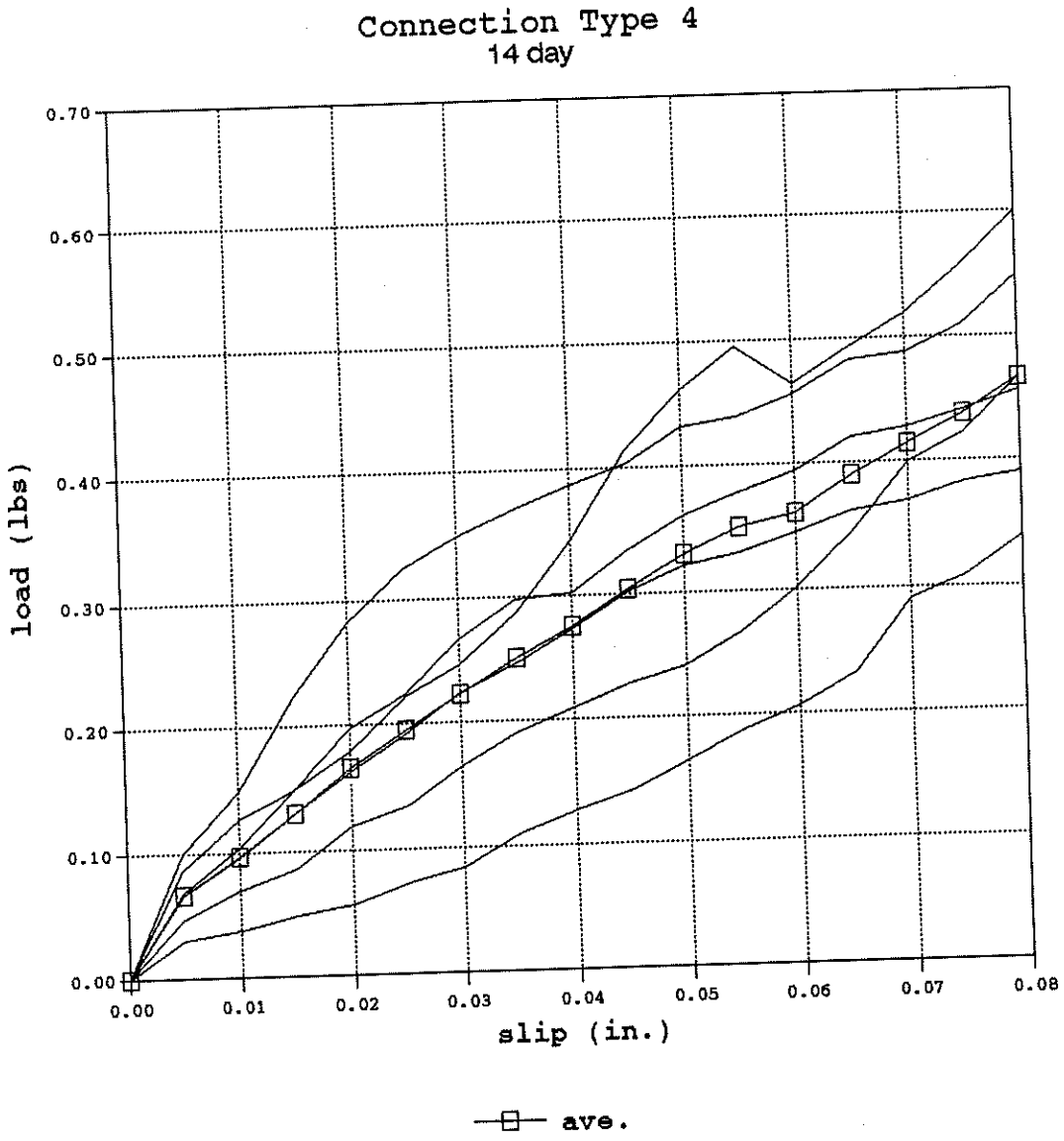

Figure A.4: The load-slip curves of specimens in connection type 4 (14 days)

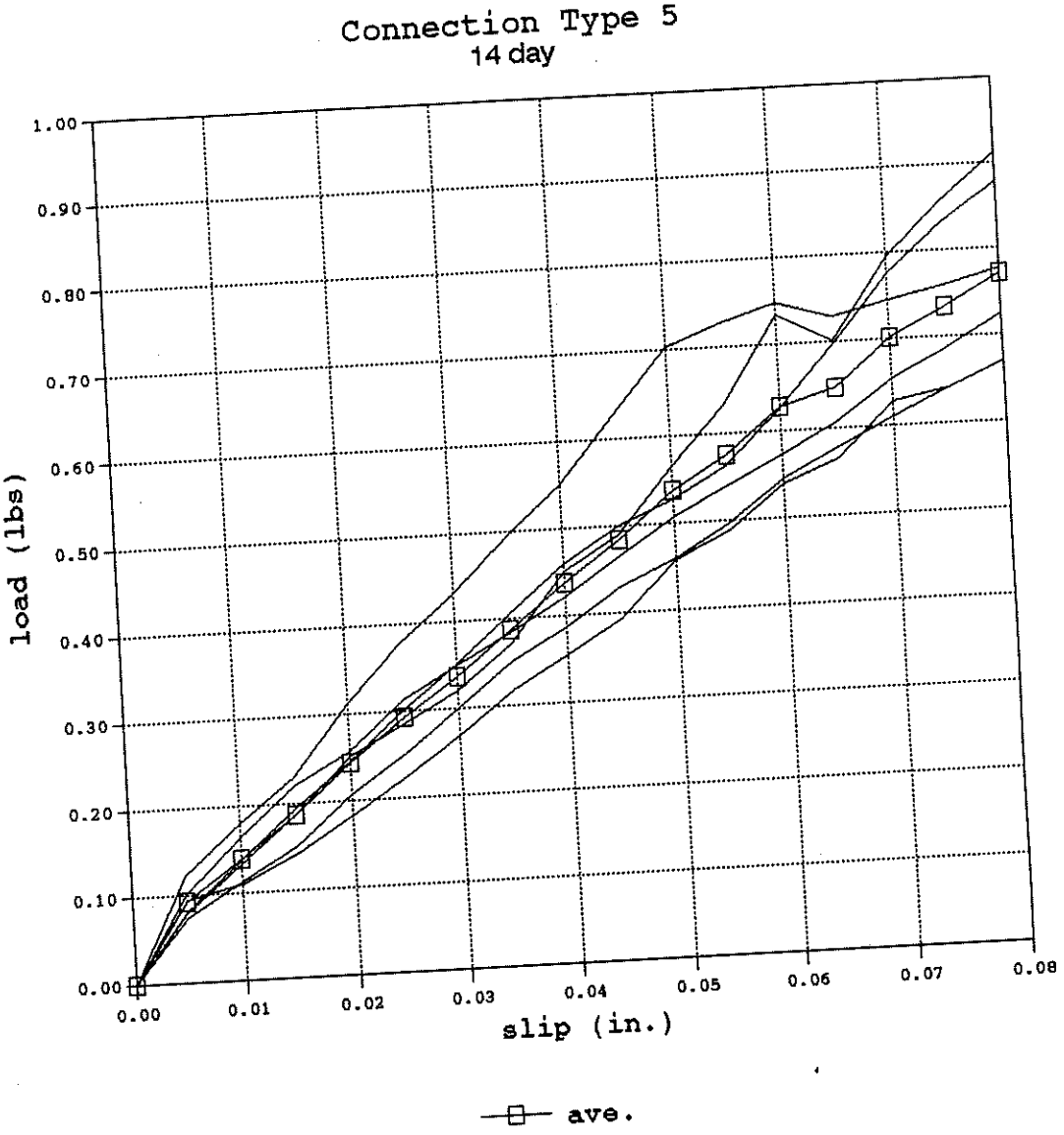

Figure A.5: The load-slip curves of specimens in connection type 5 (14 days)

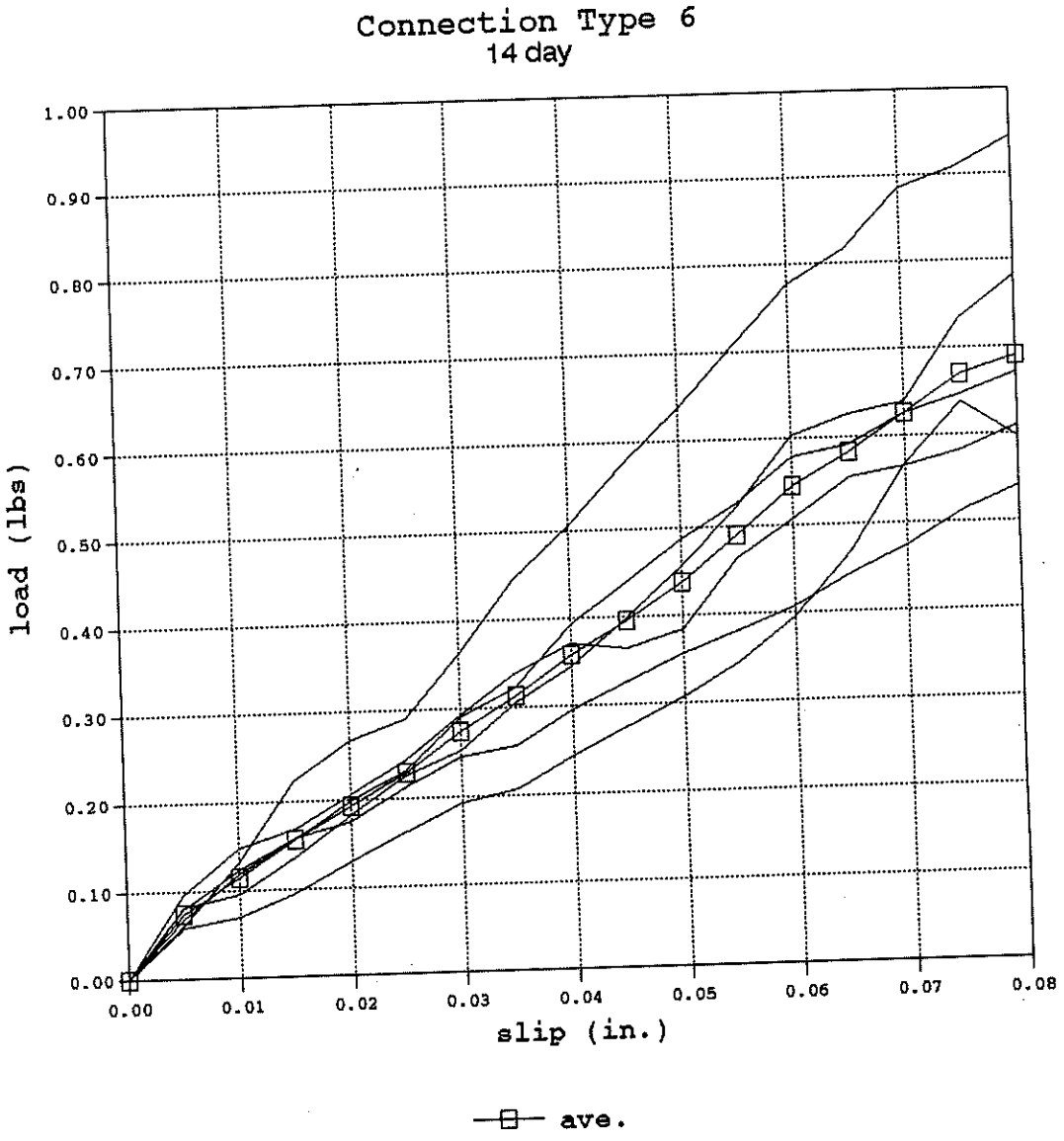

Figure A.6: The load-slip curves of specimens in connection type 6 (14 days)

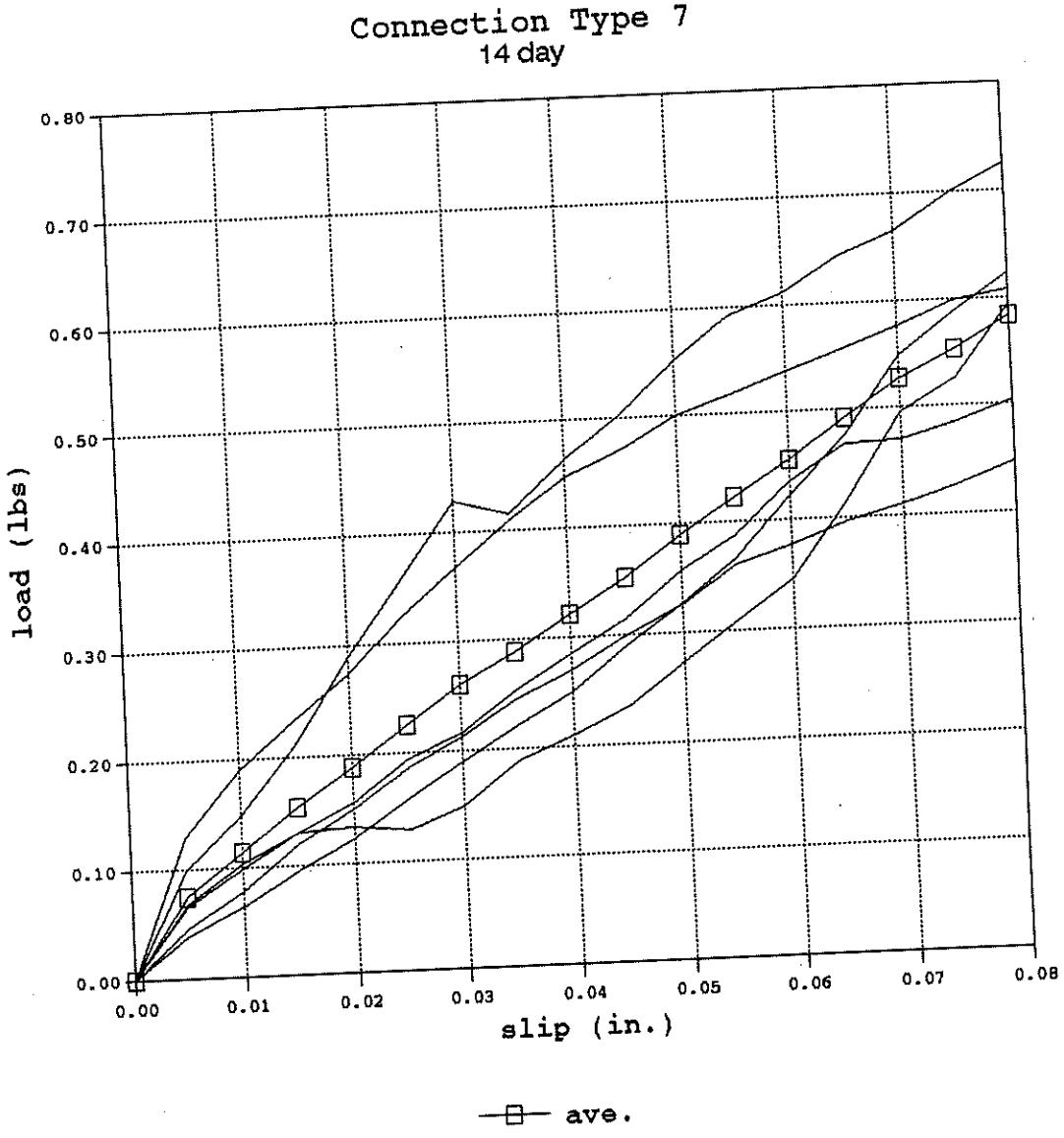

Figure A.7: The load-slip curves of specimens in connection type 7 (14 days)

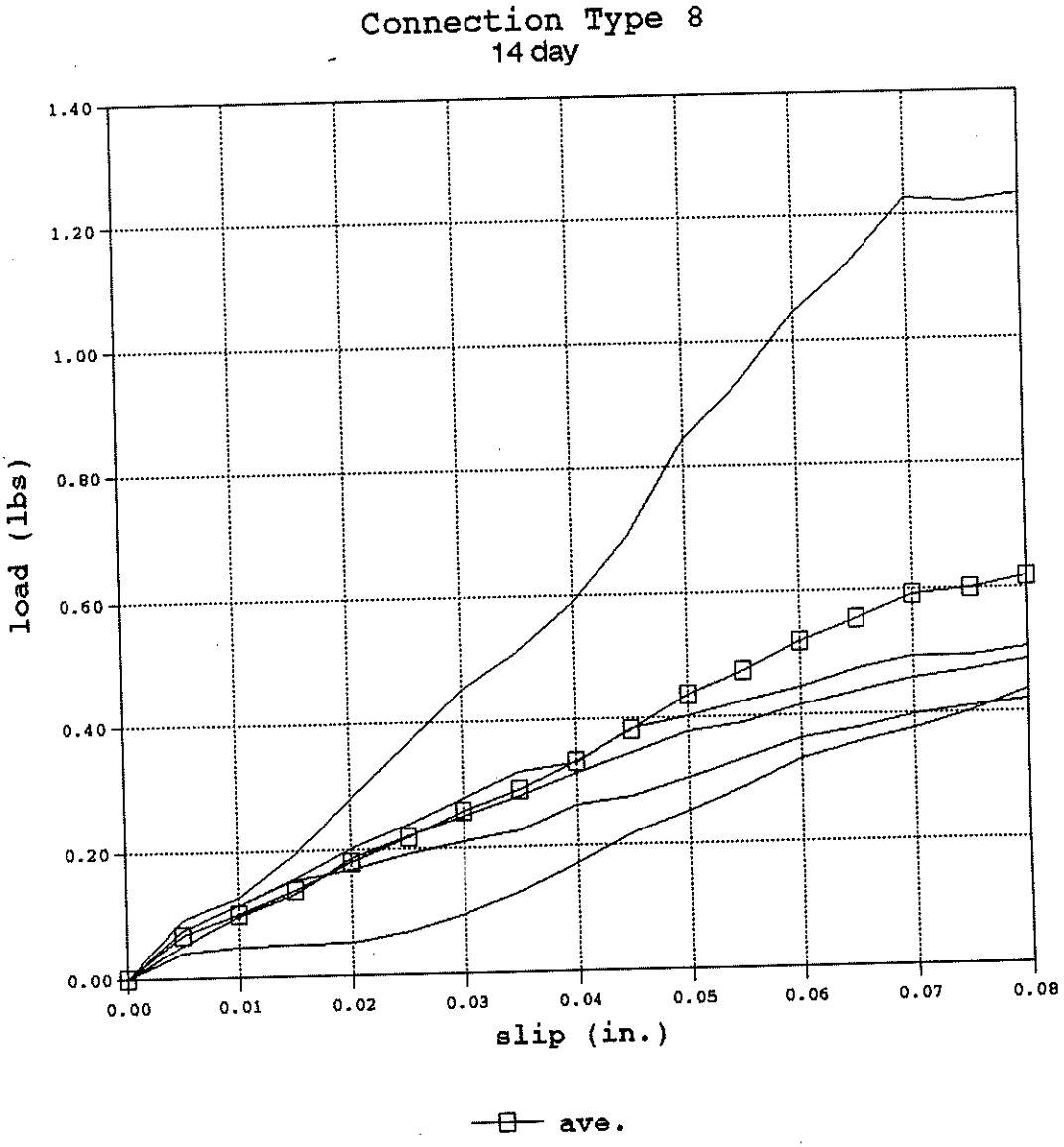

Figure A.8: The load-slip curves of specimens in connection type 8 (14 days)

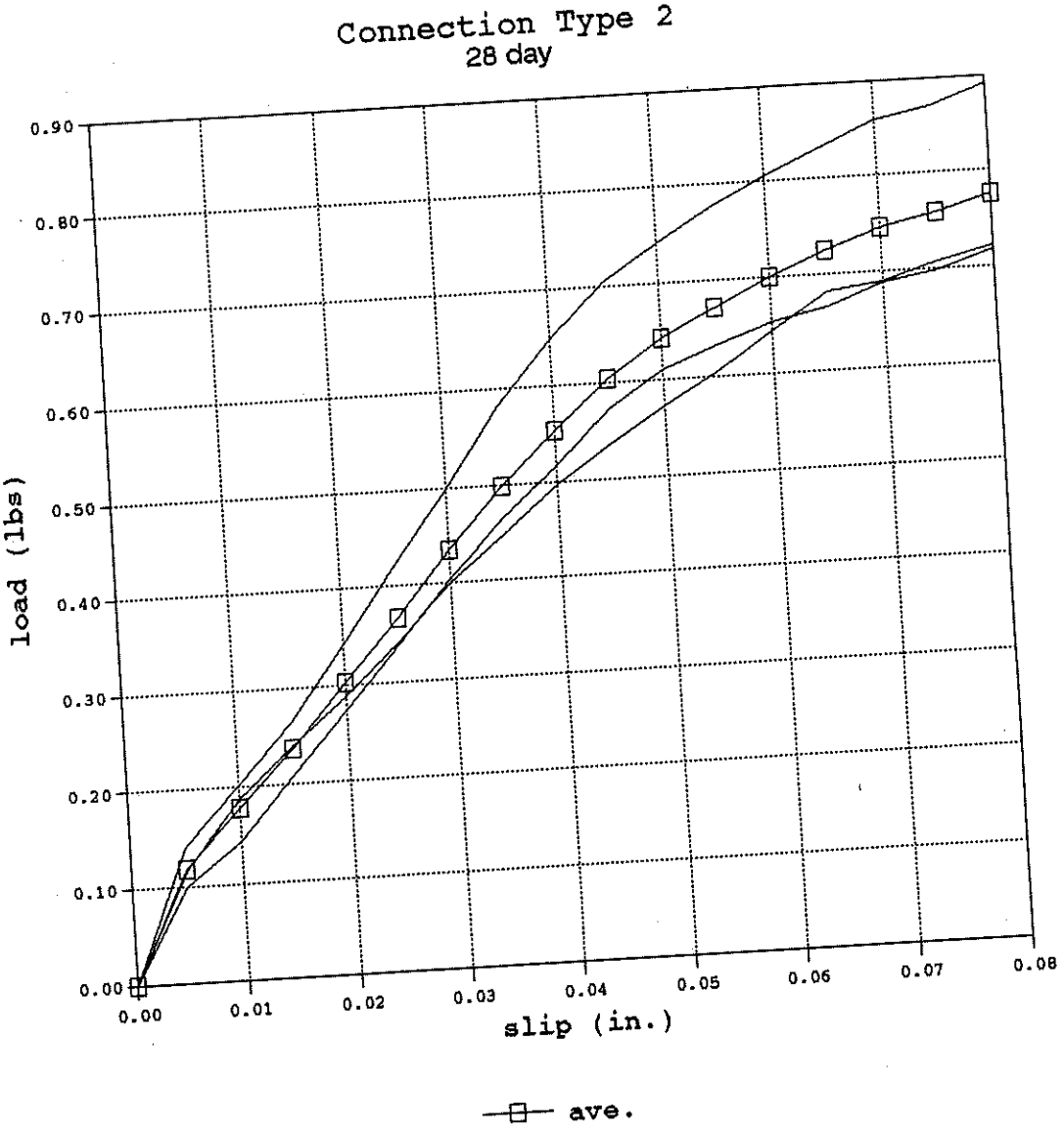

Figure A.10: The load-slip curves of specimens in connection type 2 (28 days)

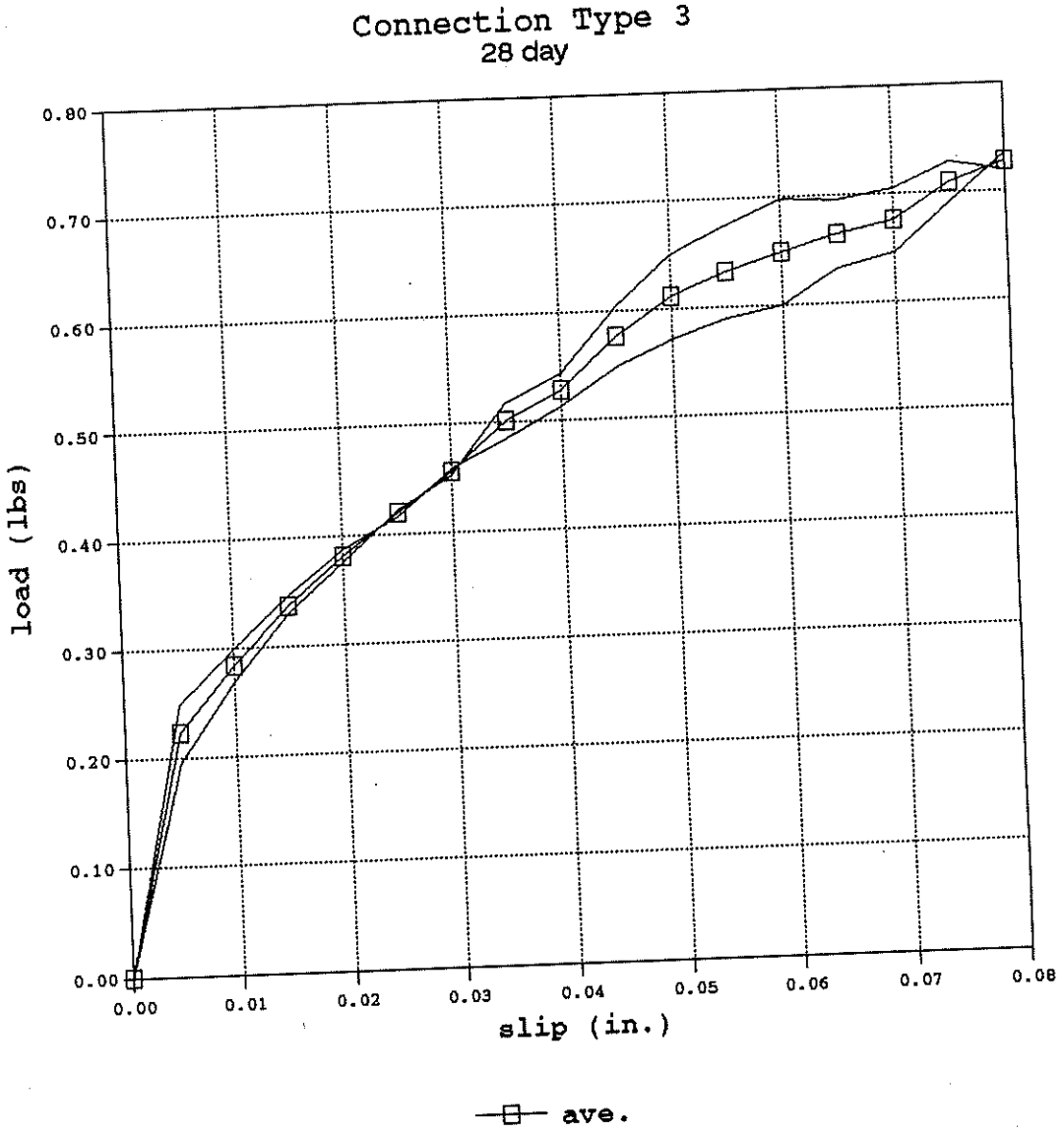

Figure A.11: The load-slip curves of specimens in connection type 3 (28 days)

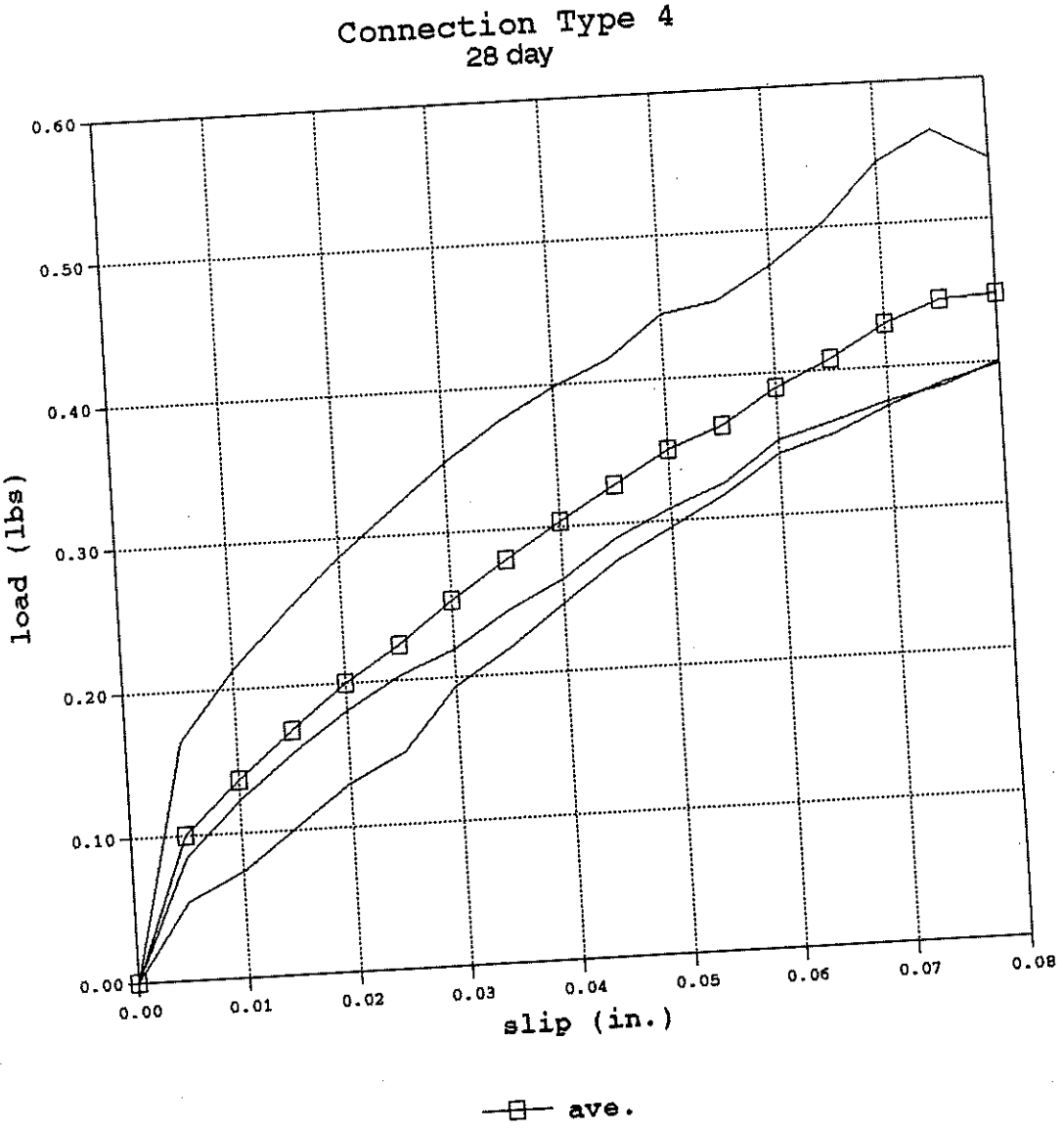

Figure A.12: The load-slip curves of specimens in connection type 4 (28 days)

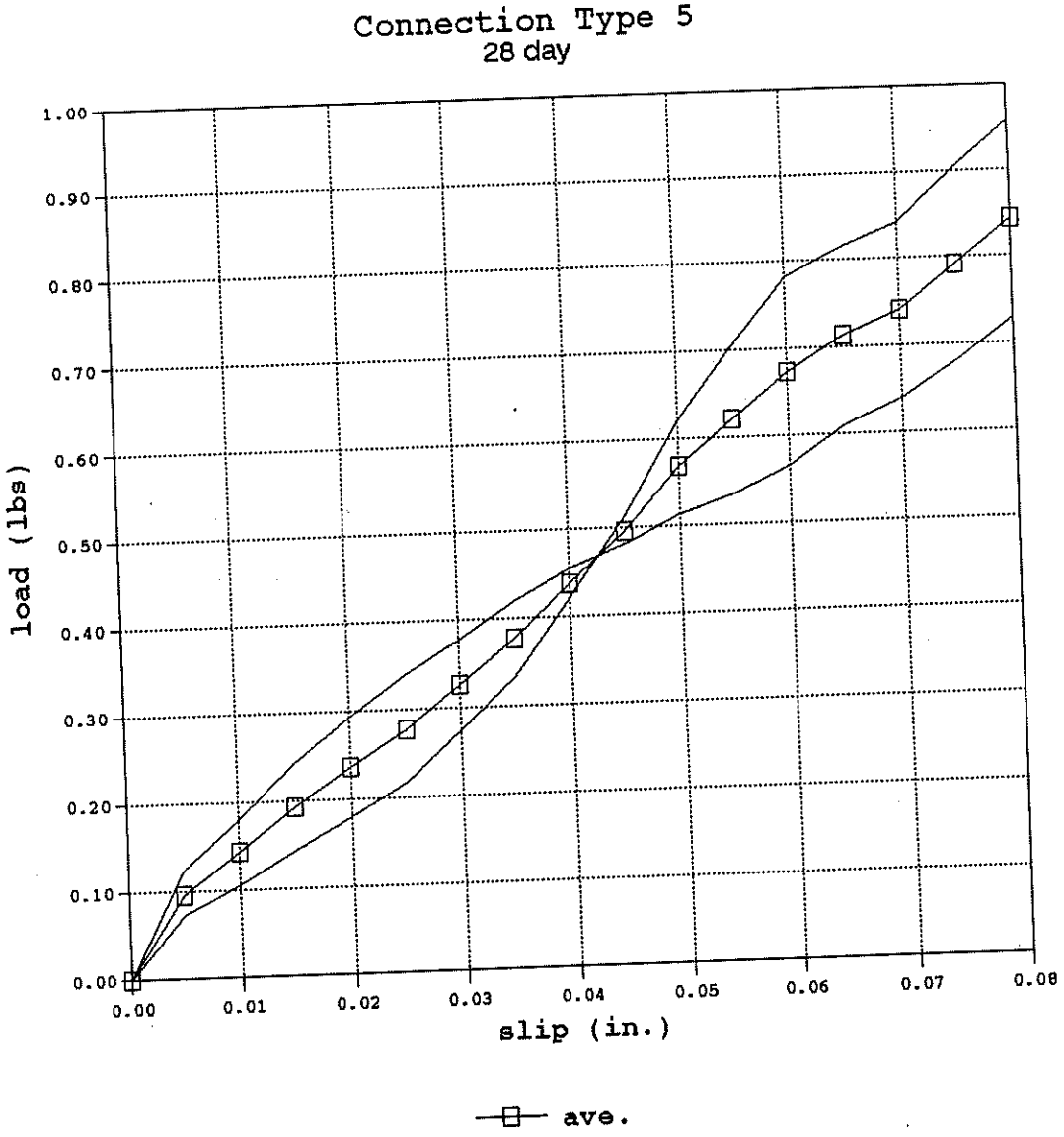

Figure A.13: The load-slip curves of specimens in connection type 5 (28 days)

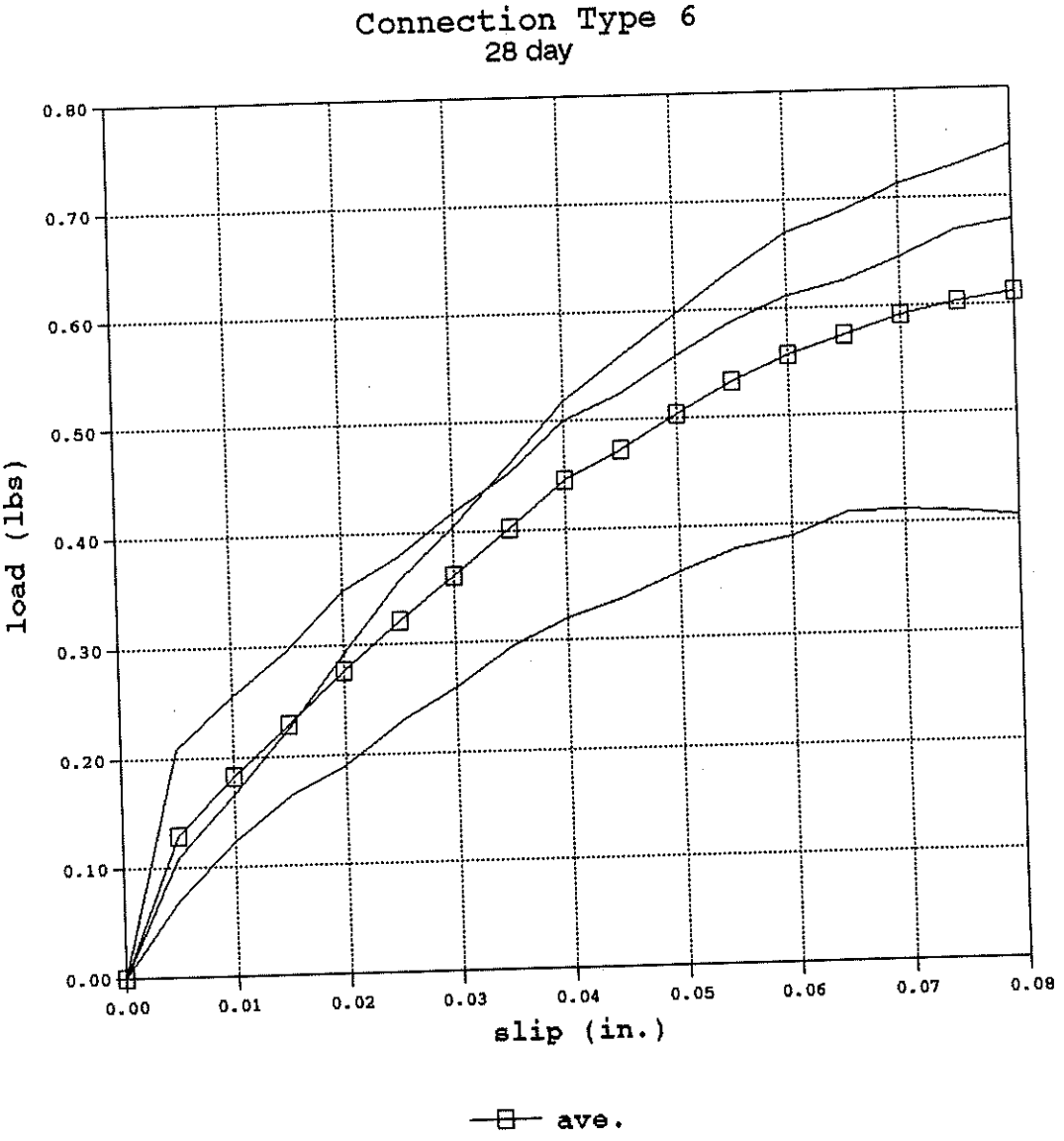

Figure A.14: The load-slip curves of specimens in connection type 6 (28 days)

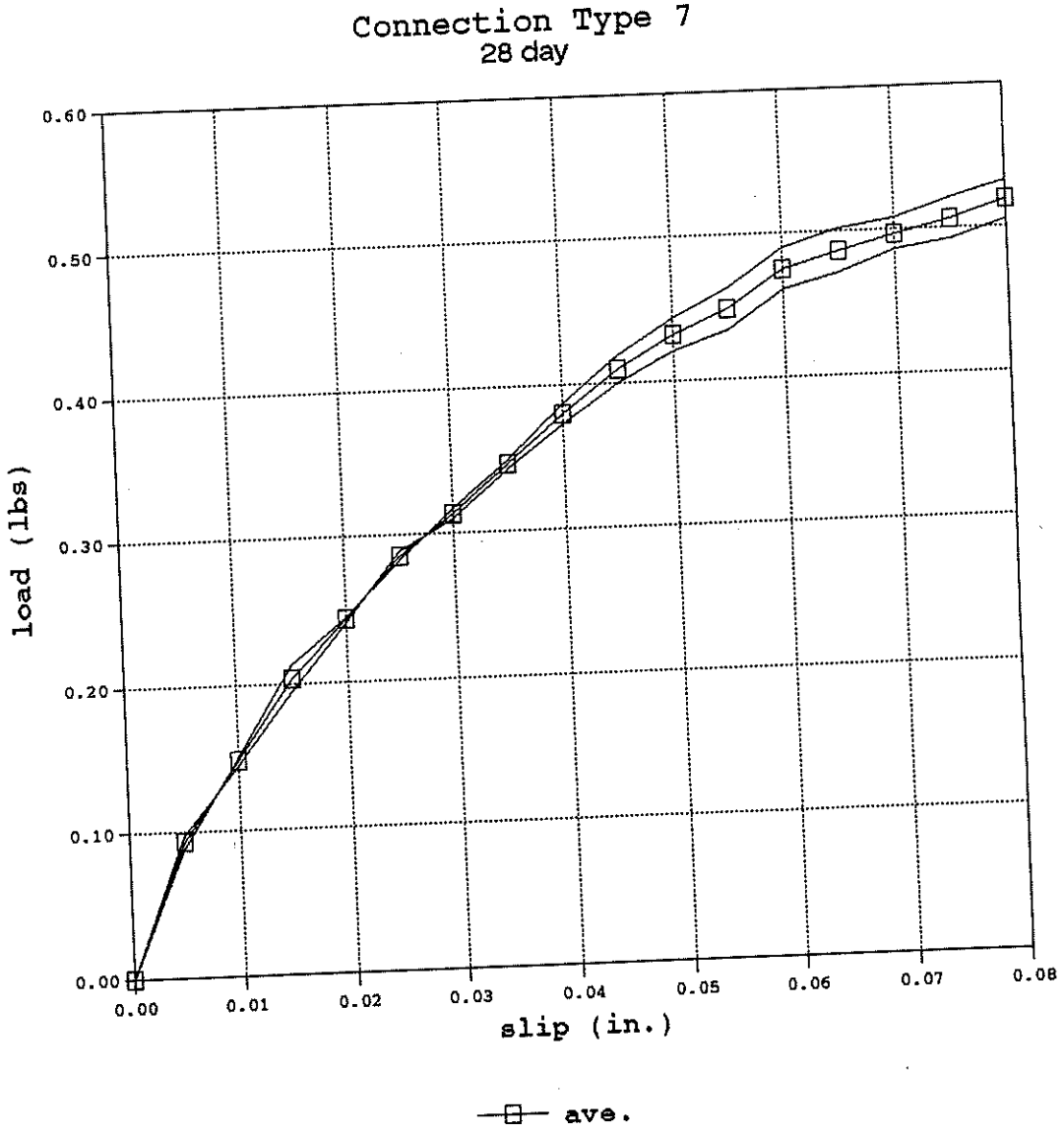

Figure A.15: The load-slip curves of specimens in connection type 7 (28 days)

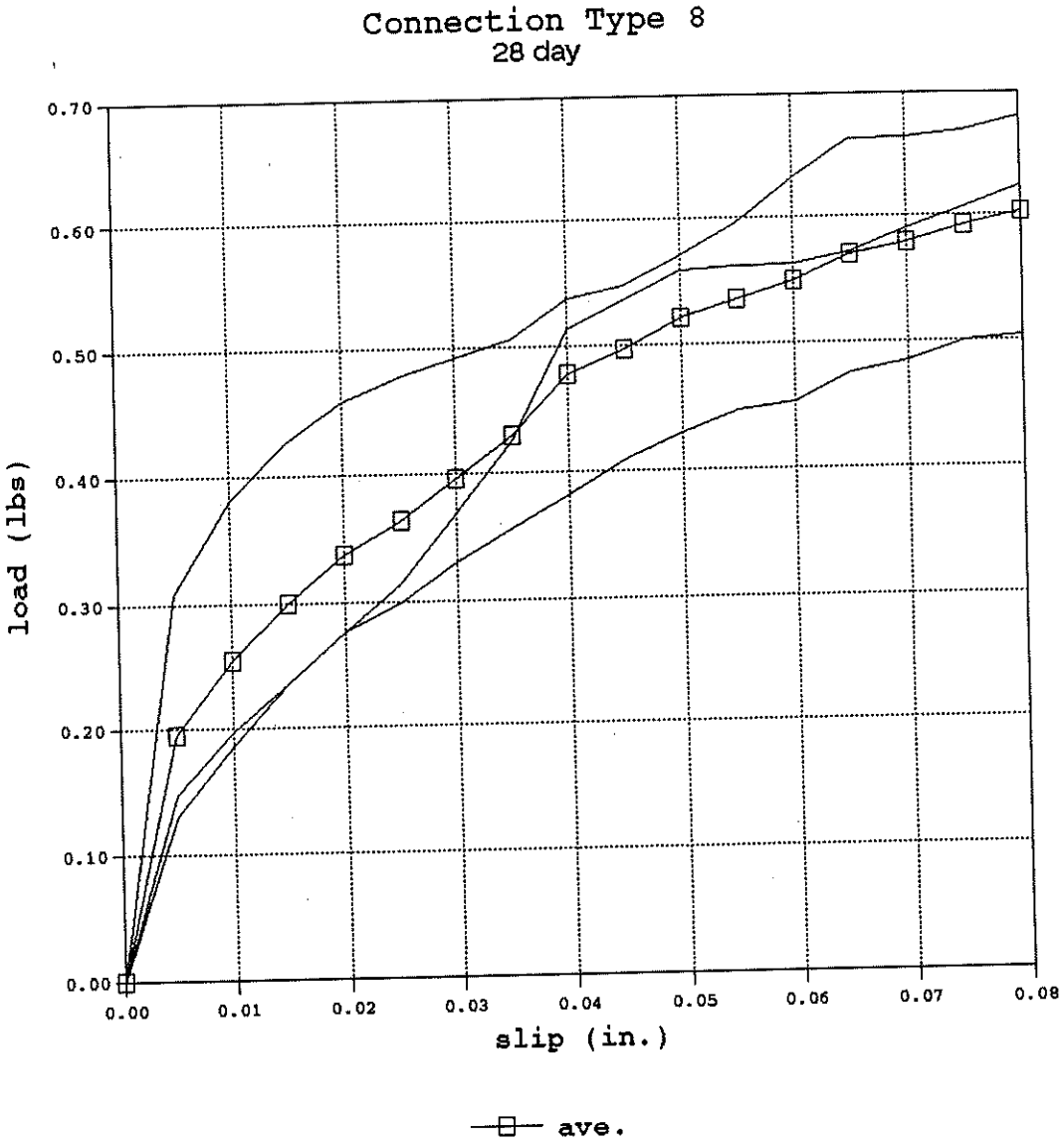

Figure A.16: The load-slip curves of specimens in connection type 8 (28 days)

APPENDIX B

THE LOAD-DEFLECTION CURVES OF T-BEAM BENDING TESTS

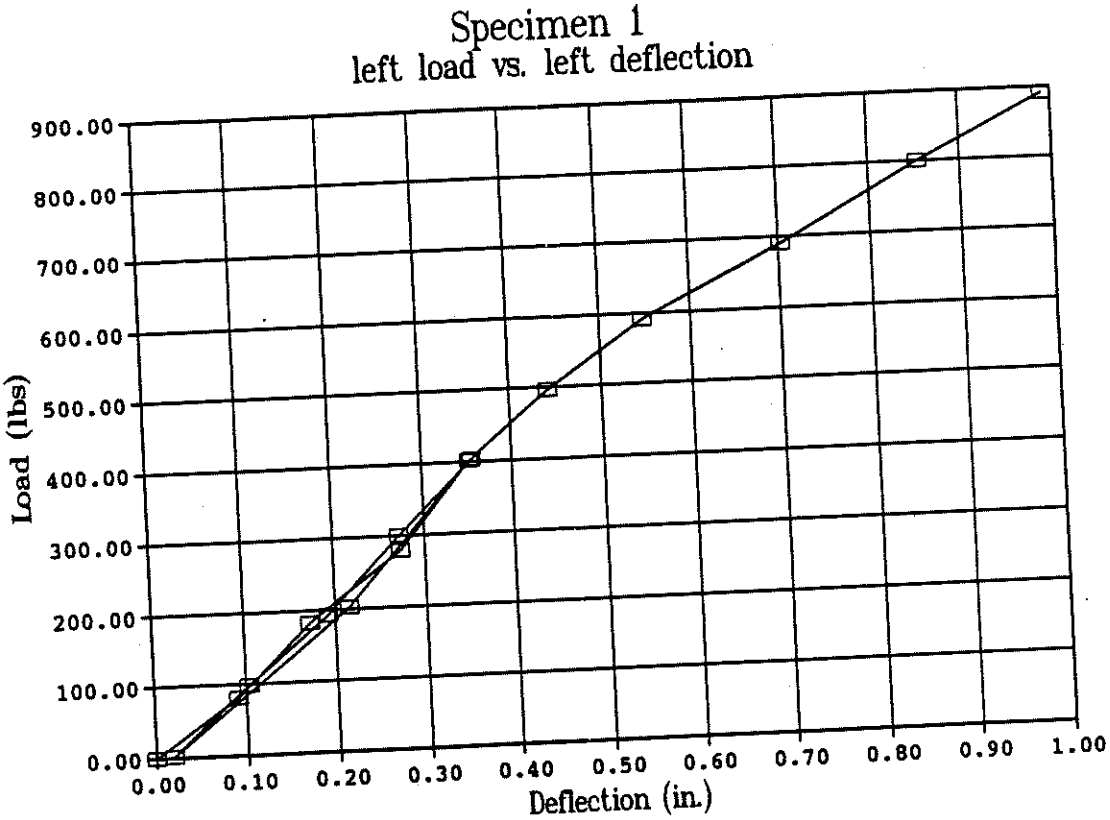

Figure B.1: Load-deflection curve of T-beam specimen 1

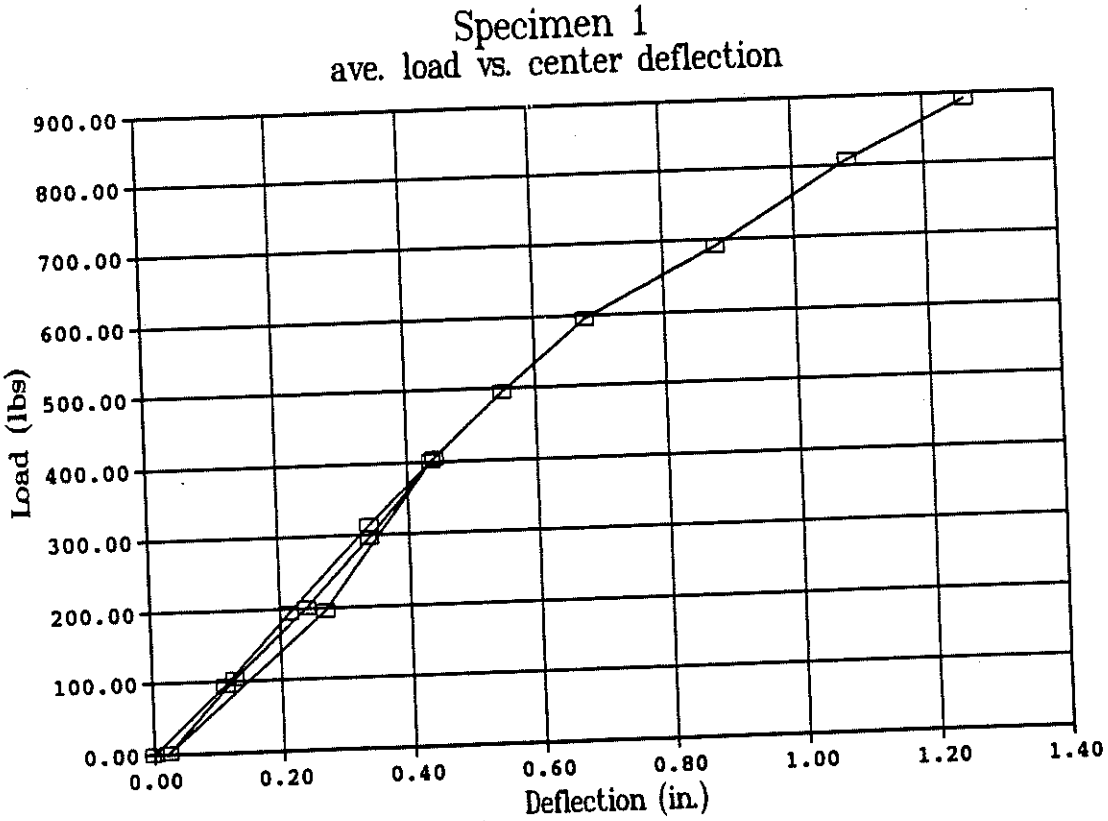

Figure B.2: Load-deflection curve of T-beam specimen 1

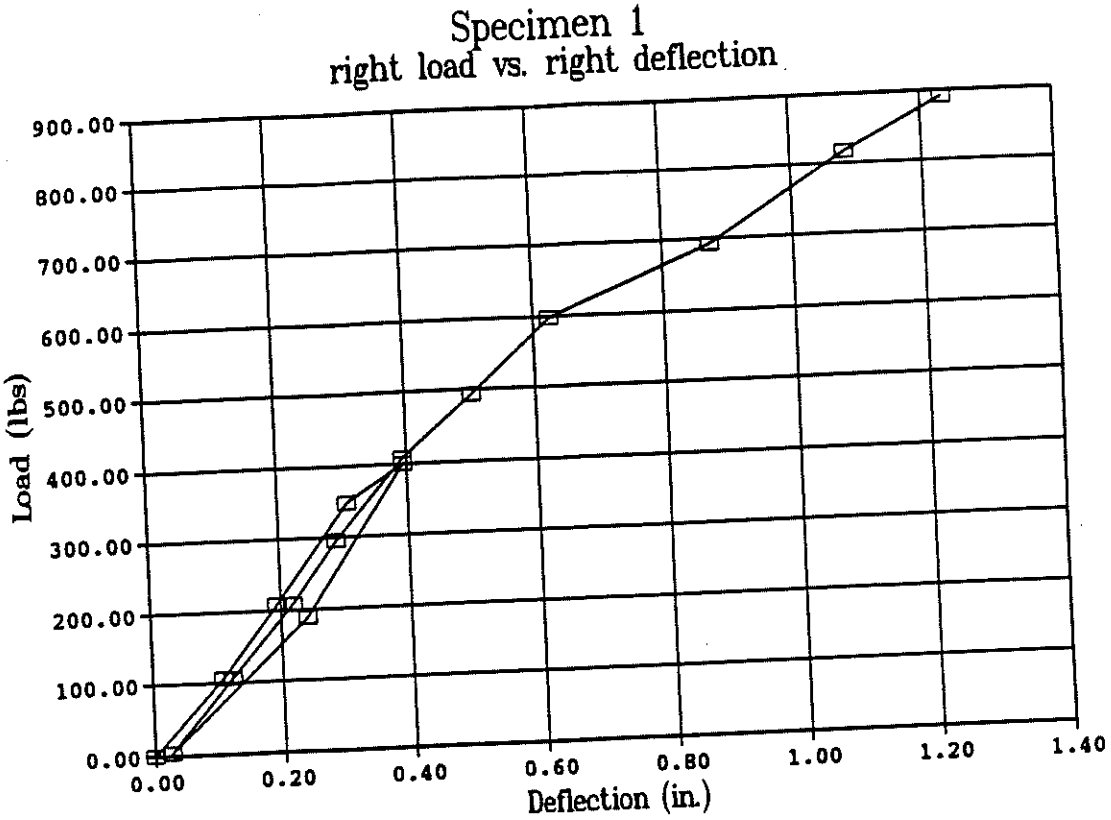

Figure B.3: Load-deflection curve of T-beam specimen 1

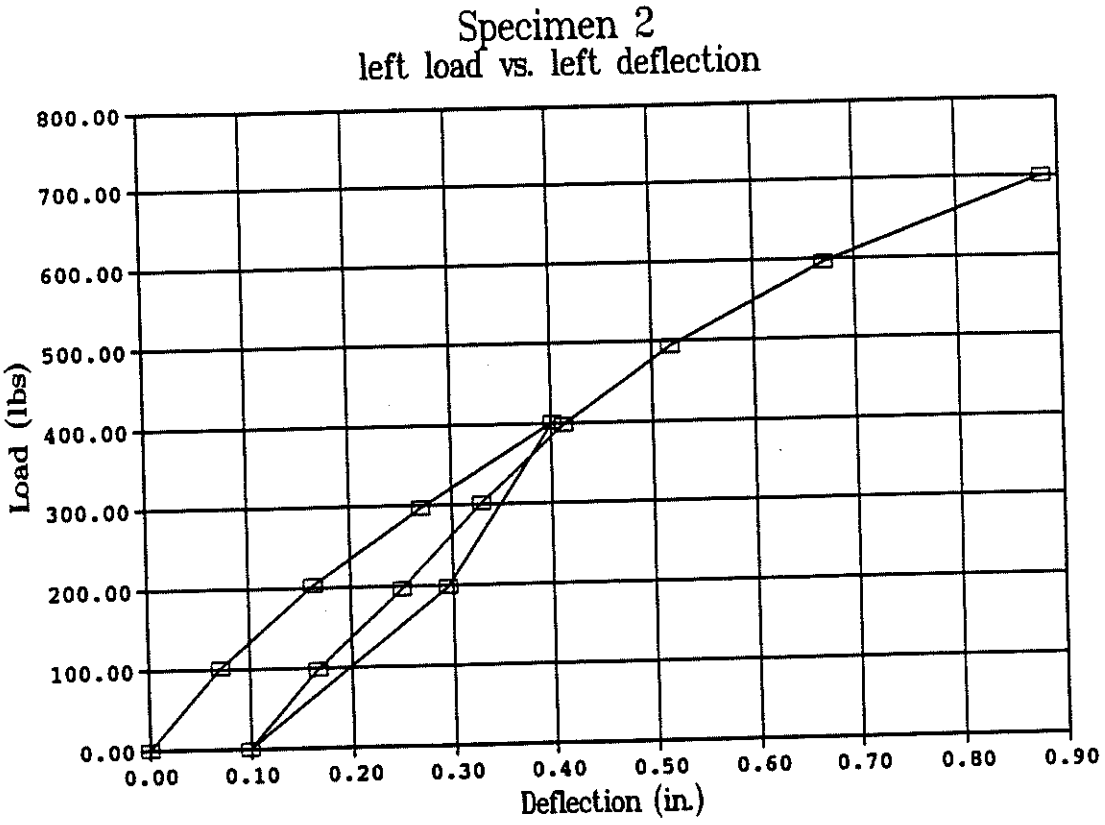

Figure B.4: Load-deflection curve of T-beam specimen 2

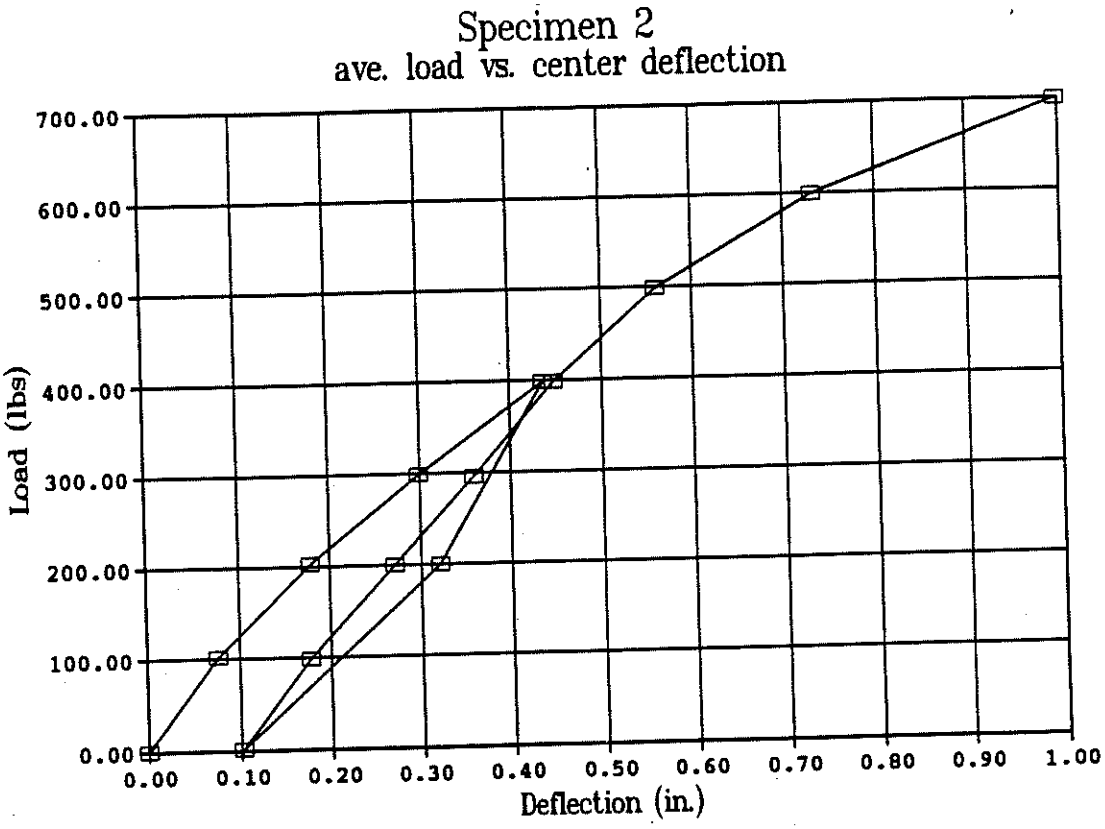

Figure B.5: Load-deflection curve of T-beam specimen 2

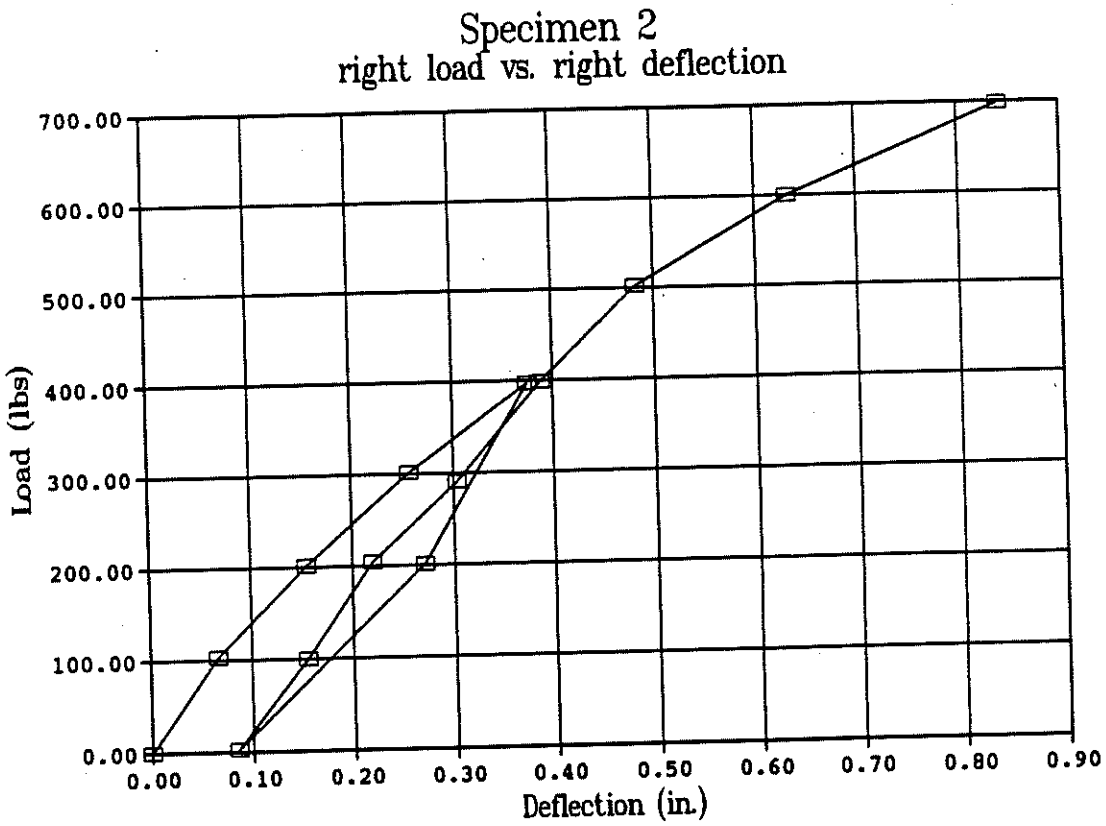

Figure B.6: Load-deflection curve of T-beam specimen 2

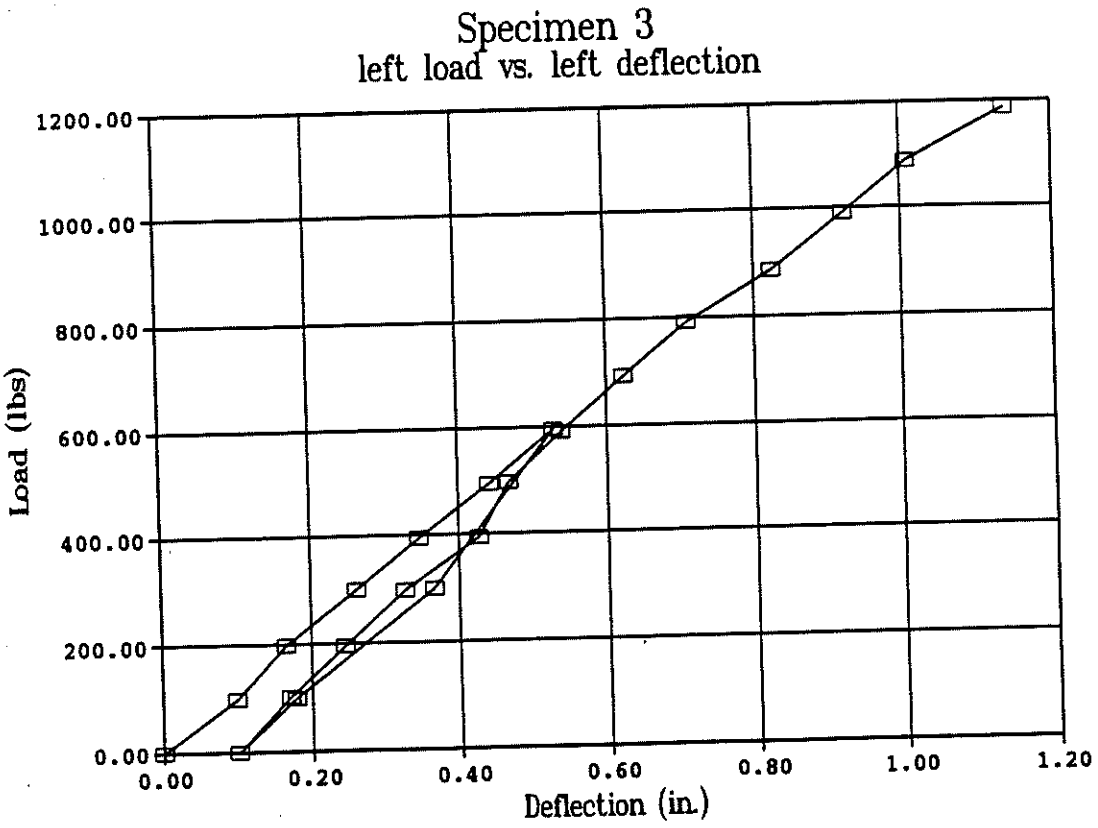

Figure B.7: Load-deflection curve of T-beam specimen 3

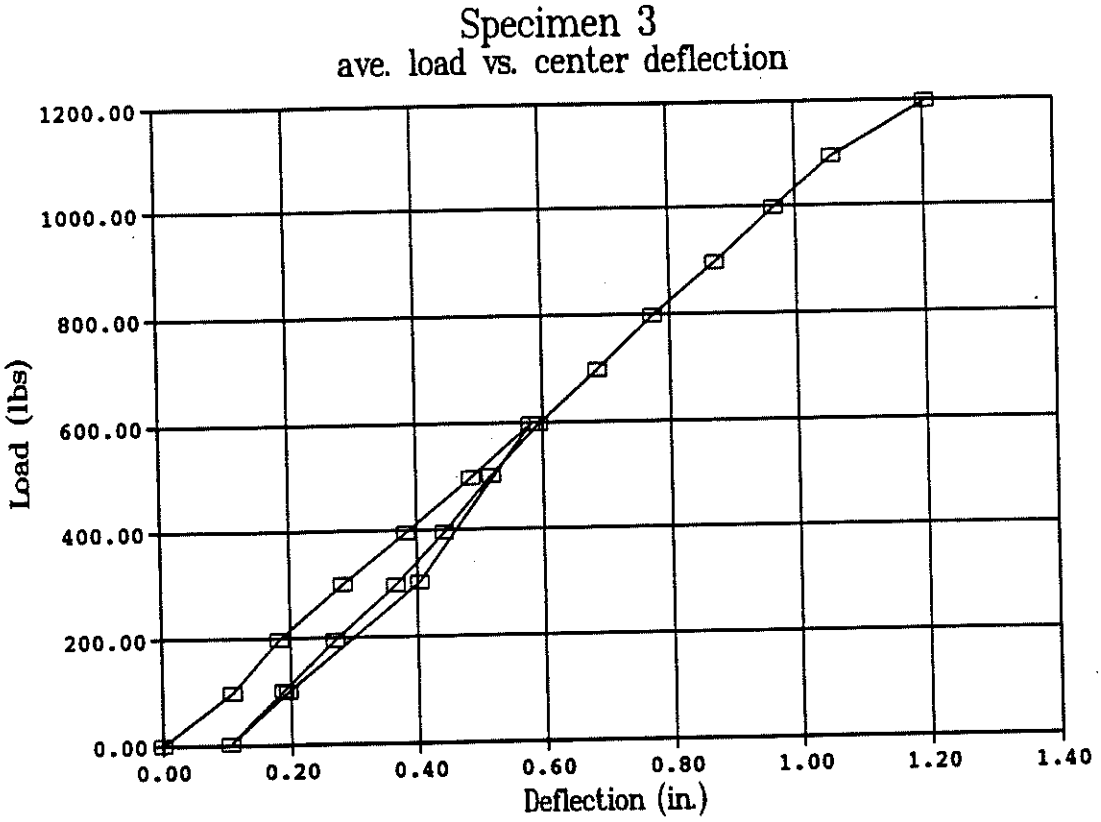

Figure B.8: Load-deflection curve of T-beam specimen 3

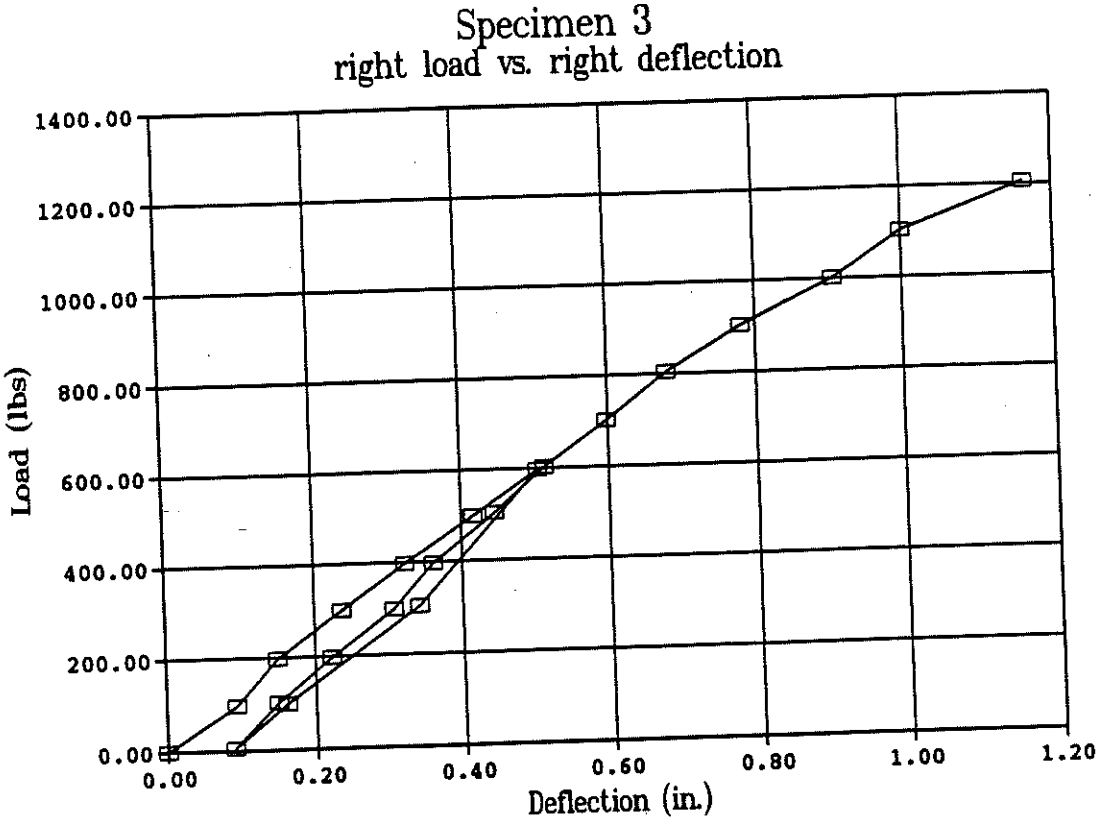

Figure B.9: Load-deflection curve of T-beam specimen 3

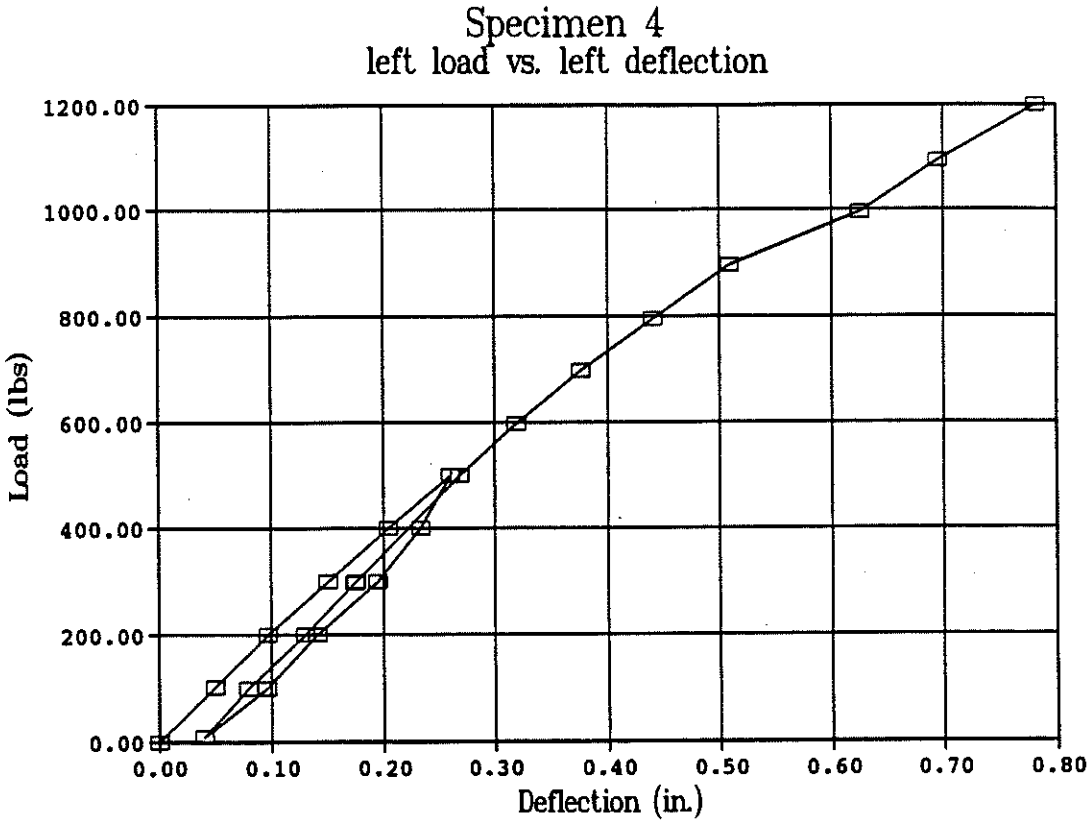

Figure B.10: Load-deflection curve of T-beam specimen 4

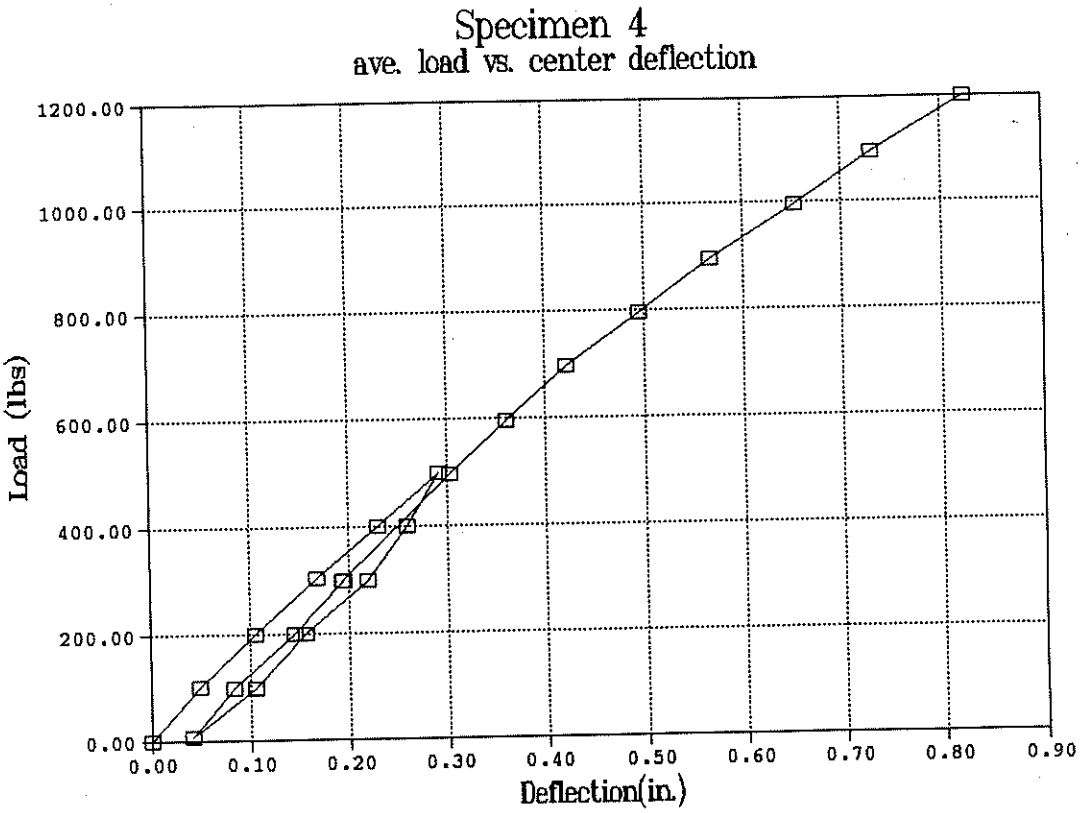

Figure B.11: Load-deflection curve of T-beam specimen 4

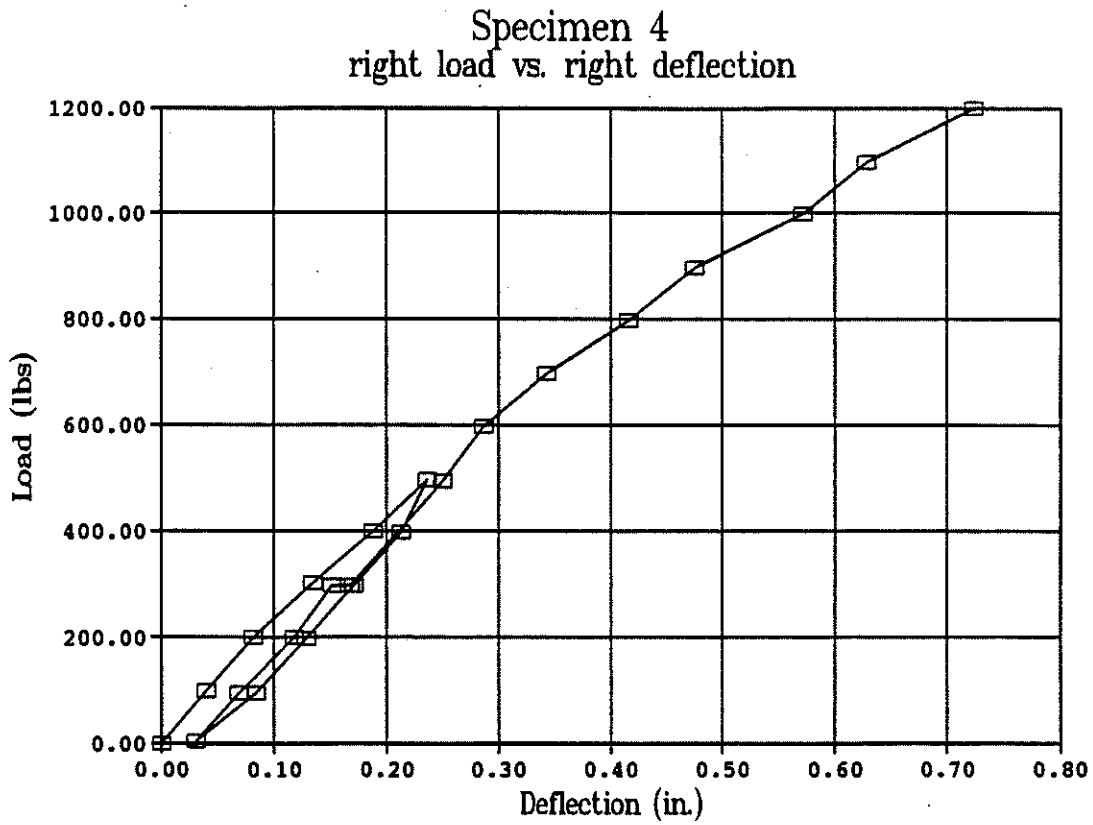

Figure B.12: Load-deflection curve of T-beam specimen 4

APPENDIX C

COMPARISON OF THE THEORETICAL AND EXPERIMENTAL RESULTS OF T-BEAM SPECIMENS

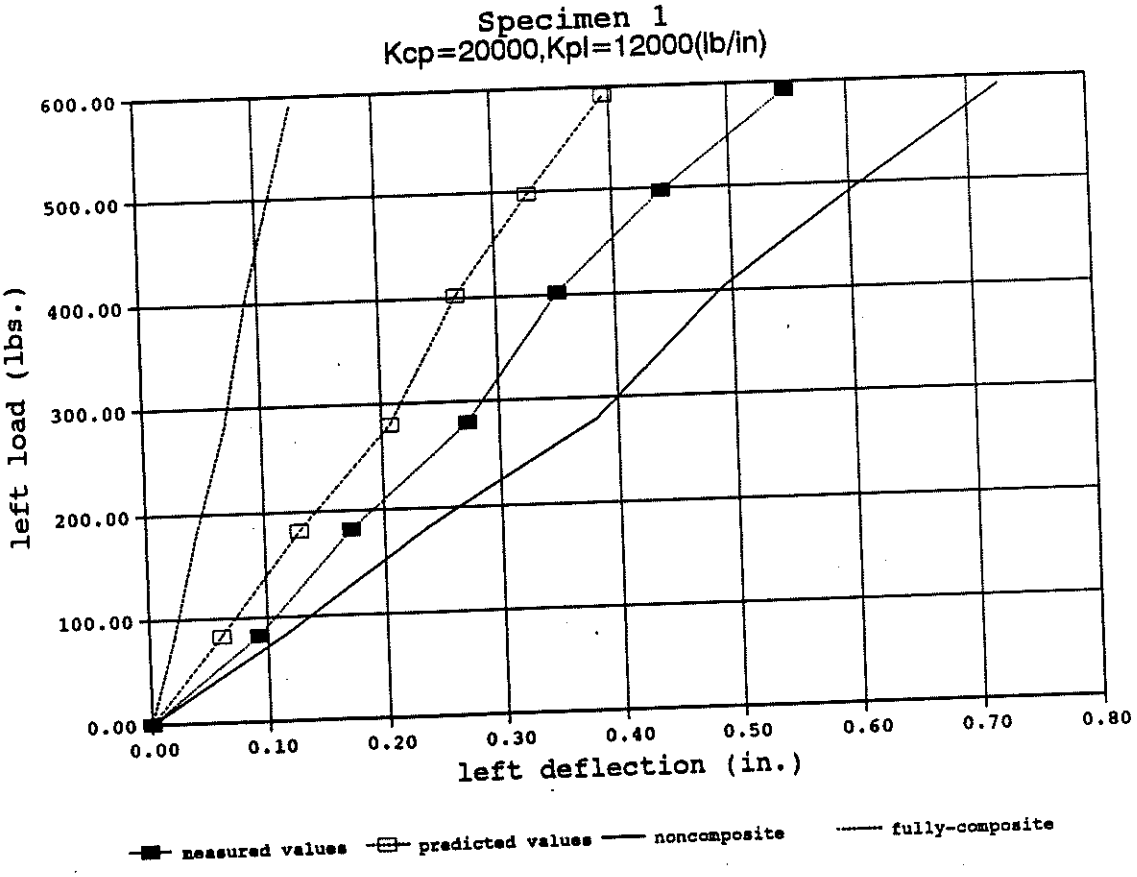

Figure C1.1: The theoretical and experimental load-deflection curves of T-beam

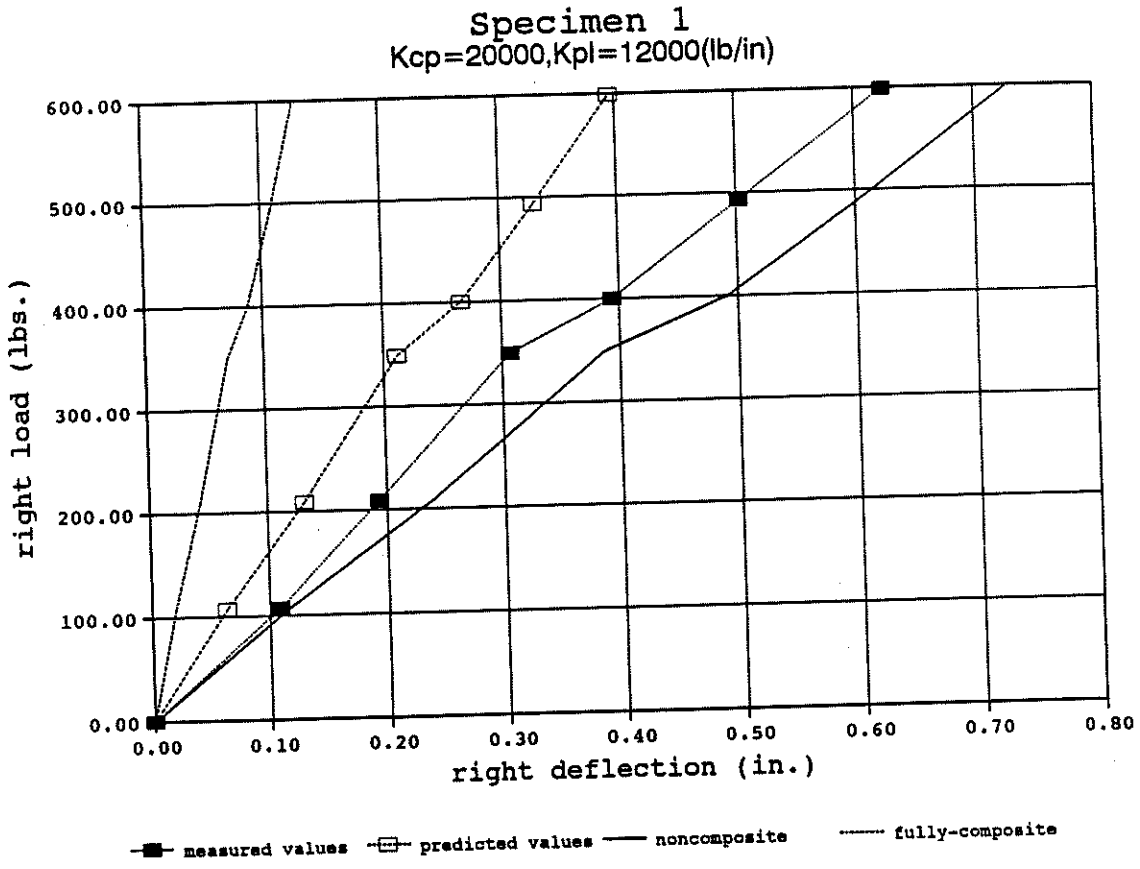

Figure C1.2: The theoretical and experimental load-deflection curves of T-beam

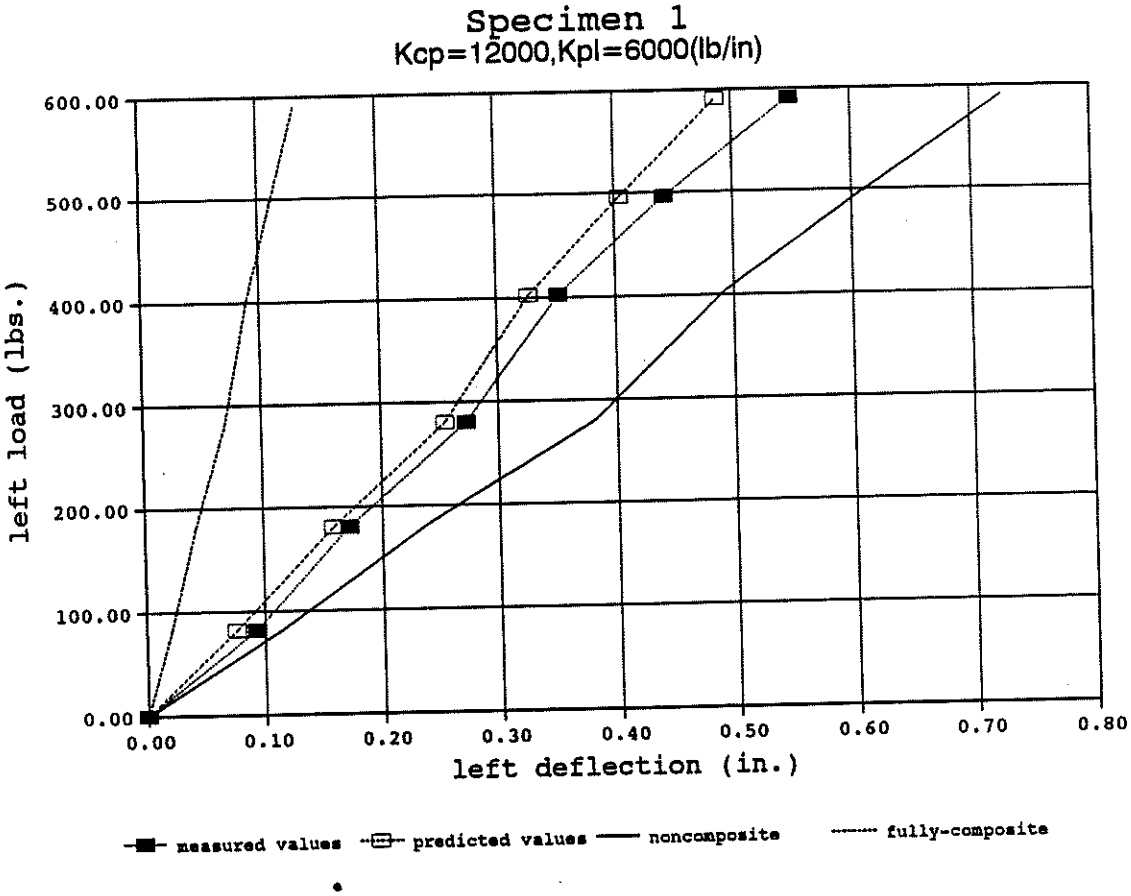

Figure C1.3: The theoretical and experimental load-deflection curves of T-beam

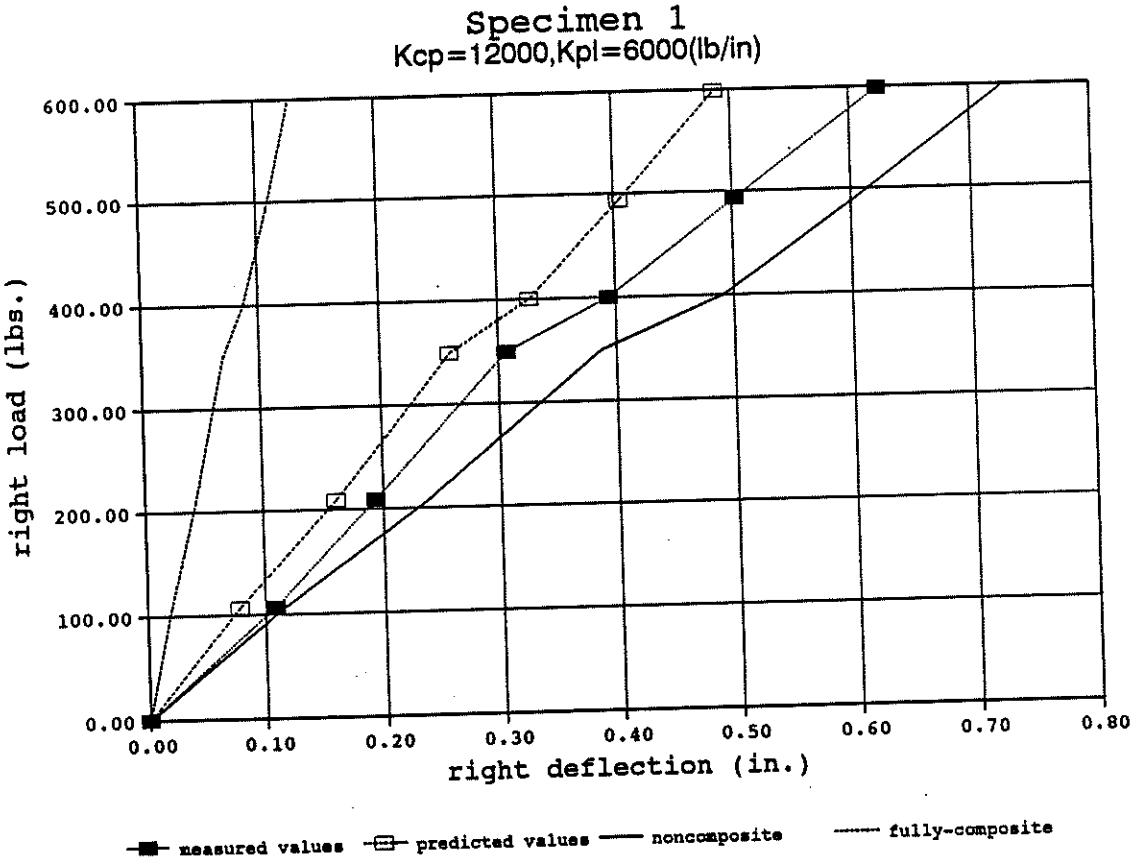

Figure C1.4: The theoretical and experimental load-deflection curves of T-beam

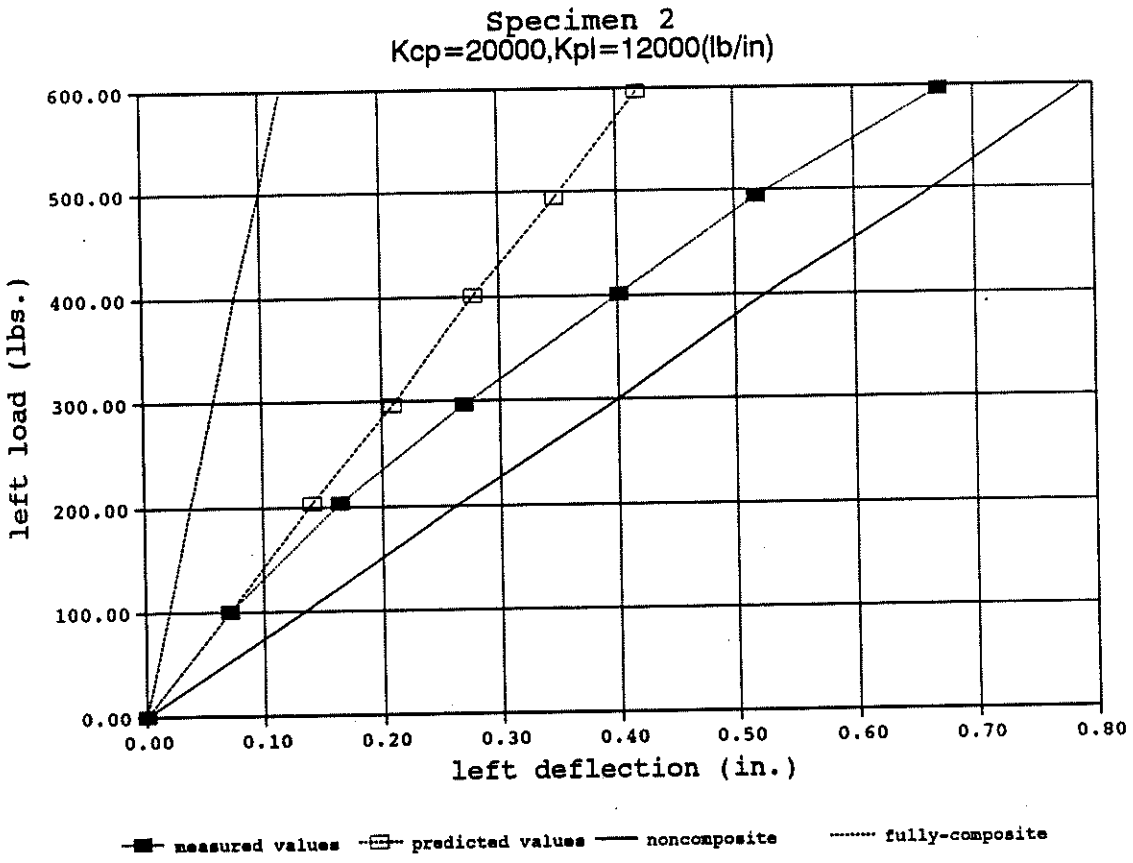

Figure C1.5: The theoretical and experimental load-deflection curves of T-beam

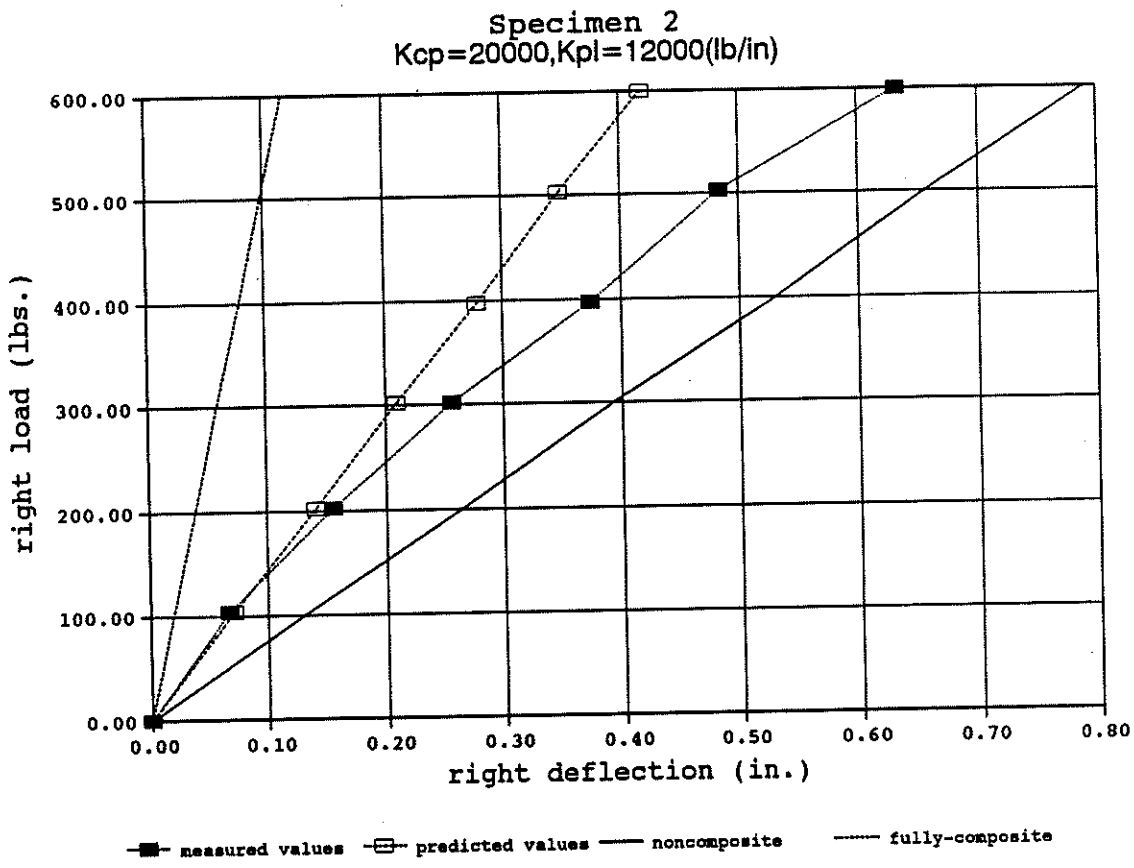

Figure C1.6: The theoretical and experimental load-deflection curves of T-beam

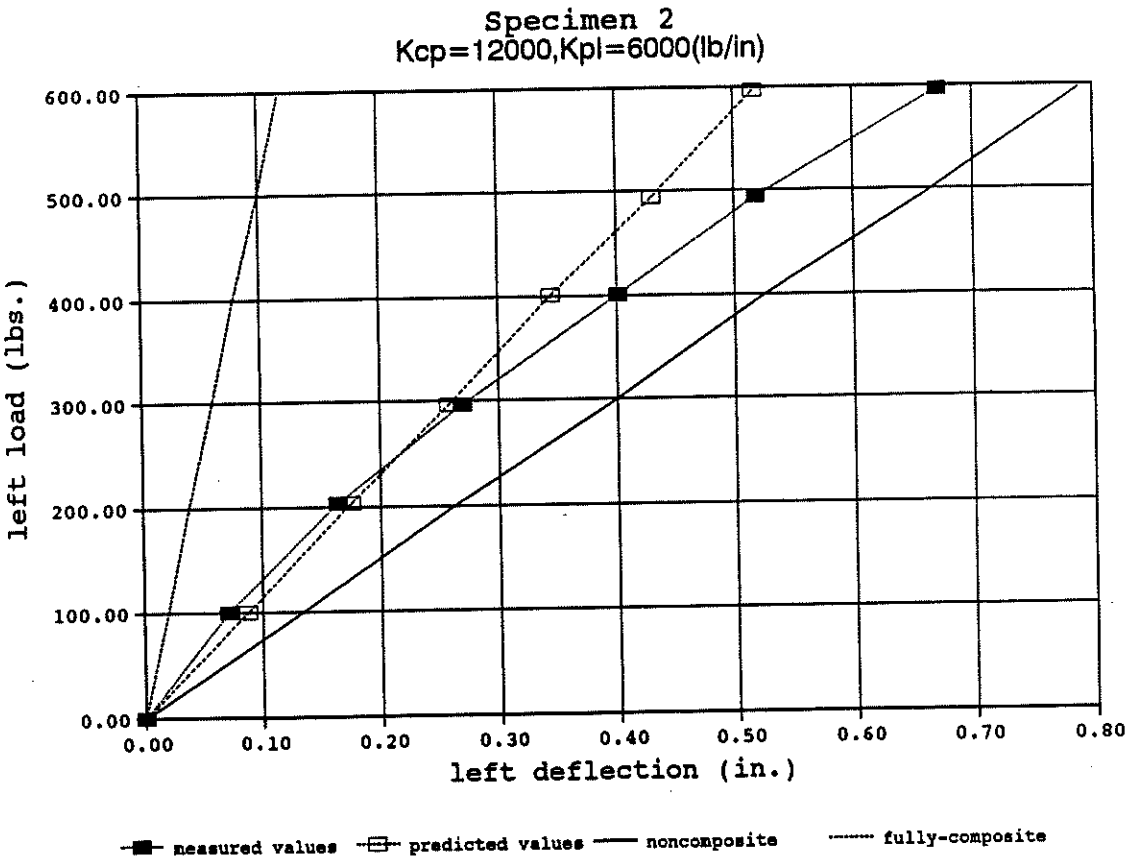

Figure C1.7: The theoretical and experimental load-deflection curves of T-beam

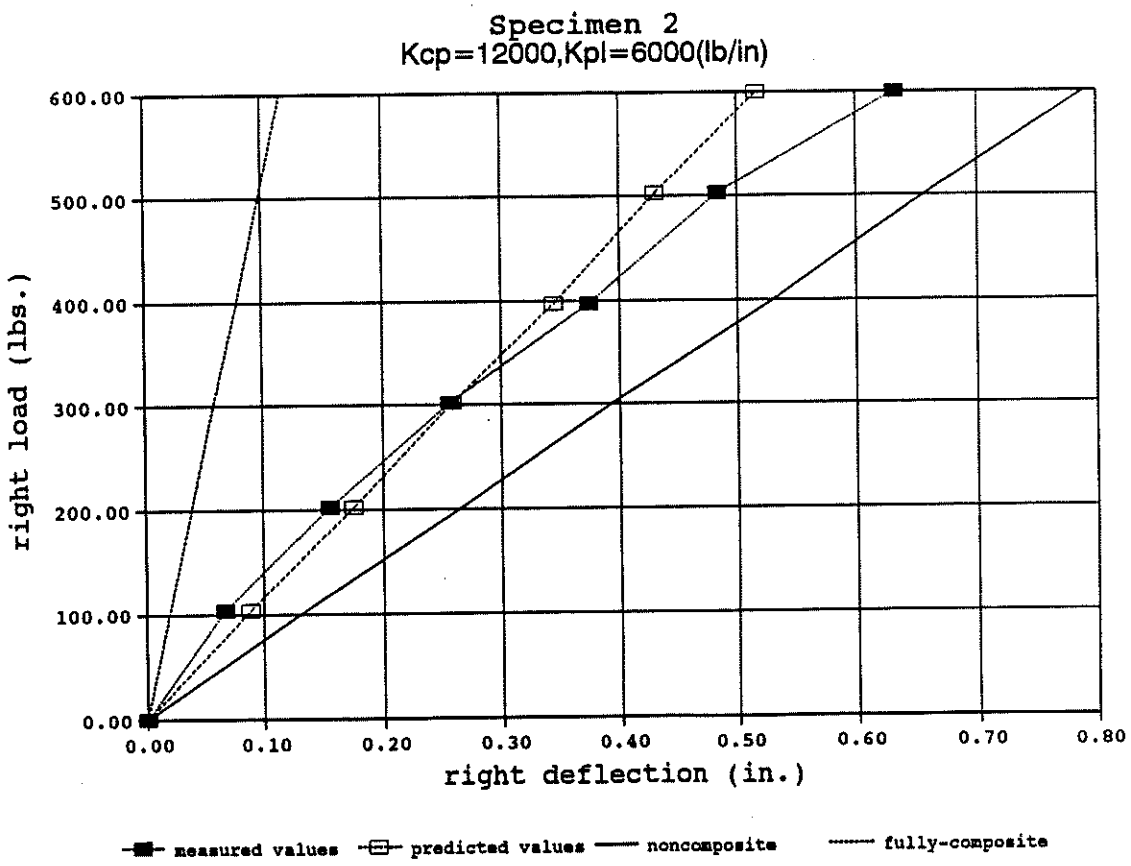

Figure C1.8: The theoretical and experimental load-deflection curves of T-beam

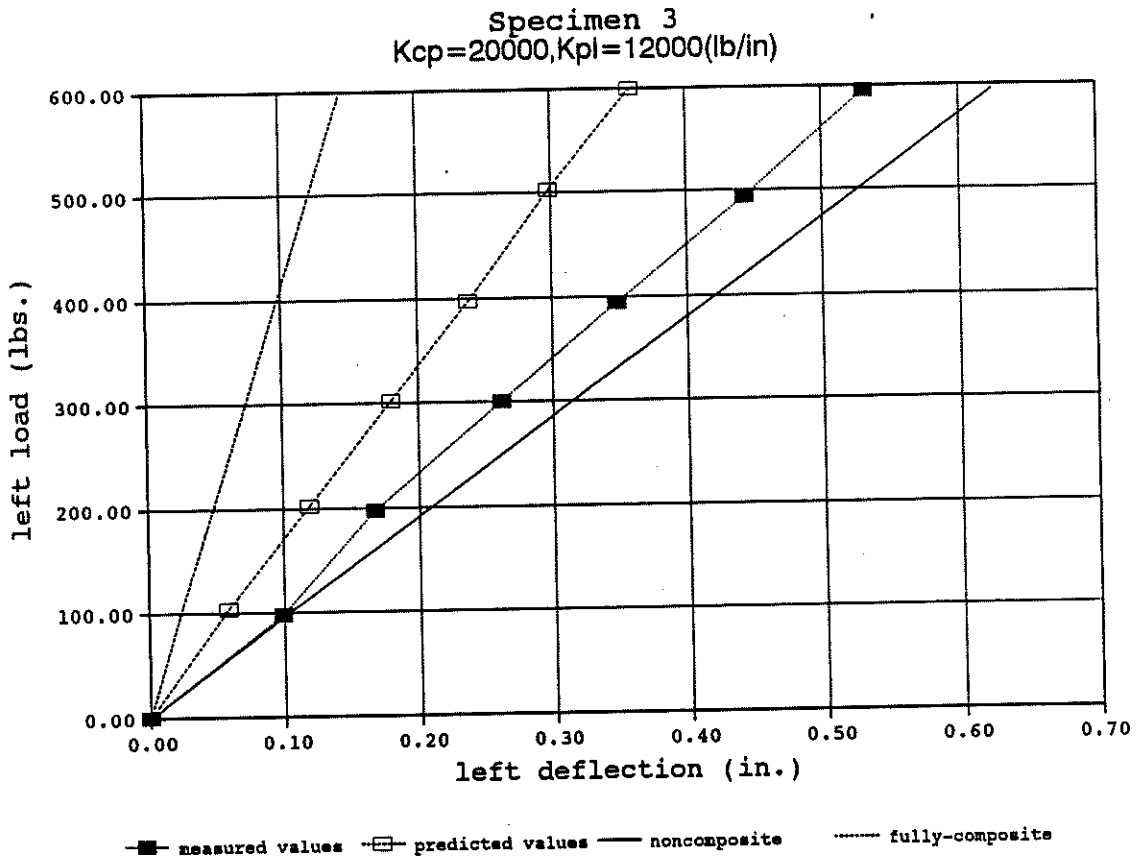

Figure C1.9: The theoretical and experimental load-deflection curves of T-beam

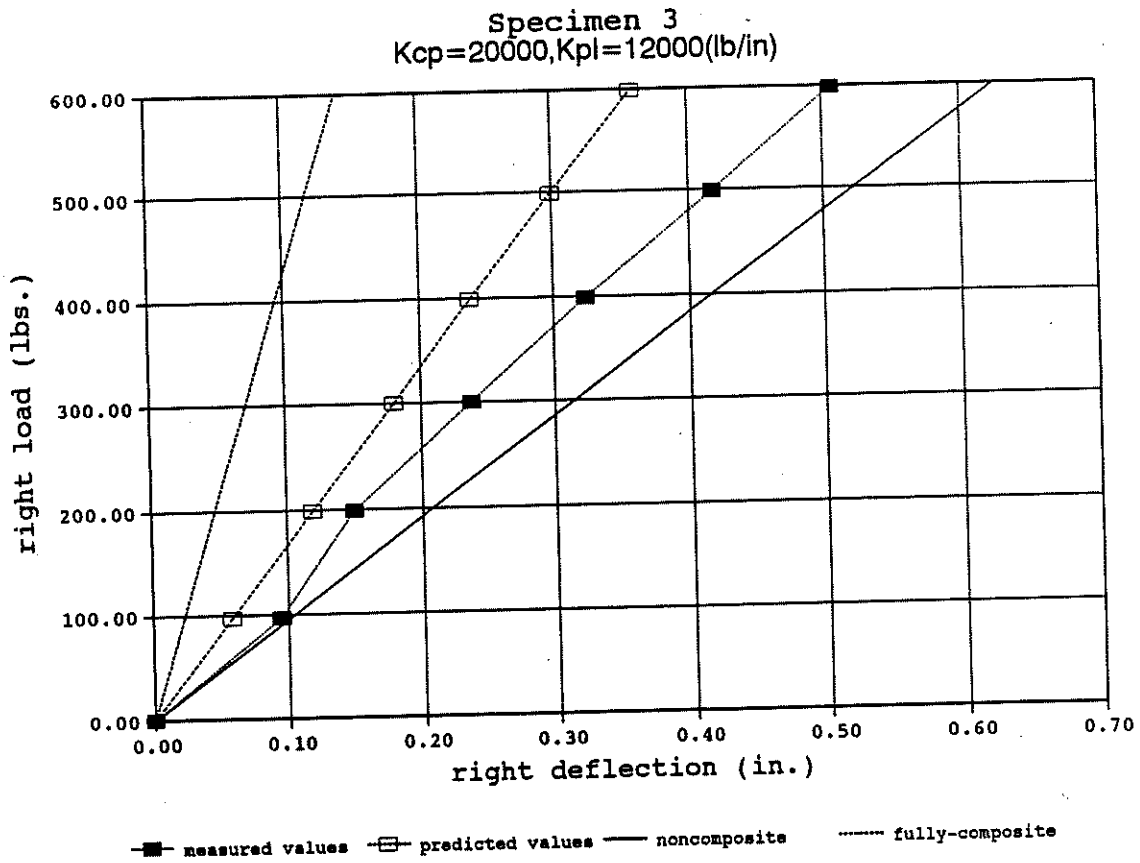

Figure C1.10: The theoretical and experimental load-deflection curves of T-beam

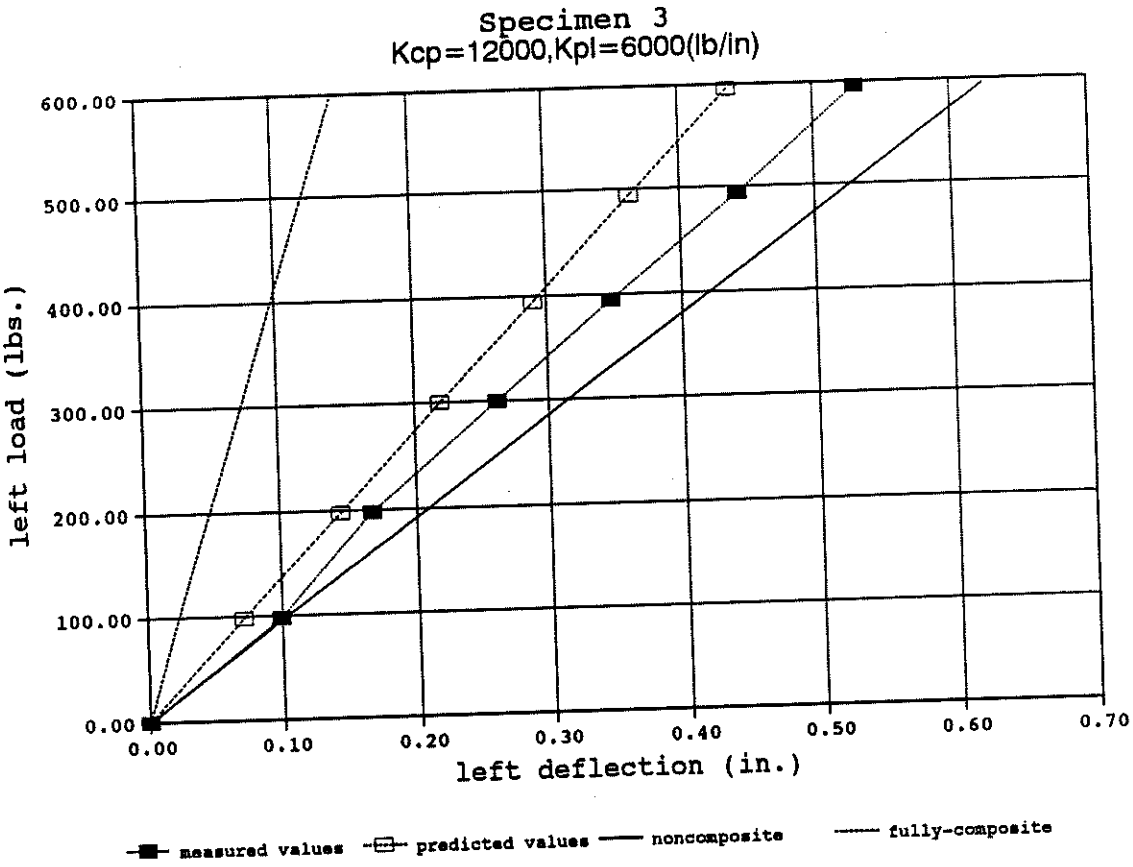

Figure C1.11: The theoretical and experimental load-deflection curves of T-beam

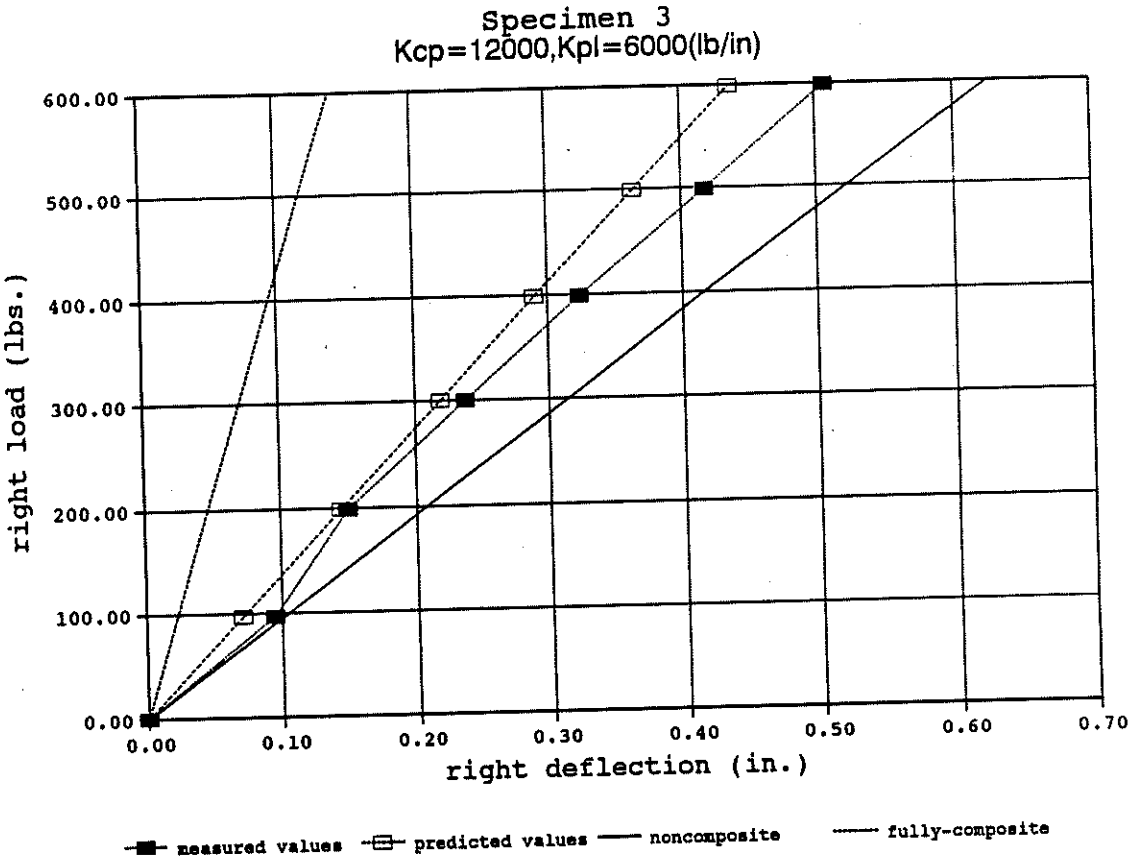

Figure C1.12: The theoretical and experimental load-deflection curves of T-beam

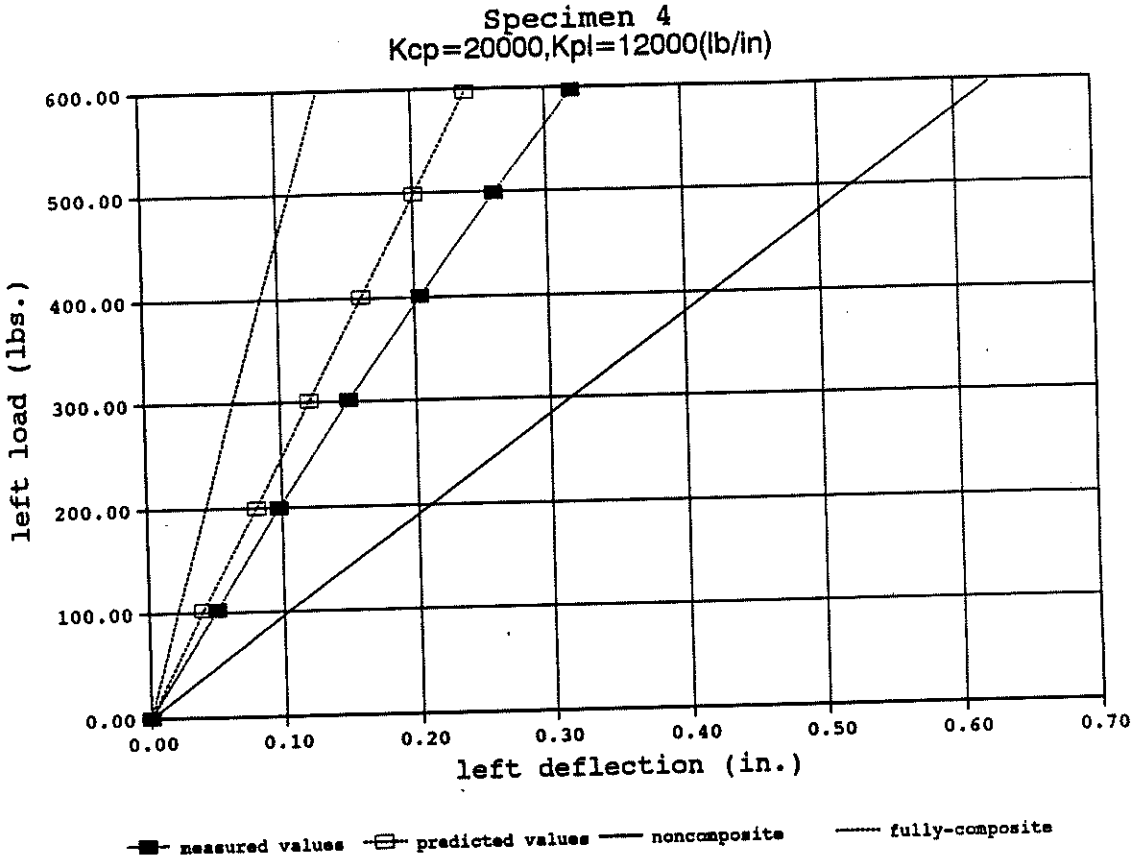

Figure C1.13: The theoretical and experimental load-deflection curves of T-beam

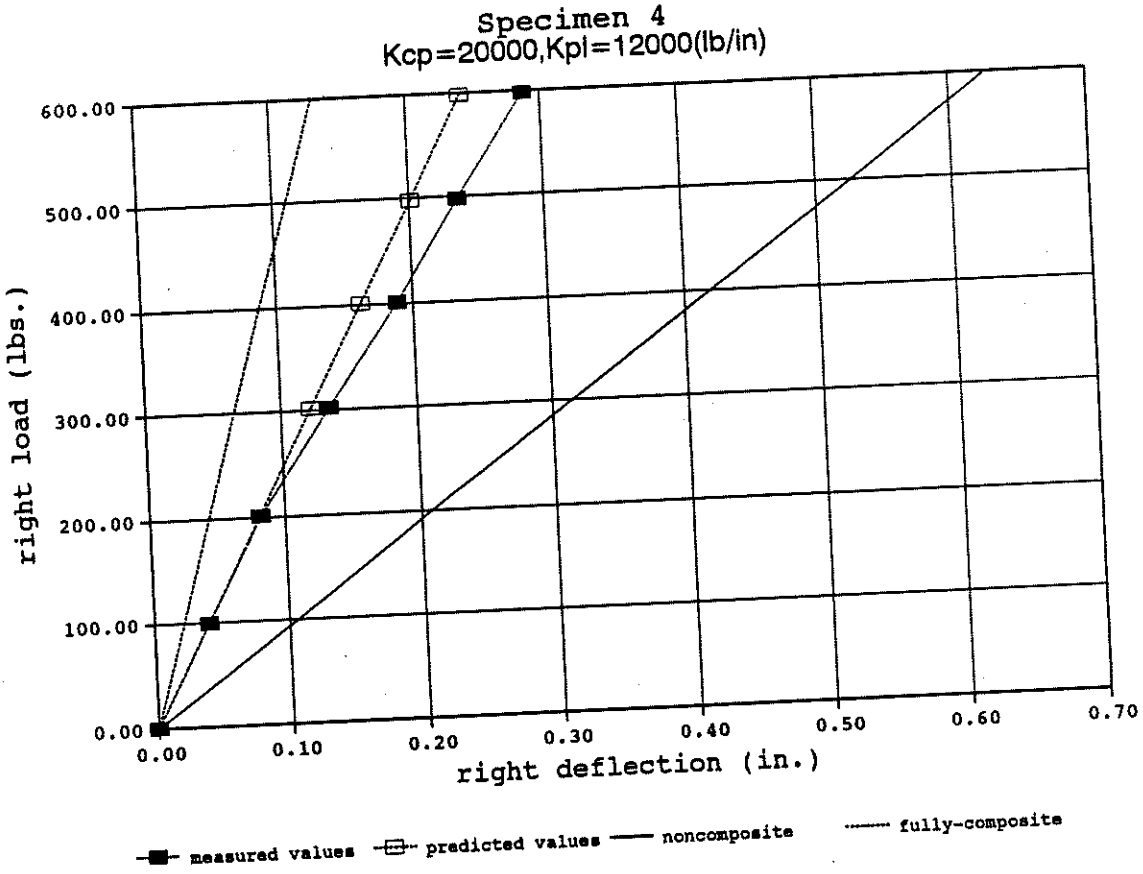

Figure C1.14: The theoretical and experimental load-deflection curves of T-beam

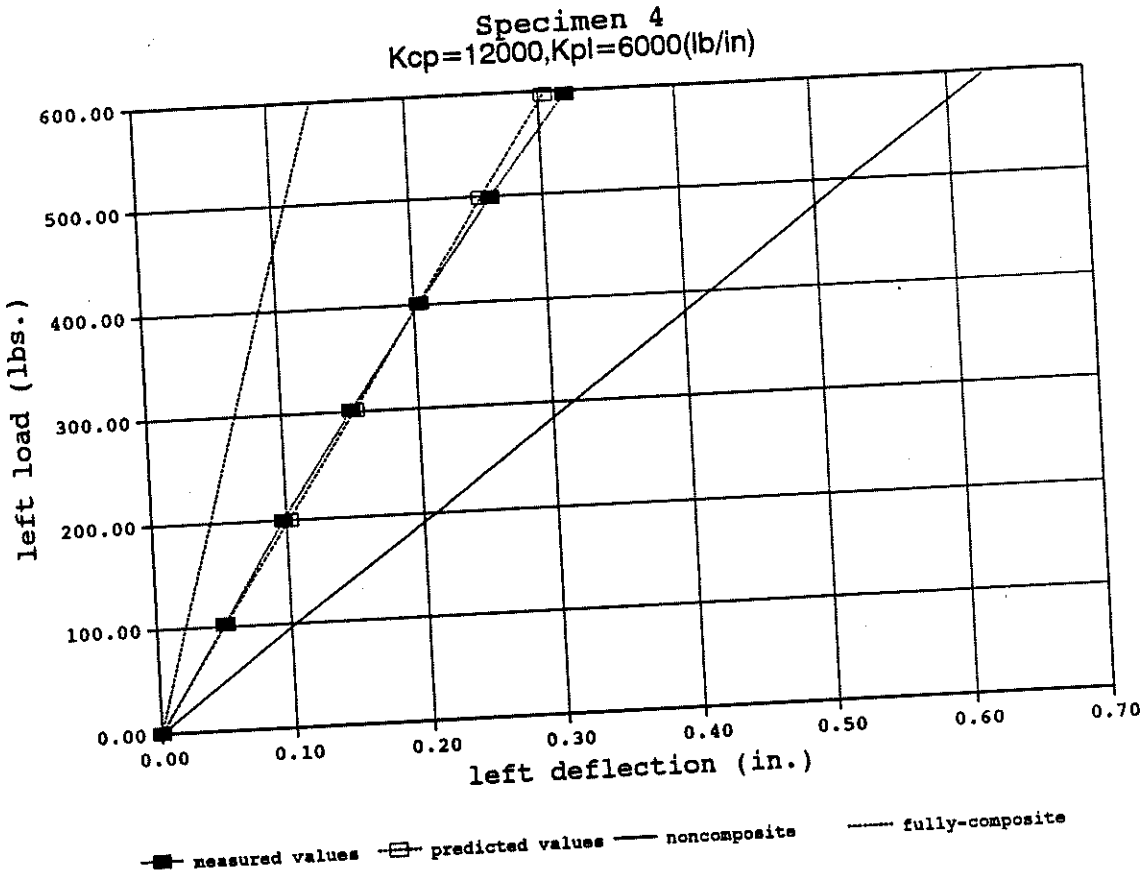

Figure C1.15: The theoretical and experimental load-deflection curves of T-beam

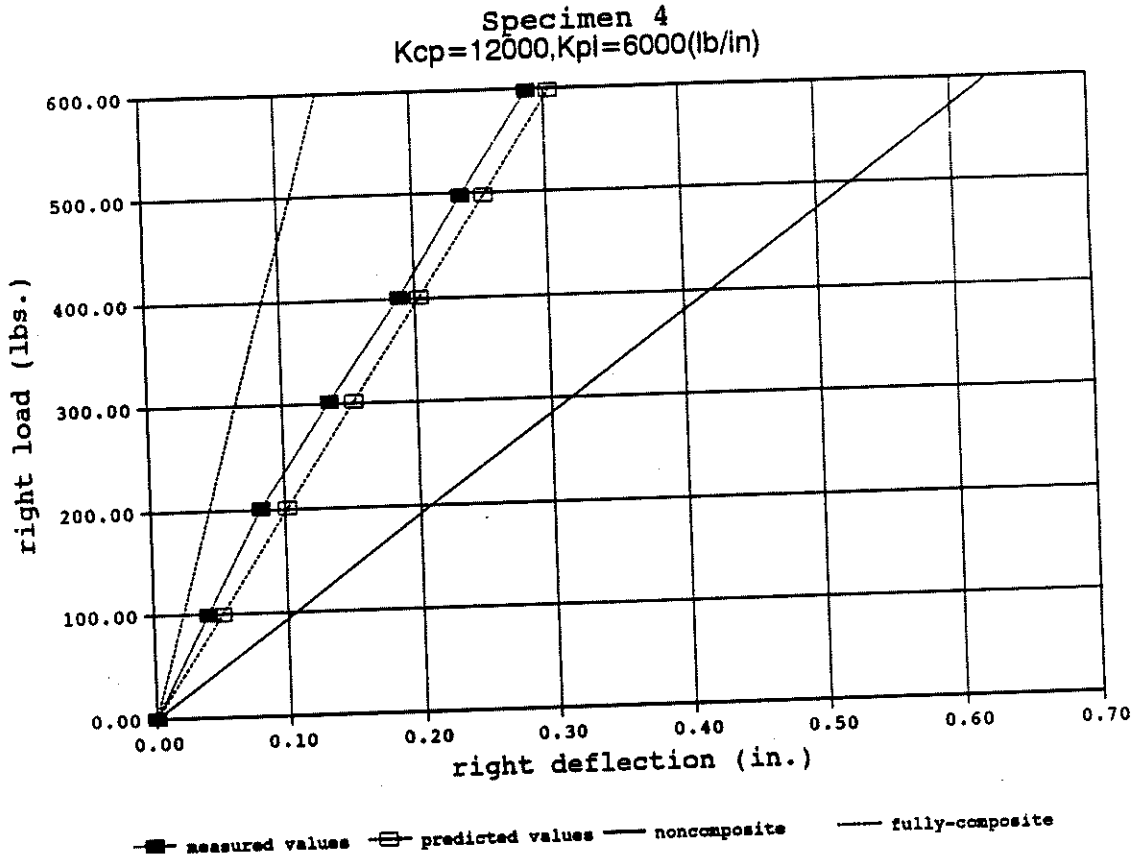

Figure C1.16: The theoretical and experimental load-deflection curves of T-beam

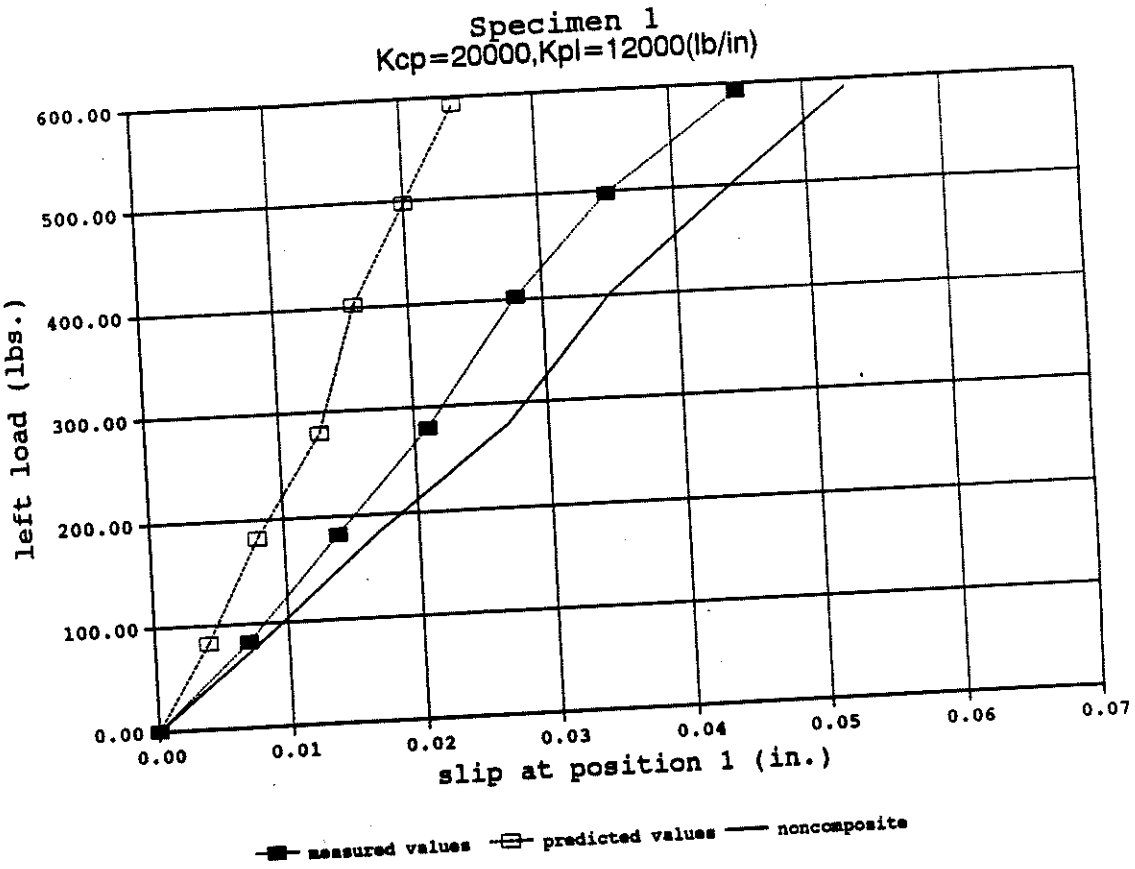

Figure C2.1: The theoretical and experimental load-slip curves of T-beam specimen 1

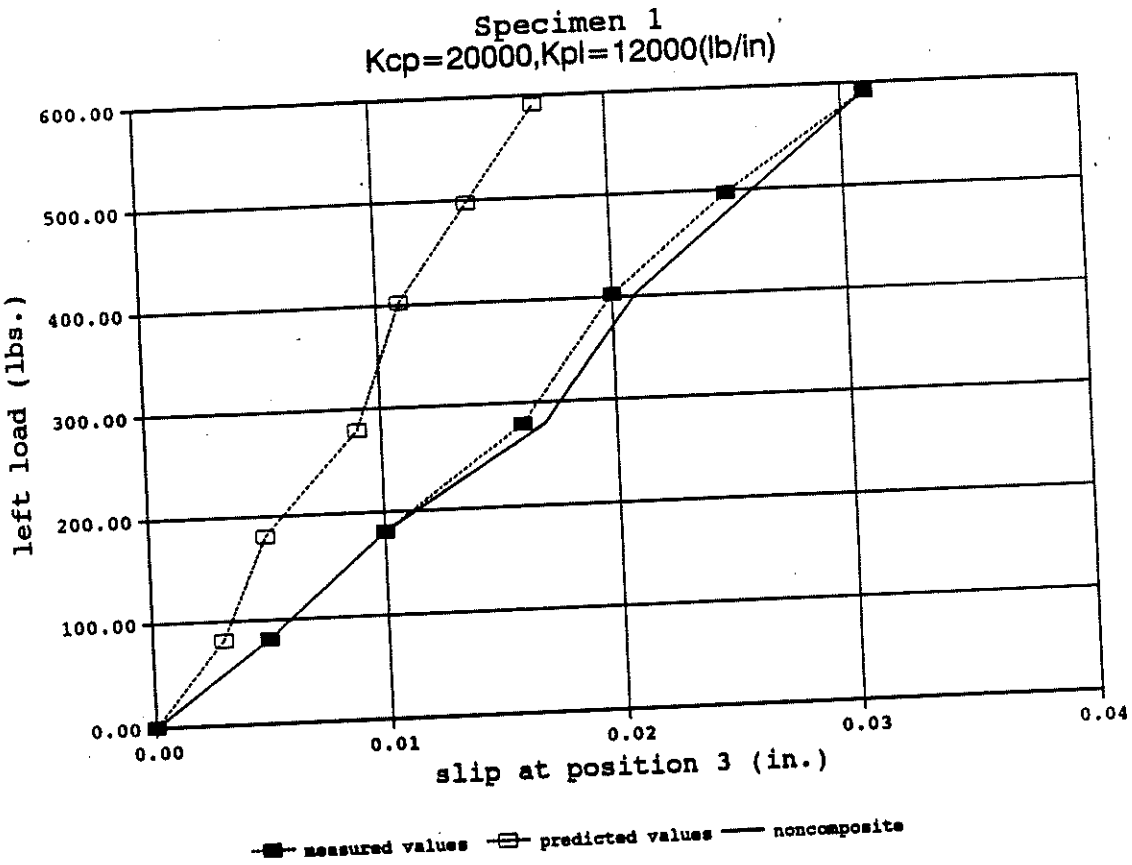

Figure C2.2: The theoretical and experimental load-slip curves of T-beam specimen 1

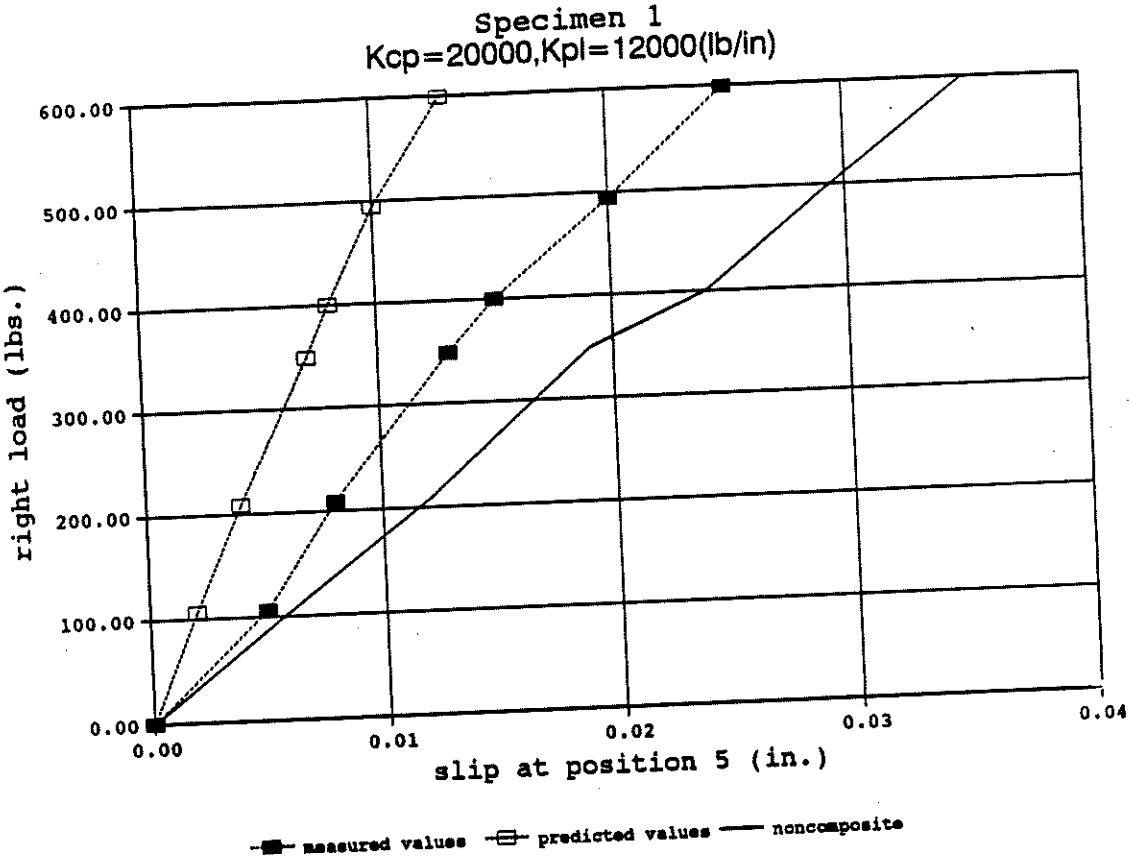

Figure C2.3: The theoretical and experimental load-slip curves of T-beam specimen 1

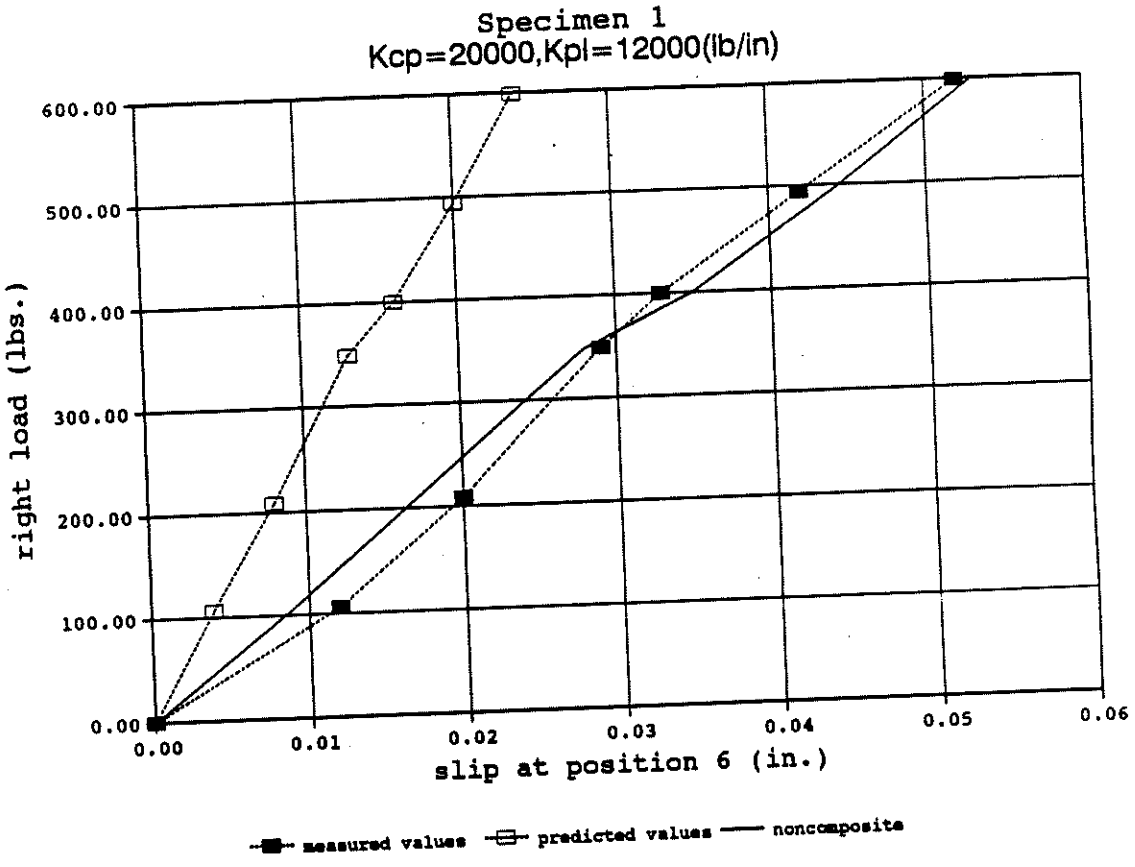

Figure C2.4: The theoretical and experimental load-slip curves of T-beam specimen 1

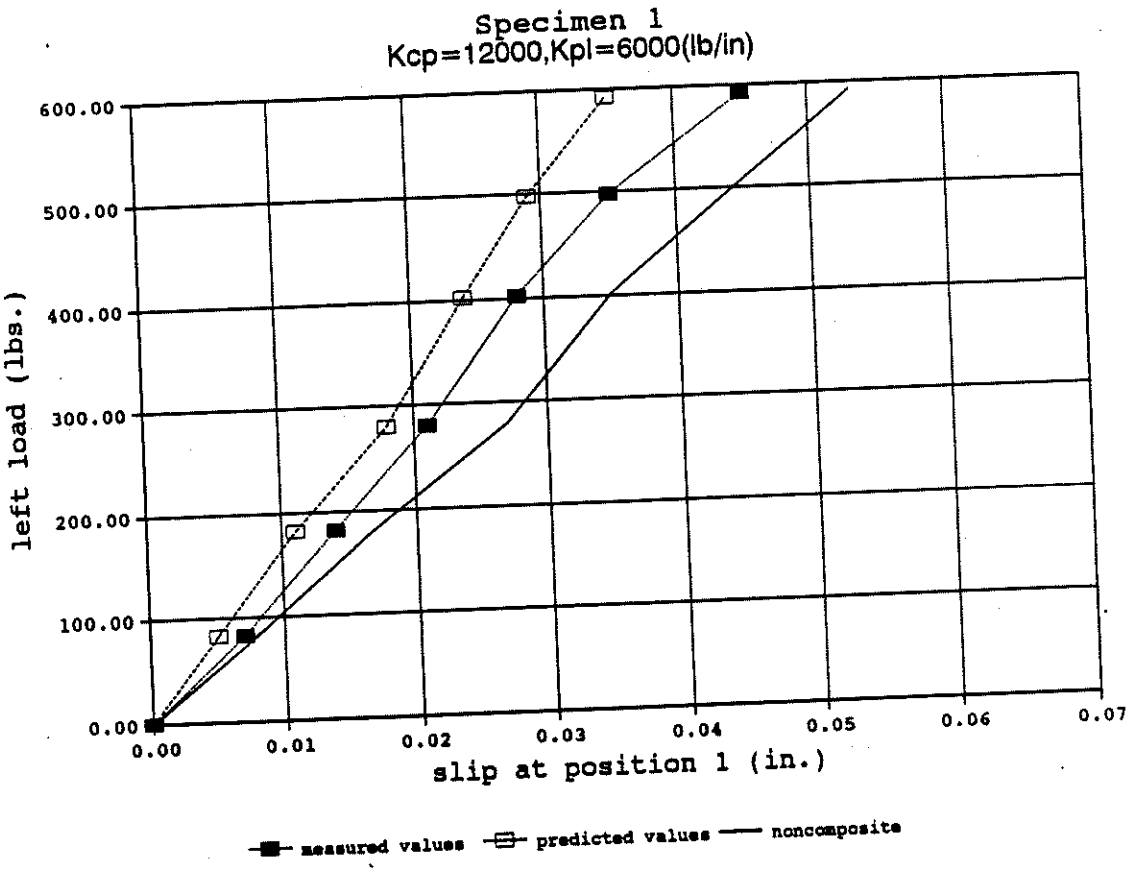

Figure C2.5: The theoretical and experimental load-slip curves of T-beam specimen 1

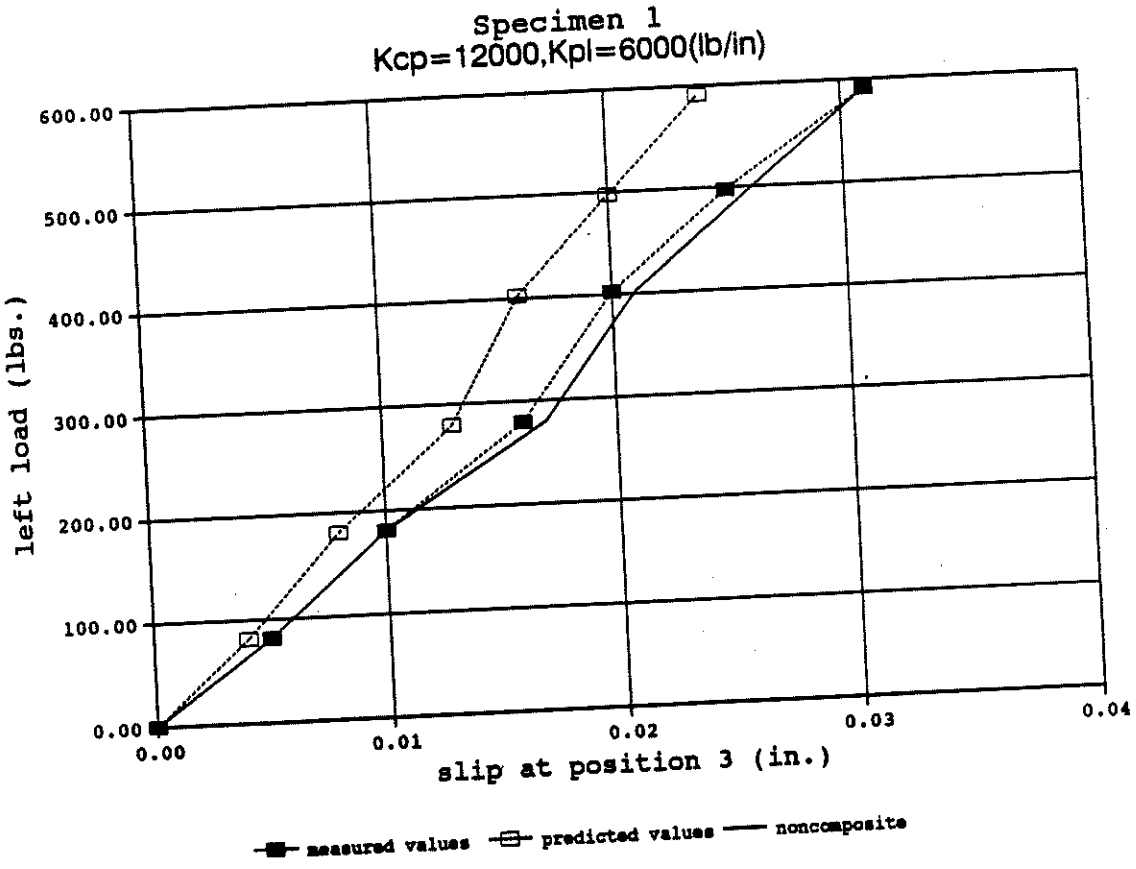

Figure C2.6: The theoretical and experimental load-slip curves of T-beam specimen 1

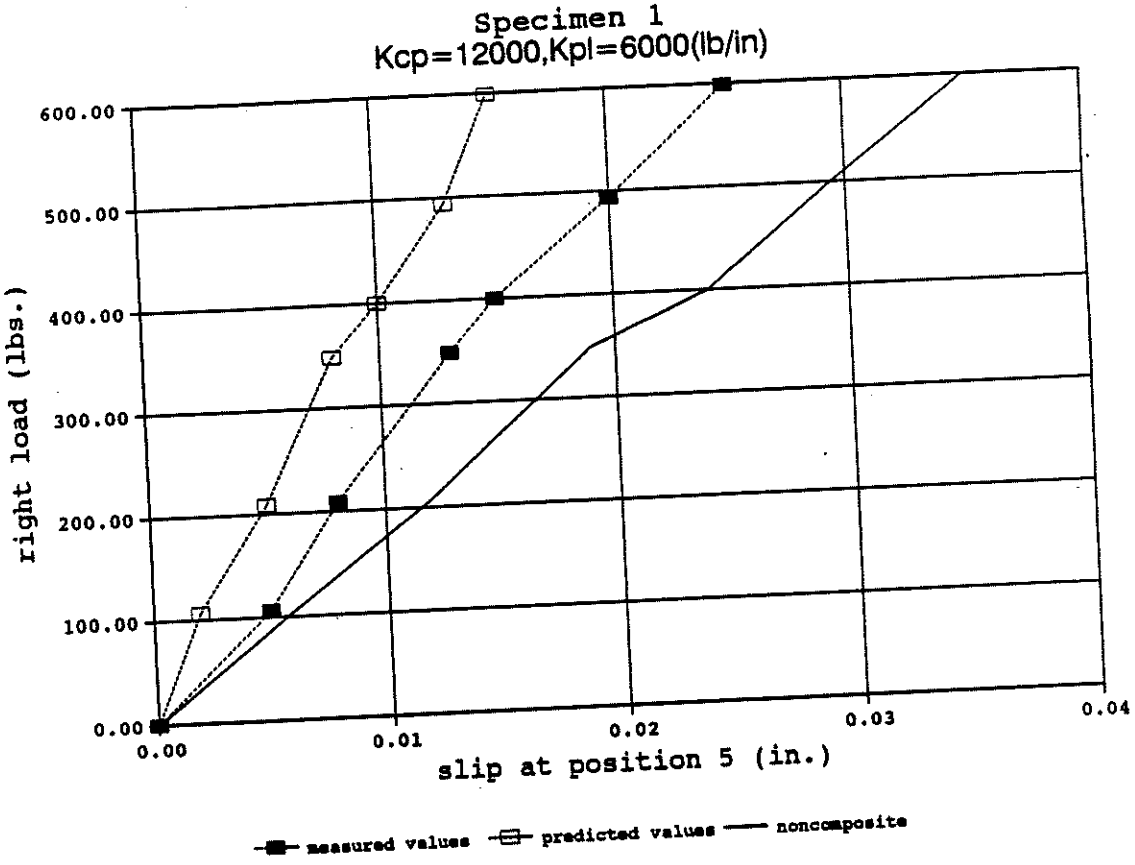

Figure C2.7: The theoretical and experimental load-slip curves of T-beam specimen 1

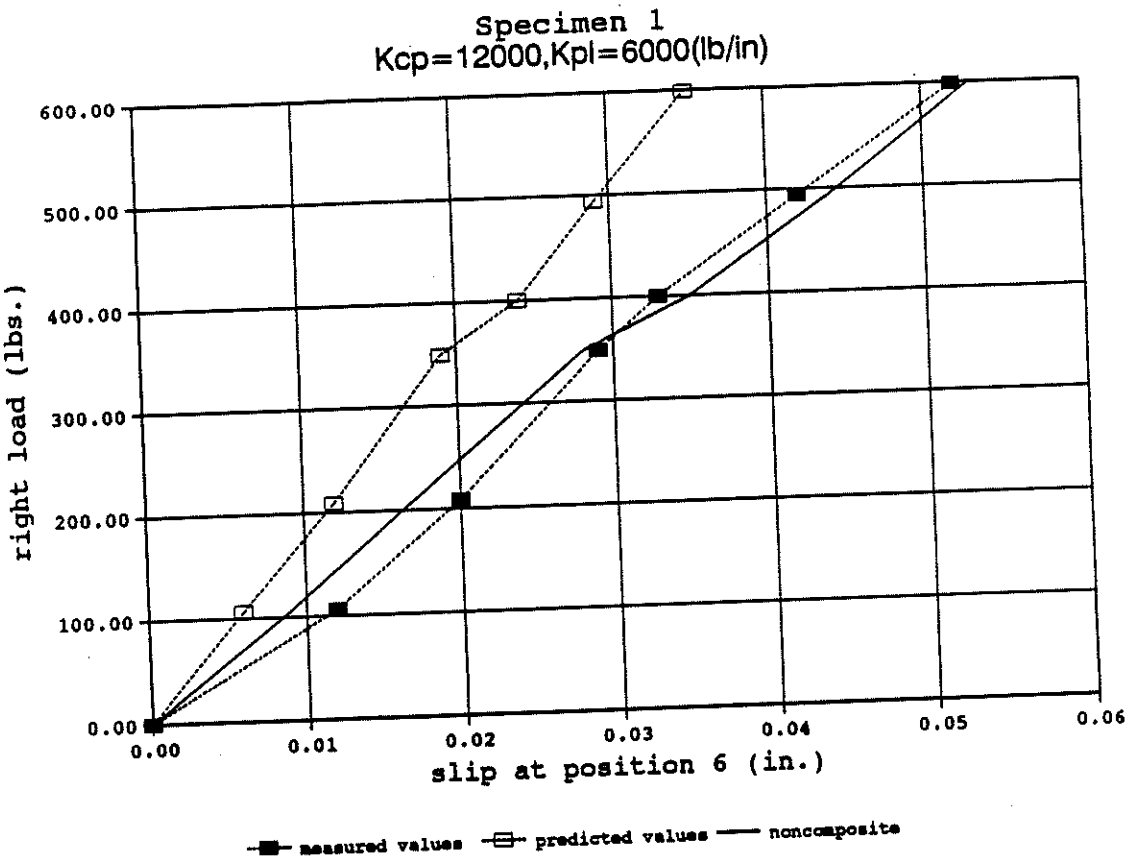

Figure C2.8: The theoretical and experimental load-slip curves of T-beam specimen 1

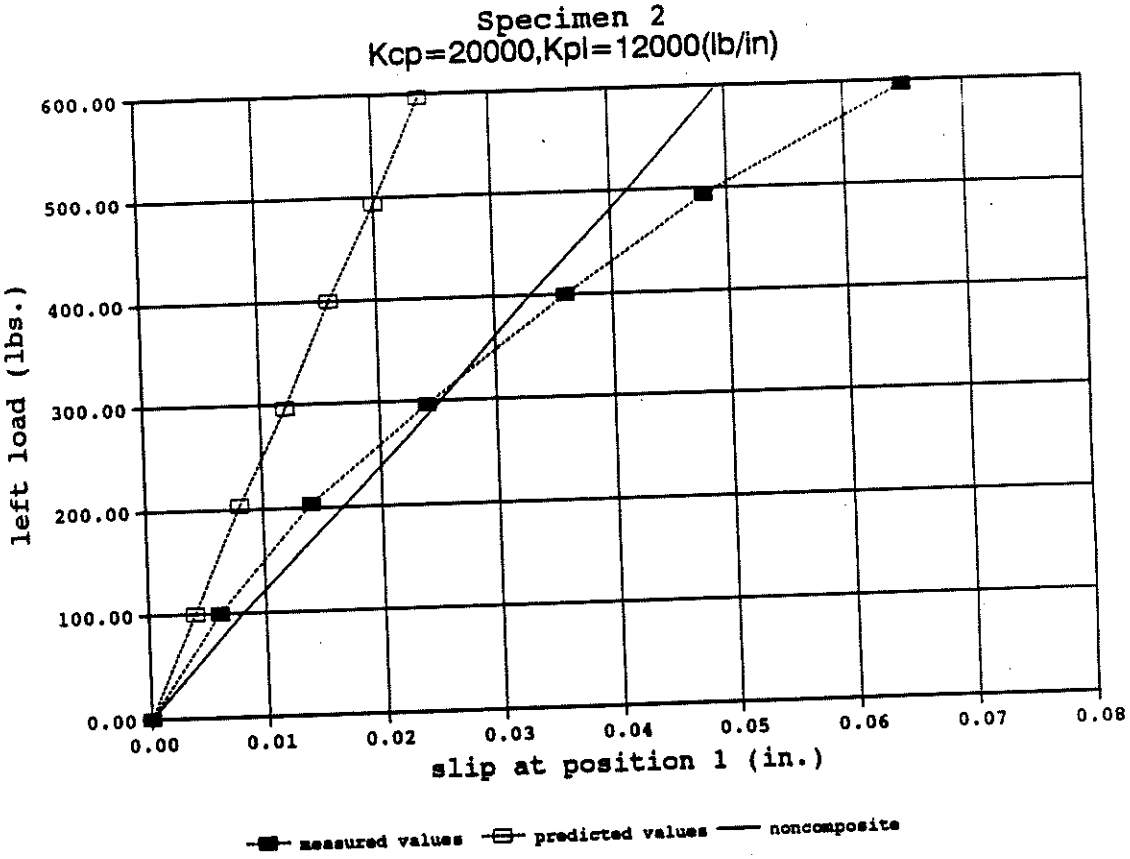

Figure C2.9: The theoretical and experimental load-slip curves of T-beam specimen 2

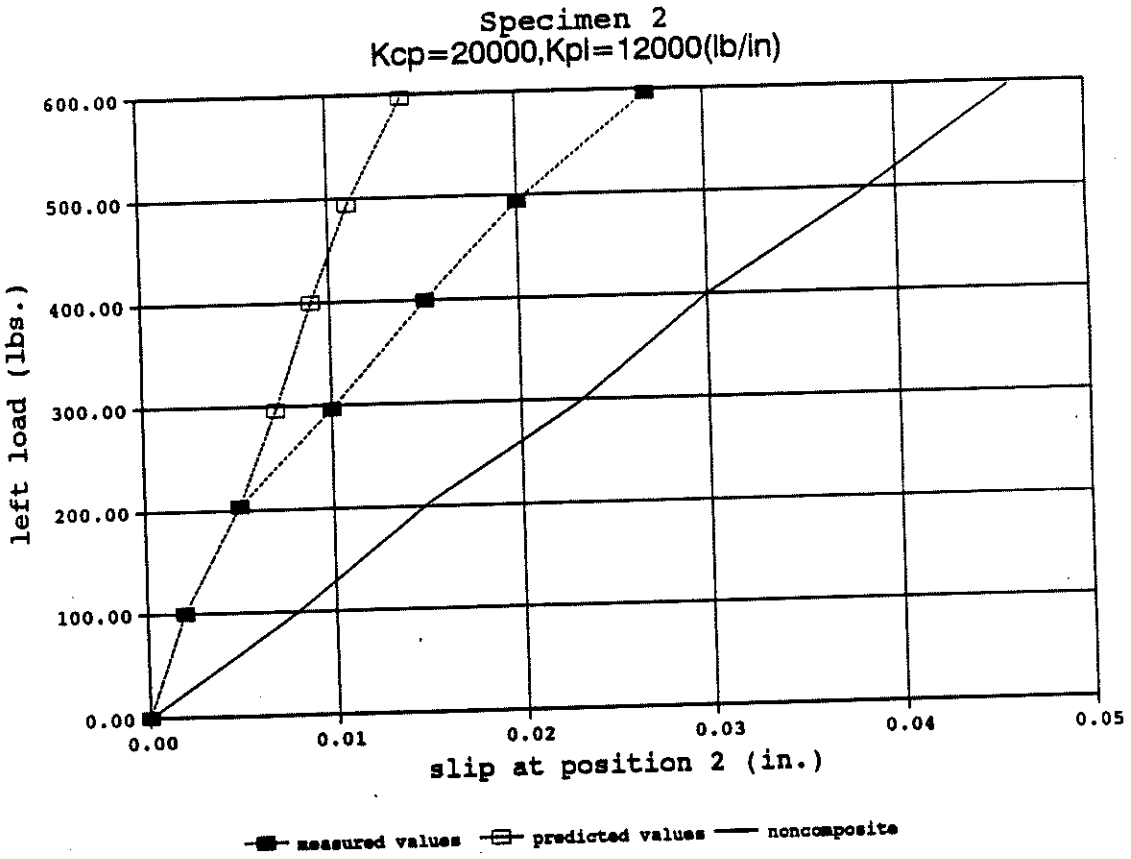

Figure C2.10: The theoretical and experimental load-slip curves of T-beam specimen 2

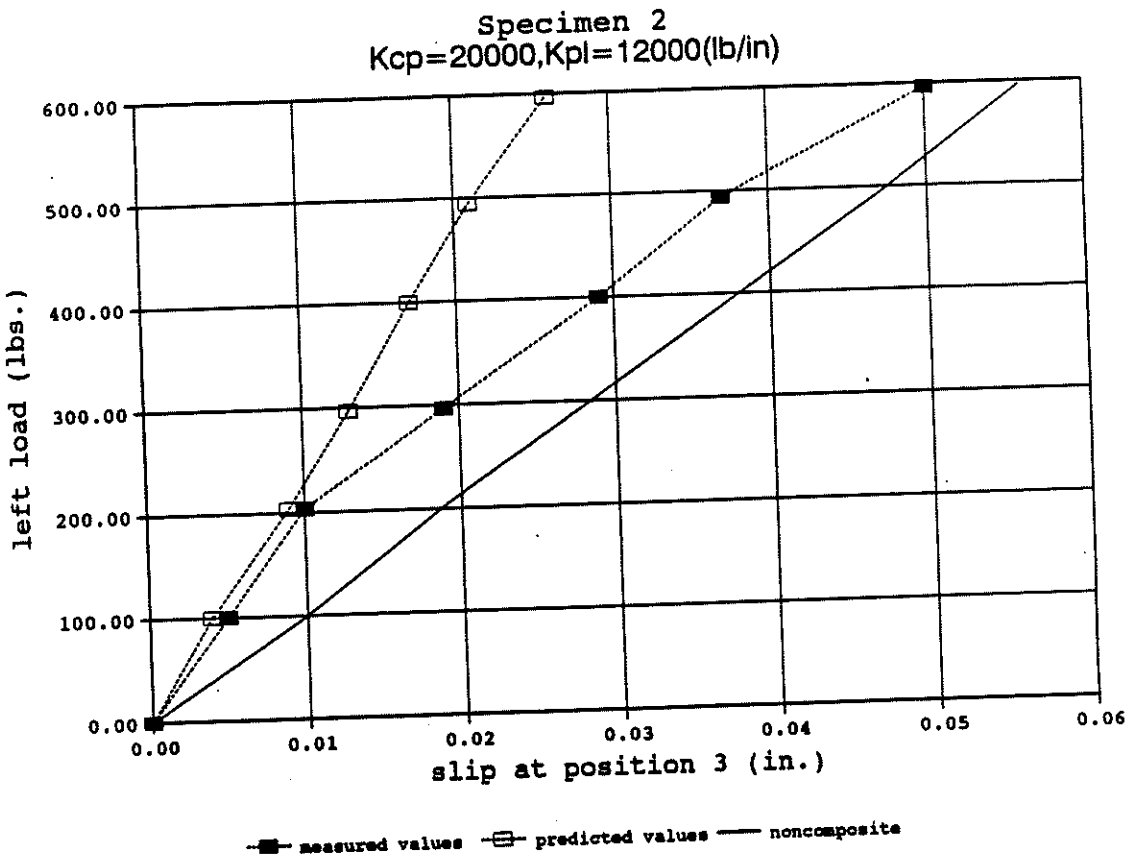

Figure C2.11: The theoretical and experimental load-slip curves of T-beam specimen 2

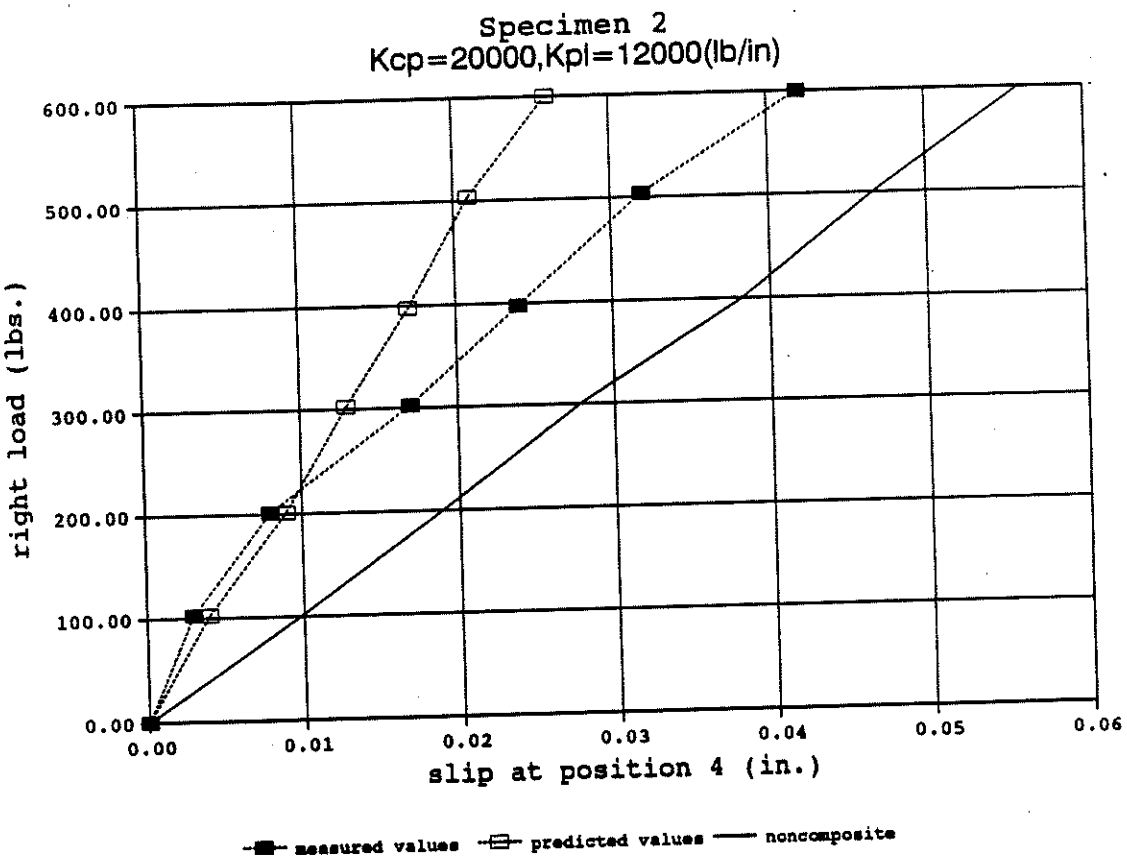

Figure C2.12: The theoretical and experimental load-slip curves of T-beam specimen 2

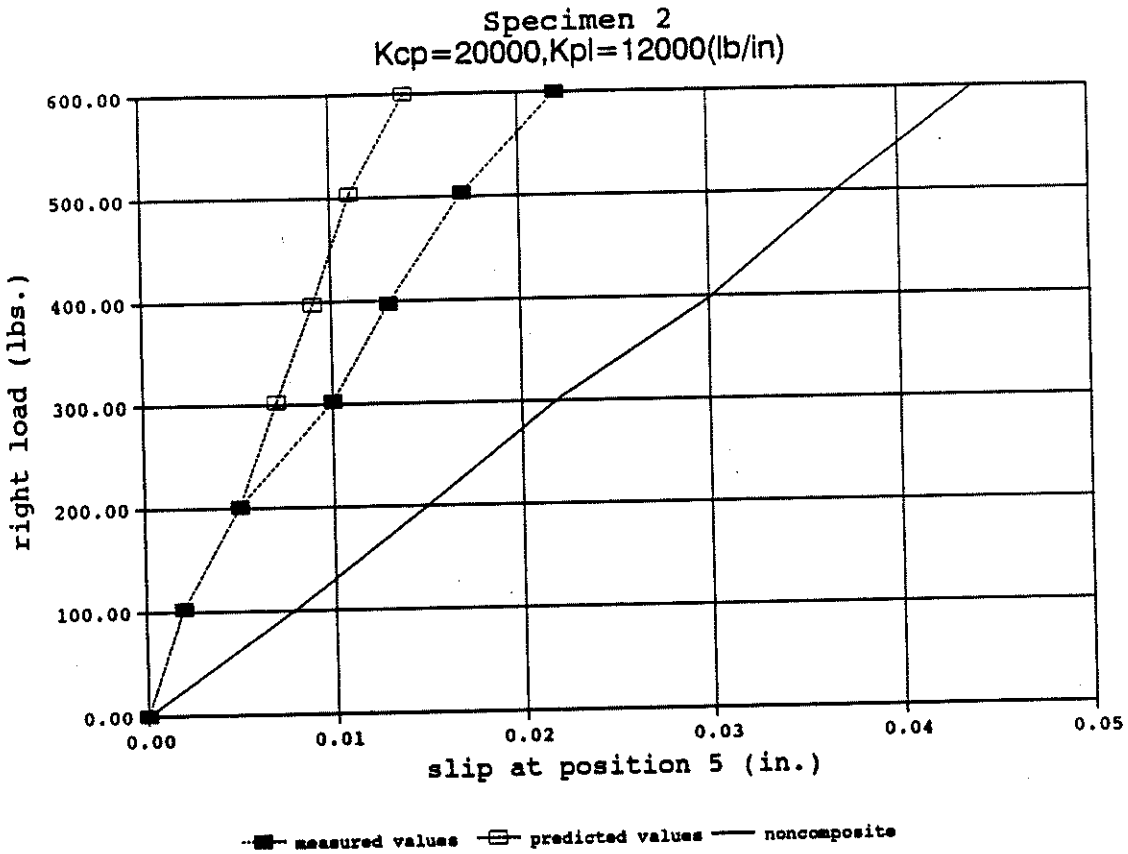

Figure C2.13: The theoretical and experimental load-slip curves of T-beam specimen 2

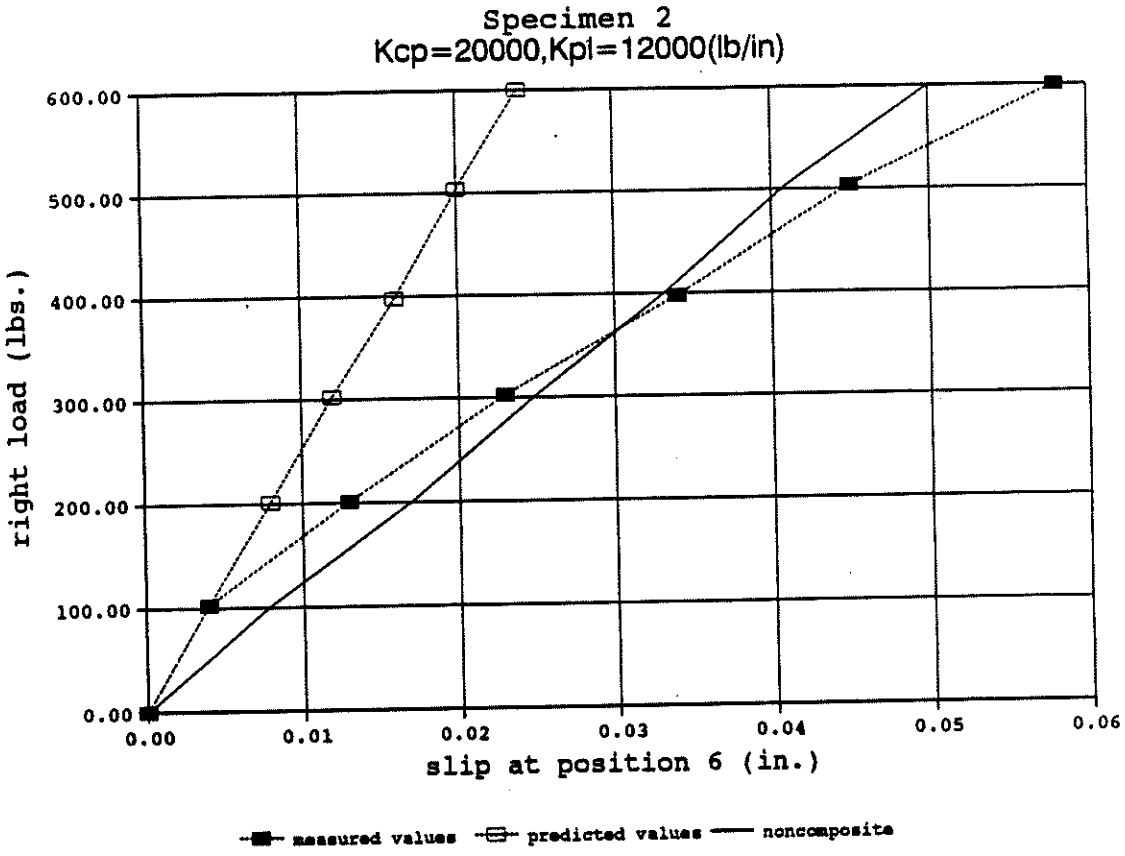

Figure C2.14: The theoretical and experimental load-slip curves of T-beam specimen 2

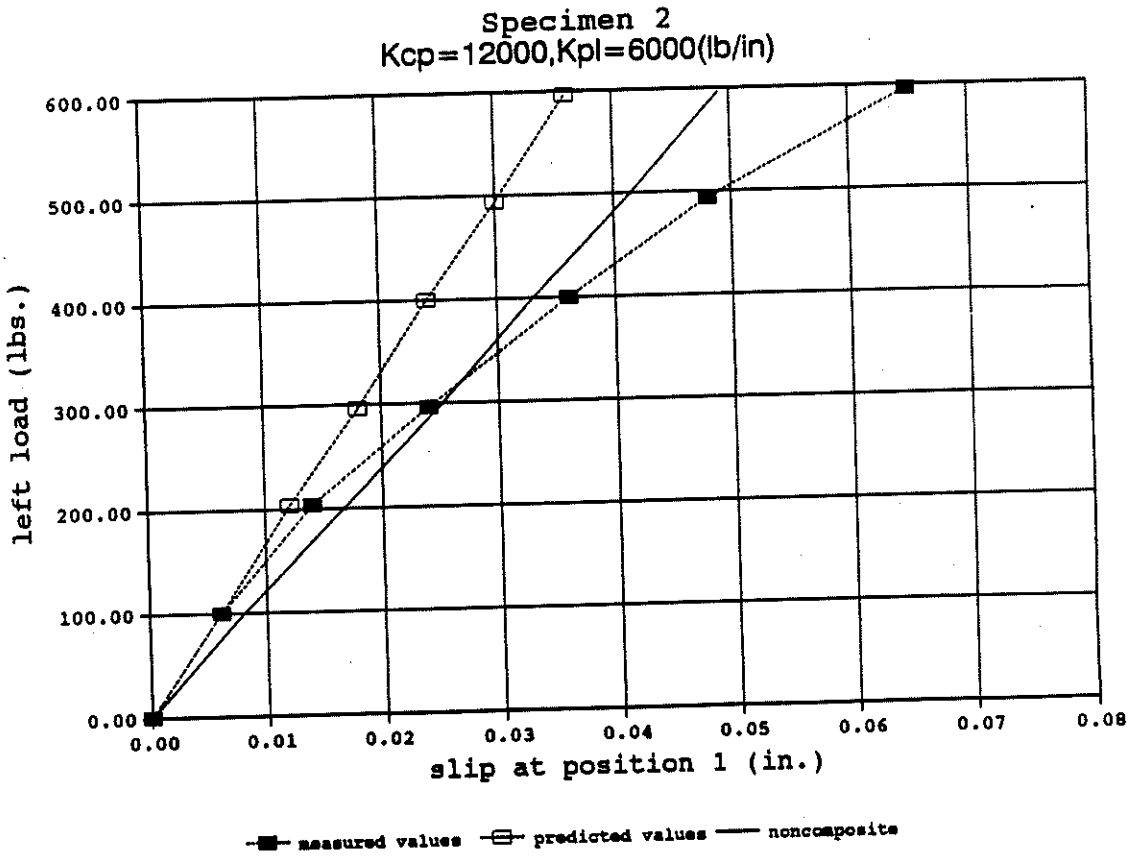

Figure C2.15: The theoretical and experimental load-slip curves of T-beam specimen 2

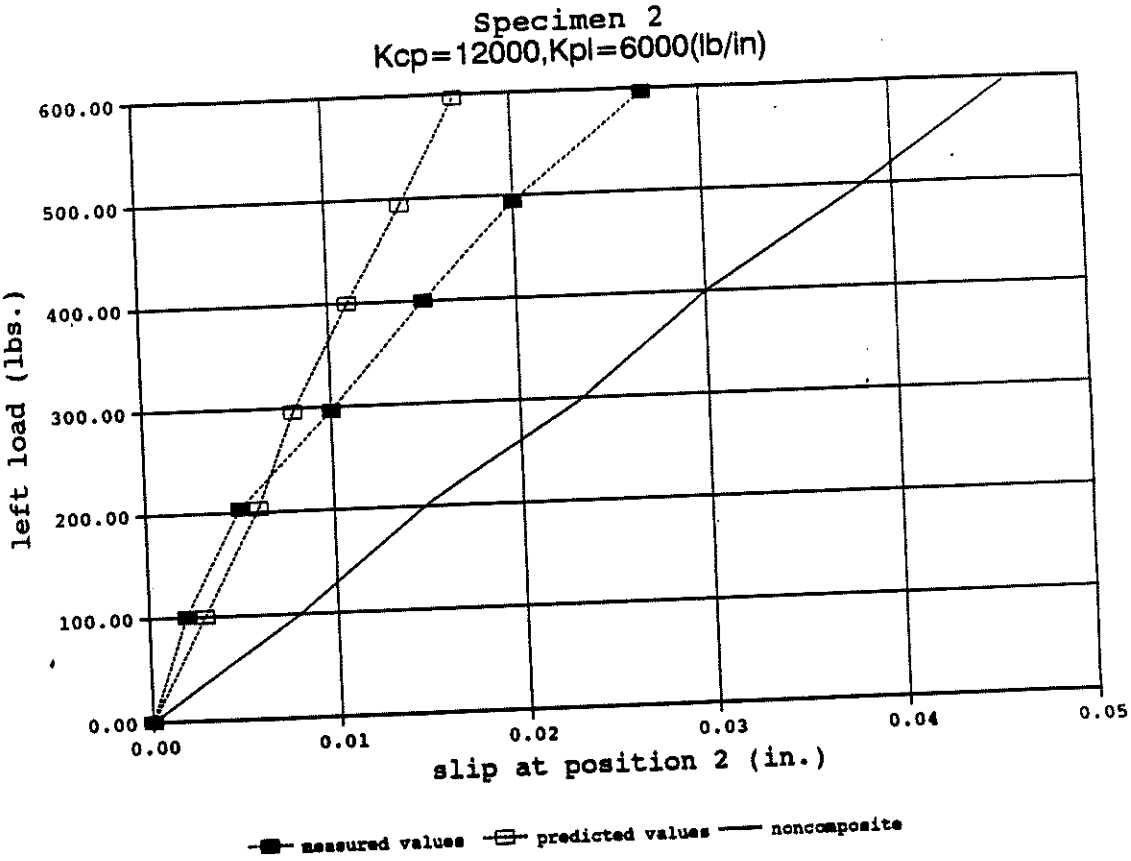

Figure C2.16: The theoretical and experimental load-slip curves of T-beam specimen 2

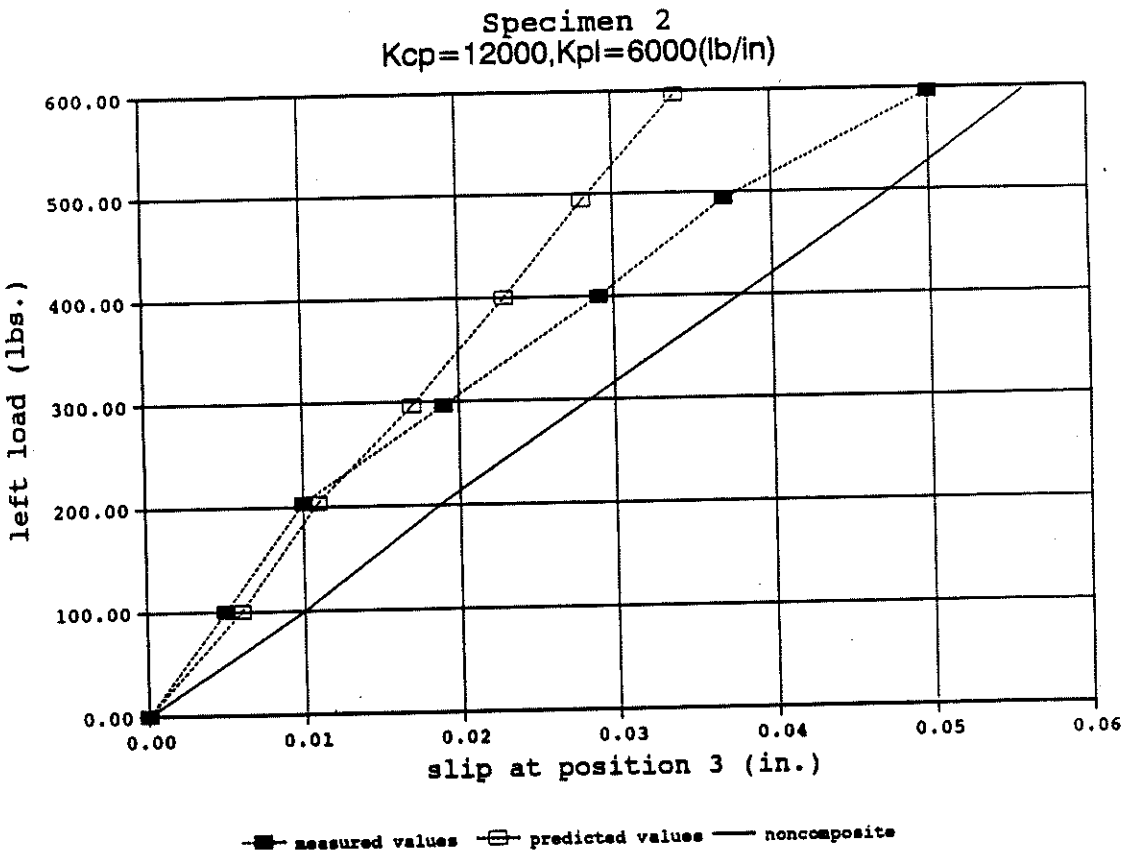

Figure C2.17: The theoretical and experimental load-slip curves of T-beam specimen 2

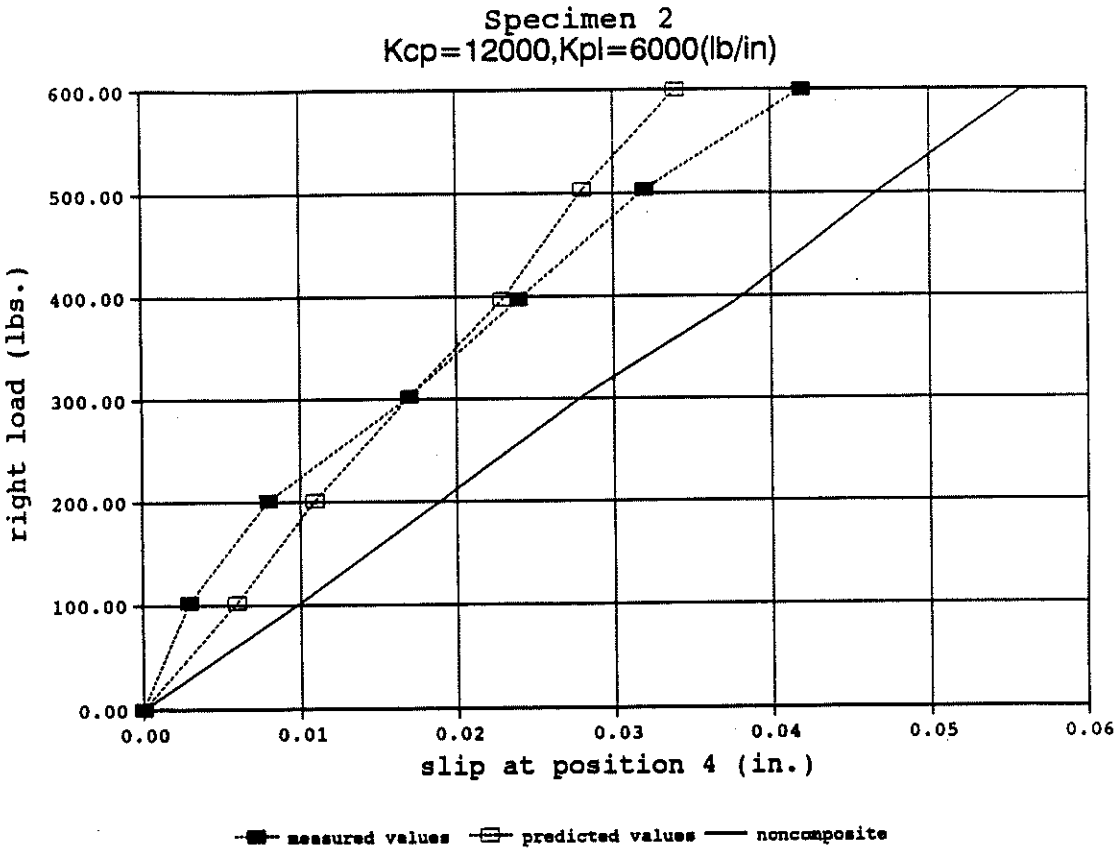

Figure C2.18: The theoretical and experimental load-slip curves of T-beam specimen 2

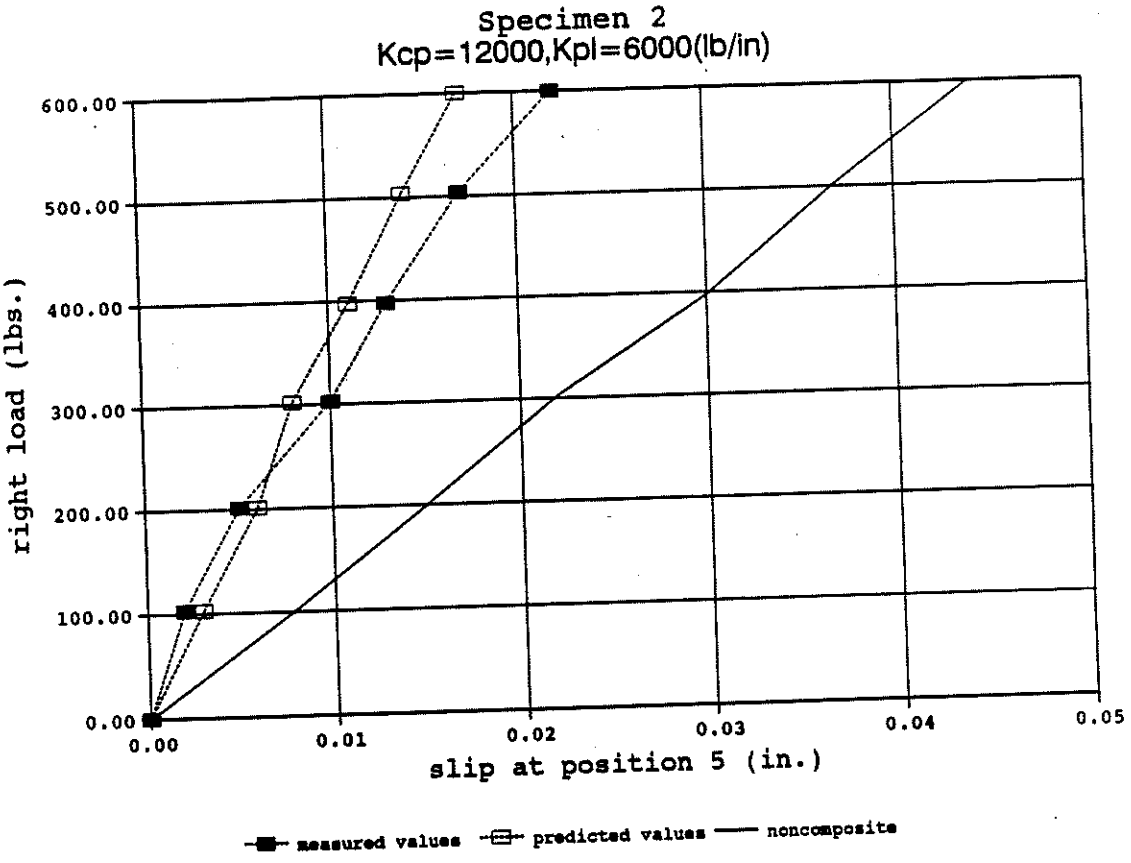

Figure C2.19: The theoretical and experimental load-slip curves of T-beam specimen 2

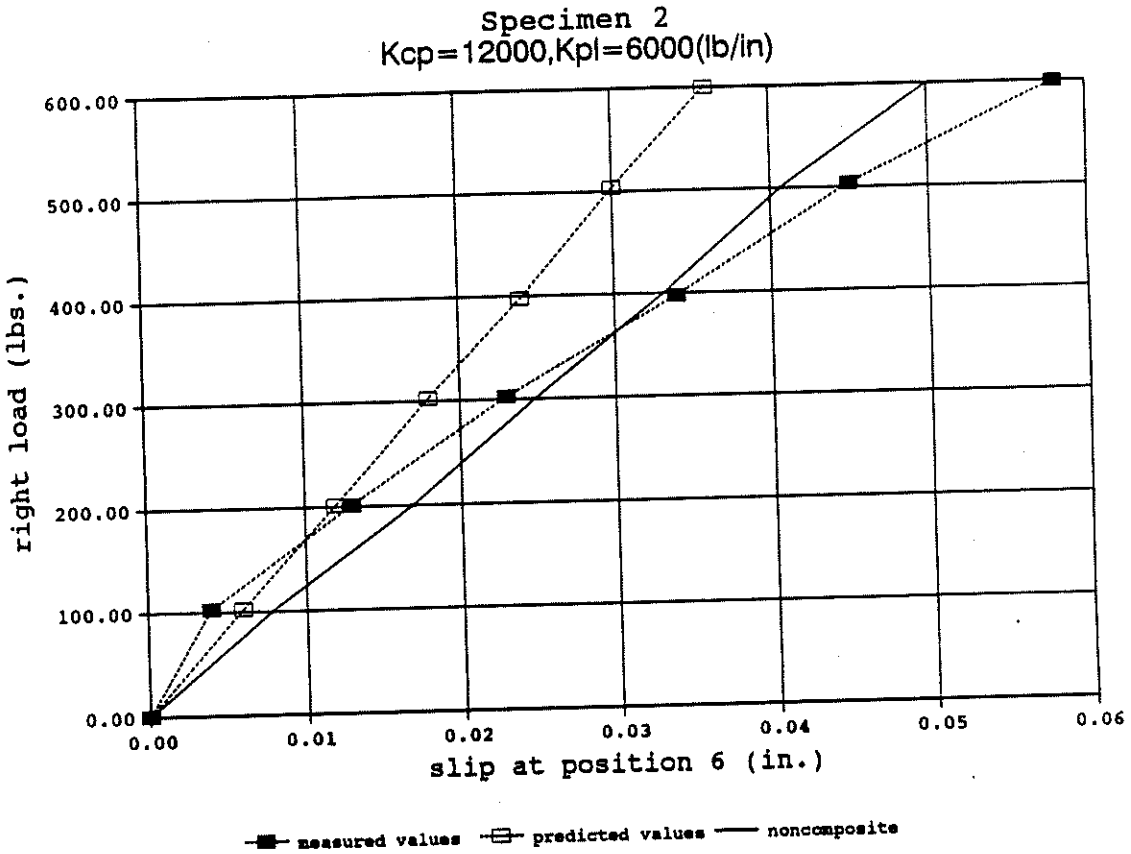

Figure C2.20: The theoretical and experimental load-slip curves of T-beam specimen 2

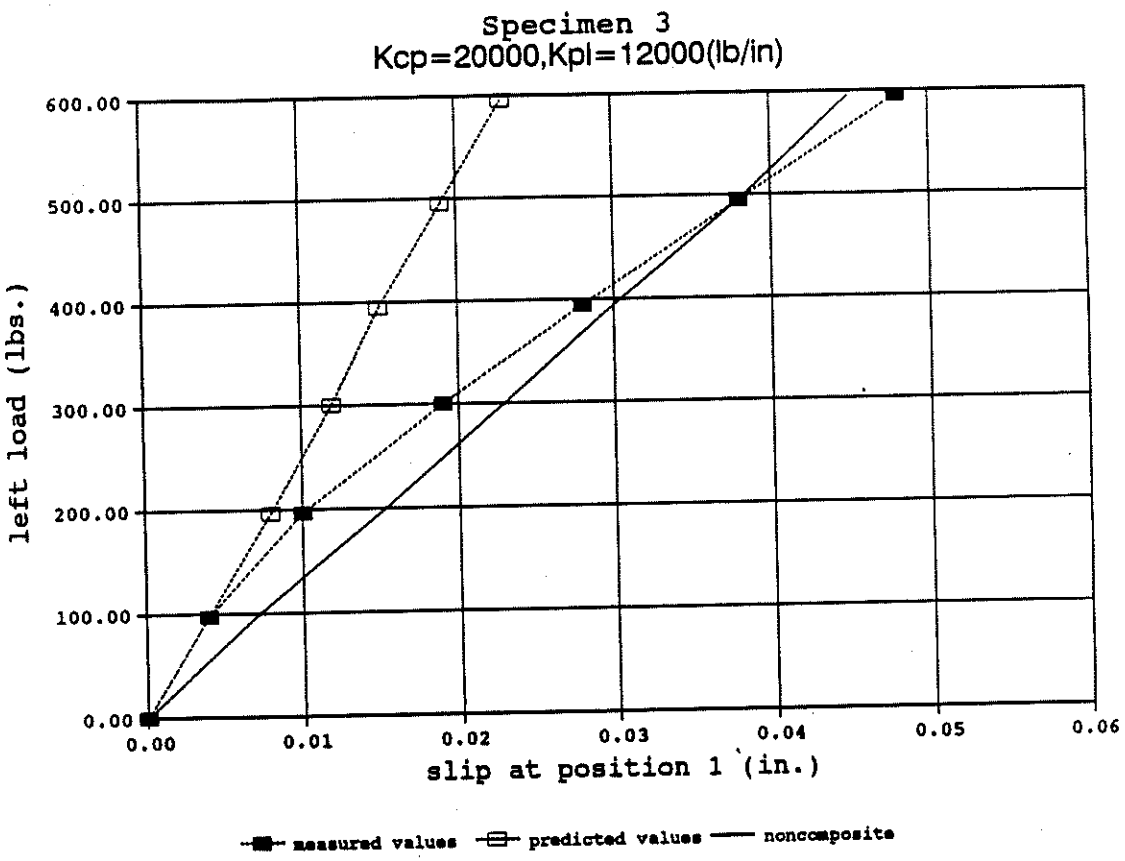

Figure C2.21: The theoretical and experimental load-slip curves of T-beam specimen 3

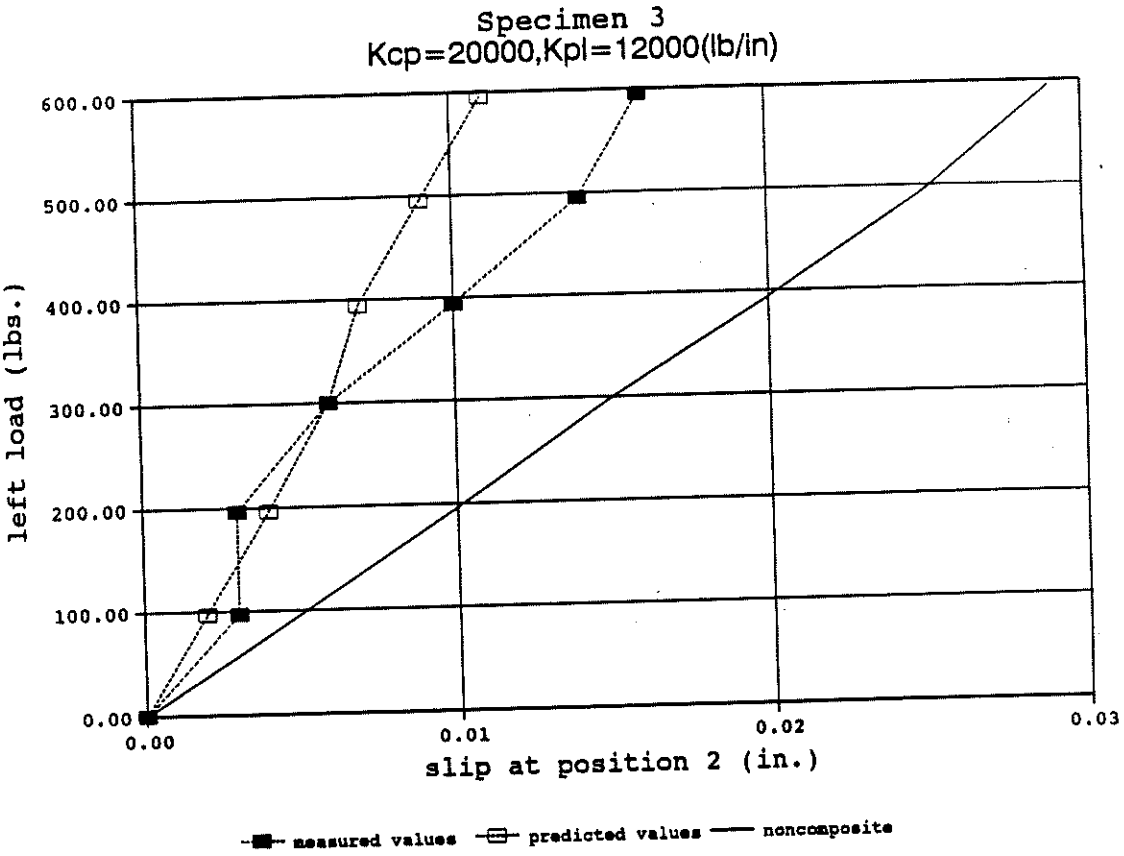

Figure C2.22: The theoretical and experimental load-slip curves of T-beam specimen 3

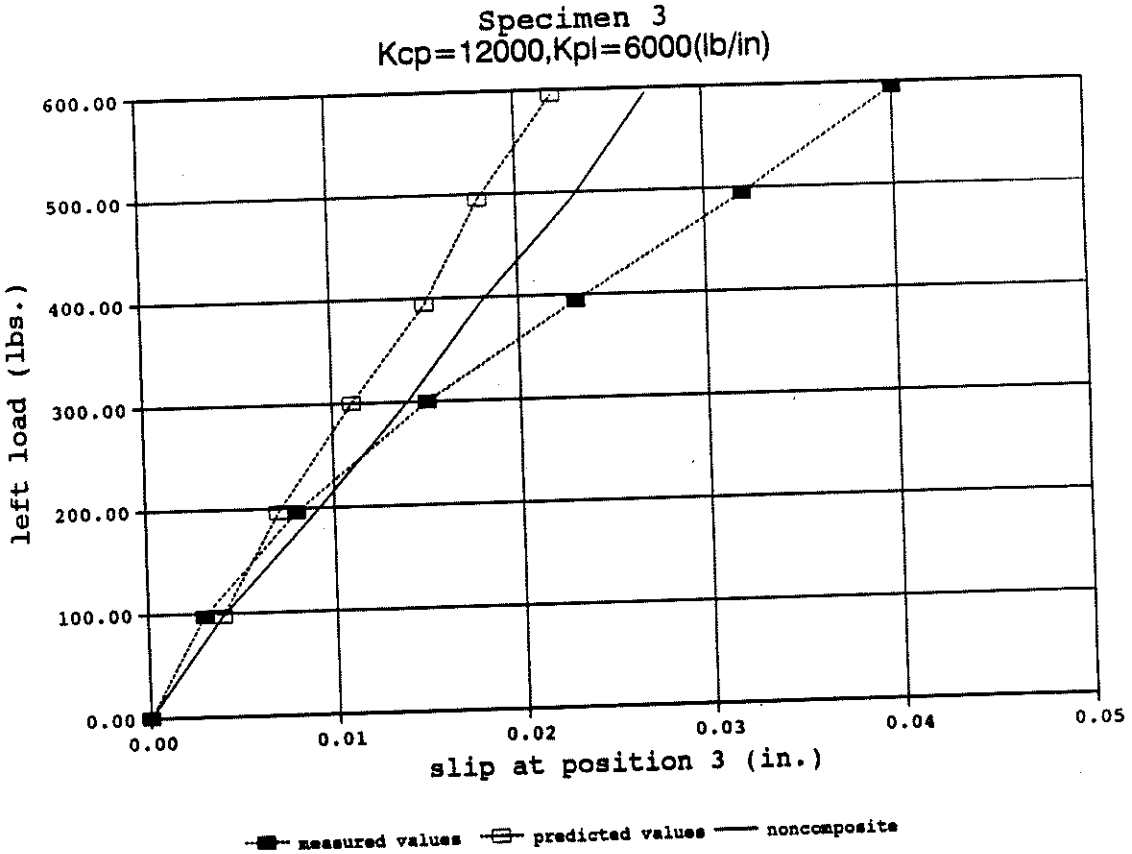

Figure C2.23: The theoretical and experimental load-slip curves of T-beam specimen 3

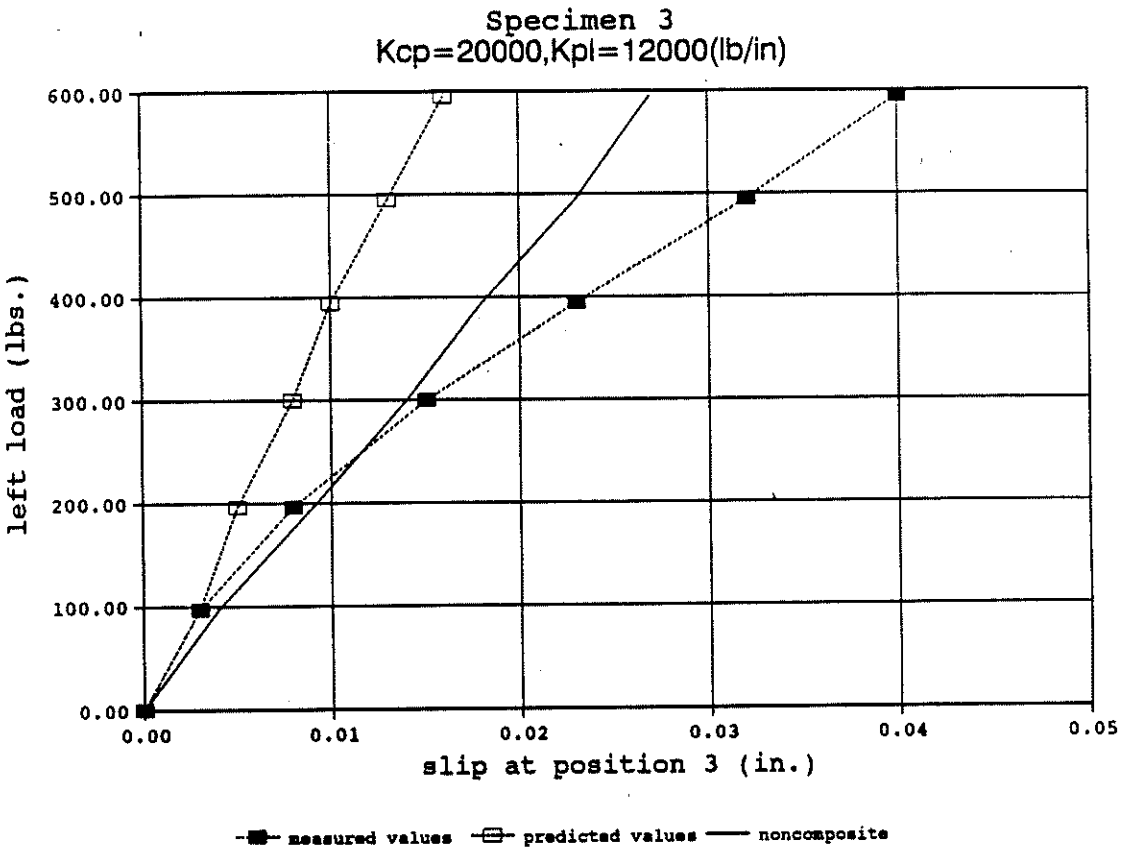

Figure C2.24: The theoretical and experimental load-slip curves of T-beam specimen 3

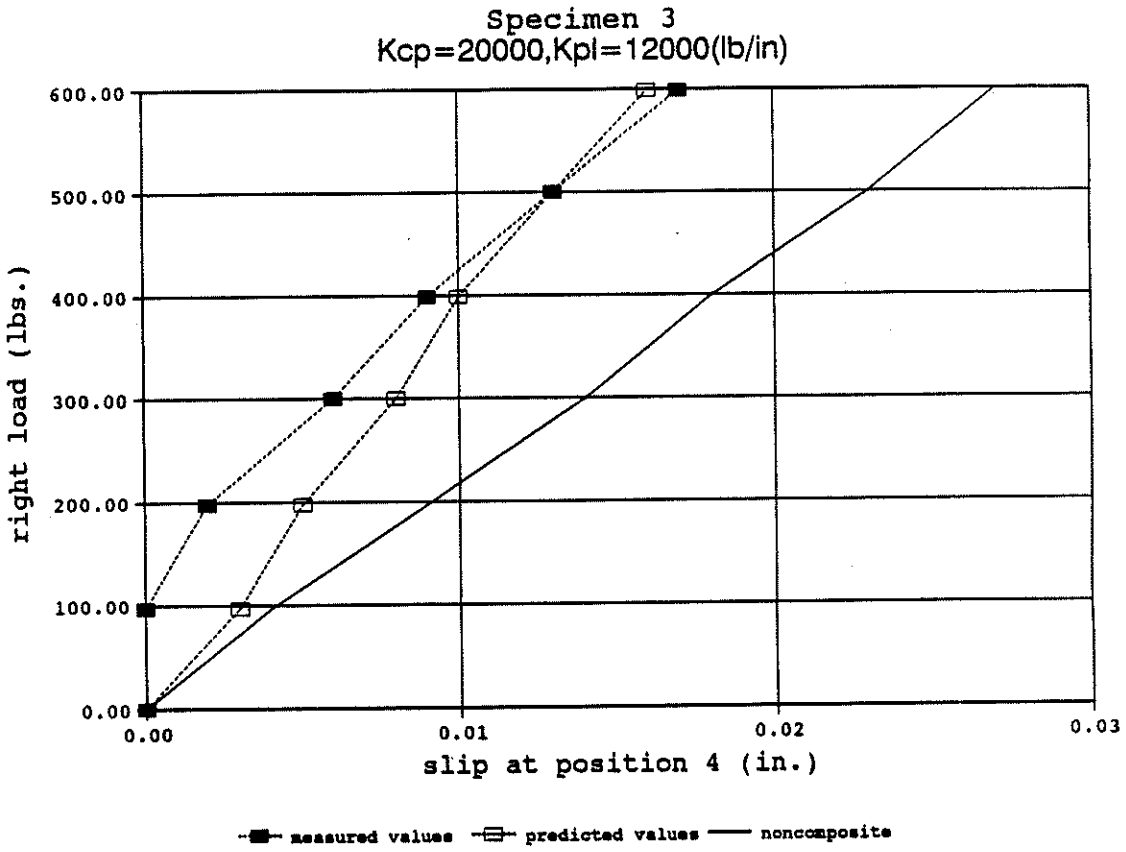

Figure C2.25: The theoretical and experimental load-slip curves of T-beam specimen 3

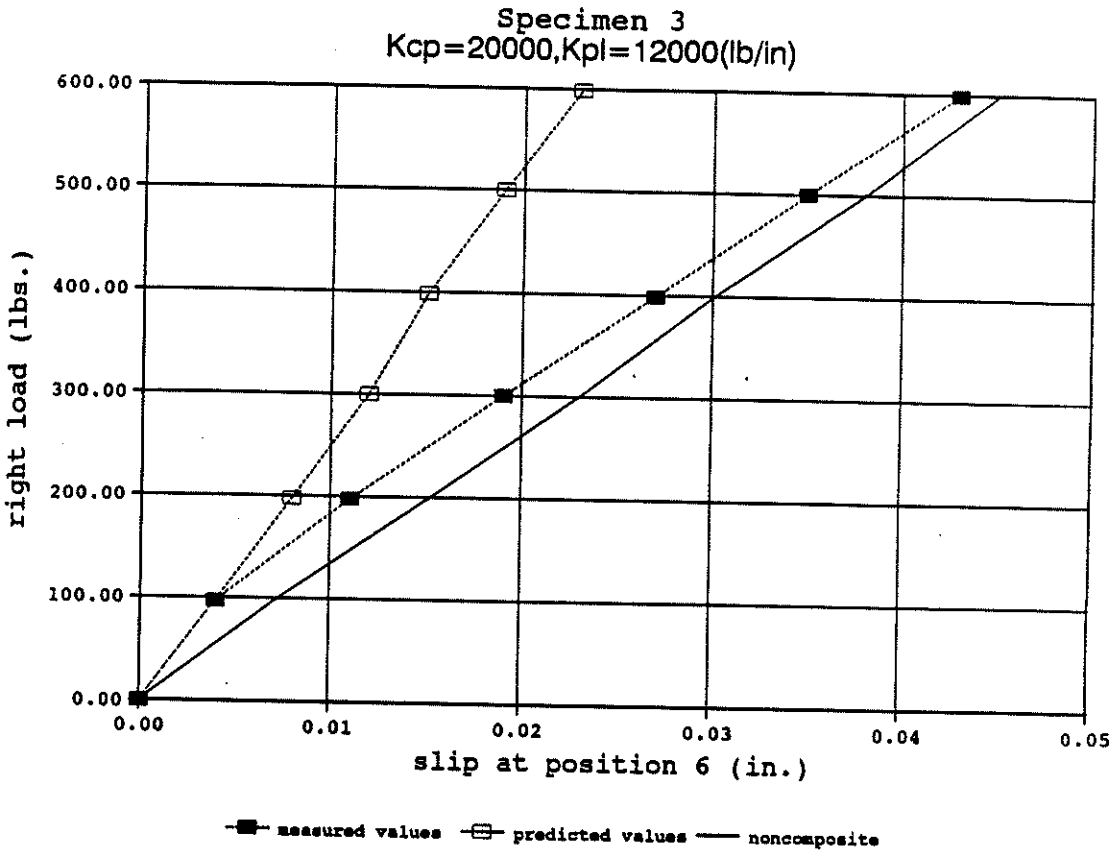

Figure C2.26: The theoretical and experimental load-slip curves of T-beam specimen 3

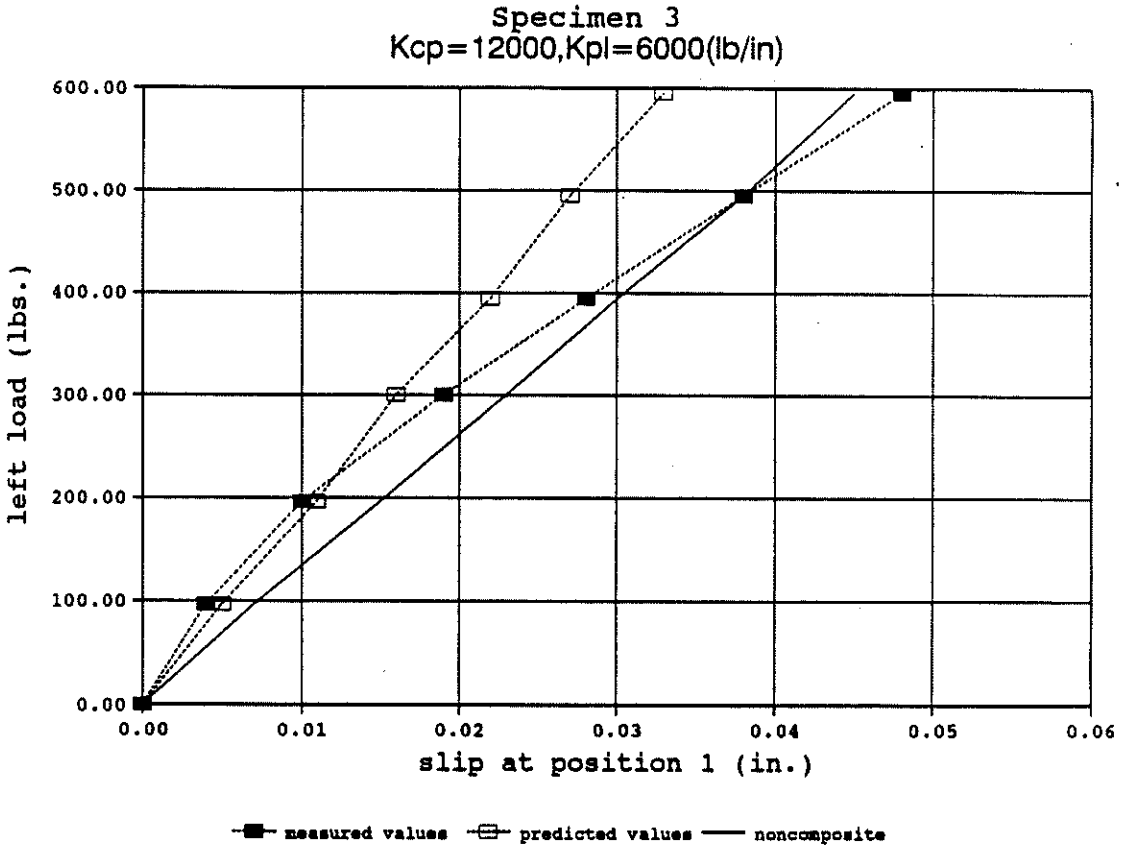

Figure C2.27: The theoretical and experimental load-slip curves of T-beam specimen 3

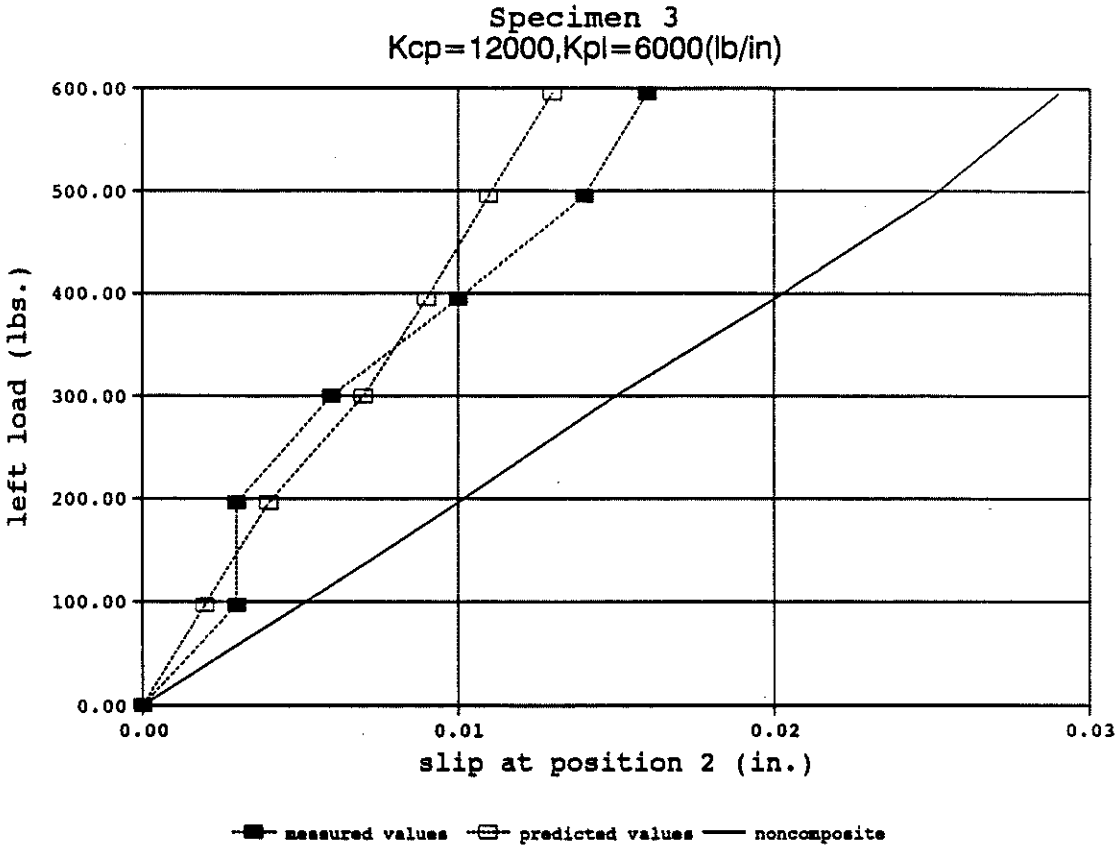

Figure C2.28: The theoretical and experimental load-slip curves of T-beam specimen 3

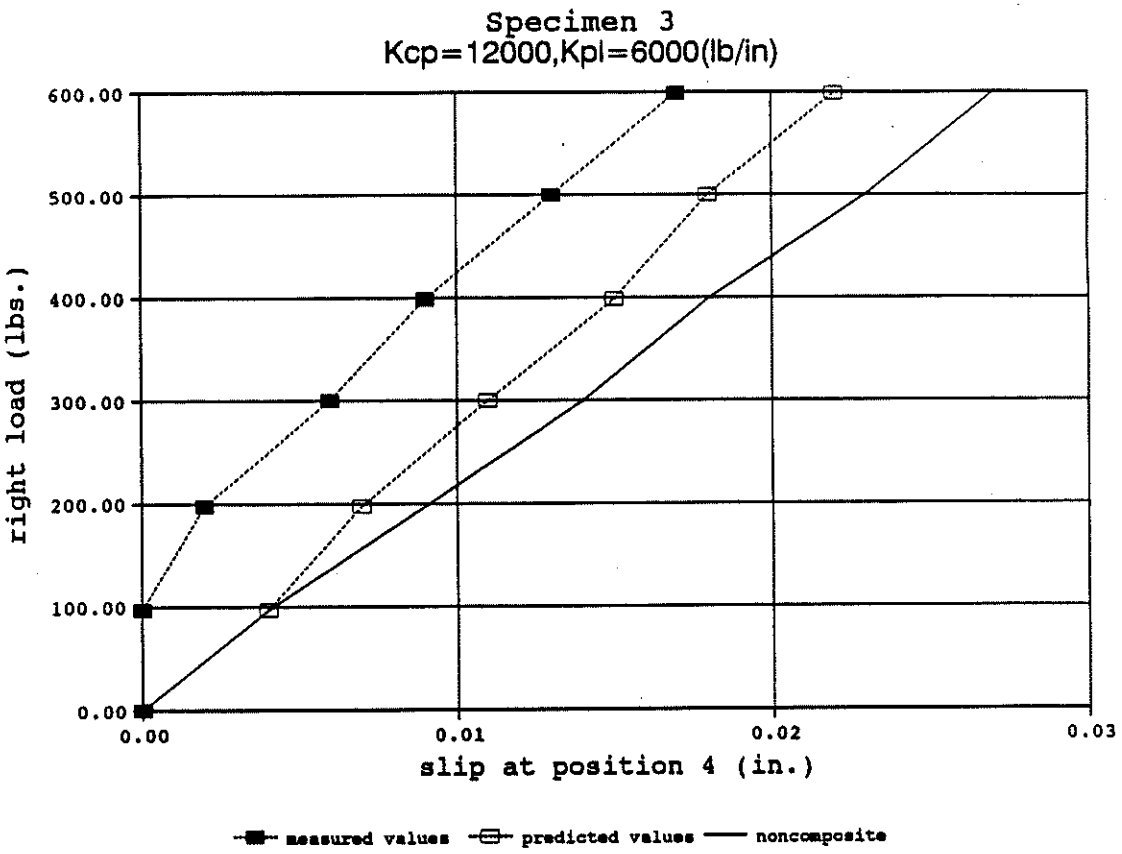

Figure C2.29: The theoretical and experimental load-slip curves of T-beam specimen 3

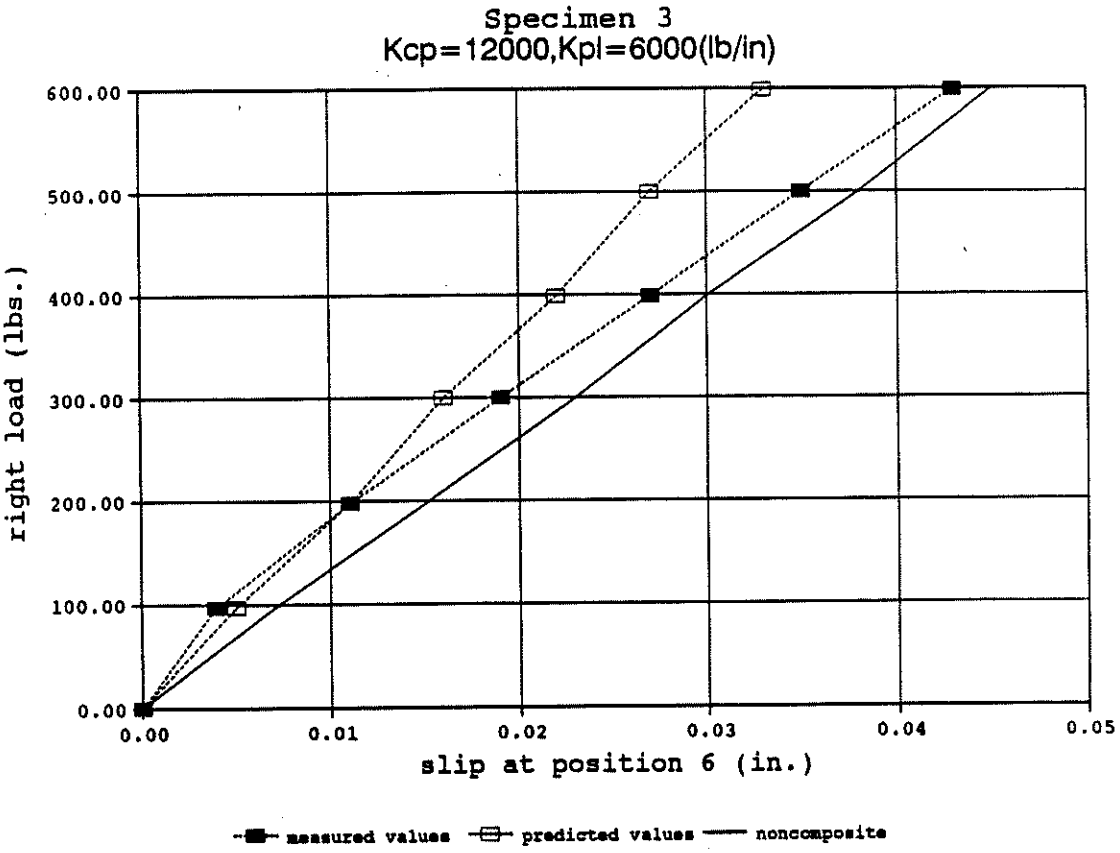

Figure C2.30: The theoretical and experimental load-slip curves of T-beam specimen 3

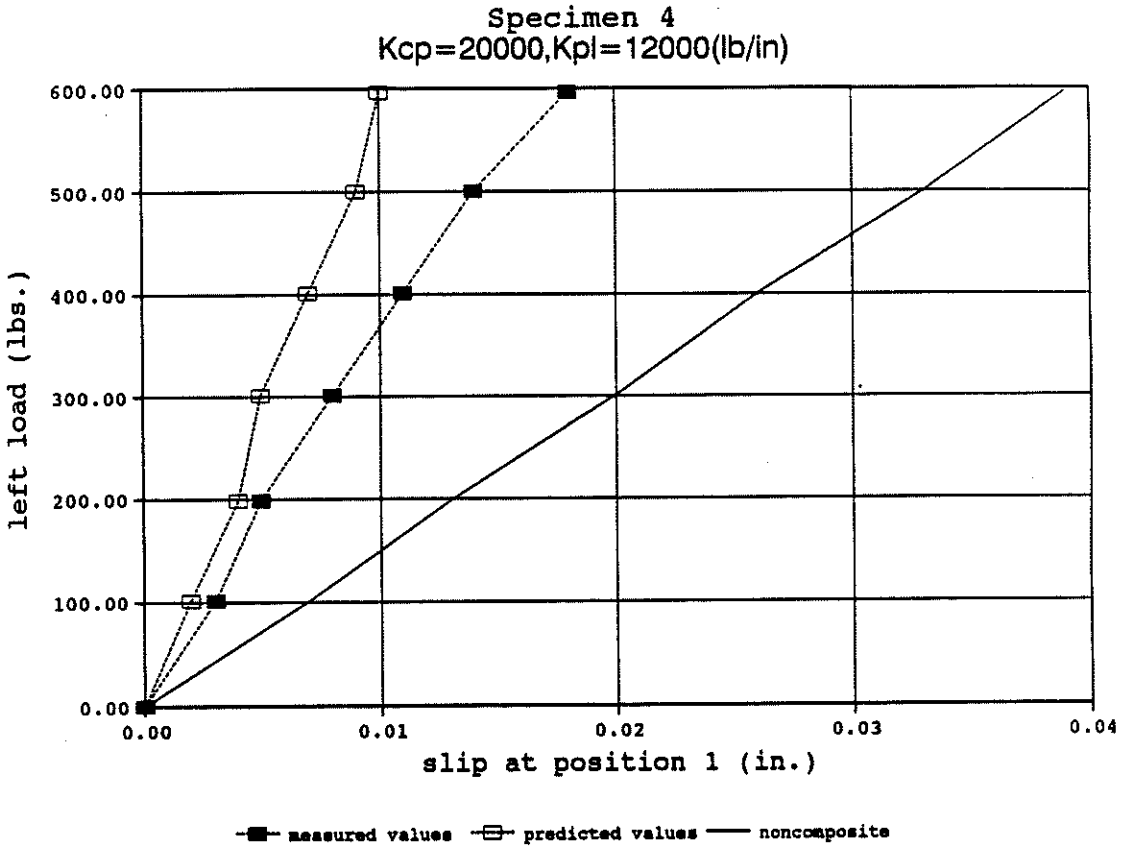

Figure C2.31: The theoretical and experimental load-slip curves of T-beam specimen 4

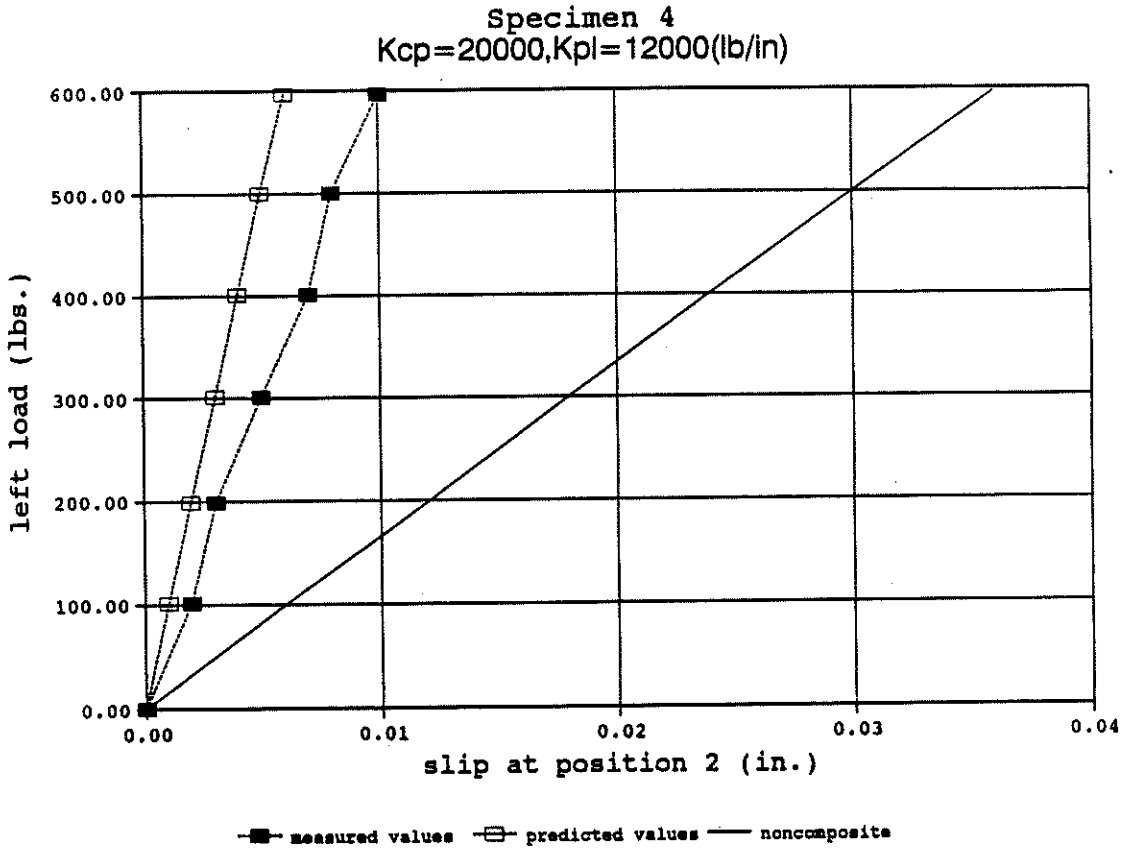

Figure C2.32: The theoretical and experimental load-slip curves of T-beam specimen 4

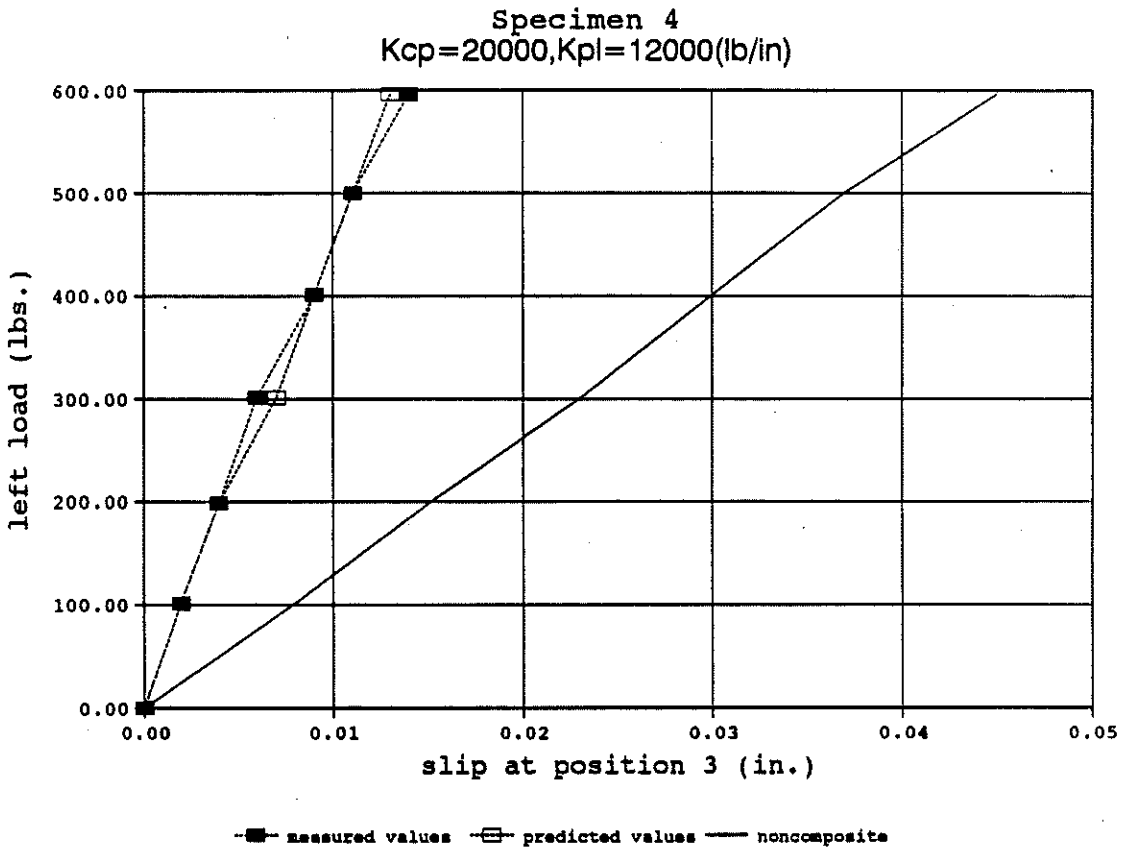

Figure C2.33: The theoretical and experimental load-slip curves of T-beam specimen 4

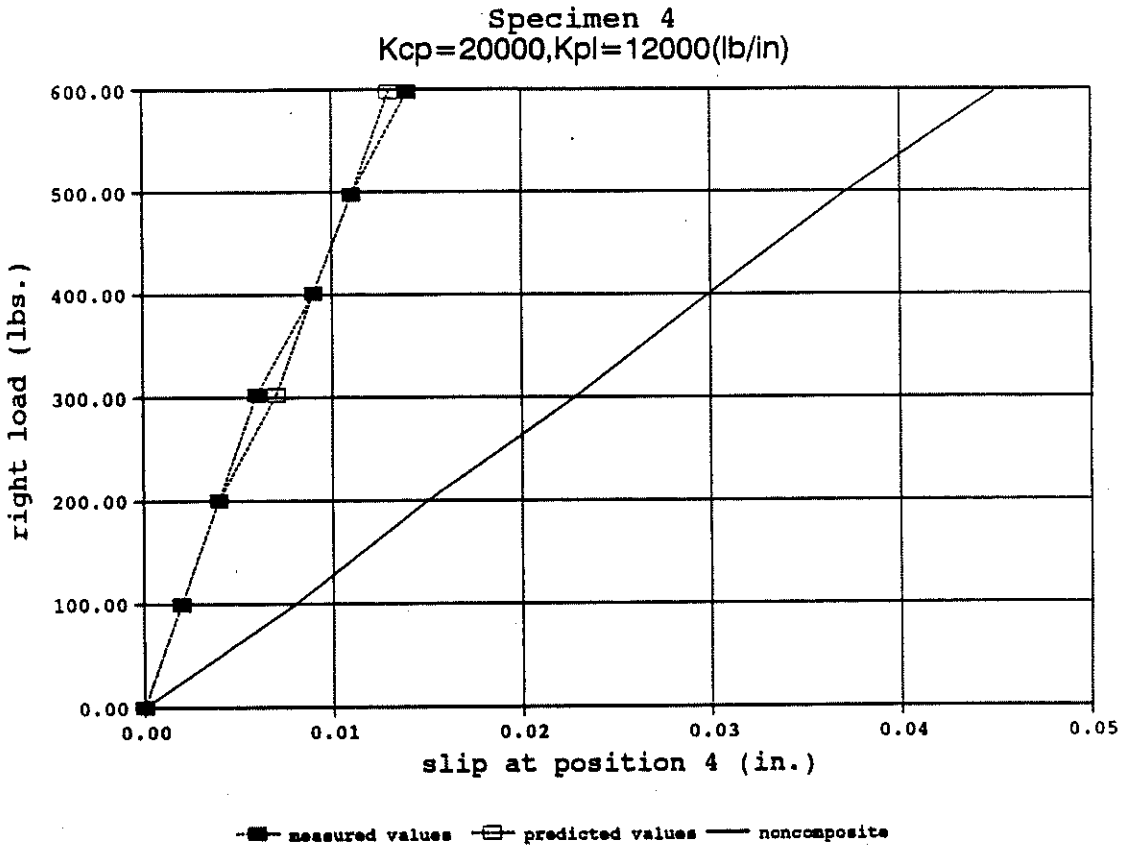

Figure C2.34: The theoretical and experimental load-slip curves of T-beam specimen 4

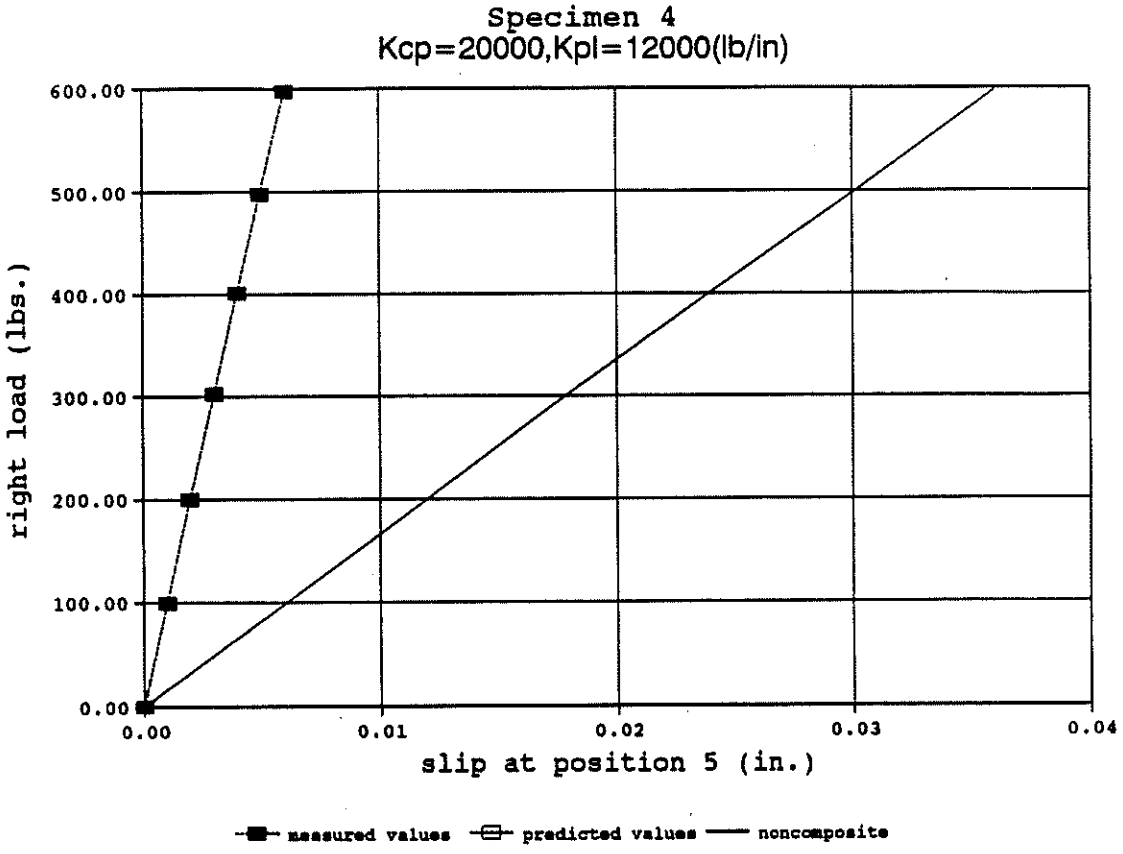

Figure C2.35: The theoretical and experimental load-slip curves of T-beam specimen 4

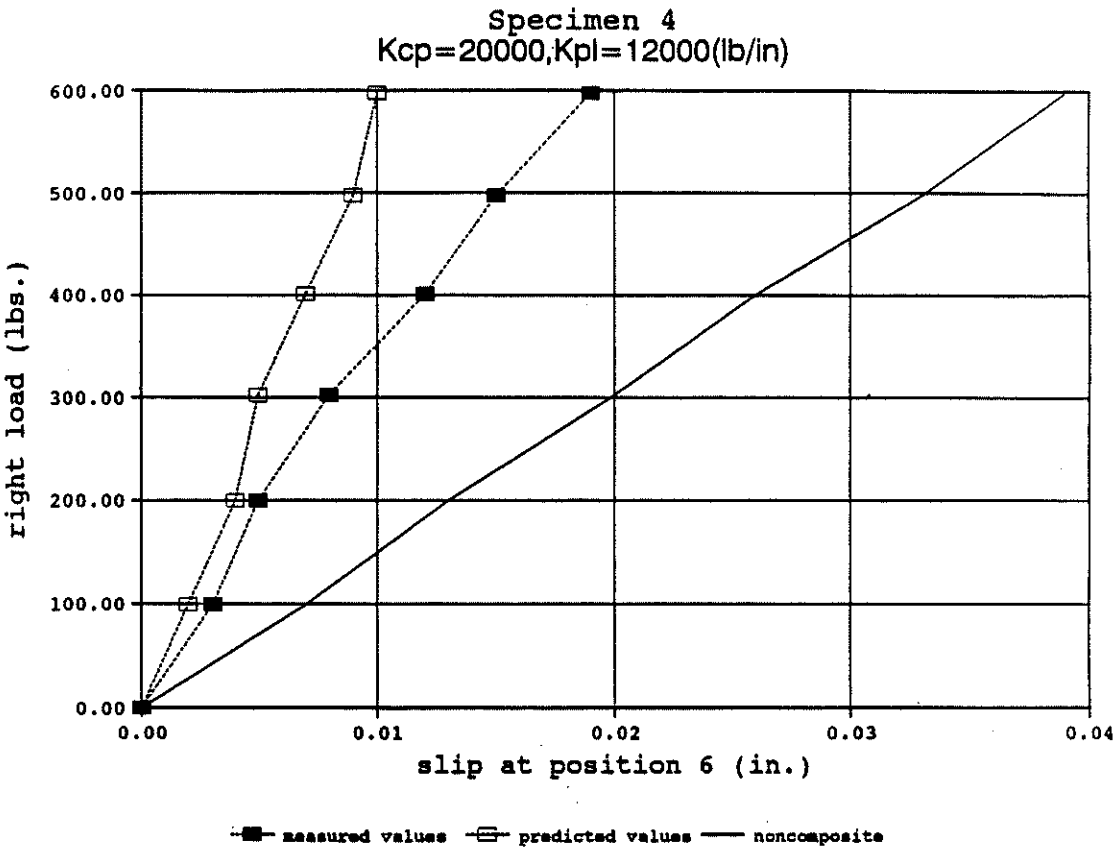

Figure C2.36: The theoretical and experimental load-slip curves of T-beam specimen 4

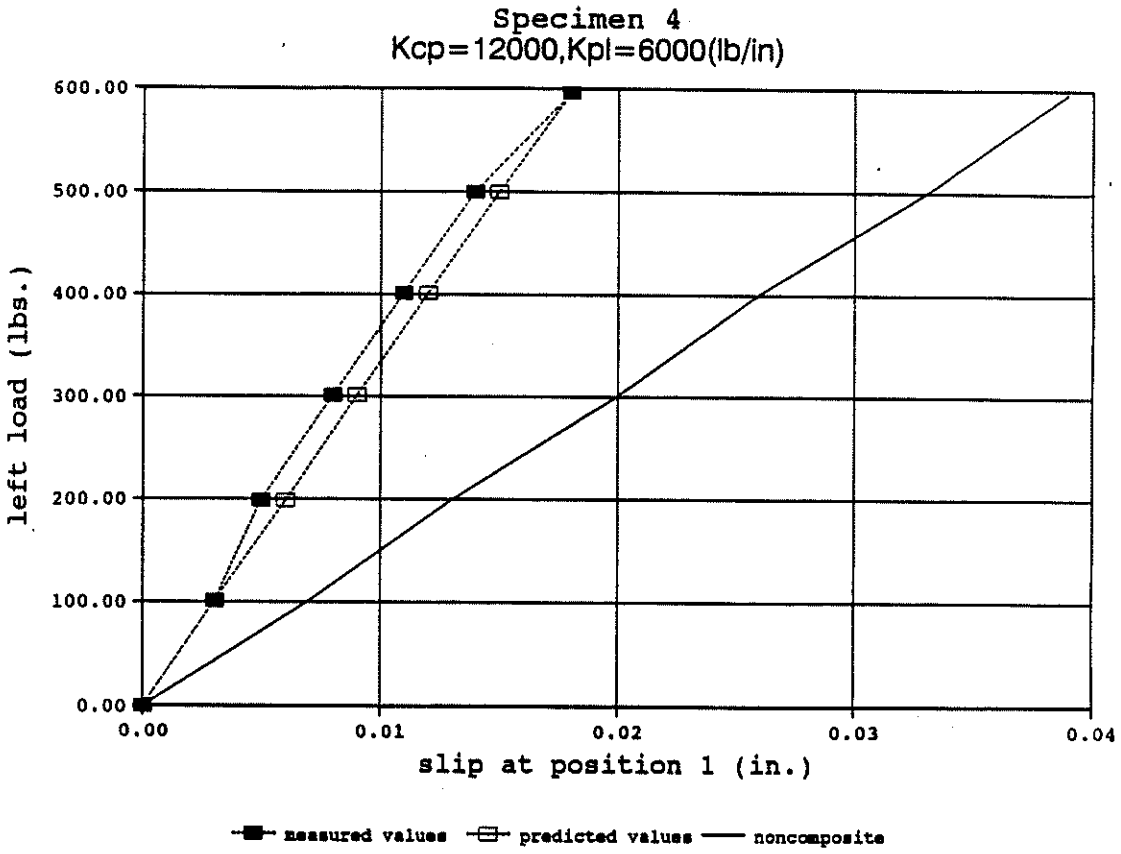

Figure C2.37: The theoretical and experimental load-slip curves of T-beam specimen 4

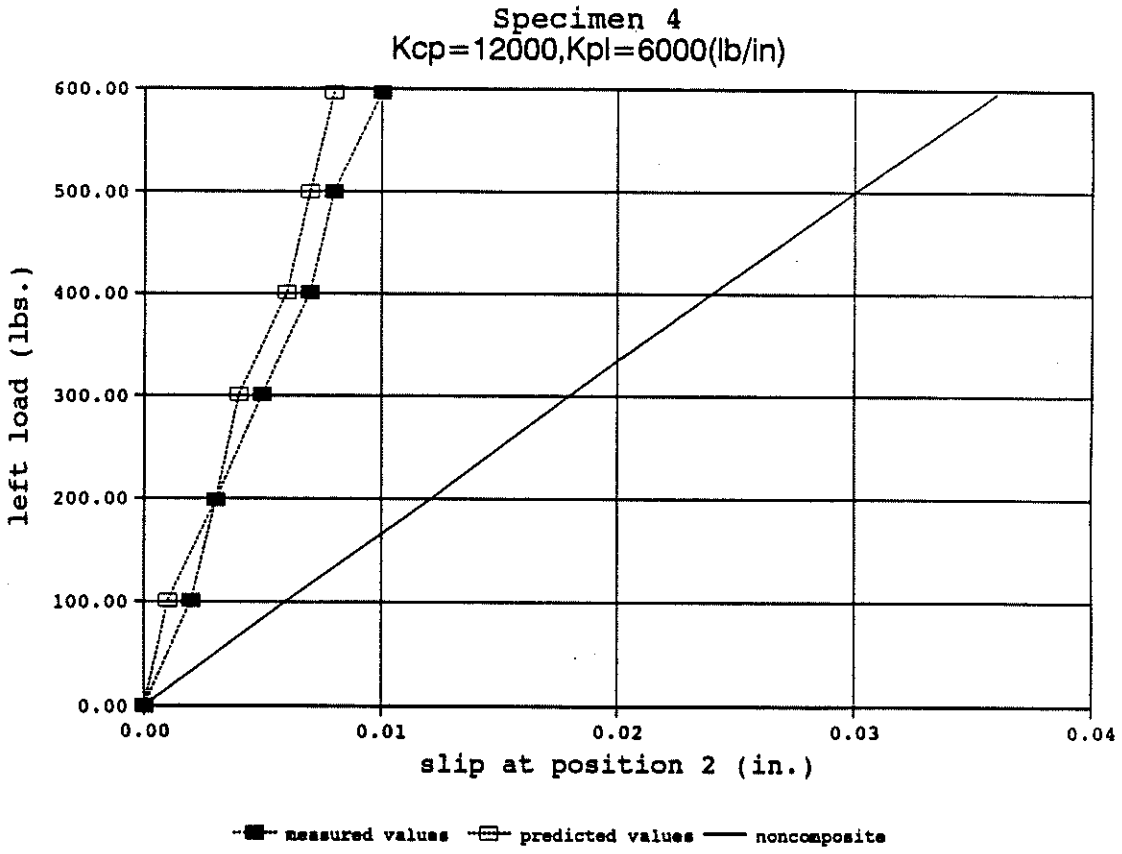

Figure C2.38: The theoretical and experimental load-slip curves of T-beam specimen 4

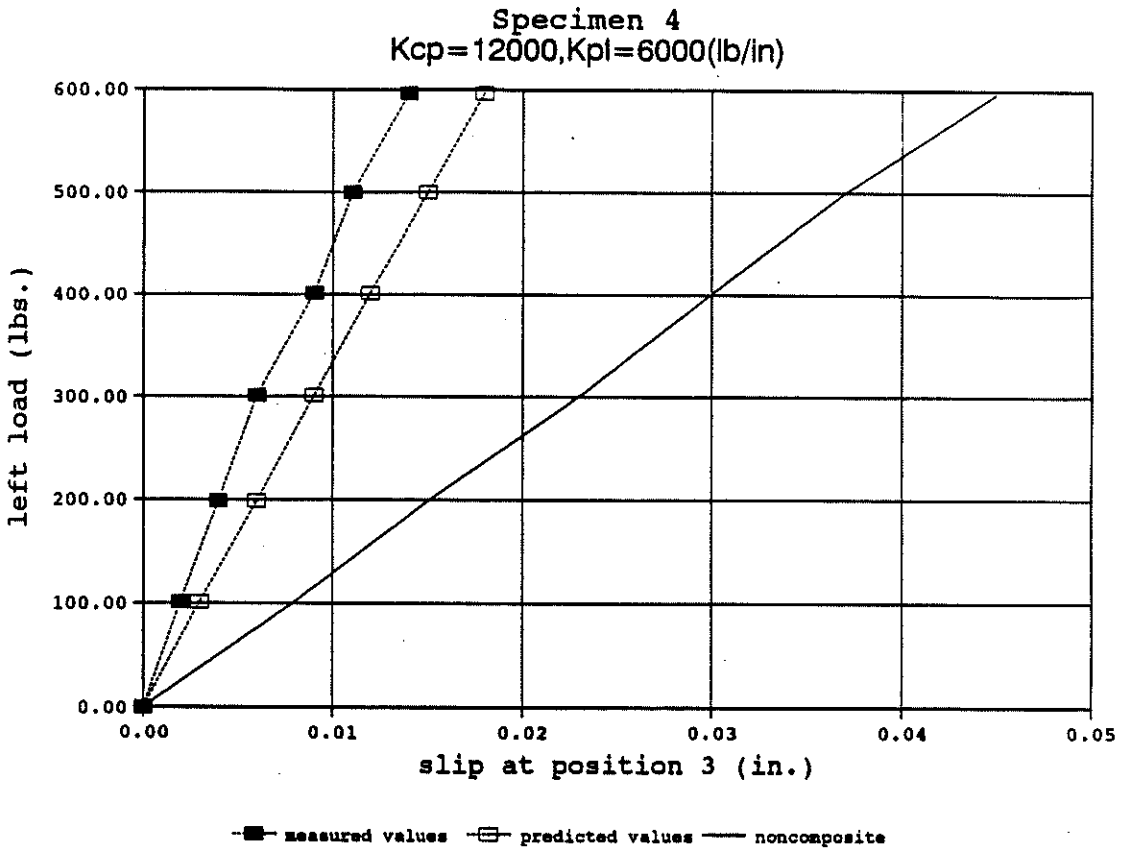

Figure C2.39: The theoretical and experimental load-slip curves of T-beam specimen 4

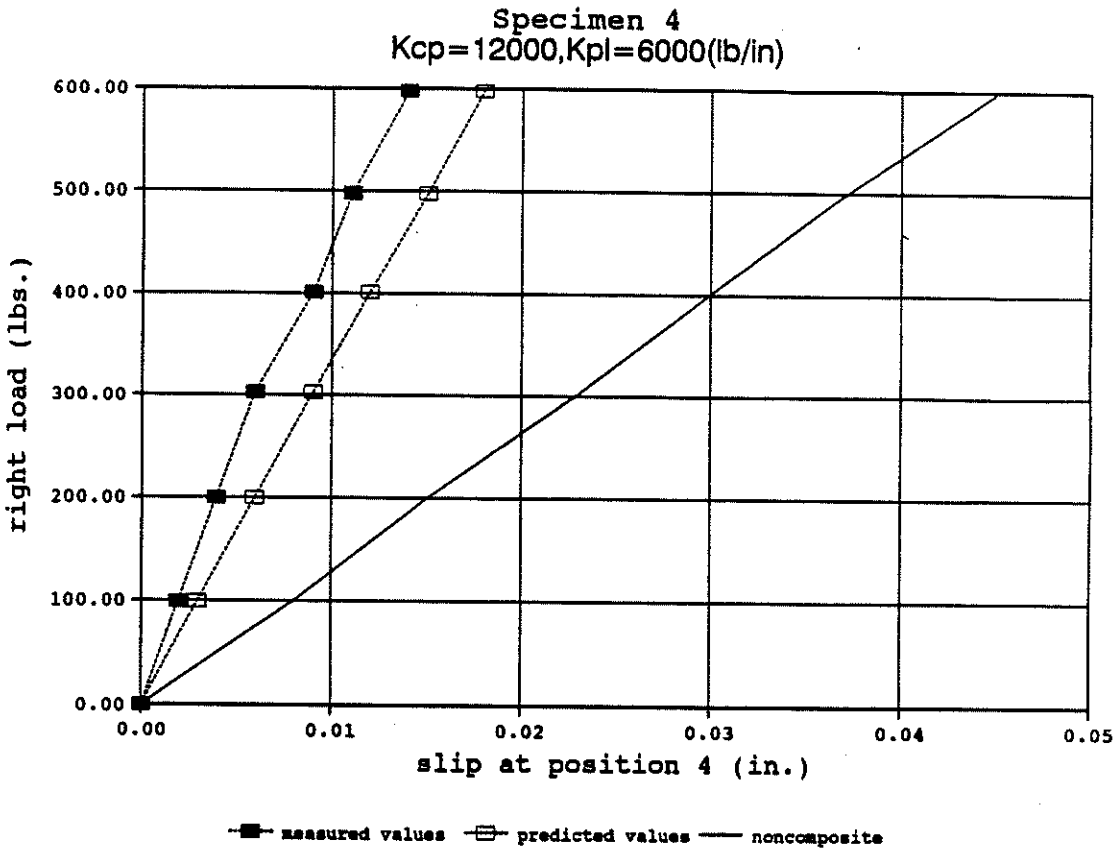

Figure C2.40: The theoretical and experimental load-slip curves of T-beam specimen 4

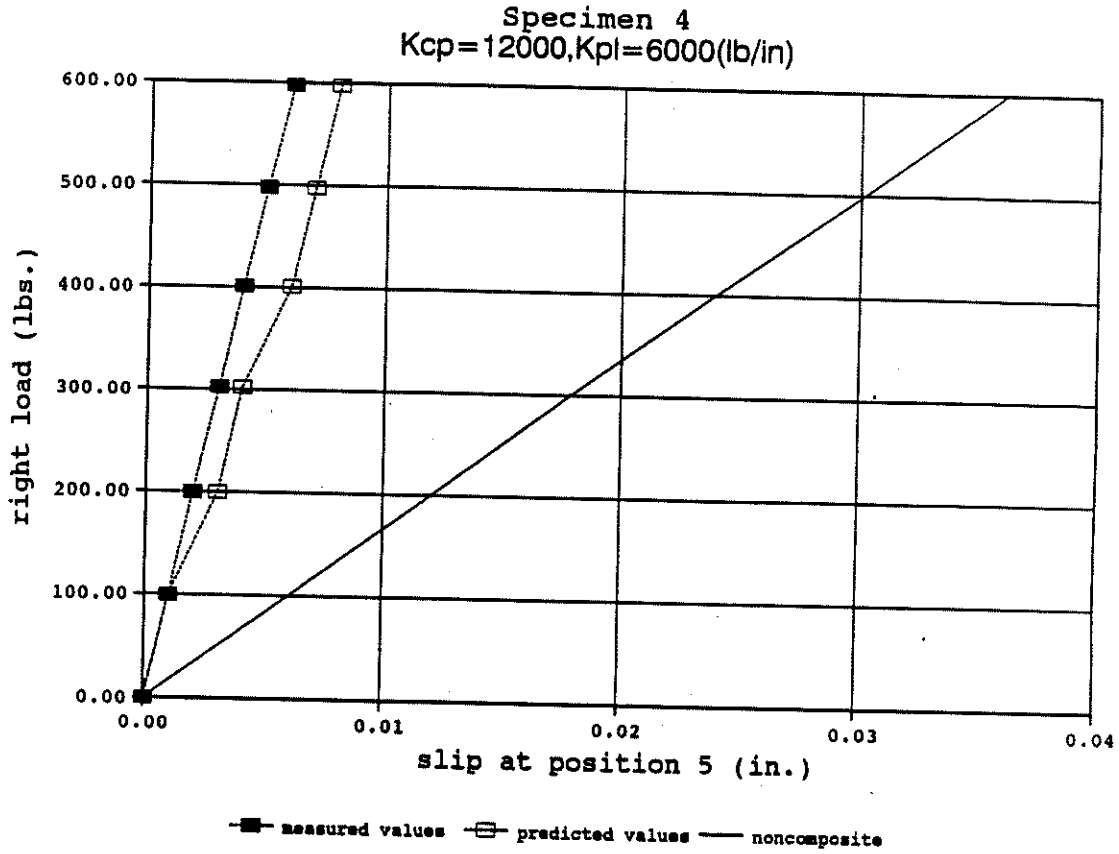

Figure C2.41: The theoretical and experimental load-slip curves of T-beam specimen 4

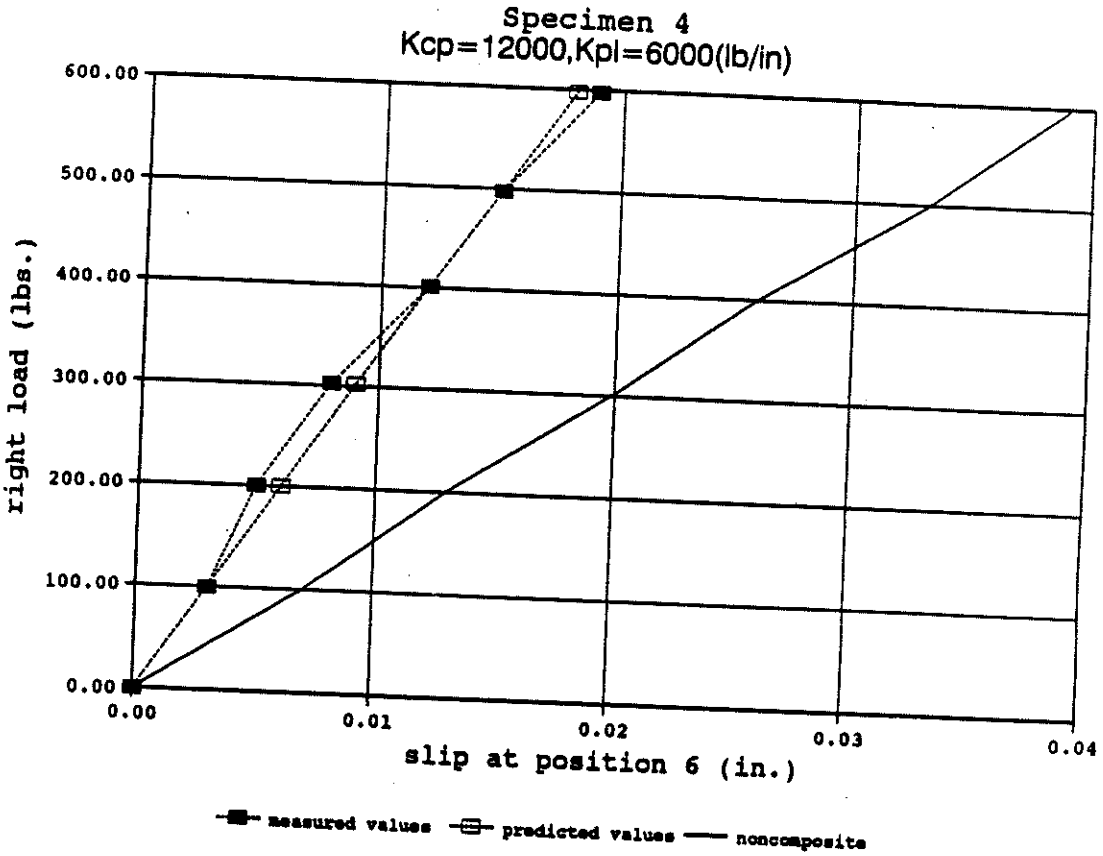

Figure C2.42: The theoretical and experimental load-slip curves of T-beam specimen 4